TEAR STRENGTH OF FILLED RUBBERS

by

AZEMI BIN SAMSURI

A Thesis submitted to the Council for National Academic Awards, England, in partial fulfilment of the requirements for the degree of Doctor of Philosophy

Collaborating establishment:

The Malaysian Rubber Producers' Research Association
Brickendonbury,
HERTFORD SG13 8NL

Sponsoring establishment:

London School of Polymer Technology
The North London Polytechnic,
Holloway Road,
LONDON, N7 8DB

May 1989

DECLARATION BY THE CANDIDATE

I declare that while registered as a candidate for the degree of Doctor of Philosophy, I have not been a registered candidate for another award of the CNAA, or of a University.

PROGRAMME OF RELATED STUDIES

The author has undertaken a programme of guided study on the phenomenological and theoretical aspects of the reinforcement of rubbers by particulate fillers under the guidance of Professor A.G. Thomas and Dr. G.M. Bristow of MRPRA. The author has also made two presentations of his own research results at two colloquia at MRPRA and presented a joint paper with Prof. A.G. Thomas at the International Rubber Technology Conference in Penang, October 1988. The abstract of the paper presented at the conference is attached in the thesis. Besides that, the author has attended a seminar at MRPRA Golden Jubilee Celebration and the weekly colloquium held at MRPRA.

ABSTRACT

The strength of black-filled rubbers has been investigated under a variety of test conditions using various compounding formulations, of both strain-crystallizing and non-strain-crystallizing elastomers. The enhancement in the tear strength is substantial when knotty tearing occurs. In knotty tearing, the crack tip grows perpendicularly to the general direction of propagation. This effectively increases the tip diameter and thus the tear strength. A strong correlation between tearing energy and knot diameter (measured in the unstrained state) has been found in the present investigation. Factors which affect the development of knotty tearing were investigated. It was found that knotty tearing is affected by the degree of strain-crystallization, molecular mobility, nature and concentration of crosslinks, the type and concentration of carbon black, temperature and tear rate.

The onset of knotty tearing appears to be related to the development of strength anisotropy at the tip of the tear. The effect of this anisotropy on the energy to propagate tearing in the direction of pre-straining was investigated using split tear test-pieces. The tearing energy for crack propagation in the direction of molecular orientation gives a quantitative measure of strength anisotropy developed in the vulcanizate as a consequence of pre-straining. It was found that, in a stretched vulcanizate, the tearing energy to propagate tearing in this direction was a factor of about 20 lower than the tearing energy of the unstretched vulcanizate.

In a certain type of black-filled vulcanizate, the anisotropy introduced during pre-stressing to large extension still persisted even after the pre-stretch was removed. The present investigation shows that the anisotropy introduced by pre-stressing is associated with the set. The tearing energy of a pre-stressed vulcanizate was found to correlate strongly with the set.

ACKNOWLEDGEMENTS

The author is very grateful to Dato' Dr. Hj. Ani Arope and Dr. Abd. Aziz S.A. Kadir, the past and the present Director of the Rubber Research Institute of Malaysia for the opportunity of his secondment to the Malaysian Rubber Producers' Research Association (MRPRA). The author would like also to thank the Director of MRPRA for the provision of the experimental facilities described in this thesis.

The author is extremely grateful to Professor A.G. Thomas who is his Director of Studies at MRPRA for his valuable advice and guidance during the course of the research work. The assistance of Dr. G.M. Bristow of MRPRA as an adviser to this research work is also highly appreciated and acknowledged. The author is also greatly indebted to Dr. D.C. Blackley, his supervisor at the London School of Polymer Technology for his valuable comments and constructive criticisms during the course of the writing of the thesis.

Thanks are also due to Dr. G.J. Lake of MRPRA for helpful discussions, and also the staff members of the Physical Testing Group, Chemistry Group and Photography Group of MRPRA for their assistance.

Finally, the author would like to thank his beloved wife, Zalaha, and his three children, Hafiza, Hafizi and Aadila for their patience and understanding during the course of the writing up of the thesis.

LIST OF ABBREVIATIONS AND SYMBOLS

NR	natural rubber
SMR L	Standard Malaysian Rubber grade L
SBR	styrene butadiene rubber
ENR	epoxidised natural rubber
INR	isomerised natural rubber
HAF black	high abrasion furnace carbon black
MT black	medium thermal carbon black
MBS	morpholinylbenzothiazole-2-sulphenamide
Flectol H	polymerised 2,2,4-trimethyl-1,2 dihydroquinoline
CBS	N-cyclohexyl benzothiazole-2-sulphenamide
TMTD	tetramethyl thiuram disulphide
M 100	tensile stress at 100% strain
M 300	tensile stress at 300% strain
E.B. (%)	percentage elongation at break
DBTS	di-n-butyl tetrasulphide
RH	rubber hydrocarbon
U_b	stored energy density at break
$[X]_{phy.app.}$	physically (apparent value) manifested crosslink concentration
$[X]_{phy.act.}$	physically (actual value) manifested crosslink concentration
υ_r	volume fraction of rubber in the swollen vulcanizate
N	number of crosslinks per unit volume of rubber
n_1/N	percentage of crosslink broken
n_2/n_1	recombination efficiency
ζ	set
σ	stress
ρ_{RH}	density of rubber hydrocarbon
S	surface energy
s	rate of extension (crosshead speed)
T	tearing energy
T_R	tearing energy ratio
θ	temperature
θ_g	glass-transition temperature
ϕ	volume fraction of carbon black in a rubber vulcanizate
r	tear rate
C_1	elastic constant
d	tear-tip diameter referred to the unstrained state
λ	extension ratio
c	crack length referred to the unstrained state
h	thickness referred to the unstrained state

w	width referred to the unstrained state
l	length referred to the unstrained state

CONTENTS

CHAPTER ONE

INTRODUCTION

1.1 General introduction

Pure gum natural rubber vulcanizates, although high in physical strength, are suitable for relatively few commercial applications. Copolymers synthetics without reinforcing materials are too low in strength to warrant their consideration for use. For most type of service, relatively large amounts of materials known to increase hardness, stiffness, strength and abrasion must be present in any given formulation. These include materials like carbon blacks, siliceons materials such as calcium silicate, fine particle precipitated calcium carbonates and hard clays to name a few examples. These materials are commonly known as fillers. Fillers are incorporated into rubbers for a variety of reasons, among which are control of physical properties of the rubber and cost reduction. The required physical properties depend on the application for which the rubber is intended, and usually a combination of properties. For example, a rubber intended for a tyre tread may require a combination of abrasion and skid resistance. Among these fillers, carbon black is the most popular. It was quoted by Dannenberg (1), that carbon black is second only to rubber as the most critical and widely used raw material of the rubber industry. About 94% of the production of all carbon black is consumed by the rubber industry (1979 statistical figure, reference (1)). When fine particles of carbon black are incorporated into rubber, the physical properties and the resistance to mechanical failure are greatly improved. Thus carbon blacks are incorporated into rubber with a view to improve both the performance and the service life of the rubber products. Rubber products like tyres and conveyor belts are susceptible to fail in service due to failure associated with crack-growth, which is related to tearing.

Currently, the tear behaviour of black-filled rubber vulcanizates is much less well understood than that of unfilled (gum) vulcanizates. This is not surprising, since most of the work on tearing of rubbers was based on the unfilled vulcanizates where the material presented few complications in the interpretation of

the results. In black-filled vulcanizates, the failure shows complicated features, for example if the crack does not follow the intended path. In view of the poor understanding of the failure process in black-filled vulcanizates, the work described in this thesis was carried out, with the hope that it will shed some light on the matter.

The approach which has been widely used for studying the strength behaviour of rubbers is based upon fracture mechanics, in which crack propagation is described in terms of energy required to create new surface, called the tearing energy. The same approach is adopted here. There are four main areas of investigations:

(i) To establish the factors which affect the development of knotty tearing which appears to be the principal mechanism by which carbon black enhances the tear resistance. Rubber products like tyres are subjected to a variety of conditions viz, temperature of surrounding environment, temperature rise in the rubber component during running of the tyre and also the rate of deformation the tyres are subjected to during driving. Tear tests on carbon-black-filled vulcanizates were carried out at different temperatures and tear rates to see how the resistance to tearing are affected by these conditions. Other factors investigated will be discussed in Chapter Three.

(ii) To investigate the effect of anisotropy induced by pre-straining during the tear test. Although rubbers are seldom used in tension, however there are a few exceptional cases where they are used in tension. Conveyor belts and cables are two examples of uses of rubber in tension. The resistance to tearing propagating in the direction of pre-straining was also investigated.

(iii) To investigate the effect of anisotropy introduced by pre-stressing prior to tear testing. The term pre-straining used in (ii) above refers to a situation where the stress giving the orientation was maintained during the actual tear tests. The term pre-stressing as applied to (iii) refers to

a situation where the stress giving the orientation was maintained for one minute and then the stress was completely removed. In other words the tear tests were carried out on vulcanizates which were previously deformed prior to the test. There are a few instances where the rubber is stretched prior to use either unintentionally or deliberately for example, when rubber goods are removed from the mould. The resistance to tearing in the direction of pre-stressing was also investigated.

(iv) To seek explanations for the high tearing energy and the smooth fracture surface produced by steady tearing.

1.2 Introduction to science and rubber technology

1.2.1 Glass-transition temperature and crystallization

Rubbers belong to a class of high molecular weight material known as polymers. Polymers consist of long chain molecules made up of many basic units called monomers joined end-to-end to form a continuous chain. Like many other polymeric materials, rubbers are viscoelastic, i.e., they exhibit both liquid-like and solid-like characteristics. This is manifested by creep and stress-relaxation. In creep, the stress is suddenly applied to a sample and maintained constant, and the strain is measured as a function of time. However, being a viscoelastic material, the strain will not be constant but will increase slowly with time, i.e, it creeps. On release of the stress, the molecules slowly recover their former spatial arrangement and the strain simultaneously returns to zero. In stress-relaxation, the sample is suddenly brought to a given deformation, and the stress required to maintain it is measured as a function of time. Being a viscoelastic material, the stress will not be constant but will decrease slowly with time. When the rubber molecules are crosslinked, it shows another important characteristic in that it can be deformed to large deformation (a few hundred percent strain), and recovers its shape and size almost instantaneously when the deforming force is removed.

Rubbery behaviour depends on the ability of the molecular units to move readily past one another so that the inherent flexibility of

the molecules can permit large deformations. Thus the intermolecular forces have to be sufficiently small so that thermal energy can produce the necessary mobility. As the temperature is lowered the thermal energy decreases and a state is reached where it is no longer sufficient to overcome the forces between the molecules. When this happens the chain segments become frozen like the molecules of in an ordinary solid. Under these conditions the rubber then becomes hard and brittle like glass. The transition temperature above which it is rubbery and below which it is glass-like hard is called the glass-transition temperature. The conventional symbol for the glass-transition temperature is T_g, but in this thesis, in order to avoid confusion with the tearing energy symbol, T, thus the symbol θ_g was adopted.

Rubber can also lose its rubbery properties by hardening through crystallization. The basic requirement for crystallization is regularity of chain structure. Thus rubbers that have a regular structure like natural rubber and chloroprene can crystallize. However, there are distinctive differences between the hardening below θ_g and hardening associated with crystallization. The hardening below θ_g is almost instantaneous. However, hardening associated with crystallization is rather gradual because crystallization is a rate process. For crystallization to occur, it is necessary for segments of molecules to move relatively to one another and to arrange themselves in a regular pattern on a crystal lattice. This process of rearrangement requires an appreciable amount of time for its accomplishment. This is why crystallization in rubber is so much slower than hardening brought about by the glass-transition temperature since hardening below θ_g involves only an instantaneous `freezing-in' of the amorphous structure of the rubber.

The rate of crystallization is also temperature dependent. For natural rubber, the temperature at which maximum rate of crystallization occurs is about -26°C (2). Low temperature crystallization is a disadvantage because it poses some problems to handling. One of the changes in properties as a consequence of low temperature crystallization is a considerable increase in hardness or stiffness. However, the material still retains a degree of flexibility and is not brittle as the glassy material.

Nevertheless, it is still a nuisance because it imposes additional difficulties in processing. Apart from leading to possible damage of machinery, rubber containing unmelted crystallites can prevent the uniform mixing of vulcanizing ingredients during the compounding stage and hence, the production of vulcanizates with inferior properties. Fortunately, crystallization is a reversible physical process, and by storing the rubber above the melting temperature the crystallized rubber reverts to its original amorphous state.

Another type hardening is called a storage hardening occurs only in natural rubber. This type of hardening is chemical in origin and it is irreversible (3). This hardening is believed to be connected with a functional group or groups such as the aldehydes, present in the natural rubber molecules (3). Storage hardening occurs when the rubber is stored at ambient temperature. However, it can be prevented by incorporating a suitable chemical (eg hydroxylamine) into the latex during processing to inhibit the crosslinking reaction during storage of the bale rubber.

Unvulcanized rubber is tacky when hot and dissolves completely in a suitable solvent. Its uses are limited to making rubber solutions and adhesives. For any rubber to be of practical use, the long chain molecules must be crosslinked together at various points to form a three dimensional network by a process known as vulcanization. The process of vulcanization transforms the moulded compound into a stable, elastic and resilient material which can perform over a wide range of temperature. When a vulcanized rubber is immersed in a solvent it does not dissolve but swells to a certain degree depending on the crosslink concentration of the vulcanizate and the nature of the solvent. Because crystallization depends on the regularity of the polymer molecule, it proceeds less readily if this regularity is disturbed. Thus the normal natural rubber vulcanizates crystallize perhaps a hundred times more slowly than the unvulcanized natural rubber because the crosslinks themselves constitute such irregularities and, in addition, there is usually sulphur combined elsewhere with the rubber molecules which act similarly. Andrews and Gent (2) suggested that the effect of crosslinking is primarily to retard the attainment of the crystalline state, either by reducing the rate of nucleus formation or by affecting the rate of growth of a growing crystal, or both.

The retardation of crystallization by crosslinks is an advantage because the vulcanized rubber can now be used in service at low temperature, even at temperatures down to -40°C (4) provided the right vulcanizing system is used. Such vulcanizing systems characteristically make use of high dosages of sulphur and accelerator, so that the sulphur is always inefficiently used for crosslinking and becomes combined extensively as side groups (e.g. cyclic, mono- and disulphides) in the rubber chain (4). The maximum degree of crystallinity detected in natural rubber is about 30% (2). The limited extent of crystallization in solid polymers can be attributed to a number of factors, including molecular imperfections (branch points, crosslinks, chain ends) and chain entanglements. Although only a small proportion of the material may become crystalline, the consequences are striking. For example the hardness of natural rubber increases by a factor of over 100, and its extensibility and elasticity are greatly reduced (2). Among other physical changes which accompany crystallization are the increase in density (i.e., decrease in volume), evolution of heat of fusion and the optical properties of the rubber, i.e., the crystallized rubber loses its optical transparency and aquires a yellowish waxy appearance.

The low temperature crystallization of some rubbers may be a disadvantage if it occurs too readily, but parallel the effect of crystallization induced by high strains at ordinary temperatures has a beneficial effect on strength properties. For example, a natural rubber compound containing no carbon black has a tensile strength of about 27 MPa whereas a similar compound made from styrene-butadiene copolymer rubber which does not strain-crystallize the figure is only about 3 MPa. However, there is a subtle difference between strain-crystallization of vulcanized NR and unvulcanized raw (uncompounded) NR. In a vulcanized NR, the crystallization produced by extension is not permanent but disappears as soon as the stretching force is removed. The rubber reverts to its original unstrained condition. Raw NR, however, when crystallized at high extension, remains in the extended state and does not return to its original state unless subsequently heated. This can easily be demonstrated by stretching a strip of raw NR to a high extension and then cool it in a stream of cold water from the tap for a few

minutes. On removal of stretching force the rubber remains in the fully extended state. When it is warmed in a stream of hot water from the tap, the crystals melt, whereupon it reverts to the unstrained state. In contrast, a strip of unfilled vulcanized NR will return to its original unstrained state almost instantaneously when the stretching force is removed. The difference in recovery behaviour between vulcanized and unvulcanized NR after crystallization may be explained by the presence of a permanent crosslinked network structure in the vulcanized material (5). This network structure leads to a strong elastic restoring force which is sufficient to break down the crystalline structure formed on stretching. In unvulcanized NR, molecular slippage can take place on extension, and the elastic restoring force is not sufficient to break down the crystalline structure. It is only when the temperature is raised sufficiently to melt the crystallites (ca. 30°C) that the rubber returns elastically to its original state (5).

The effect of crosslinks on the glass-transition temperature is small. Increasing the degree of chemical crosslinking raises the θ_g by a few degrees, the effect being due partly to the increase in the intermolecular forces provided by more sulphur being combined with the rubber and partly to the restraining influence of the crosslinks themselves (6). Besides that, the glass-transition temperature of the rubber is also affected by the chemical nature of the rubber molecules. For example, the size and the number of side groups, and the polarity of the side groups. Generally, rubbers having polar side groups such as nitrile rubber and chloroprene have high θ_g. These side groups reduce the mobility of the molecules since the thermal energy has to overcome intermolecular forces associated with polar attraction and steric effects. The glass-transition temperature can be depressed substantially by incorporating liquid plasticizers in rubber. Plsticizers are low molecular weight viscous liquid(which are compatible with rubber, have high molecular mobility at low temperatures, low volatility at vulcanization temperatures and should not interfere with the vulcanization process. Plasticizers reduce the glass-transition temperature by generating free volume (i.e the volume available for segmental motion) in the material because of their high molecular mobility. Generally, plasticizers usually reduce strength.

1.2.2 Characteristics of carbon blacks

Vulcanized rubber is basically defined as a cross-linked elastomeric polymer. Rubber vulcanizates which contained only ingredients necessary for vulcanization process for example, sulphur, zinc oxide, stearic acid and protective agents such as aromatic amines are termed as unfilled or gum vulcanizates. As mentioned earlier in the general introduction, gum vulcanizates have limited uses. Fillers are usually incorporated into rubber to meet the properties and specifications required in service. The present investigation is concerned only with carbon black as the reinforcing filler. The subject of reinforcement of carbon blacks in rubbers is very wide and complex. Some general background about carbon blacks and a few relevant established theories will be presented and discussed briefly in this section. Carbon blacks are essentially elemental carbon and are composed of particles which are partly graphitic in structure (7). Carbon blacks are produced by converting either liquid or gaseous hydrocarbons to elemental carbon and hydrogen by partial combustion or thermal decomposition. There are three methods of producing commercial carbon blacks. One is known as the Furnace Process, which is the most popular method. This process consists of the incomplete combustion of natural gas or heavy aromatic residue oils from petroleum or coal industries in refractory-lined steel furnaces at reaction temperatures range from about 1200°C to 1700°C. The second process is called a Thermal Process where natural gas is thermally decomposed at 1300°C in the absence of air. This is done in a cylindrical furnace filled with an open checkerwork of silica brick. The third is called Channel or Impingement Process. Natural gas is burned in literally millions of small flames issuing from lava or steatite tips. The smoky flames produced by these burnings are impinged on channel irons. Carbon soots deposited on relatively cool channel iron surfaces are then scraped off into a suitable container. Channel Process is obsolete and is abandoned because of pollution it creates in the surrounding environment.

The term reinforcement has been widely used by the rubber technologists to denote the improvement in the resistance to tearing and abrasion and also the increase in the tensile strength conferred

by the carbon blacks. The extent of the reinforcement produced by the carbon black is affected by the properties of the carbon black which are listed below.

(i) Particle size: The particles of carbon black are not discrete but are fused ``clusters'' of individual particles (7). The reinforcement conferred by the black is not influenced to any extent by the size of the unit but predominantly by the size of the particles within the unit. Particle size of itself has relatively little effect on the modulus. Tensile strength and tear strength are affected by the particle size and both properties are normally enhanced as the surface area increases (7) (i.e surface area increases with decreasing particle size).

(ii) Structure: The term ``structure'' refers to the joining together of carbon particles into long chains and tangled three-dimensional aggregates (7). This aggregation of particles takes place in the flame during the manufacture of carbon black. The oil furnace process using highly aromatic raw materials, gives blacks of high structure. The higher the structure of a carbon black, the more irregular the shape of the aggregates, hence the less these aggregates are capable of packing together. The thermal process produces blacks with little or no structure. There is some particle aggregation in blacks produced by the channel process. The effect of structure is more noticeable on processing properties than on the properties of the vulcanizates (7). In general, the higher the structure the stiffer the unvulcanized compound and the harder the vulcanized material.

(iii) Physical nature of the surface: The carbon atoms in a carbon black are present in layer planes. In thermal blacks, the layers are highly orientated, parallel to the surface. Furnace blacks on the contrary, show less crystalline crystallite orientation than thermal blacks (7). The role of the physico-chemical nature of the surface in rubber reinforcement is not fully understood. There were suggestions (7) that the high modulus produced by the high structure blacks was not because the carbon black

agglomerates restricted the crosslinked network, but because these aggregates when broken down during mixing produced active free radicals capable of reacting with the rubber. This black-rubber interaction is evident by the existence of the so called ``bound rubber'' which gives a measure as the amount of rubber insolubilized by the presence of filler when the mix is exposed to a solvent (toluene) in which the rubber alone is readily soluble (8). It was reported also (8), that when a carbon black was progressively graphitised by heat treatment, tensile and tear strengths progressively decreased, indicating that the physico-chemical nature of the surface is important.

In summary, particle size is the most important feature of carbon black. 'Structure' of black appears to show no significant effects on vulcanizates properties. The present knowledge of the relationship between surface chemistry and rubber properties is still not complete.

1.3 Mechanisms of reinforcement

The enhancement of strength properties by fine particles of carbon black provides an interesting paradox. It is well known that the presence of small amounts of impurities in the rubber, for example, sand and grit will reduce the strength of the rubber vulcanizates because such impurities act as local stress concentrations and thereby initiate failure. It is therefore at first sight difficult to envisage how the introduction of these rigid particles can result in the enhancement of strength properties. Some hypotheses and postulations by previous investigators in the past are discussed below regarding the mechanisms of reinforcement of carbon blacks in rubbers.

(i) Load sharing mechanism: According to Bueche (9), the reinforcement is due to a load-sharing effect arising from the attachment of several molecules to one filler particle. When a highly stressed molecular chain breaks, the tension it carried is believed to be distributed over a substantial number of other chains via the filler particle, instead of being imposed upon its immediate neighbours. Thus, a catastrophic failure is avoided.

(ii) Slipping mechanism: Dannenberg (10) suggested that some slipping of molecular chains occurs over the surface of the filler particles, thus allowing highly stressed chains to relieve their tension.

(iii) Detachment of filler particles: Andrews and Walsh (11) suggested that the detachment of rubber from filler particles in the highly strained region around an advancing tear is an important source of energy dissipation which can contribute to enhancement in strength. This will be discussed further in Chapter Three.

(iv) Stress softening: Filled materials show pronounced stress softening (12). Consequently, they do not return a large fraction of the energy put into deforming them; i.e., they exhibit hysteresis to a marked degree. The cause of this phenomenon is not fully understood. Bueche (13) reckoned that the phenomenon was attributed to breakage, detachment, or slippage of abnormally short chains to two filler particles. On the other hand, Harwood et al (14) observed a rather similar effect in unfilled natural rubbers under large stresses. They then attributed the phenomenon to the rubber network itself rather than to details of the rubber-particle interface. Whatever the details of the mechanism, stress-softening is a means of energy dissipation wich can contribute to enhancement of strength.

Those hypotheses discussed above all have one thing in common, which is energy dissipation. Although, it is generally accepted that energy dissipation is important in enhancing strength properties, however in tearing, there is a perculiar feature known as knotty tearing which appears to be the principal mechanism of enhancement of tear resistance in black-filled rubber vulcanizates (15, 16). The present investigation is concerned with the enhancement of tear resistance of black-filled rubber vulcanizates in particular to shed some light on the mechanism of knotty tearing.

CHAPTER TWO

LITERATURE SURVEY

2.1 General introduction on the strength of solid materials

Fracture creates free surfaces. The strength of a solid material can be defined as its ability to resist fracture. The resistance can be measured in terms of stress, strain and work done to break, tearing and etc. The mechanics of failure of a solid body containing a flaw or other imperfections began when Griffith (17) carried out a classical work on the fracture of glass. Griffith's fracture criterion can be stated as follows: a pre-existing crack in an elastic body will grow only if, in so doing, the elastic stored strain energy released at the instant of rupture is equal to or greater than the amount of surface energy required to create new surfaces. This can be expressed in a mathematical form by

$$-\left(\frac{\partial W}{\partial A}\right)_{l} \geq 2S \qquad (2.1)$$

where W is the elastic strain energy stored in the body, A is the new interfacial area of the fractured surface, and S is the surface energy of the material. The minus sign indicates that, there is a reduction in the stored energy as A icreases. W continues to decrease until the strain energy is zero, that is, when the crack has spread across the body. A factor of 2 appears on the right hand side of equation 2.1, because there are two surfaces to a crack. The suffix, l, of the partial differentiation denotes that the crack spreads under conditions such that the external forces on the test-piece do not move and do no work. Equation 2.1 implies that all the mechanical work appears as surface energy. The term $-(\partial W/\partial A)$ is defined as the strain energy release rate, or the fracture energy (18). The word ``rate'' normally means rate with respect to time. However, in this context, the word ``rate'' refers to the rate of releasing elastic strain energy in propagating a fracture over an increment of area δA, and not the time.

Griffith's theory of brittle fracture is applicable only to

materials which are perfectly elastic. Polymeric materials, on the other hand, show non-linear elasticity, and are capable of being deformed to large strain, the strain being usually accompanied by irreversible energy dissipation. Clearly, Griffith's theory is not applicable to polymeric materials.

2.2 Tearing energy theory of Rivlin and Thomas

Tearing is the term used to denote fracture of a vulcanized rubber. Conventional tear tests usually express the tear resistance in terms of the force to produce tearing per unit thickness, referred to the unstrained state. Such tear tests often produce different ratings because the tearing force depends in a rather complex manner on the geometry of the test-piece and nature of tear tip. It is clear that such tests do not measure the same tear resistance, and thus the tear strength so measured is not a fundamental property of the material.

In order to circumvent these problems, Rivlin and Thomas (19) treated the whole problem from the stand point of energy rather than force. In so doing, they applied Griffith's fracture criterion, but with a little modification to allow for the irreversible deformation which occurs at the highly-strained regions around the neigbourhood of the tear tip. The energy required to create new surfaces by the tearing process is defined as the tearing energy. Like Griffith, they also postulated that a cut in a strained body would spread only if the elastically-stored strain energy released at the point of tearing, equalled or exceeded the critical tearing energy. This definition can be expressed by the mathematical relation given below

$$-\frac{1}{h}\left(\frac{\partial W}{\partial c}\right)_{l} \geq T_c \qquad (2.2)$$

where W is the total elastic strain energy stored in the test-piece, h is the original thickness measured in unstrained state, c is the length of a cut, and T_c is the characteristic tearing energy of the material. The suffix l again denotes that external forces do not move, so do no work. Equation 2.2 is analogous to equation 2.1, except that T now takes into account not

only the surface energy but also the associated energy losses. The mechanism by which this strain energy is lost, presumably by the sudden relaxation of small regions of the highly-strained rubber at the tip of the crack when tearing takes place. According to Rivlin and Thomas, tearing is a very localised process. Thus this irreversible energy losses would take place in a region immediately around the tip, and the amount of energy dissipated would then depend on the strain and the physical properties of the rubber there. Also, at the point of tearing, the rubber would approach its limiting strain, which is characteristic of the material. Therefore it seems likely that energy dissipation would be dependent only on the physical properties of the material and not on the overall shape of the test-piece. Tearing energy should therefore provide a true measure of the tear resistance independent of the geometry of the test-piece and the way the forces are applied.

To verify the tearing energy criterion, Rivlin and Thomas evaluated the term $-(\partial W/\partial A)$ in equation 2.2, using NR gum vulcanizate. Rivlin and Thomas defined the term $-(\partial W/\partial A)$ as the tearing energy and denoted by the symbol, T. They first attempted this by computing the elastic stored strain energy, W, from the measured force extension curves on test-pieces of different shapes and sizes containing various cut lengths, c, and estimated $(\partial W/\partial c)$ at the point of tearing from curves of W versus c. They found that the results agreed to within about 30% because of the inherent irreproducibility of the tearing process. In their second approach, they used two test-pieces of different geometries which gave deformations known as a simple extension and a pure shear, as shown in Figure 2.1a and 2.1b respectively. These test-pieces enabled them to calculate the strain energy release rate directly from measured applied forces and strains. In the case of a simple-extension test-piece, commonly known as a ``trouser'' test-piece, its tearing energy is given by

$$T = \frac{2F\lambda}{h} - wU \qquad (2.3)$$

where F is the applied tearing force, λ is the extension ratio in each leg, h is the original thickness in unstrained state, w is the total width of the test-piece, and U is the strain energy density in the legs of the test piece that are in simple extension.

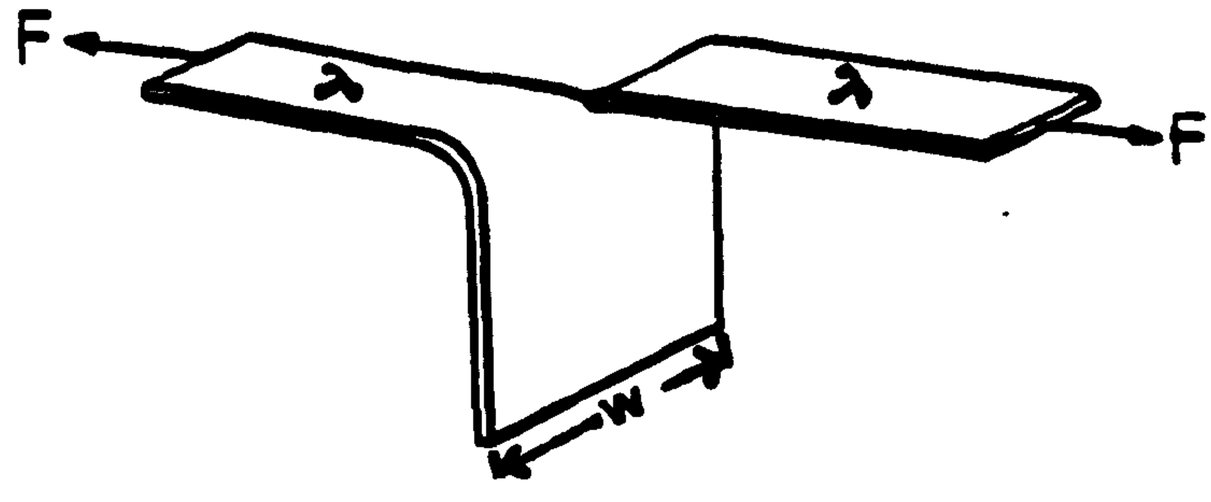

a

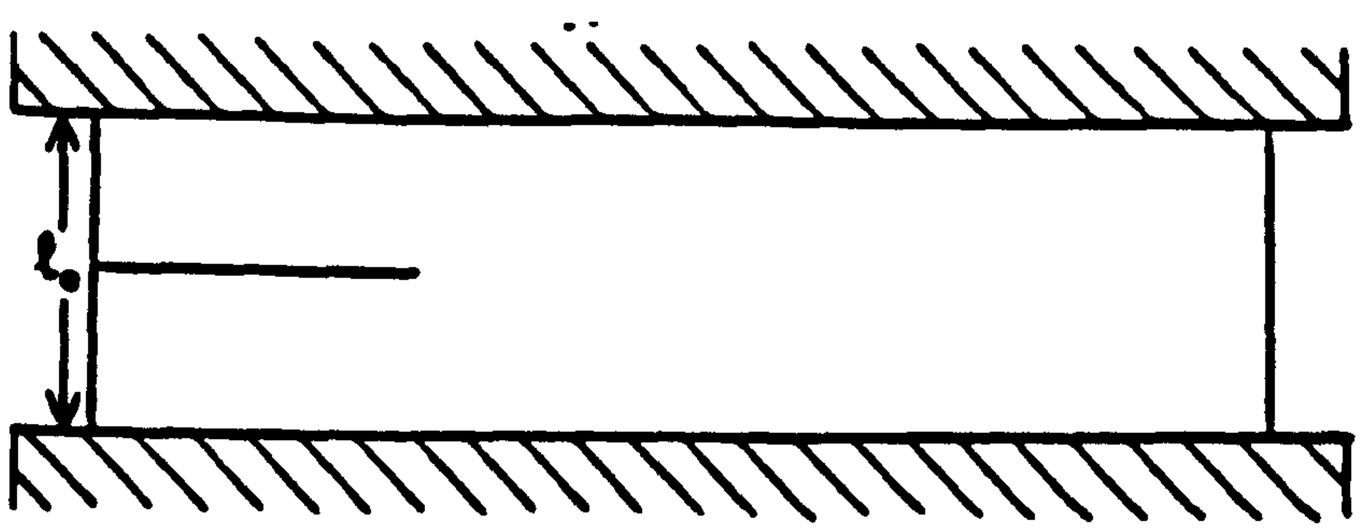

b

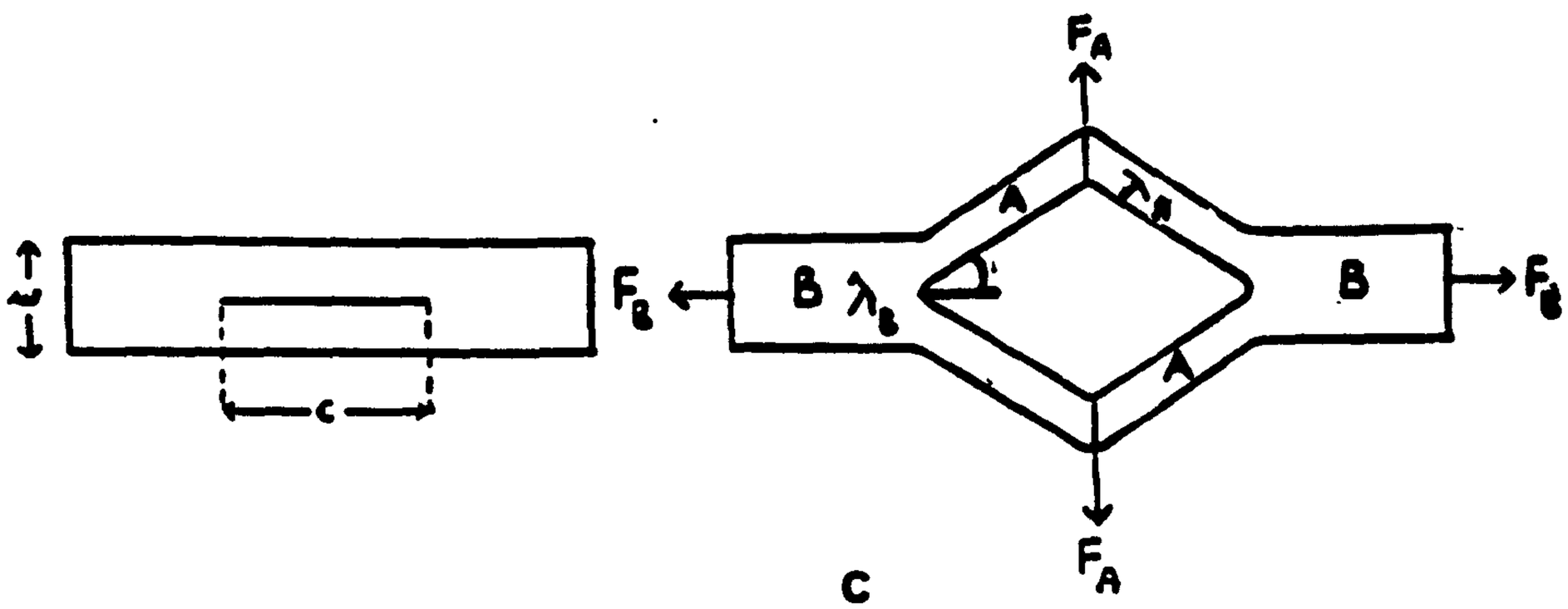

C

d

Figure 2.1: Types of tear test-pieces (a) simple extension (trouser) test-piece (b) pure shear test-piece (c) split test-piece (d) angled test-piece.

A useful approximation is obtained when the legs of the test piece are not extensible, for example, by using wider legs test piece so that $\lambda \cong 1$ and U=0. When this is the case, equation 2.3 reduces to

$$T = \frac{2F}{h} \qquad (2.4)$$

In the case of a pure-shear test-piece, its tearing energy is given by

$$T = Ul_o \qquad (2.5)$$

where U is the strain energy density in that region of the test piece which is in a state of pure shear, and l_o is the distance between the two parallel clamps.

When the results were expressed in terms of tearing energy, similar values were obtained from both types of test-pieces, indicating that tearing energy gives a quantitative measure of a material property. Later investigations by Thomas et al (20,21) using other test-pieces, such as split tear test-piece (Figure 2.1c) and angled test-piece (Figure 2.1d), have confirmed the earlier findings. For the split tear test piece, its tearing energy is given by

$$T = \frac{F_A \lambda_A \sin\phi}{h} + \frac{F_B(\lambda_A \cos\phi - \lambda_B)}{h} - w(U_A - U_B) \qquad (2\cdot6)$$

where λ_A, λ_B and U_A, U_B are the extension ratios and stored energy densities in regions A and B respectively, $\tan\phi = F_A/F_B$, and w is the width. In the case of the angled test-piece, its tearing energy is given by the relation

$$T = \frac{2F}{h} \sin\alpha \qquad (2.7)$$

where h, F and c have the same meaning as in equation 2.3 and α is the is the angle between the clamps.

Figure 2.2 shows that the three test-pieces of widely differring geometries all giving similar relationships between tearing energy and tearing rate, thus confirming that tearing energy gives a true quantitative measure of tear resistance. The magnitude

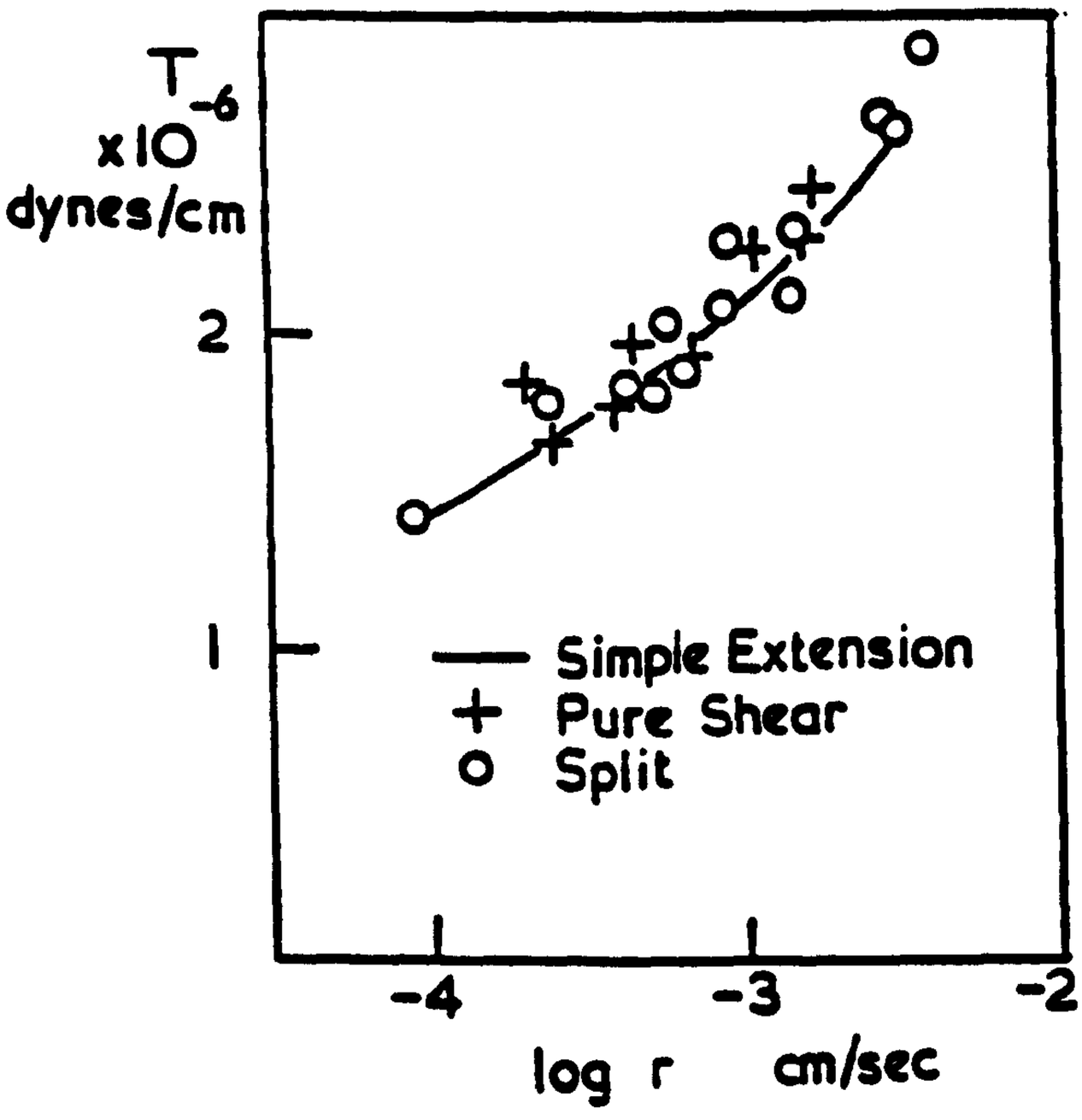

Tear results for a gum SBR rubber obtained on the three test pieces shown in Fig. 2·1

Figure 2.2: Tearing energy vs tear rate.

of the tearing energies they obtained ranged from 1.0 kJ m^{-2} to 100 kJ m^{-2}. These values exceed substantially the surface energy, which is about 0.1 kJ m^{-2} for many materials. This clearly implies that energy losses or hysteresis play a major contribution in the tearing process of a vulcanized rubber, and probably may be the major factor in determining its strength.

2.3 Relationship between tearing energy and tear tip diameter

Thomas (22) made furthur progress by relating the tearing energy to the strain distribution around the tip of a crack. Based on a semi-circular crack tip model for a vulcanized rubber, he showed that the tearing energy, T, is approximately related to the diameter of a crack tip, d, by the relationship below

$$T = dU \qquad (2.8)$$

where U is the elastically stored energy per unit volume of rubber. If a test-piece is taken to break, the relationship becomes

$$T = dU_b \qquad (2.9)$$

where U_b denotes the work to break per unit volume of rubber. Thomas verified this relationship experimentally by measuring the tearing energy of test-pieces having model tips of diameter in the range of 1 mm to 3 mm. He found that the ratio T/d was substantially constant. Furthermore, it agreed well with the work to break in tensile-tests carried out independently on different vulcanizates of various strengths.

Later, Greensmith (23) followed up this work more extensively by using both unfilled and black-filled SBR vulcanizates. The rates of extension of the rubber at the tip of an incision, and in stress-strain measurements were made approximately the same by making the measurement at similar time to break. This is given by the relationship

$$r = Asd \qquad (2.10)$$

where A is a dimensionless constant (A = 0.75), s is the average

rate of extension for the rubber approaching the tip of the tear, and r is the rate of crack propagation. In this way, he was able to compare U_b from tensile and tear measurement done independently. The results were expressed by plotting T/d and U_b against the reciprocal of the time to break, t, as shown in Figure 2.3a and 2.3b for unfilled and black-filled vulcanizates respectively. In both cases, T/d and U_b were comparable in magnitude and showed a similar dependence on time, t. The U_b values, however, were consistently lower than T/d by about 30%, which Thomas (22) attributed in part to the imperfect elasticity of the material which was not allowed for in the theory leading to equation 2.8, and in part to the considerable difference in effective size of the test piece in the two types of measurement. In the case of the tensile test-piece, its length is of the order of a centimeter, whereas, in the tear measurement with a tip diameter of 2 mm, the breaking point is confined to a region of a fraction of a millimeter in size. This reduction in size may increase the apparent tensile strength appreciably because it is less likely to be affected by flaws there than it is in the tensile test-piece. It is interesting to note that, when equation 2.9 was applied to tear tests where the tip was formed naturally by tearing, use of the same value of the work to break indicated a tip diameter of the order of 0.2 mm. The size of the irregularities on the torn surface was observed to be of the same order of magnitude. In the case of black-filled rubbers that failed in a knotty manner, the tip diameter is of the order of 2 mm consistent with the average size of the knot formed (16). This suggests that, in carbon-black-filled rubbers, the enhancement in tear strength is associated with the increase in tear tip diameter, d, rather than with increase of the work to break, U_b.

2.4 Threshold tearing energy theory of Lake and Thomas

Although equation 2.8 is only an approximate relationship, it has been applied successfully to account not only for macroscopic tearing process, but also for microscopic tearing. Lake and Thomas (24), used that relationship to predict the threshold tearing energy, T_o. Lake and Thomas, defined T_o as the minimum tearing energy at which mechanical crack growth can occur. At tearing energies less than T_o crack growth is attributable solely to

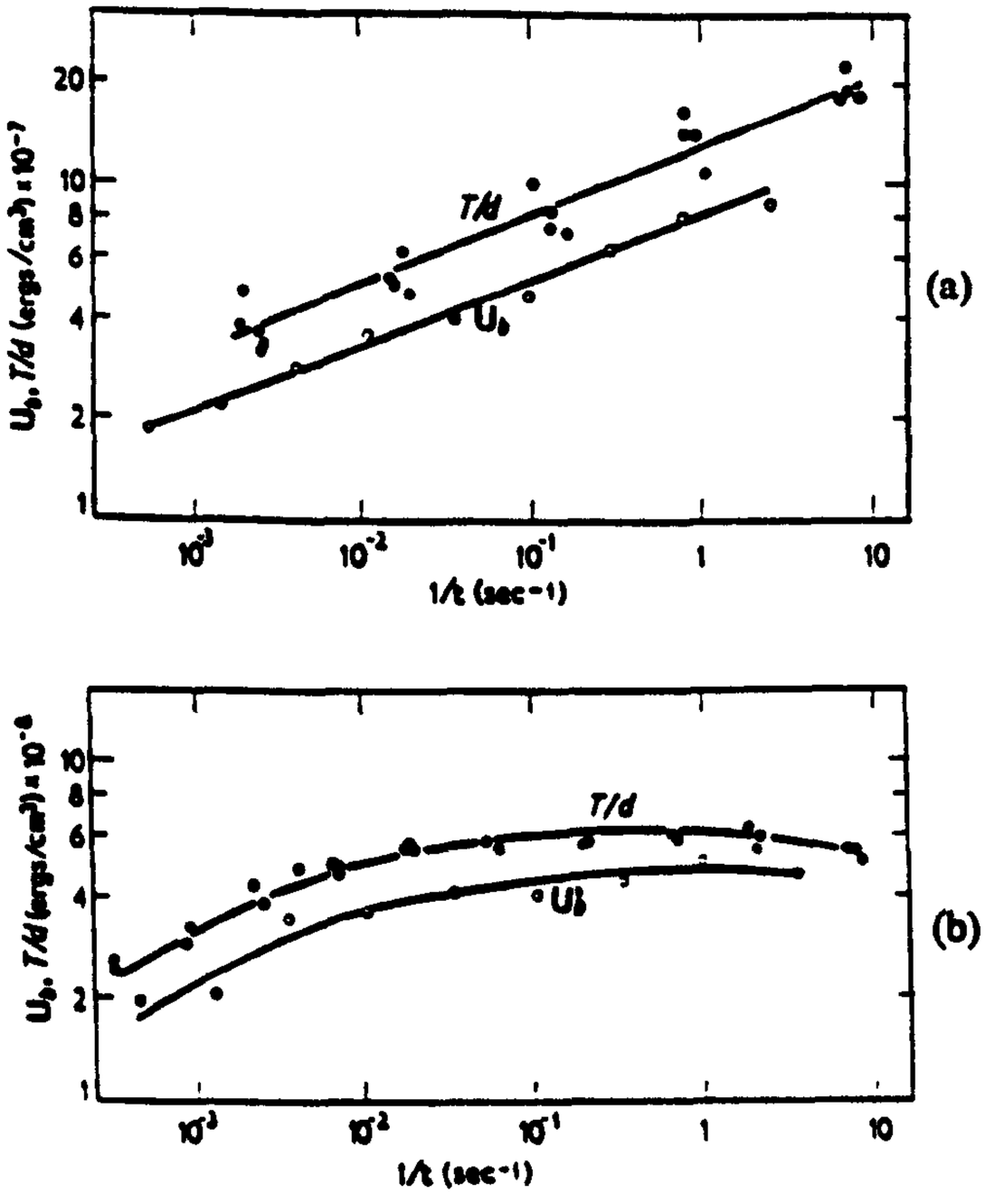

Comparison of U_b *vs.* $1/t$ and T/d *vs.* $1/t$ for (a) pure gum SBR vulcanizate, (b) SBR vulcanizate containing SRF black. *J. Appl. Polym. Sci.*, 1960, 3, 186, Fig. 3, and 187, Fig. 4, respectively

Figure 2.3: Comparison of strain energy density from tensile and tear measurements

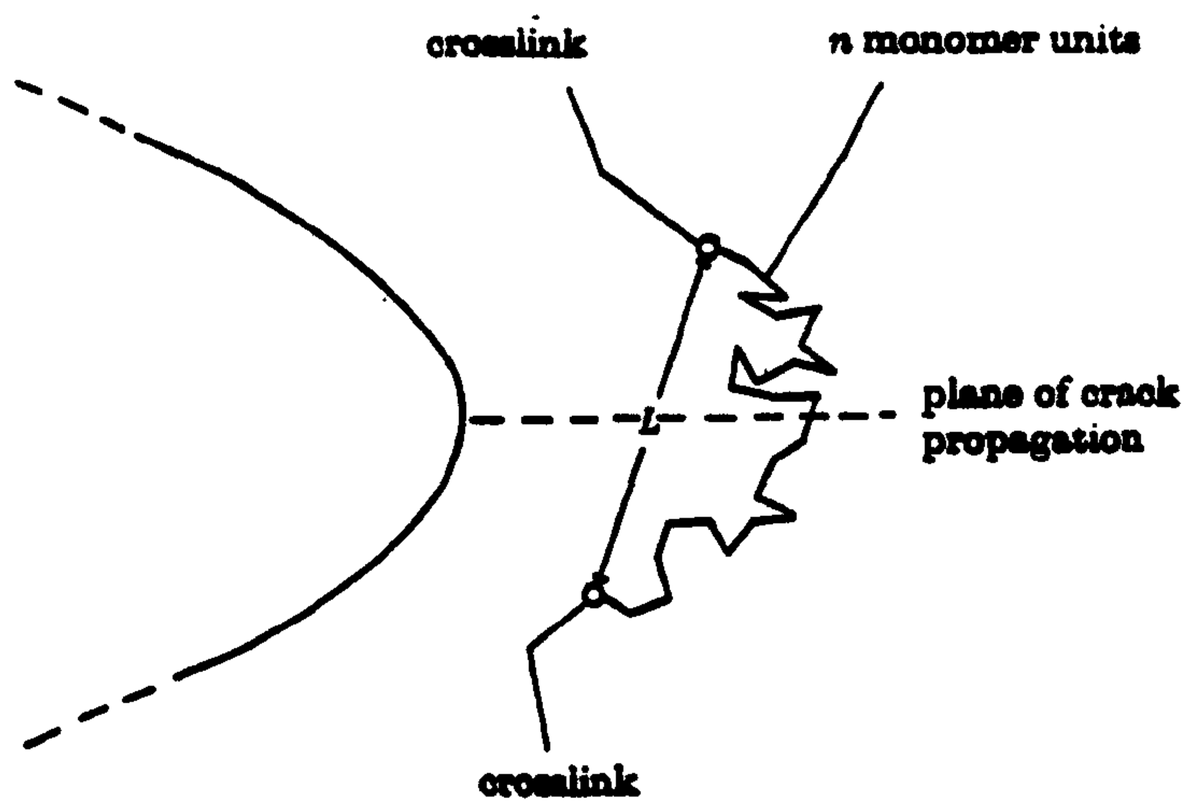

Schematic diagram showing a polymer chain lying across the plane of crack propagation.

Figure 2.4: Schematic diagram showing a model of a crack

chemical attack by ozone, and is normally very much slower than T_o (25). All rubbers whose molecular backbones contain carbon-carbon double bonds are susceptible to ozone attack and cause cracking. Since ozone crack growth is chemical in origin, thus the rate of growth is independent of tearing energy. Lake and Thomas (24) found that the magnitude of T_o was more-or-less similar for a wide range of elastomers, including both crystallizing and non-crystallizing rubbers which differ widely in other strength properties such as tensile strength and tear strength. The magnitude of T_o for a range of polymers is about 0.05 kJ m^{-2}, suggesting that it may be related fairly directly to the strengths of the chemical bonds of the molecules which comprise the material. Lake and Thomas calculated T_o from the molecular structure of a rubber and the strength of primary chemical bonds. Figure 2.4 shows a schematic diagram of molecular chains lying across the fracture plane. In the theory for T_o, Lake and Thomas assumed that d has the minimum possible value (d_o) for an elastomer while U has the maximum possible value of (U_o) determined by the bond strength. Thus, on a molecular scale equation 2.8 becomes

$$T_o = U_o d_o \qquad (2.11)$$

where d_o is the diameter of the tear tip and U_o is the strain energy density at the tip. U_o is given by

$$U_o = \varepsilon N n \qquad (2.12)$$

where ε is the maximum energy which can be stored in each monomer unit and N is the number of chains per unit volume of rubber which contain on average n monomer units per chain. The tear-tip diameter, d_o, is interpreted as the smallest and sharpest possible. However, in the case of a rubber, because of its structure it cannot be of atomic dimensions, but must be of the order of the distance between adjacent crosslinks in the unstrained state. According to the statistical theory of rubber elasticity (26), this distance is given by

$$d_o = \xi l n^{1/2} \qquad (2.13)$$

where ξ is a factor determined by the freedom of rotation about

bonds in the chain and l is the length of a monomer unit. Substituting U_o and d_o into equation 2.11, gives

$$T_o = \xi l \varepsilon N n^{3/2} \qquad (2.14)$$

The value of T_o estimated from this theory is about 25 J m^{-2}, whereas the value obtained experimentally is about 50 J m^{-2}, i.e., higher by a factor of 2. In view of the uncertainties in the approximations and assumptions of the theory, the agreement between theory and experiment is regarded remarkably good. To determine T_o experimentally, the tear measurements have to be carried out using swollen vulcanizates at slow rate of tearing and at high temperature to eliminate hysteresis. This is known as the threshold conditions (27).

The effect of carbon black on T_o has been studied by Bhoumick, Gent and Pulford (27). To attain threshold conditions they used pre-scored ``trouser'' tear test-pieces swollen with paraffin oil, and carried out the tearing at high temperatures (80°C - 150°C) and slow tear rate (less than 1 mm/min.). The value of T_o was found to be around 200 J m^{-2}, which indicates that, the minimum tearing energy (T_o) for mechanical crack growth in black-filled rubbers rubbers is about three to four times higher than the unfilled rubbers. Bhoumick, Gent and Pulford (27) attributed the increase in T_o to detachment of adhering polymer molecules from particles of carbon black at forces somewhat below those which cause main-chain fracture.

The uniqueness of the above theory is that, just like Griffith's theory, it relates fracture to molecular parameters. Indeed, T_o would be the surface energy (2S), if intermolecular separation only was involved. However, this is not the case, since in order to break a bond crossing the fracture plane, it is necessary to take many other bonds in the same chain between crosslinks up to essentially the breaking point. Thus the energy required is correspondingly magnified. A rather intriguing question may arise as to why failure does not occur in bulk when T_o is reached? The answer might be associated with the irreversible dissipation of energy as the crack grows when T_o is exceeded. When the crack begins to propagate, there is retraction of the rubber in the vicinity of the crack which gives rise to mechanical

hysteresis. This reduces the stress concentration at the tip, and no furthur growth occurs until either the stress is increased or it is removed and re-applied.

Andrews (28) has provided a generalised theory of fracture of solid materials involving T_o and mechanical hysteresis. This proposes the general relationship

$$T = T_o\gamma(v,\theta,e) \qquad (2.15)$$

where γ is a loss function whose value depends on the material, the crack velocity, v, the temperature, θ, and the overall state of strain, e, in the body. For a perfectly elastic body, γ reduces to unity and T_o becomes the surface energy, 2S.

2.5 Types of tear failure

There are basically two types of tear failure which may affect the magnitude of the tearing energy of a particular vulcanizate. These have been classified qualitatively as steady and stick-slip tearing respectively (29). Steady tearing is controlled by a basic tear process which is predominantly viscoelastic in nature. In this case, the tearing energy increases continuously with the rate of crack propagation. Stick-slip tearing is a secondary tear process where the tearing energy increases as the tear rate decreases. This is attributed to the development of strengthening structures, for example, crystallization and strength anisotropy induced by carbon black at the tip of a tear. According to Greensmith (16,29), both crystallization and strength anisotropy induced by carbon black require an appreciable time to form.

The most convenient way to distinguish between the two types of tear process is to do tear measurements at a constant rate separation using a trouser test-piece. The fluctuations of tearing force with rate will reflect the nature of tear process. Typical tearing force-time curves for this type of tear measurement are illustrated in Figure 2.5. In the case of steady tearing, the tearing force and rate of propagation remain essentially constant

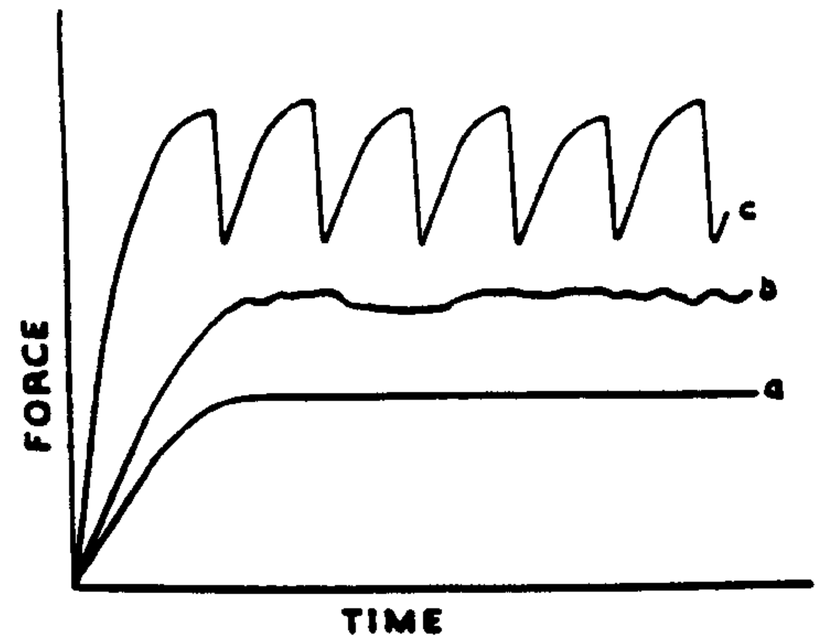

Figure 2.5: Schematic tearing force–time curves for constant rate of extension of the test-piece: (a) and (b) steady tearing; (c) stick-slip tearing.

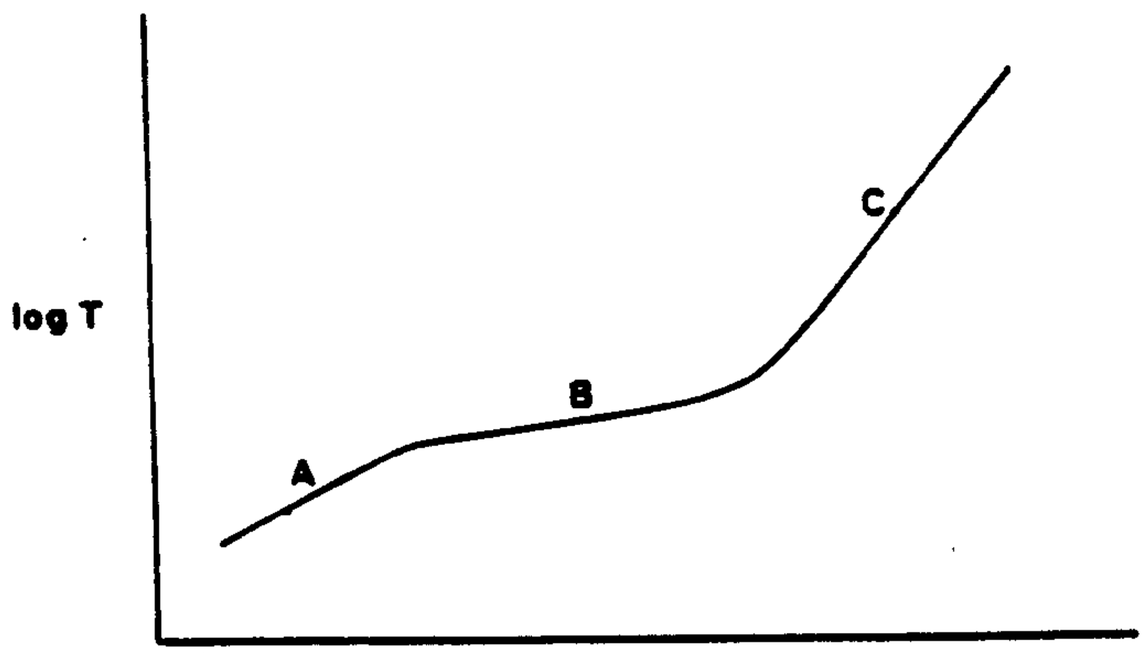

a) Schematic T against rate diagram. A. rough tearing: B. stick-slip tearing: C. smooth tearing.

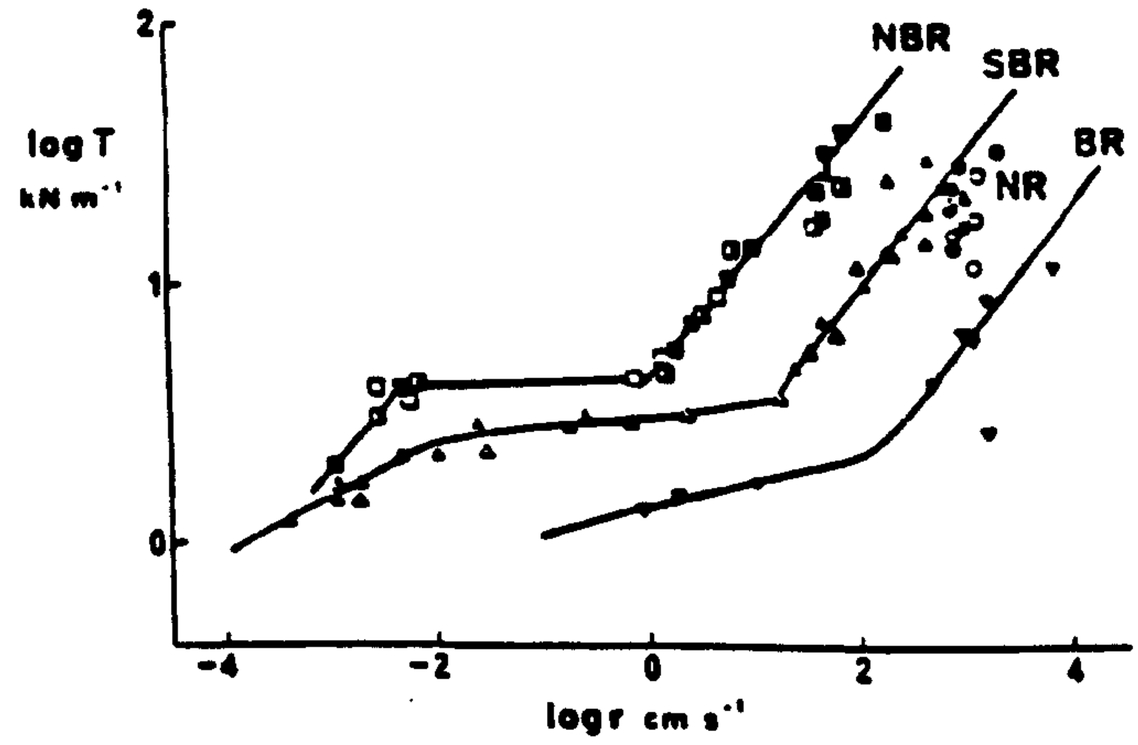

b) Tearing energy against rate relations for NBR. □. □. ■: SBR. △. △. ▲: NR. ○. ○. ●: BR. ▽. ▽. ▼. The l_0 values are 2.0. 3.0. 4.0 cm. respectively.

Figure 2.6: Regimes of tearing

apart from random fluctuations, once tearing has commenced. Curve (a) denotes small fluctuations of tearing force with rates and curve (b) denotes marked fluctuations of tearing force with rates. The appearance of the torn surface depends on the degree of fluctuation which in a way reflect the nature of the tearing process. If the fluctuations are relatively small, a smooth torn surfaces are produced. Otherwise rough and irregular torn surfaces are produced. In the case of stick-slip tearing, a tear does not propagate continuously but rather arrests and reinitiates at fairly regular intervals. This would result in a more pronounced fluctuations of the tearing force with the rate of propagation (curve c). The torn surface appears to have both smooth and rough regions. The rough surface corresponds to the stick period (tear arrests) where the force is building up, and the smooth surface corresponds to tear moving (tear initiates).

2.6 Effect of tear rates on tear failure

Kadir and Thomas have carried out some work on the crack propagation of unfilled elastomers over a very wide range of tear rates (30). The rates from 10^{-7} m s^{-1} to some 50 m s^{-1} were covered using pure-shear test-pieces. Three regimes of tearing were identified, viz, rough, stick-slip and smooth tearing as shown in Figures 2.6 a and 2.6b.

2.6.1 Rough tearing

Rough tearing occurs at the lower range of tearing rates from about 1 μm s^{-1} to about 100 μm s^{-1}. The fractured surfaces appear to be very rough, the scale of roughness being of the order a few tenths of a millimeter. The degree of roughness tends to decrease with increasing rates. It has been suggested that the mechanisms responsible for rough tearing are associated with cavitation of the tensile hydrostatic component of the stress field ahead of the tip of the tear. The stress necessary to produce this cavitation is of the order of the Young's modulus of the material (about 10^6 N m^{-2} for gum NR). The local tensile stress developed just ahead of the crack must be very high in order to break

primary chemical bonds, and should be more than adequate to cause such cavitation.

2.6.2 Stick-slip tearing

Stick-slip tearing occurs at tearing energies and rates between rough and smooth tearing regions. The variations in the instantaneous rates was reported to be very large. Stick-slip tearing has been attributed to structural changes at the tip of the tear. There is also a suggestion that it could be due to a frozen stress field around the tip of the tear which results in the tear propagating in the direction of decreasing stress (28).

2.6.3 Smooth tearing

Smooth tearing occurs at very high tear rates above 10 m s^{-1}. The rate of extension ahead of the tip of the crack at this rate is extremely high, and the material approaches its glassy state and becomes stiffer. Thus at such high tear rate, rupture of the chain occurs first before cavitation can take place. In the absence of cavitation, the fractured surface thus appears very smooth. It is interesting to note that in this region the tear strength follows the ranking order of the glass-transition temperature of the material. The fact that the tear strength of NR is intermediate between SBR and butadiene rubbers suggests that it cannot strain crystallize at this high tear rate (about 10 m s^{-1}). This indicates that crystallization requires a finite time to form.

2.6.4 Knotty tearing

In knotty tearing, like stick-slip tearing the crack does not propagate continuously, but tends to deviate sideways, perhaps, at right angles to its intended tear path. It has been suggested that the mechanisms responsible for these tear deviations, and hence for knotty tearing, are associated with the development of strengthening structures due to local strength anisotropy at the tip of the tear (15,16). Apart from this strength anisotropy, the properties of the tear zone also play a major influence on tip blunting. As pointed out by Lake and Yeoh (31), the existence of the relatively weak zones between latex particles might be responsible for the tear

deviations and hence knotty tearing observed in films dried down from sulphur-prevulcanized natural rubber latex.

The range of tear rates over which knotty tearing can occur depends upon the types of rubber and the size of filler particles. Natural rubber which crystallizes on straining gives a wider range of tear rates and temperatures of knotty tearing regions than does SBR which does not strain-crystallize, as is shown in Figures 2.7a and 2.7b respectively. Thus crystallization enhances further the strengthening structure so that the net effect is much greater than that given by carbon black alone. The results also indicate that fine black particles are more effective in inducing strength anisotropy for the occurrence of knotty tearing than are large black particles.

2.7 Dependence of tearing energy on rate and temperature

Tearing energy is not a constant quantity. Its magnitude depends both on the rate and the temperature of tear measurement. The effects are best described by 3-dimensional plots of tearing energy versus tear rate and temperature (32), as shown in Figures 2.8 a, b and c, for unfilled SBR and NR and black-filled SBR respectively. In the case of unfilled SBR, the tearing energy increases either when tear rate increases or temperature decreases, i.e., the conditions where viscoelastic energy dissipation are high. In the case of a strain-crystallizing rubber like NR, the dependence of tearing energy on rate and temperature becomes less marked. This could be associated with the crystallization, which outweighs the dependence of the viscous component on rate and temperature of tearing. The high tearing energy displayed by NR over a relatively wide range of temperature and rate could be associated with the high energy losses which appear as heat of crystallization.

Figure 2.8c shows the effect of loading carbon black particles into SBR. The flat plateau surface shown in Figure 2.8c represents knotty tearing regions where there is a marked increase in the tearing energy. Outside this range, where knotty tearing does not operate, carbon black produces a relatively small increase in strength. This suggests that the development of knotty tearing is

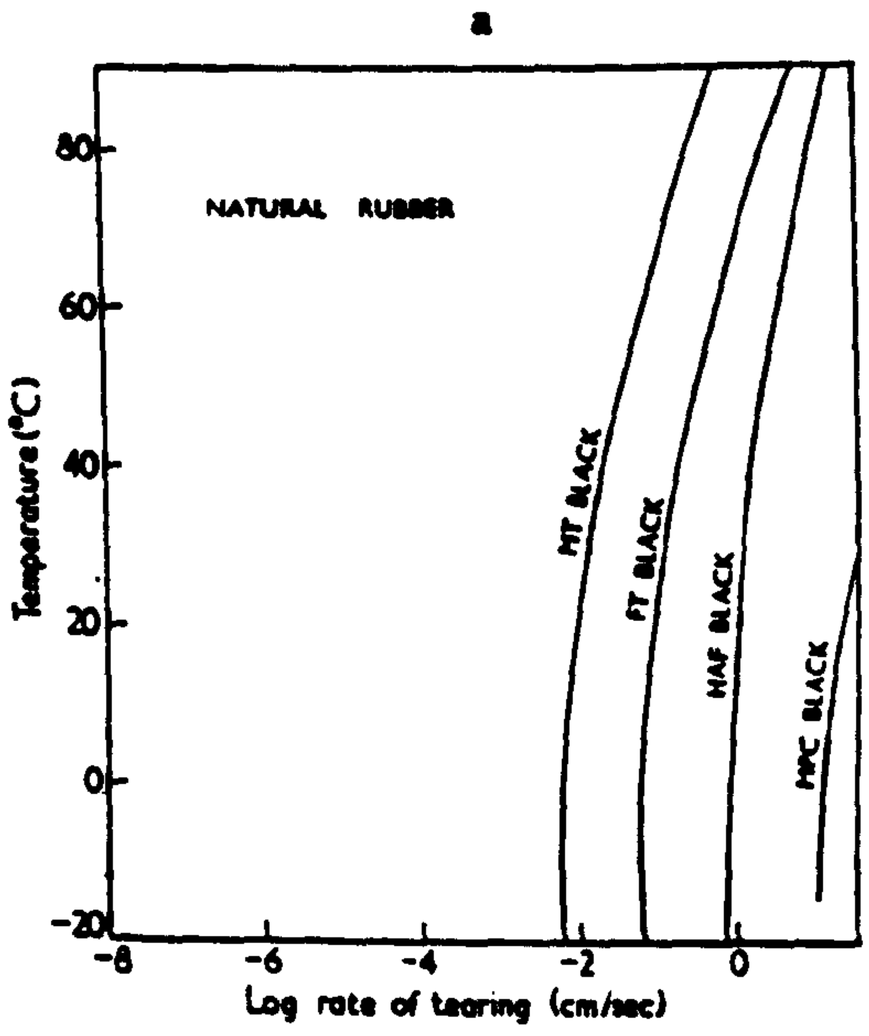

Regions of knotty tearing for NR containing various blacks. The regions lie to the left of the appropriate curves. *J. Polym. Sci.*, 1956, 21, 186, Fig. 4b

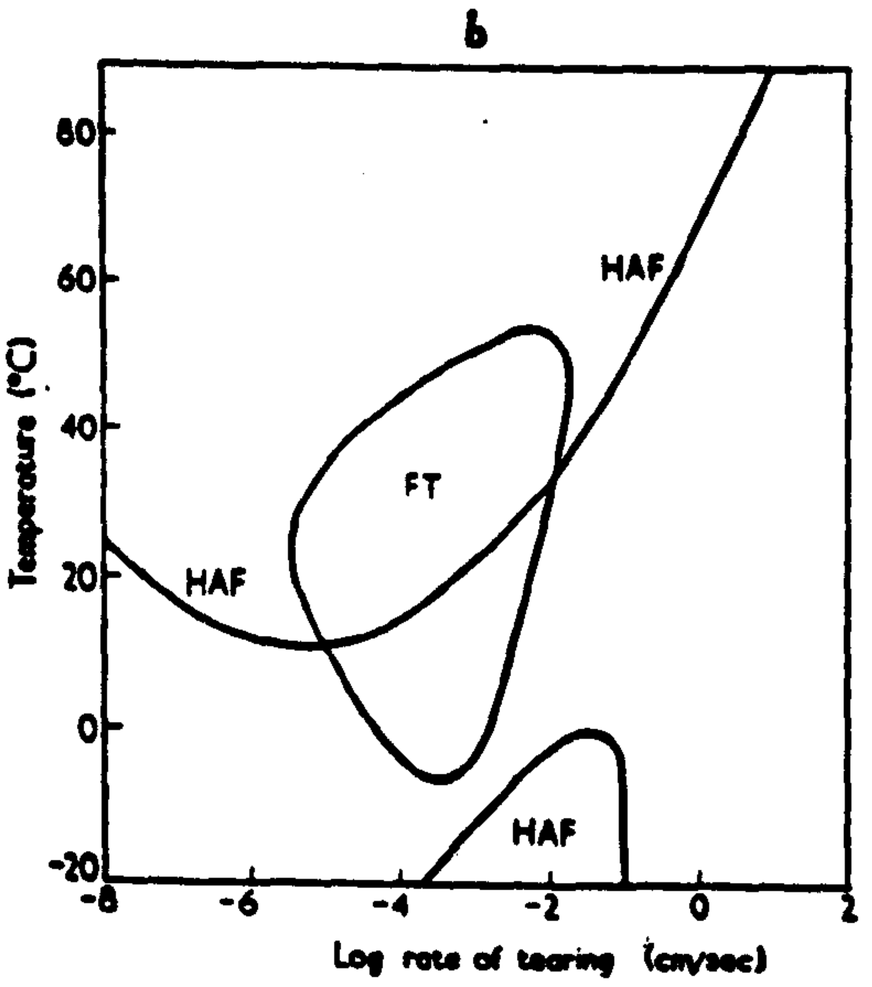

Regions of knotty tearing for SBR containing various blacks.
J. Polym. Sci., 1956, 21, 186, Fig. 4a

Figure 2.7: Regions of knotty tearing as a function of tear rate, temperature and types of carbon black

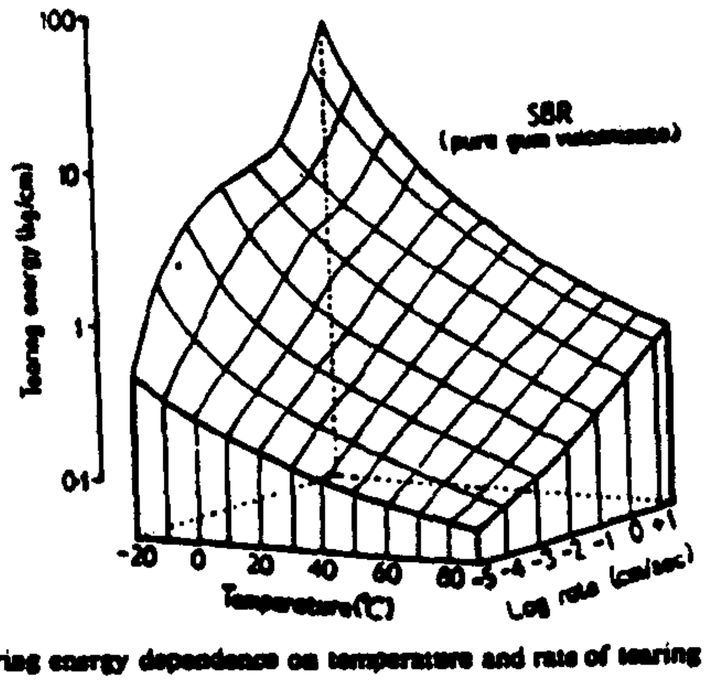

a) Tearing energy dependence on temperature and rate of tearing for gum SBR

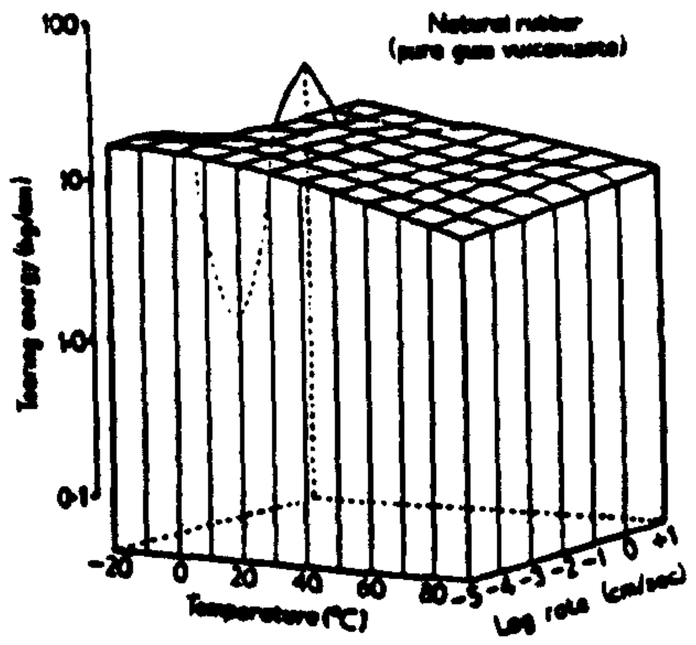

b) Tearing energy dependence on temperature and rate of tearing for gum NR

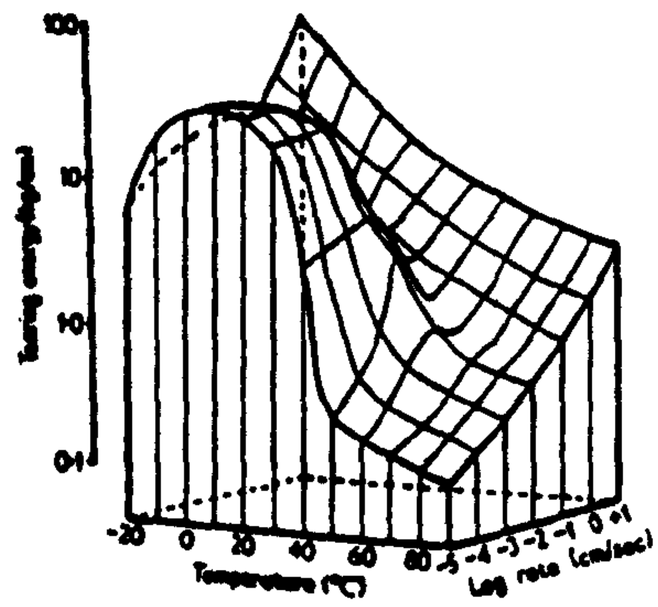

c) Tearing energy surface for SBR vulcanizate containing FT black.
Trans. Soc. Rheol., 1960, 4, 184, Fig. 5

Figure 2.8: Effects of tear rates and temperatures on tearing energy

also rate-dependent, implying that a finite time is required for the strength anisotropy to form at the crack tip.

2.7.1 Time-temperature superposition principle

In the absence of crystallization or any filler particles, the mechanical energy loss (hysteresis) is predominantly associated with viscoelastic effects. The amount of energy dissipation is controlled by the internal viscosity of the material. Under these conditions, the material should display the law of corresponding states, better known as the time-temperature superposition principle. This relates the time or rate of deformation to the temperature of deformation. It is the case that measurements at high frequencies (short response times) are equivalent to measurements at low temperatures, and that measurements at low frequencies (long response times) are equivalent to measurements at high temperatures. This is a matter of some practical importance since it is not normally convenient to measure very short or very long response times. This difficulty can be avoided by doing measurements at several temperatures. Williams, Landel and Ferry (33) who investigated the variation of viscosity with temperature for glass-forming liquids, developed an equation that can be used to explain the temperature dependence of viscosity and other rate processes in glass-forming liquids. This well-known equation is known as the WLF equation, and is given by

$$\log a_\theta = \frac{-C_1(\theta - \theta_s)}{C_2 + \theta - \theta_s} \qquad (2.16)$$

where θ_s is the reference temperature, usually taken as θ_g+50^{0}C, θ is the temperature of measurement, θ_g is the glass-transition temperature of the material, and a_θ is the shift-factor. Williams et al (33) claimed that they could obtain the universal constants for glass forming liquids, if the glass-transition temperature was chosen as the reference temperature, with C_1 = 40 and C_2 = 52. However, these constants (40 and 52) are not absolutely universals, discrepancies do arise if the temperature of measurements is raised too far from the glass-transition temperature (34). Thus, glass-forming liquids obey WLF equation within the range $\theta_g < \theta < \theta_g$+120°C.

Mullins (35) found that the WLF equation could be used to explain the dependence of tearing energy of the amorphous rubber on rates and temperatures of deformation. Using tearing energy results for unfilled SBR of Greensmith and Thomas (32), Mullins (35) found that they were amenable to the WLF transformation. A single mastercurve was found to represent data covering a wide range of rates and temperatures of deformation, as is shown in Figure 2.9a. Kadir and Thomas (30) have also shown that data for tearing energy in the smooth regions are also amenable to the WLF transformation, as is shown in Figure 2.9b. However, Kadir and Thomas found that it was possible to obtain a master curve only by taking θ_s as $\theta_g + 20^0$C. This was necessary to take account of depression of the glass-transition temperature of the material ahead of the crack by about 30^0C. This occurs because of the hydrostatic component arising in the material due to the high tensile stresses, perhaps around the tip approaching the breaking strain. The WLF equation is only applicable to steady tearing only (35).

2.8 Dependence of strength on type of crosslink

In a vulcanized rubber, the crosslinks are also part of the structure. It is well-known that, if a rubber is vulcanized to the same crosslink concentration by different vulcanizing systems, the resultant vulcanizates may have widely differing strength properties like tensile strength, cut growth and tear resistance. This arises because different types of vulcanization system produce different types of crosslink. For example, in natural rubber, there are three types of sulphur-vulcanizing system. The first is called the conventional vulcanizing system which produces predominantly polysulphidic crosslinks. The second is called the efficient vulcanizing (EV) system which produces mainly mono-sulphidic crosslinks. The third is called a semi-EV vulcanizing system which is a compromise between the two systems. The word ``efficient'' acknowledges the efficiency of the sulphur atoms to form useful crosslinks. The fewer the sulphur atoms in a given crosslink, the more efficient is the system said to be. The types of crosslink produced depend upon the exact conditions of vulcanization, i.e., the ratio of sulphur and accelerator used, the temperature and period of vulcanization. Table 2.1 provides general guidance concerning the relative proportions of sulphur and accelerator for

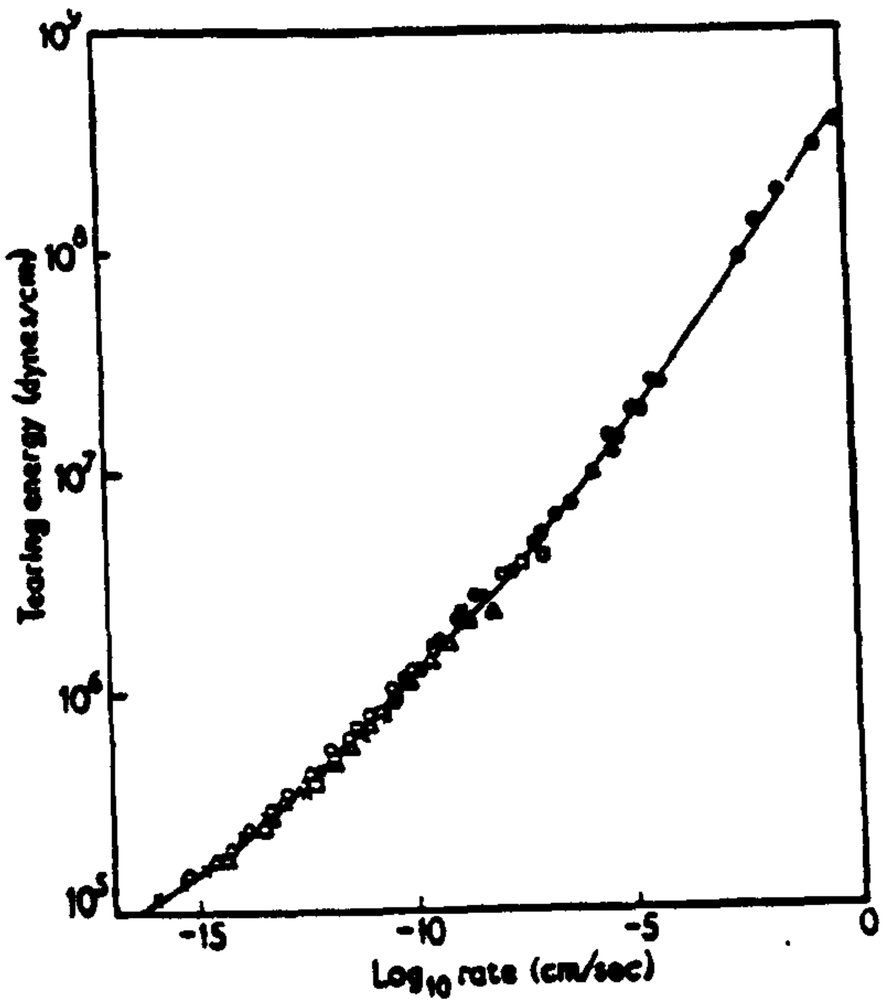

a) Tearing energy as a function of reduced rate of tearing for SBR gum vulcanizate. *Trans. IRI*, 1959, 35, 216, Fig. 3

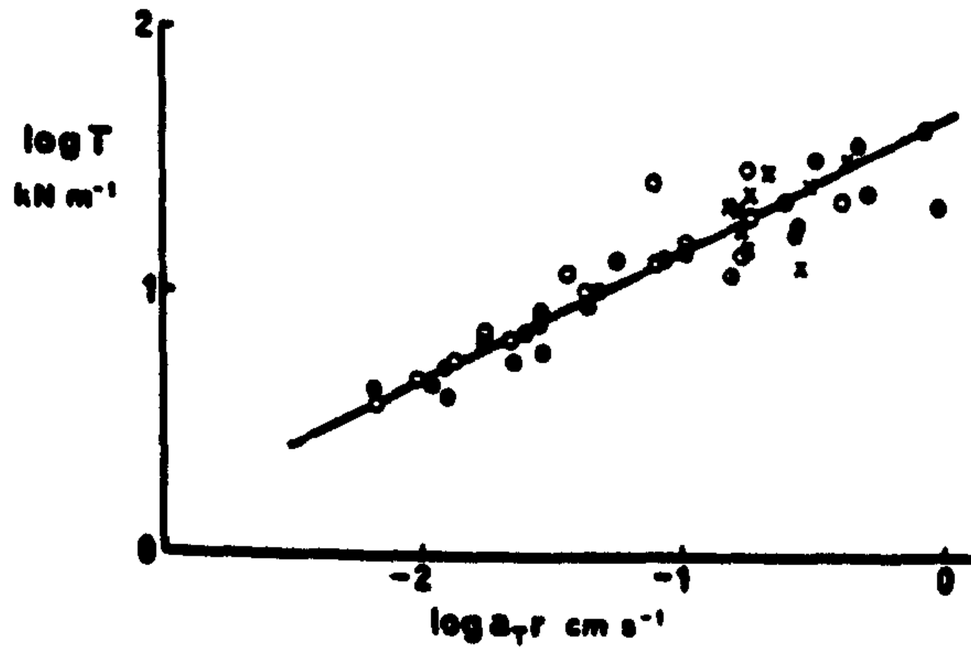

b) Composite curve for smooth tearing. ● NBR. ○ SBR. × NR ◑ BR. The shift factor a_T is given in the text.

Figure 2.9: Tearing energy mastercurve in steady and smooth tearing regions

the three sulphur vulcanizing systems employed in NR (36). Table 2.2 shows the relative proportions (percentage) of the types of crosslink present in vulcanizates given by the three systems. Besides elemental sulphur, organic peroxide and urethane reagent (36) are two alternative vulcanizing systems. Organic peroxides, such as dicumyl peroxide, forms carbon-carbon crosslinks, whereas, urethane reagents forms crosslinks which are essentially of the urea type (36). Both these systems produce crosslinks which are more thermally stable than are sulphur crosslinks. In particular, polysulphidic crosslinks have the least thermal stability.

The effect of type of crosslink on tensile strength of unfilled NR vulcanizates is well documented (37). The tensile strengths of vulcanizates are ranked in the inverse order to the bond energies of the crosslinks (37). Weak crosslinks such as the polysulphidic type usually give higher tensile strength than do stable crosslinks such as the mono-sulphidic type, because of their ability to relieve local stress through 'yielding', thereby permitting a more uniform distribution of stress. This hypothesis has been supported by an independent investigation into the breaking and reforming of crosslinks during stressing (38). Here, the permanent set provides an indication of the number of bonds which have recombined whilst in the deformed state, and changes in equilibrium volume swelling indicate the fraction of crosslinks which break. Figure 2.10 shows the dependence during stressing of the fraction of crosslinks broken, n_1/N, and the recombination efficiency n_2/n_1, where N is the initial number of chains per unit volume, and n_1 and n_2 are the number of chains which break and reform respectively. The results show that for weak and labile crosslinks (polysulphidic type), the permanent set and the changes in the equilibrium volume fraction of rubber in swollen vulcanizate, υ_r, (shown in Figures 2.11 and 2.12 respectively) increase as the applied stress increases. The recombination efficiency after stressing was always below 100% indicating that there was no gain in the concentration of crosslinks. According to Thomas (38) the observed increase in υ_r after stressing therefore was not associated with increase in crosslink concentration but was a consequence of a two-network present in the vulcanizates. The set observed after stressing clearly indicates the existence of a two-network present in the vulcanizates. In the case of carbon-carbon crosslinks, the set was

Table 2.1: Relative proportions of sulphur and accelerator in sulphur-curing systems for natural rubber.

Curing systems	Sulphur	Accelerator
Conventional	2.0 - 3.5	0.4 - 1.0
Semi-EV	1.0 - 1.7	1.6 - 2.5
EV	0.3 - 0.8	2.5 - 6.0

Table 2.2: Relative proportions of types of crosslinks present in vulcanizates given by the three vulcanizing systems at optimum cure.

	Conventional	Semi-EV	EV	Peroxide
Poly (-S-S_3-S-) and disulphidic (-S-S-)	95%	50%	20%	-
Monosulphidic	5%	50%	80%	-
Carbon-carbon	-	-	-	100%

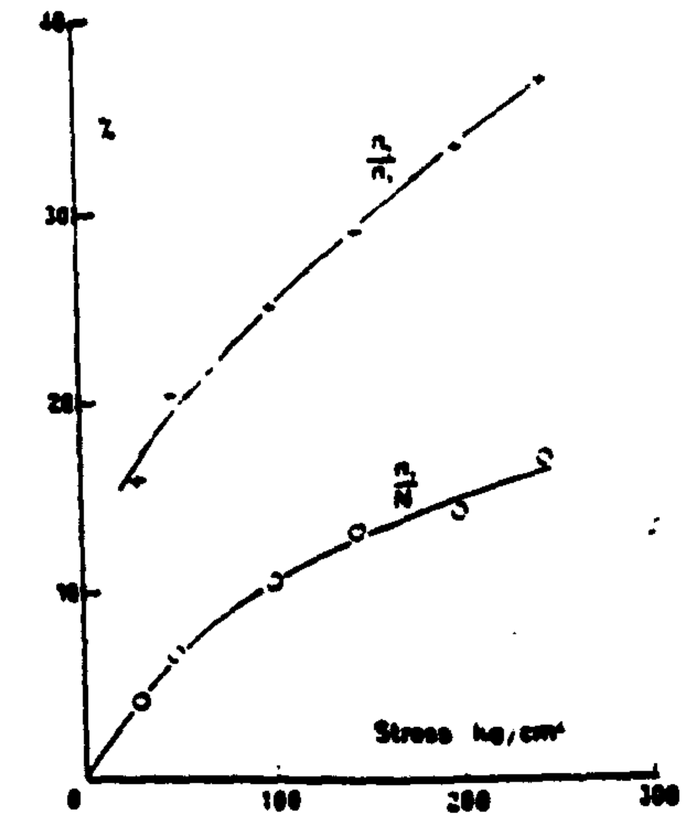

Dependence of the fraction of crosslinks broken and recombination efficiency on the applied stress.

Figure 2.10: Network breakdown and reformation on stressing

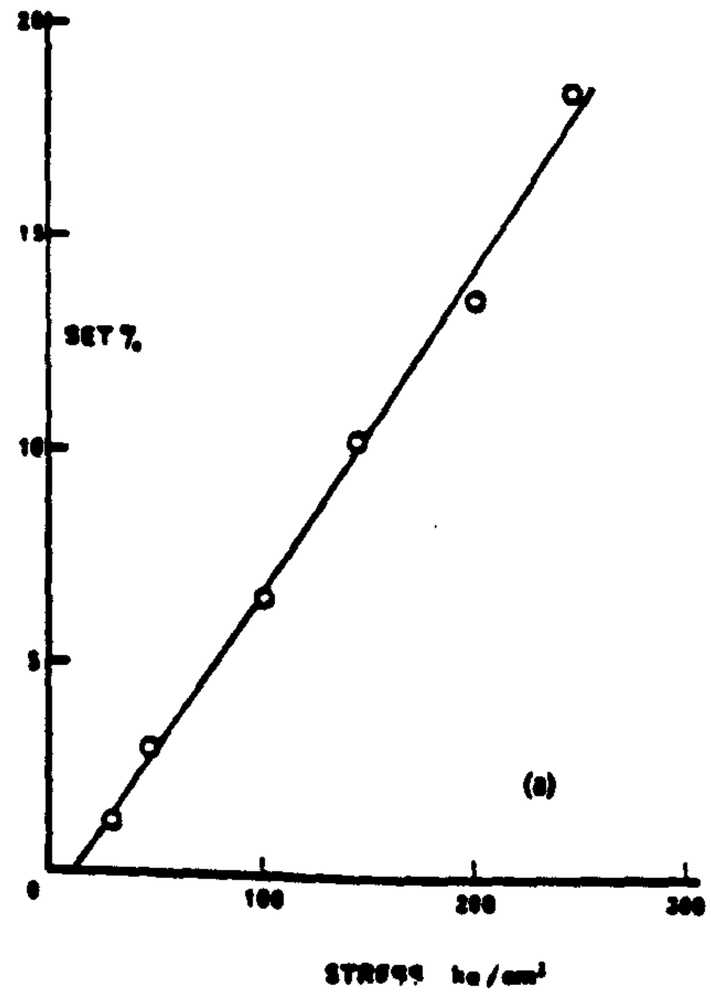

Figure 2.11: Changes in set with stressing

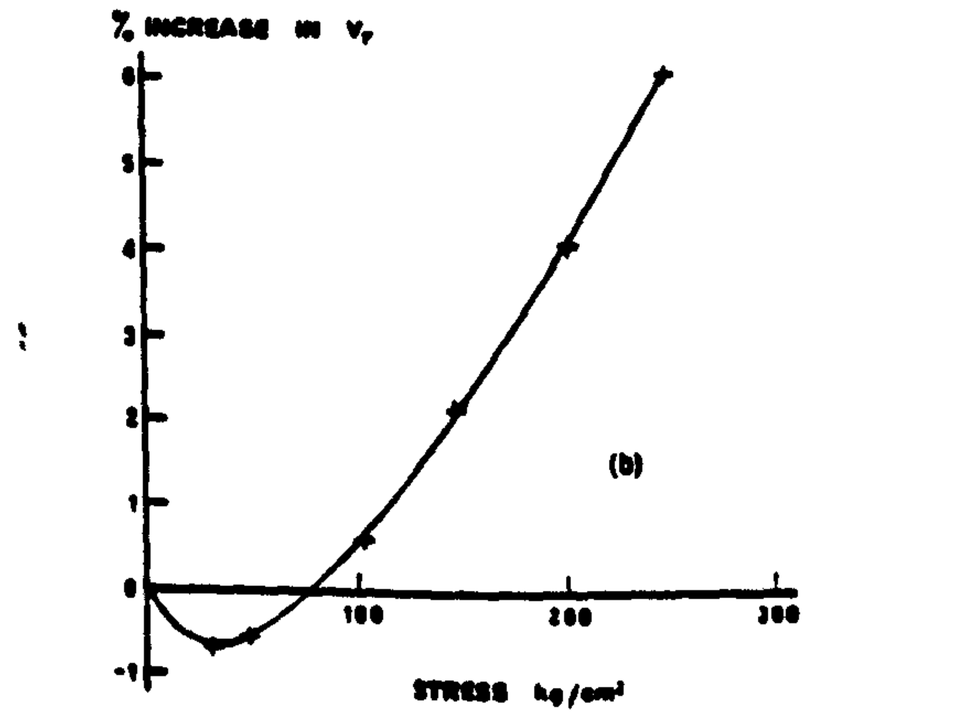

Changes in equilibrium swelling produced by stress on a vulcanizate containing polysulfidic crosslinks.

Figure 2.12: Changes in volume fraction of rubber in a swollen vulcanizate.

less than a quarter of that of a polysulphidic network, and the number of broken crosslinks calculated was about half. Mono-sulphidic networks show intermediate behaviour, and their recombination effeciency is about a quarter that for polysulphidic networks which explains why this type of network produces low permanent set (38). To check furthur this hypothesis, about 5% of di-n-butyl tetrasulphide was incorporated into the polysulphidic network through swelling, so that it would interfere with the recombination process. Thomas (38) found a substantial reduction in set and calculated recombination efficiency was reduced to about 10%. Recent work by Brown et al (39) have confirmed earlier findings of Thomas.

Recent work by Brown, Porter and Thomas (40) provides some information concerning the influence of type and concentration of crosslink on tearing energy, as shown in Figure 2.13 where tearing energy is plotted against shear modulus (reflecting the crosslink concentration). The tearing energy decreases as the shear modulus increases for each of the three vulcanizing systems investigated. Just like tensile strength, the tearing energy decreases in the following ranking order (at any level of crosslink concentration) polysulphidic> mono-sulphidic > carbon-carbon crosslink, i.e., in the inverse order of their thermal stability.

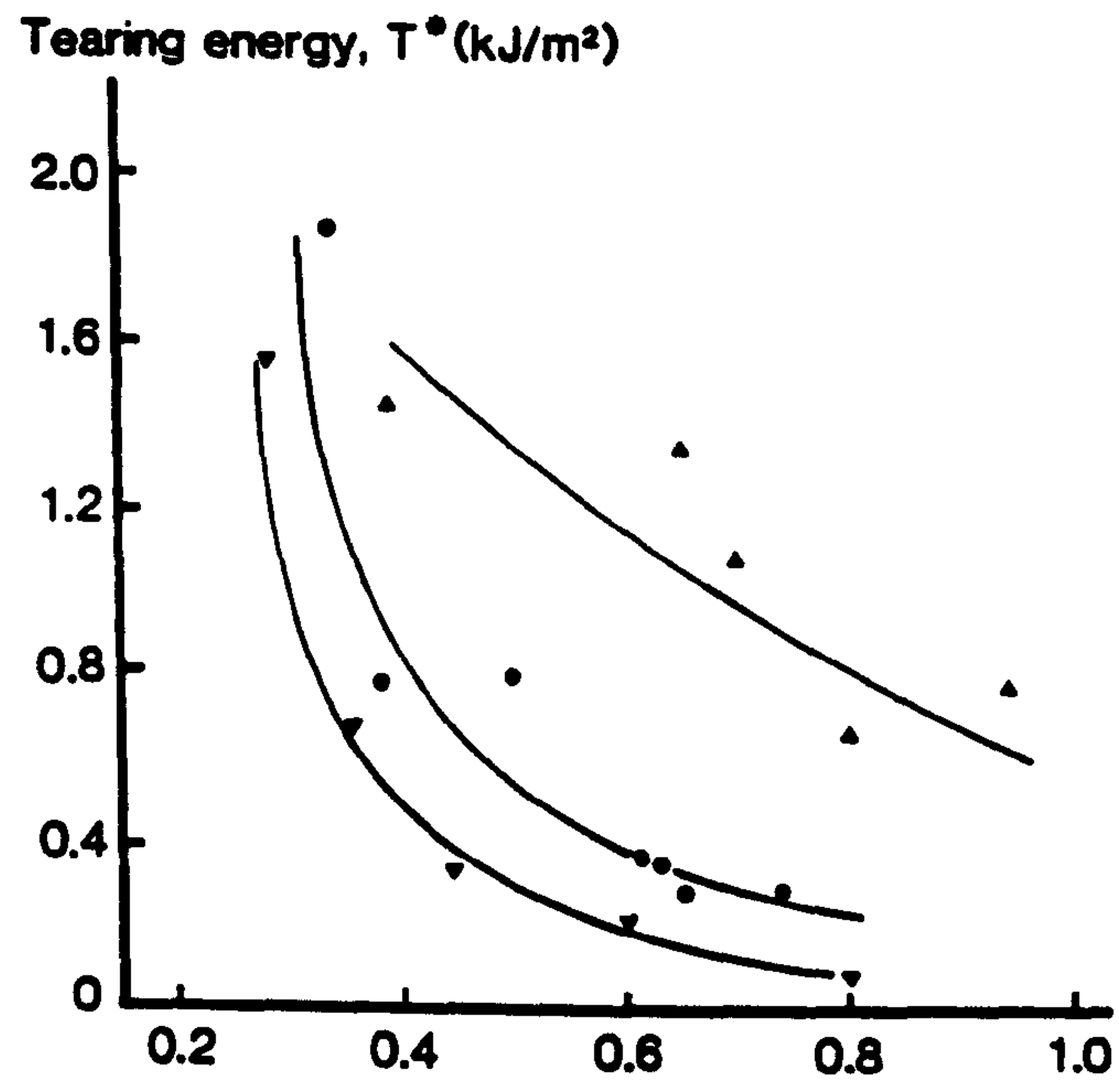

Influence of vulcanizing system on tearing energy (T^*), measured at 10^{-3} cm sec $^{-1}$, for isomerized natural rubber: (▼) peroxide (carbon-carbon crosslinks); (●) EV (mainly monosulphide crosslinks); (▲) conventional (mainly polysulphide, crosslinks).

Figure 2.13: Dependence of tear strength on types of crosslink

CHAPTER THREE

PREVIOUS WORK ON TEAR STRENGTH OF BLACK-FILLED RUBBER

3.1 Introduction

The enhancement of tear strength of black-filled rubbers has always been associated with the development of an anisotropic zone perpendicular to the direction of the advancing tear, this zone forming barriers in the path of the tear and resulting in knotty tearing (15,16). According to Greensmith (16), these barriers are associated with the oriented structures formed at the tip of the tear. He referred to these barriers as the ``strengthening structures''. In black-filled strain-crystallizing rubbers, ``strengthening structures'' include both polymer crystallites and ``carbon black'' structure. According to Medalia (49), in black-filled non-strain crystallizing rubbers, it appears that the ``strengthening structures'' can be formed by alignment of carbon black aggregates and their linkage into chains or strands. The strongest evidence for formation of strands of aggregates comes from the measurement of electrical conductivity. The conductivity in the direction of stretching increases substantially on stretching. A 20-fold increase in longitudinal conductivity was reported by Medalia (49). The phenomenon of knotty tearing, together with the factors which affect its development, have been discussed in Section 2.6.4. This chapter reviews and discusses the work that has been done in the past in an attempt to explain the mechanisms of enhancement in tear strength of black-filled rubbers in terms of the experimental, observations and consequent findings. At the end of the chapter, the aims and scope of the present work will be discussed.

3.2 Examination of the torn surface

Andrews and Walsh (11) studied the fractured surfaces of black-filled rubbers by means of replica electron microscopy. The rupture process was deduced from the micrograph of the replica, since it reflected an exact copy of the rupture path through the material. The amount of extracted filler lifted out by the

replicating material (gelatine) reflected the relative strength of the adhesion of filler particles to the rubber matrix. Poor adhesion is reflected by a high amount of filler extracted. Some of the interesting findings from this work are summarised below.

(1) The adhesion of filler particles is affected by the particle size, the cure systems and the mode of failure. MT black, which has large-sized particles, showed relatively poorer adhesion than did fine particles of HAF black. The latter showed stronger adhesion because of their higher surface area per unit volume than did the former type of black. It was also found that peroxide-cured rubbers showed stronger adhesion than did sulphur-cured rubbers. Andrews argued that the difference could lie in the strength of the bond at the rubber-filler interface, which could be stronger in peroxide-cured rubbers than sulphur-cured rubbers.

(2) There was a correlation between good adhesion and high tear resistance. Good adhesion at the rubber-filler interface usually produced high tear strength. Small-sized particles showed higher tear strength than did large-sized particles, since the former adhered more strongly at the rubber interface than did the latter.

However, although the adhesion of filler particles at the rubber matrix was stronger in peroxide-cured rubbers than in sulphur-cured rubbers, the tear strength of the former was relatively poorer than that of the latter. Thus, it appears that the bond between rubber and filler particles must be neither too strong nor too weak. If the adhesion is too strong, as was the case with the peroxide-cured rubbers, then breakdown occurs in the matrix near the particle and the latter remains attached to the rubber. If the adhesion is too poor, then breakdown occurs at low stresses. Thus the importance of a good adhesion is necessary only to a level where it could withstand stresses high enough to develop the necessary hysteresis to enhance strength. From the experimental observations and findings Andrews suggested the followings:

(i) The rupture paths in filled material seem to travel from one filler unit to an adjacent one. Since the path followed

would be that requiring least energy, it would seem probable that filler particles (or groups) or their immediate environment were zones of relative weakness. These weak zones lead to branching and broadening the tip of a growing tear, and thus raise the energy to propagate tearing.

(ii) Carbon black can also exert an indirect influence on the propagation of rupture by providing a mechanism for hysteresis at high stress. The breakdown hysteresis in filled rubbers must operate at the actual point of rupture, which explains why poorly-adhering fillers which seperate at low stresses exert no influence on tear strength.

Recently, Gent (41) proposed a mechanism for the rupture process in black-filled rubbers, more-or-less similar to that suggested by Andrews earlier. By careful examination of the photographs taken at the tear tip, there was evidence that the tear tip seemed to be split by numerous vertical tears, each being associated with a carbon black particle. Thus it appears that each carbon black particle acted as a local stress-raiser and provided a potential nucleus for a small secondary crack to grow. When this small secondary crack linked up with other cracks through crack deviations, it grows in size. This in turn causes the blunting of the effective tip by increasing in tip diameter, thus providing an enhancement of tear strength.

3.3 Prevention of lateral tear deviation

Gent and Henry (42) developed a technique whereby possible deviations of the tear from a linear path was restricted. This was achieved by bonding thin steel strips on opposite sides of the two legs of the trouser-tear test-pieces as shown schematically in Figure 3.1. The advantage of this technique is that, in addition to restricting extension of the legs of the trouser tear test-pieces, proper alignment of these steel strips allows a degree of control over stick-slip tear path deviations and tear tip diameter, and thus permitted estimates to be made of their importance. The width of separation of bonded metal were varied from 0.01cm to 3cm, so that variations in lateral tear deviation could be investigated. They carried out the tear measurements at temperatures ranged from -50°C

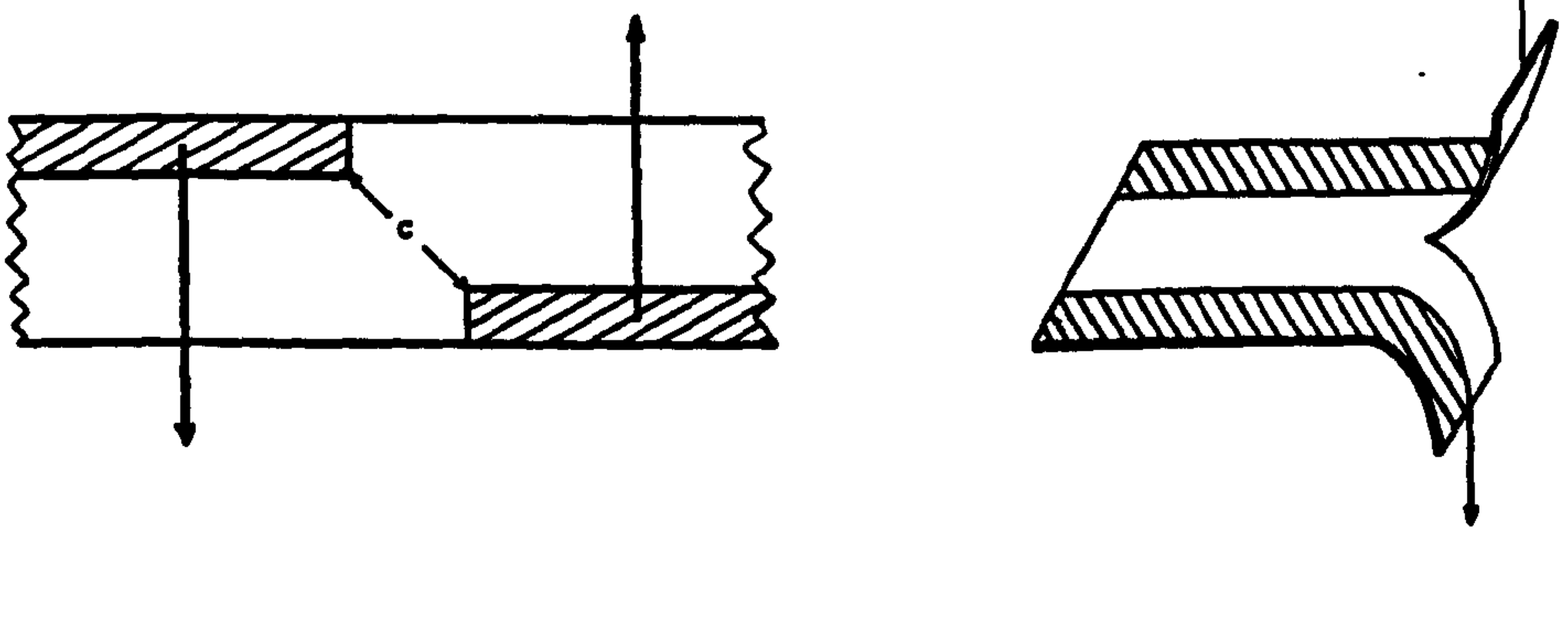

Figure 3.1: Schematic diagram showing a `constraint' trouser tear test-piece.
(a) sketch of the cross-section for a narrow-gap test-piece
(b) method of tear.

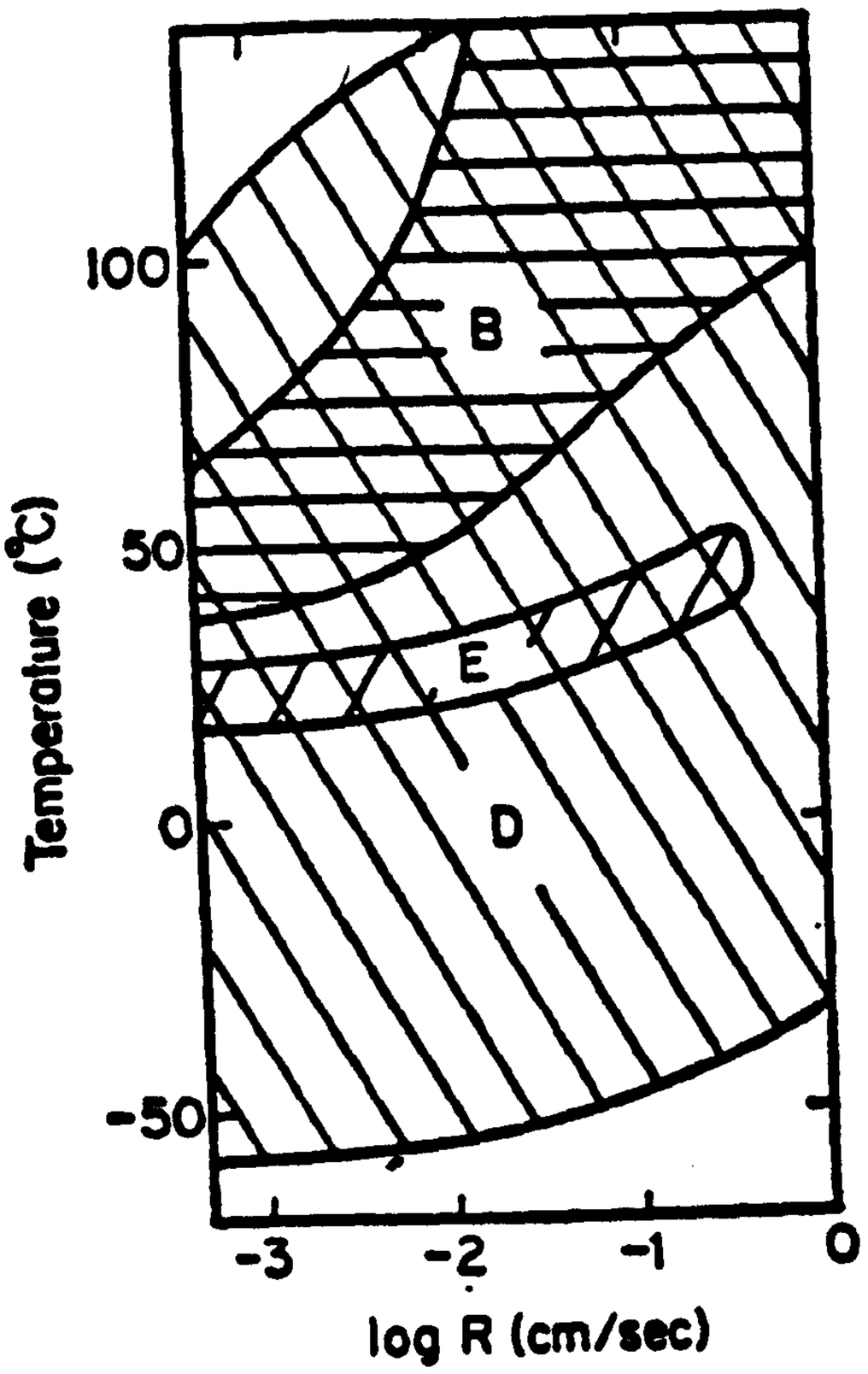

Figure 3.2: Regions of knotty tearing for carbon-black-filled vulcanizates of SBR(B), NR(D), and cis-polybutadiene(E).

to 100°C, and at tear rates ranged from 0.0004 cm s^{-1} to 1 cm s^{-1}

In the case of black-filled rubbers, the wide-gap test-pieces displayed knotty tearing over a well-defined range of tear speeds and temperatures. Different rubbers gave different range of knotty tearing regions as shown in Figure 3.2. Black-filled natural rubber vulcanizates gave wider range of knotty tearing regions than did black-filled SBR. Their results were consistent with the results of Greensmith (16). Outside this range, they all tore relatively smoothly. However, when the separation of the metal shims was narrowed, large-scale tear deviation was not observed. The tearing energy for the filled rubbers was about twice as large as that for the unfilled rubbers.

It was suggested that the increase tear strength in black-filled rubbers was due primarily to large-scale lateral tear deviations. Thus the mechanism of reinforcement of tear strength is associated with the increase in effective diameter of the tear tip resulting from lateral tear deviation, and not with a pronounced increase in the intrinsic strength. Although the true mechanism of tear deviation was not known exactly, it was suggested that the development of strength anisotropy (controlled by the internal viscosity of the rubber/black system) was necessary for its occurrence. Recently, Stacer et al (43,44,45) investigated the phenomenon of lateral tear deviation in more detail by considering how it would be affected by factors such as temperature, rate and strain. A technique similar to that used by Gent and Henry was employed, the minor difference being the use of brass instead of steel as the shim material. The advantage of this change lay in the natural ability of brass to bond to sulphur-cured rubbers. This simplified sample preparation (43). They varied the spacing of the bonded brass from 3mm to as close to zero as possible. Their results were consistent with the results of Gent and Henry (42). When the spacing of the bonded brass was wide, knotty tearing occurred, and when the spacing of the bonded brass was closed to zero, steady tearing occurred. Some other interesting observations and findings are listed below.

(i) They found a linear relationship between tear initiation energy and shim spacing distance, as shown in Figure 3.3. In

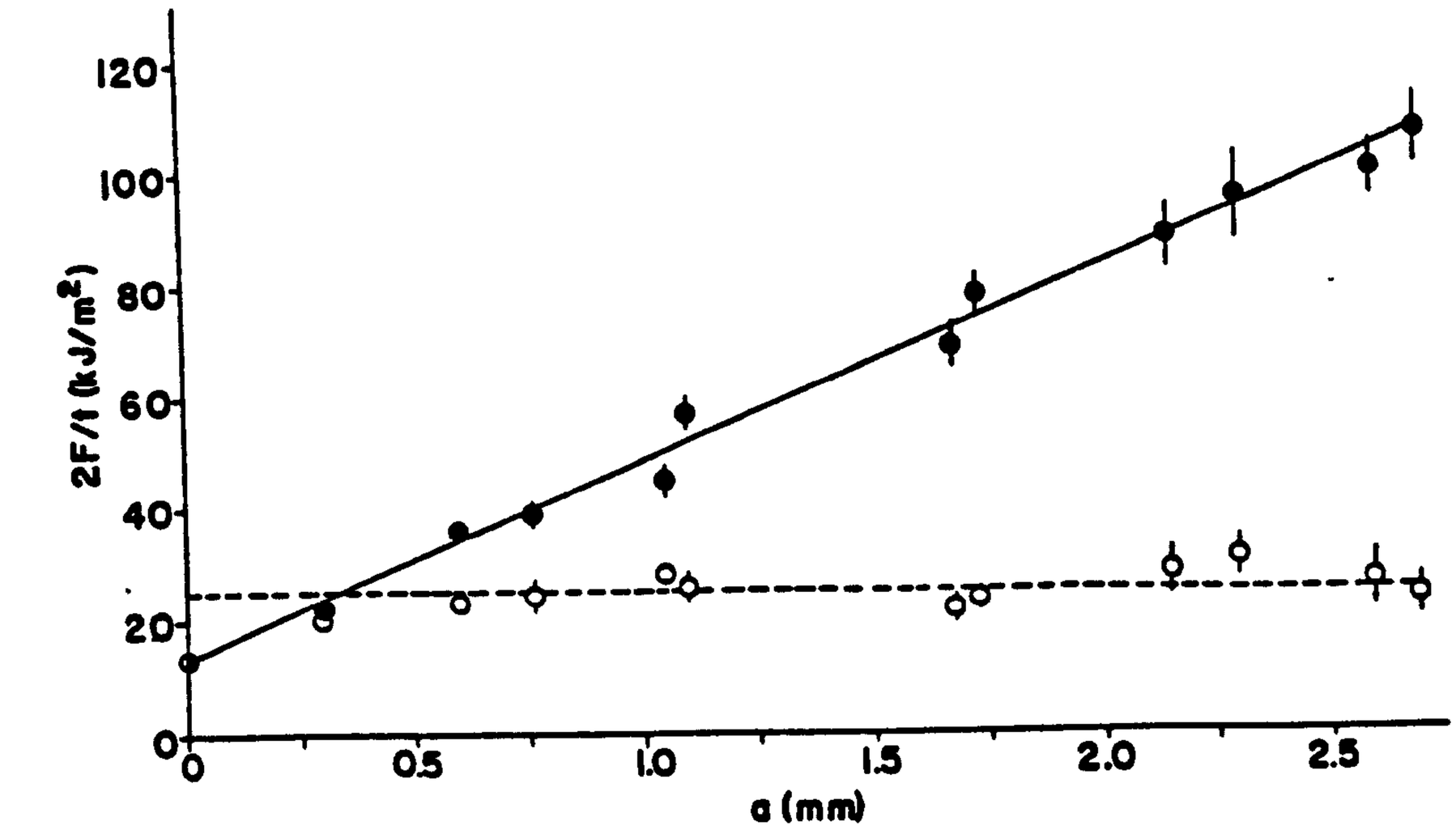

Figure 3.3: Effect of shim separation distance on tear arrest and initiation energies for filled NR tested at -40°C, and tear rate 1.7 mm s^{-1}; ◑ , constrained; ○ , arrest; and ● , initiation.

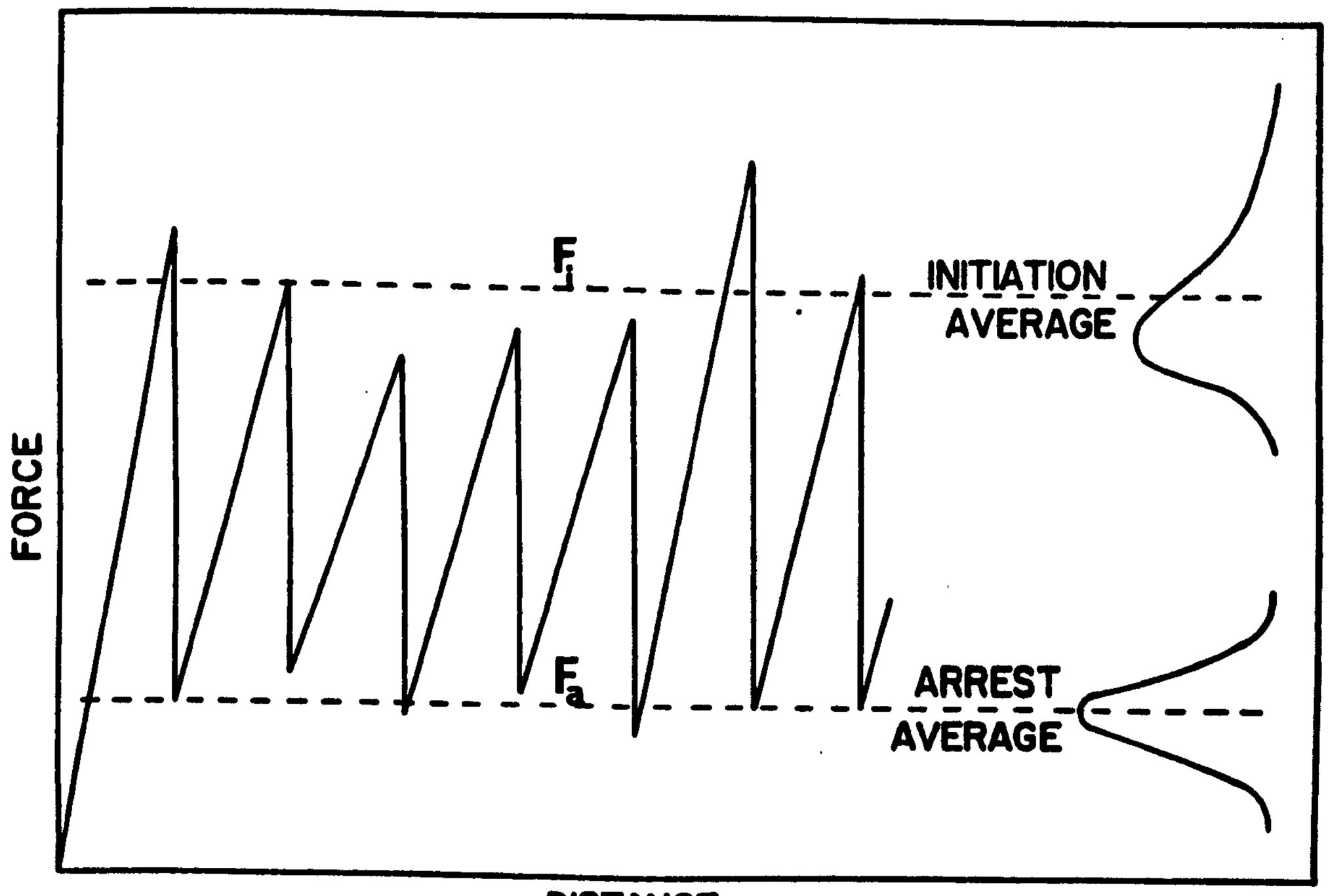

Figure 3.4: Schematic diagram showing the tearing force-distance chart. F_i tearing force at tear initiation, F_a tearing force at tear arrest.

contrast, the tear arrest energy is independent of shim spacing distance, with the average arrest value being slightly higher than the contrained tear energy (assuming zero shim separation). The tear initiation energy refers to the tearing energy calculated using the maximum tearing force F_i given by the upper peak of the tearing force-distance chart. The tear arrest energy refers to tearing energy calculated using the minimum tearing force F_a given by the lower peak of the tearing force-distance chart, as shown schematically in Figure 3.4.

(ii) There were regions of tear rate and temperature where knotty tearing could develop. If the temperature and rate are such that the deforming material at the tear tip did not extent beyond a critical extension ratio, λ_c, where λ_c corresponds to the upturn in the tensile stress-strain curve for the rubber, unstable tearing did not occur. No explanation was put forward to account for this behaviour. At low temperatures (short times), the boundary between stable and unstable tearing was controlled by a characteristic time, t_c, associated with the onset of the rubber-glass transition. At times shorter than t_c, unstable tearing did not occur because of the plastic yielding of the material which interrupted the formation of the anisotropically-reinforced structure at the tear tip.

3.3.2 Effect of molecular orientation on tear strength

The tear strength of carbon black-filled rubbers shows a marked dependence on the direction of molecular orientation. This effect was first recognised by Busse (15), who demonstrated that it was easier to move a pin in a highly-stretched black-filled NR system along the stretching direction than to move it in the transverse direction. Houwink and Janssen (46), investigated this effect using the Delf tear test-piece. The samples were first pre-strained to the required elongation before punching out the test-pieces either parallel or perpendicular to the direction of pre-stretching. They found that, in the parallel direction, the tear resistance was reduced to that of the corresponding unfilled rubber. However, in the transverse direction, the tear resistance was equivalent to the

tensile strength. They found that, after heating for some hours at 100°C, the effects disappeared and the tear resistance reverted to its normal value. They explained that the tear resistance in the parallel direction was low because the filler particles which were oriented parallel to the molecular orientation produced a marked splitting effect. In the transverse direction, however, the tear resistance increased because this highly-oriented zone acted against the tearing process. The disappearance of the effects after heating was attributed to the elastic recovery which helped to revert the filler particles to the unoriented state.

A similar investigation was reported by Gent and Kim (47). Here, trouser tear test-pieces were scored on both surfaces either along or transverse to the pre-stretching direction in order to control the tear path. The samples were held in the extended state for a minute or two before releasing the load and allowing them to relax prior to tearing. Three important conclusions emerged from their work:

(i) In non-strain crystallizing rubbers (SBR), no significant effect of pre-strectching on tearing energy was observed, either in unfilled or black-filled rubbers.

(ii) In strain-crystallizing rubbers (NR), the effect of pre-stretching on tearing energy was substantial particularly the black-filled rubber. The tearing energy in the parallel direction fell by a factor of about 5 at 300% strain. In the transverse direction, its tearing energy increased by about 30%.

(iii) They found that the effect of pre-stretching on the tear strength was relatively permanent. This is reflected by the low tearing energy in the direction of molecular orientation, even when the tear tests were carried out one month later, or after heating at 100°C for one hour prior to tear tests. This is contrary to the findings of Houwink and Janssen earlier. It could be that the reasons for the disagreement was the different length of heating time; Houwink and Janssen heated the samples at a much longer period than did Gent and Kim.

Gent and Kim explained the phenomena summarised in (ii) and (iii) using Dannenberg hypothesis which states that, crystallization in black-filled rubbers brings about segregation of filler particles because the filler particles are excluded from the crystalline domains when the rubber crystallizes. When the crystallites melt, the two components do not remix, so that domains relatively free from carbon black remain oriented in the pre-stretching direction, thus allowing easy tearing along this direction.

In another interesting investigation, Gent and Kim (47) determined tearing energy parallel to the stretching direction whilst holding the test-piece in the stretched state. They observed a very marked difference between the characteristic tearing of non-strain and strain-crystallizing rubbers. In the former, a reduction in tearing energy was very marked between 25% to 100% extension; thereafter, only a slight decrease was noted. However, in the latter, a substantial reduction in tearing energy was observed, in particular, at large strains; for example, at 250% strain the tearing energy dropped by a factor of about 40. They attributed the effect in the case of NR to strain crystallization, such crystallization providing easy fracture paths for tears to grow along the imposed strectching direction.

Earlier, Chasset and Thirion (48) also carried out some qualitative work on the longitudinal tear of stretched vulcanizates. Their method consisted of determining the instantaneous transverse force necessary to produce a longitudinal tear in a partially-split test-piece (trouser type) subjected to a constant extension. They observed that natural rubber vulcanizate containing reinforcing black filler tore in a continuous ``fibrous manner'' in which the rubber appeared to split like a fibrous material. This occured at 140% elongation and above. In the case of black-filled synthetic rubbers (butyl,SBR and chloroprene) they observed 'amorphous-type' tearing, in which the tear progressed in a slow and regular manner.

3.4 Aim and scope of the present investigation

In the previous published work on the tear strength of black-filled rubbers, the investigations were focused on tearing

measurements carried out at various tear rates and temperatures using natural rubber and one or two other synthetic rubbers. As far as the author is aware, no attempts were made to investigate the role of crystallization and effect of vulcanizing systems on the enhancement of black-filled rubbers. The aims of the present investigation were as follows:

(1) to investigate the role of strain-crystallization in promoting the occurrence of knotty tearing.

(2) to investigate the influence of nature of crosslink to promote knotty tearing.

(3) to investigate the effect of crosslink concentration on the development of knotty tearing.

(4) to investigate the importance of strength anisotropy in promoting knotty tearing.

(5) to seek correlations between the degree of crystallization and the extent of anisotropy developed during pre-straining.

(6) to seek correlations between the anisotropy introduced by pre-stressing and the permanent set.

(7) to seek explanations for smooth fractured surface observed in black-filled rubbers at tear rates where unfilled rubbers would produce rough fractured surface.

There are two schools of thought concerning the mechanisms of the enhancement of tear resistance in black-filled rubbers. The first mechanism postulates that the enhancement of tear resistance in black-filled rubbers is associated with the blunting of the tear tip as a consequence of tear diversion. The reason for tear diversion is still not fully understood. However, there are suggestions that it might be associated with the ``strengthening structures'' which form at the tear tip (15,16) and also because of the weak zones inherent in the black-filled rubbers (11). The second mechanism of enhancing the tear strength is believed to be associated with hysteresis (28). An attempt has been made to interprete the results of investigation using these theories.

CHAPTER FOUR

FACTORS WHICH AFFECT THE DEVELOPMENT OF KNOTTY TEARING

EXPERIMENTAL METHODS

4.1 Materials and formulations

In this investigation, natural rubber (NR), epoxidised natural rubber (ENR25 and ENR50), styrene butadiene rubber (SBR) and isomerized natural rubber (INR) were used. The grades of each rubber employed are listed in Table 4.1, together with its glass-transition temperature and degree of crystallinity produced at 400% extension (50). These rubbers display a wide range of glass-transition temperature, and different degree of crystallinity on straining. This is particularly significant because the effect of molecular mobility and crystallization could be investigated on a wider range than that investigated by Greensmith (16).

The effect of the nature of carbon black particles on the development of knotty tearing was also investigated. Two grades of carbon black, viz, high-abrasion furnace (HAF) and medium thermal (MT), which differ widely in particle size, were used. The former has an average diameter of about 26 nm to 30 nm and the latter has an average diameter of about 201 nm to 500 nm, according to the ASTM classifications. Another significant difference is that an HAF black has high structure while an MT black has little or no structure (7).

The base mix formulation was the same for each rubber, so as to avoid complications associated with variations in the compounding ingredients. Table 4.2 shows the standard base mix formulations for each rubber investigated. In the case of HAF black, the amount incorporated into rubbers was varied from 10 parts per hundred of rubber (pphr) to 60 pphr. In the previous published work on the tear strength of black-filled rubbers, most of the investigations were carried out using rubbers loaded with 50 pphr of carbon black. There is little or no information published as far as the author is aware, concerning the effect of carbon black loading on the development of knotty tearing. It is of interest to see if the amount of filler loading bear any significant influence in promoting

Table 4.1: Degree of crystallinity and glass-transition temperature, θg, of rubbers.

Elastomer	Commercial grade	θg °C	* Deg of crystallinity (%) (at 400% strain)
NR	SMR L	-72	11
ENR 25	ENR 25	-48	11
ENR 50	ENR 50	-27	10
SBR	Intol 1500	-63	0
INR	-	-75	0

Footnotes:

(i) SMR L is a high-quality grade Standard Malaysian Rubber with an assurance of freedom from particulate contamination, examples, sand and bark (60). The absence of contamination helps to avoid complication associated with premature failure arising from that source.

(ii) ENR 25 and ENR 50 are chemically modified natural rubber containing 25 and 50 mole per cent of epoxy groups on the main chain respectively (50, 51).

(iii) Intol 1500 is a grade produced by cold emulsion polymerization. It contains about 23.5% by weight of styrene, the molecular proportion of units in the chains being one styrene to approximately six butadiene (61).

(iv) INR was kindly supplied by Mr P. Brown of MRPRA. Isomerization was carried out on a small laboratory scale by mixing NR with butadiene sulphone. On heating at 140°C, sulphur dioxide was liberated from the sulphone which was allowed to react with NR for 48 hours. Quantitative ^{1}H-NMR analysis of the sample indicated that the final product contained 64 mole per cent of trans-1-4-isoprene units.

* See reference 50.

Table 4.2: Base mix formulations

Ingredients	Parts per hundred of rubber (pphr)
Rubber	100
Zinc oxide	5
Stearic acid	2
* Flectol H	2
Carbon black	varies (0, 10, 25, 30, 40, 50 and 60)

* Flectol H - Polymerized 2,2,4-trimethyl-1,2 dihydroquinoline

Table 4.3a: Tensile properties of unfilled vulcanizates base on semi-EV system

Base mix: Rubber 100, Zinc oxide 5, steaic acid 2, Flectol H 2
All units in parts per hundred of rubber (pphr)
Curatives: Sulphur 1.2 pphr , morpholinylbenzothiazole-2-sulphenamide (MBS) 2 pphr

Mix number	G1	G2	G3	G4	G5
Rubber	NR	ENR 25	ENR 50	SBR	INR
Cure time at 150°C (mins)	25	17	15	40	27
M100 (MPa)	0.8	0.79	0.8	0.88	0.92
M300 (MPa)	1.64	1.6	1.66	1.62	1.61
Tensile strength (MPa)	26.9	26.3	26.6	2.36	2.02
E.B. (%)	749	852	758	418	350
U_b (MJ m^{-3})	45.1	48.3	42.5	5.67	4.80

Footnotes:

cure time - time to vulcanize the rubber compound to a maximum state of cure, i.e., the time determined from the torque-cure time curve to reach maximum torque.

M100 - tensile stress at 100% strain

M300 - tensile stress at 300% strain

E.B. - elongation at break

U_b - stored energy density at break calculated from the area under the stress-strain curve at break

<u>The footnotes above are applicable to the rest of the tables in this chapter</u>

knotty tearing. In the case of MT black, the amount incorporated into rubbers was 50 pphr. Unless otherwise stated, a semi-efficient (semi-EV) vulcanization system was used throughout. Table 4.3a shows the tensile properties of unfilled vulcanizates obtained from semi-EV vulcanization system and Table 4.3b shows the tensile properties of HAF black-filled vulcanizates obtained from the same vulcanization system. Tensile measurements were carried out by pulling dumbbell test-piece to break at a rate of 100 mm per minute at 23°C using an Instron machine. The M100 and M300 refer to tensile stress at 100% and 300% strain respectively. U_b refers to stored energy density at break, determined by integrating the area under the stress-strain curve at break. The tensile results shown in all Tables were the median value obtained from three test-pieces. The tensile properties (M100, M300 and tensile strength) are included in each table to serve as quality controls. They play no part in the present investigation. The tensile strength obtained from mixes G_1, G_2 and G_3 was more-or-less the same, about 26 MPa. This is consistent with the figure reported by Davies et al (50). The tensile strength of unfilled SBR was consistent with the results of Greensmith (16). The tensile strength of unfilled isomerised NR was about the same order of magnitude reported by Brown, Porter and Thomas (40). The tensile strength of carbon-black-filled NR and SBR filled with 50 pphr of HAF and MT blacks shown in Table 4.3b and 4.3c respectively, were consistent with the results obtained by Greensmith (16). Thus this indicates that the quality of the vulcanizates prepared were as good as those prepared by the previous investigators.

Three other vulcanization systems viz, conventional and efficient (EV) sulphur vulcanization systems and peroxide vulcanization system, were also employed to see if they have any influence on the development of knotty tearing. As far as the author is aware, this aspect had not been previously investigated. Table 4.4a shows a set of formulations for conventional vulcanization system of black-filled (50 pphr HAF) NR mixes. The ratio of sulphur to accelerator was 5:1. In order to get networks with a range of crosslink concentration, rubber mixes were prepared with *pro rata* changes in sulphur and accelerator concentration, whilst keeping sulphur to accelerator ratio constant, i.e., 5:1. Table 4.4b shows a set of formulations for efficient

Table 4.3b: Tensile properties of HAF black-filled vulcanizates base on semi-EV system

Base mix: Rubber 100, ZnO 5, St. acid 2, Flectol H 2, HAF (N330) 50.
All units in parts per hundred of rubber (pphr)
Curatives: Sulphur 1.2 pphr , MBS 1.2 pphr

Mix number	H1	H2	H3	H4	H5
Rubber	NR	ENR 25	ENR 50	SBR	INR
Cure time at 150°C (mins)	30	16	15	110	30
M100 (MPa)	2.14	2.4	2.90	2.0	2.64
M300 (MPa)	11.9	11.9	14.0	10.2	8.56
Tensile strength (MPa)	27.1	27.5	25.7	25.4	12.8
E.B. (%)	547	549	487	565	322
U_b (MJ m^{-3})	57.1	59.3	50.2	52.8	-

Table 4.3c: Tensile properties of MT black-filled vulcanizates base on semi-EV system

Base mix: Rubber 100, ZnO 5, St. acid 2, Flectol H 2, MT black 50
All units in parts per hundred of rubber (pphr)
Curatives: Sulphur 1.2 pphr, MBS 1.2 pphr

Mix number	M1	M2	M3	M4
Rubber	NR	ENR 25	ENR 50	SBR
Cure time at 150°C (mins)	30	15	11	100
M100 (MPa)	1.56	1.57	1.51	1.29
M300 (MPa)	7.24	6.48	6.44	3.81
Tensile strength (MPa)	19.6	19.1	12.0	9.72
E.B. (%)	557	592	494	758
U_b (MJ m^{-3})	43.3	43.9	26.2	37.3

Table 4.4a: Conventional vulcanization system (NR) and physical properties of vulcanizates obtained

Base mix: NR 100, ZnO 5, St. acid 2, Flectol H 2, HAF (N330) 50 in parts per hundred of rubber (pphr).

Mix number	A1	A2	A3	A4	A5	A6	A7	A8
Sulphur (pphr)	1.0	1.5	1.6	1.75	2.0	2.5	3.5	4.0
MBS (pphr)	0.2	0.3	0.32	0.35	0.4	0.5	0.7	0.8
Cure time at 150°C (mins)	35	34	29	30	28	27	25	24
M100 (MPa)	1.48	1.13	1.84	2.20	2.45	2.75	3.99	3.96
Tensile strength (MPa)	18.8	19.5	21.7	25.6	26.8	25.6	27.8	27.6
E.B. (%)	550	575	511	525	526	481	433	447
U_b (MJ m^{-3})	42.9	43.0	44.8	57.6	63.3	54.5	55.4	59.0
U_r	0.2176	0.2204	0.2691	0.2964	0.3090	0.3281	0.3828	0.3837
$[X]$ x 10^{-2} mol/kg RH	3.64	3.77	6.00	7.57	8.41	9.77	14.63	14.70
$[X]_{act.}^{app.}$ x 10^{-2} mol/kg RH	2.38	2.47	3.93	4.95	5.50	6.39	9.57	9.61

Footnotes:

U_r - volume fraction of rubber in swollen vulcanizate determined by equilibrium swelling measurement

$[X]_{app.}$ - apparent crosslink concentration determined by equilibrium swelling measurement

$[X]_{act.}$ - actual crosslink concentration determined by equilibrium swelling measurement

Table 4.4b: Efficient vulcanization (EV) system (NR) and physical properties of vulcanizates obtained

Base mix: NR 100, ZnO 5, St. acid 2, Flectol H 2, HAF (N330) 50 in parts per hundred of rubber (pphr).

Mix number	B1	B2	B3	B4	B5	B6	B7
Sulphur (pphr)	0.175	0.25	0.175	0.2	0.3	0.6	0.8
MBS (pphr)	-	-	1.4	1.6	2.4	4.8	6.4
TMTD (pphr)	-	-	0.88	1.0	1.6	3.0	4.0
CBS (pphr)	2.11	3.0	-	-	-	-	-
Cure time at 150°C (min)	35	30	30	45	50	50	60
M100 (MPa)	1.11	1.68	2.15	2.19	2.71	5.08	6.76
Tensile strength (MPa)	18.9	23.0	25.8	25.0	24.1	20.1	11.7
E.B. (%)	550	533	554	527	445	289	154
U_b (MJ m^{-3})	40.6	52.4	62.7	55.3	45.9	26.7	8.86
U_r	0.2139	0.2534	0.2905	0.2965	0.3325	0.4006	0.4250
$[X]_{app.} \times 10^{-2}$ mol/kg RH	3.52	5.20	7.25	7.61	10.13	16.48	19.37
$[X]_{act.} \times 10^{-2}$ mol/kg RH	2.31	3.40	4.74	4.98	6.62	10.78	12.67

Footnotes:

TMTD - tetramethyl thiuram disulphide

CBS - N-cyclohexyl benzothiazole-2-sulphenamide

U_r - volume fraction of rubber in swollen vulcanizate determined by equilibrium swelling measurement

$[X]_{app.}$ - <u>apparent</u> crosslink concentration determined by equilibrium swelling measurement

$[X]_{act.}$ - <u>actual</u> crosslink concentration determined by equilibrium swelling measurement

For soluble EV system the following combination of curatives were used:
Sulphur 0.7, MBS 1.7, tetrabutyl thiuram disulphide (TBTD) 0.7, Zinc oxide was replaced by zinc-2-ethylhexanoate

Table 4.4c: Peroxide-vulcanizing system (NR) and physical properties of vulcanizates obtained

Base mix: NR 100, ZnO 5, St. acid 2, Flectol H 2, HAF (N330) 50 in parts per hundred of rubber (pphr).

Mix number	C1	C2	C3	C4	C5	C6	C7	C8	C9
Dicumyl peroxide (pphr)	0.5	0.75	1.0	1.5	1.7	2.0	2.3	3.0	3.75
Cure time at 150°C (mins)	80	80	90	110	120	100	100	90	90
M100 (MPa)	1.02	1.27	1.27	1.6	1.65	2.39	2.90	3.72	4.78
Tensile strength (MPa)	16.5	20.2	21.0	21.8	23.1	25.0	24.3	22.5	22.2
E.B. %	456	490	455	412	438	366	348	262	223
U_b (MJ m^{-3})	30.0	40.0	33.2	36.1	41.3	37.3	34.4	23.1	19.3
U_r	0.1936	0.2311	0.2487	0.2672	0.2778	0.3133	0.3134	0.3474	0.3766
$[X]$ x 10^{-2} mol/kg RH	2.83	4.20	4.98	5.90	6.46	8.74	8.74	11.32	13.98
$[X]^{app.}_{phys}$ x 10^{-2} mol/kg RH	1.85	2.75	3.26	3.86	4.23	5.72	5.72	7.41	9.14

Footnotes:

U_r - volume fraction of rubber in swollen vulcanizates determined by equilibrium swelling measurement

$[X]_{app.}$ - apparent crosslink concentration determined by equilibrium swelling measurement

$[X]_{act.}$ - actual crosslink concentration determined by equilibrium swelling measurement

Table 4.4d: Conventional vulcanization system (SBR) and physical properties of vulcanizates obtained

Base mix: SBR 100, ZnO 5, St. acid 2, Flectol H 2, HAF (N330) 30 in parts per hundred of rubber (pphr).

Mix number	S1	S2	S3	S4	S5
Sulphur (pphr)	1.5	2.0	2.5	3.0	3.5
MBS (pphr)	0.37	0.5	0.72	0.75	0.88
Cure time at 150°C (mins)	120	80	80	60	60
M100 (MPa)	1.06	1.32	1.75	2.03	2.54
M300 (MPa)	3.95	5.61	9.23	11.1	15.8
Tensile strength (MPa)	22.3	25.8	26.1	26.3	24.9
E.B. (%)	797	645	528	482	392
U_b (MJ m^{-3})	65.3	58.0	50.5	47.2	37.7
U_r	0.3922	0.4423	0.4766	0.5033	0.5209
$[X]$ x 10^{-2} mol/kg RH	2.75	5.93	8.94	11.83	14.02
$[X]^{app.}_{act.}$ x 10^{-2} mol/kg RH	2.03	4.38	6.61	8.75	10.37

Footnotes:

U_r - volume fraction of rubber in swollen vulcanizate determined by equilibrium swelling measurement

$[X]_{app.}$ - <u>apparent</u> crosslink concentration determined by equilibrium swelling measurement

$[X]_{act.}$ - <u>actual</u> crosslink concentration determined by equilibrium swelling measurement

vulcanization (EV) system base on HAF black-filled NR mixes. The ratio of sulphur to accelerator was about 1:12. Table 4.4c shows a set of formulations for peroxide vulcanization system, also base on HAF black-filled NR mixes. Table 4.4d shows a set formulations for conventional vulcanization system base on black-filled (30 pphr HAF) SBR mixes. The crosslink concentration and the volume fraction of rubber in swollen vulcanizates shown in Tables 4.4a, 4.4b, 4.4c and 4.4d, were determined by equilibrium swelling method which will be discussed later. In all cases, the crosslink concentrations used were both substantially greater and substantially less than those used in normal technological vulcanizates (ca 6 x 10^{-2} mol per kg of rubber hydrocarbon).

4.2 Experimental methods

4.2.1 Mixing and moulding

The base mix was prepared in a laboratory internal mixer (batch volume ca 1400 cm^{-3}). The weights before and after mixing were checked to ensure that the carbon black was incorporated in the rubber. Carbon black dispersion was assessed using the 'microtomed section' method. All the mixes prepared were rated 'A' indicating that the carbon black particles were well dispersed in the rubber matrix, as shown in Figure 4.1. Mixes lower than 'A' rating were rejected. Vulcanization was carried out using a compression mould in a steam heated press to produce a flat vulcanized sheet of uniform thickness. The vulcanization temperature and the time taken to vulcanize (cure time) to a maximum state of cure are given in each table.

4.2.2 Preparation of test-pieces

All the tear measurements were carried out using simple-extension (trouser type) test-pieces. The test-pieces were prepared by stamping a die on a flat 230 mm x 230 mm x 2 mm vulcanized sheet. The nominal dimensions of the test piece are given in Figure 4.2a.

4.2.3 Tearing measurement

Tearing was done by separating the legs of the test-piece at a

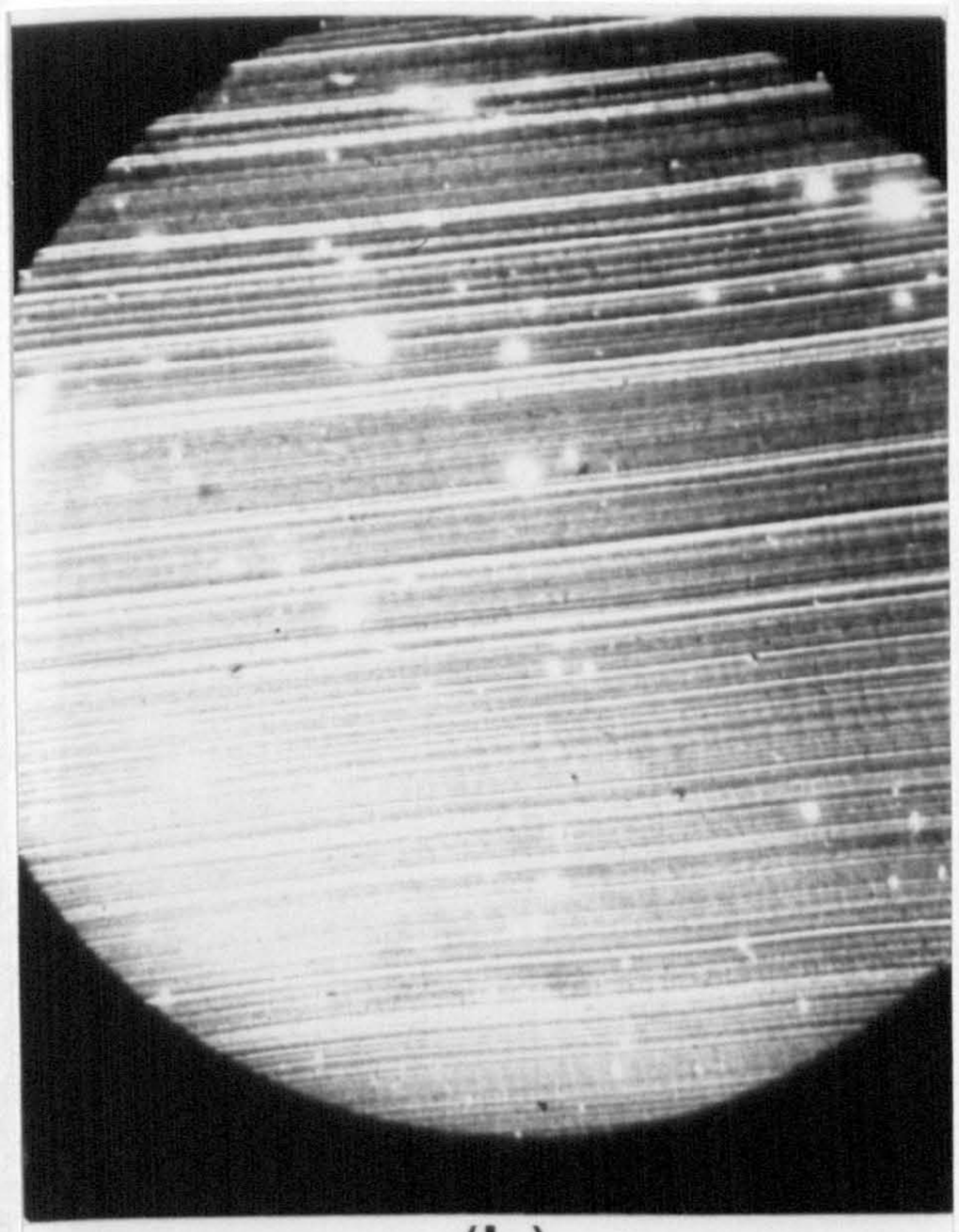

(b)

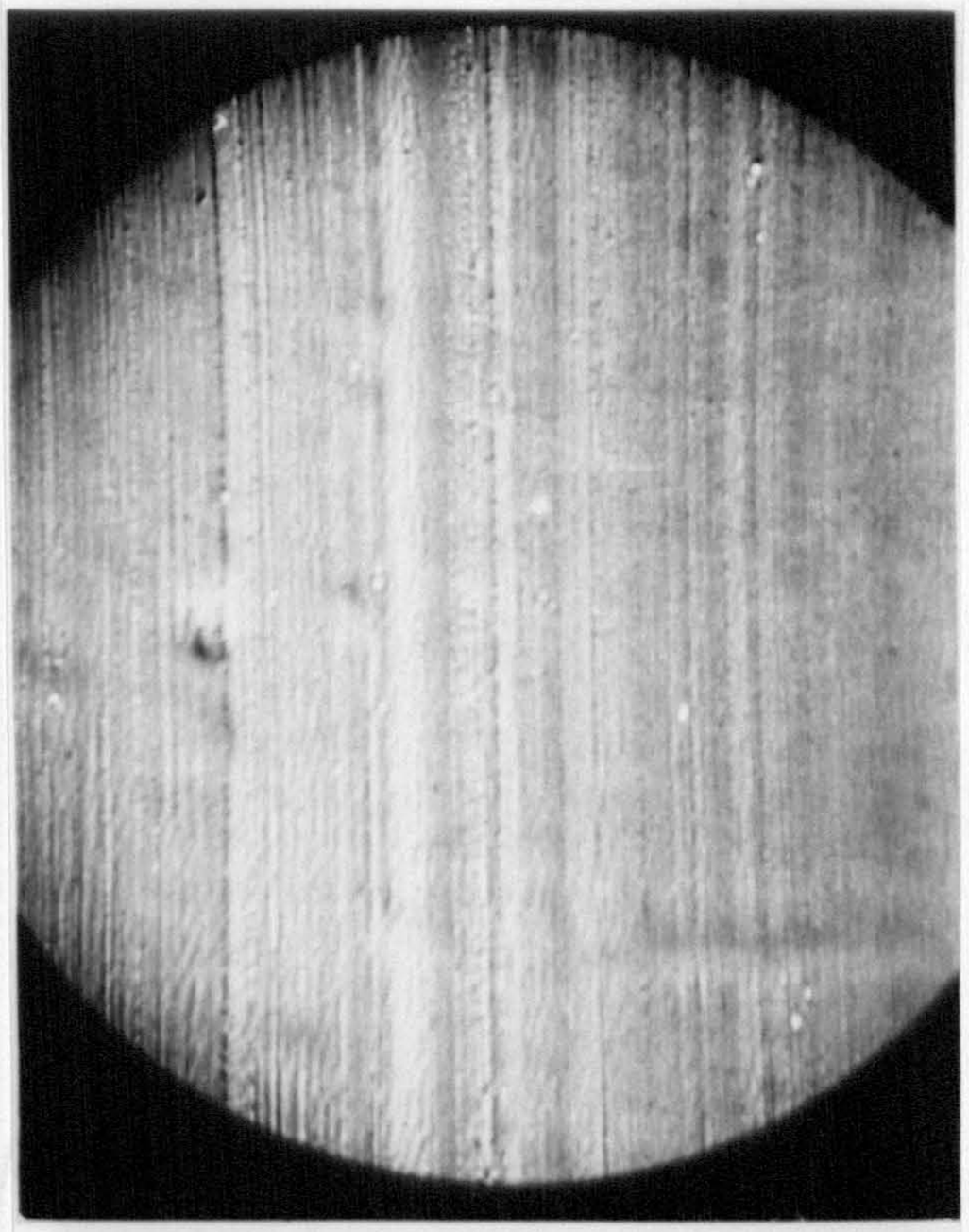

(a)

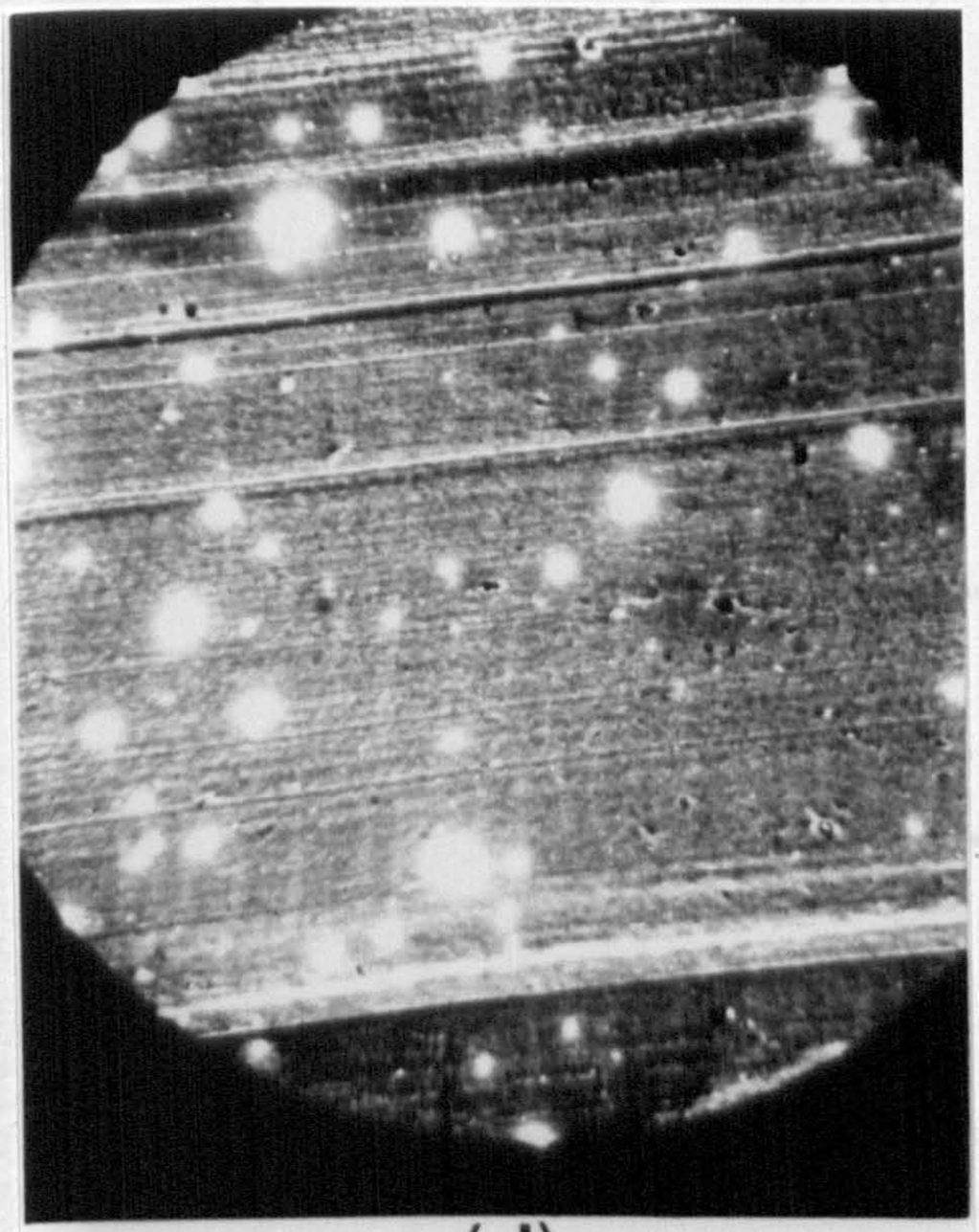

(d)

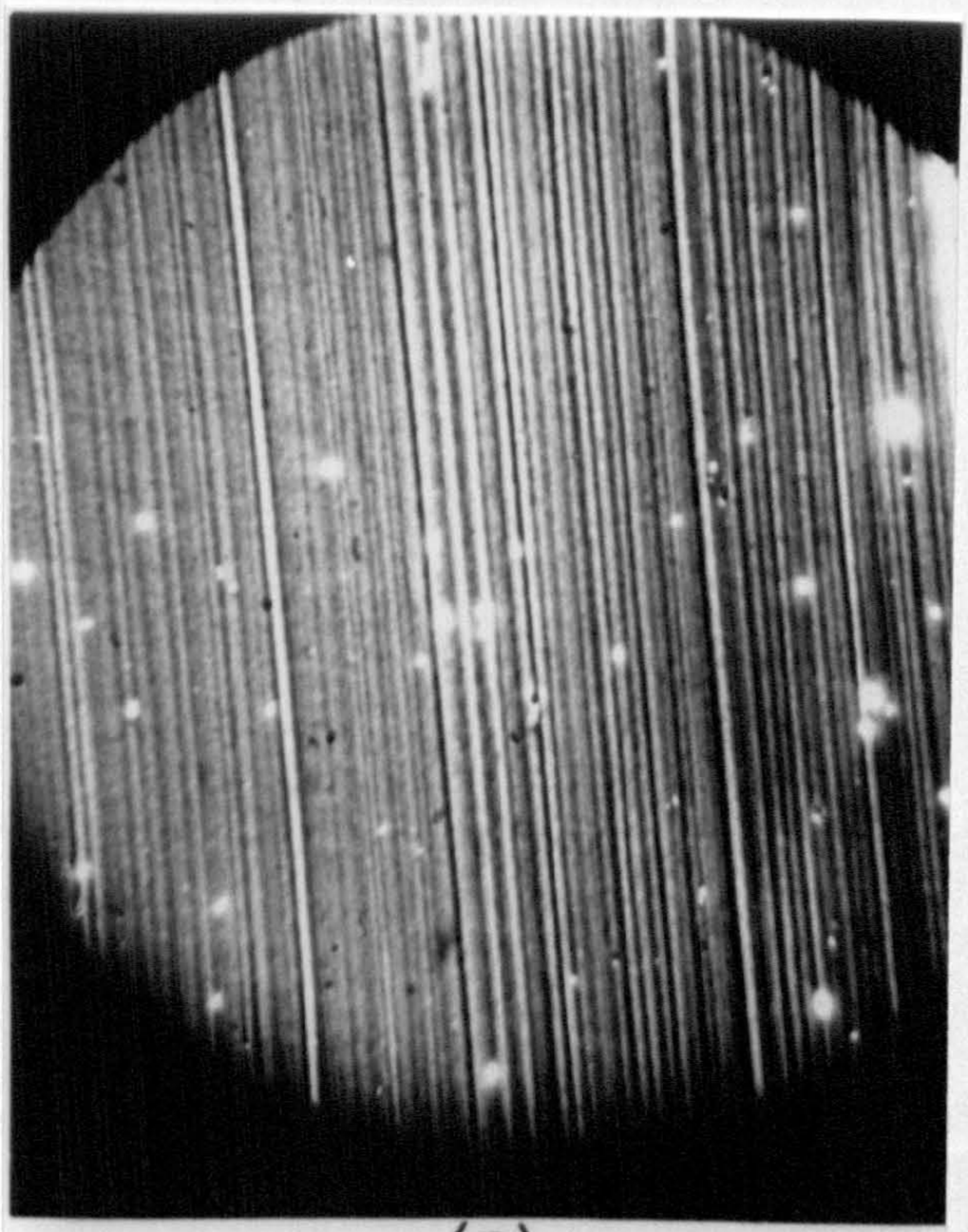

(c)

Figure 4.1: Carbon-black dispersion rating (a) NR (b) ENR 25 (c) ENR 50 (d) SBR. Full formulations given in Table **4·3b**
Black-dispersion rating = A, for each rubber mix.

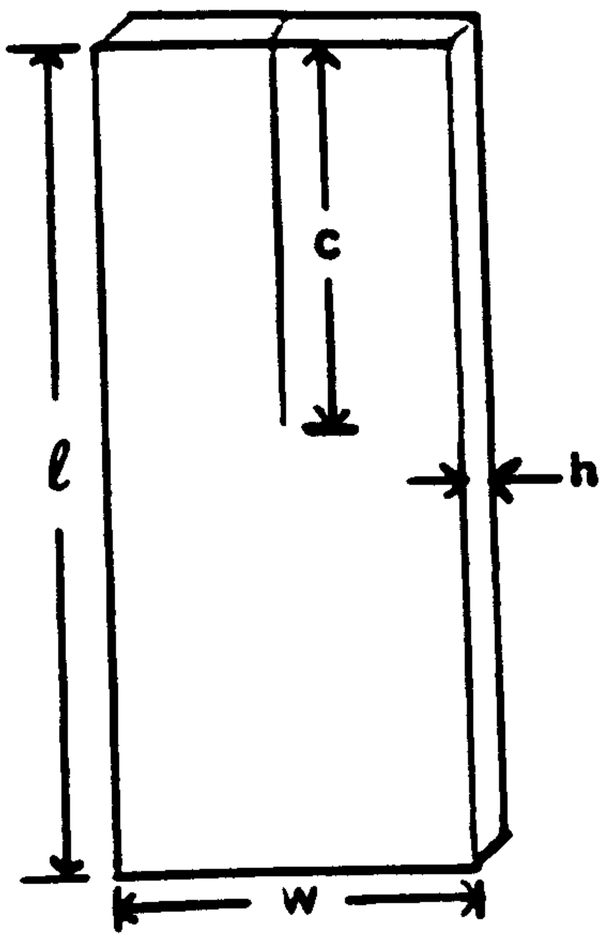

(a)

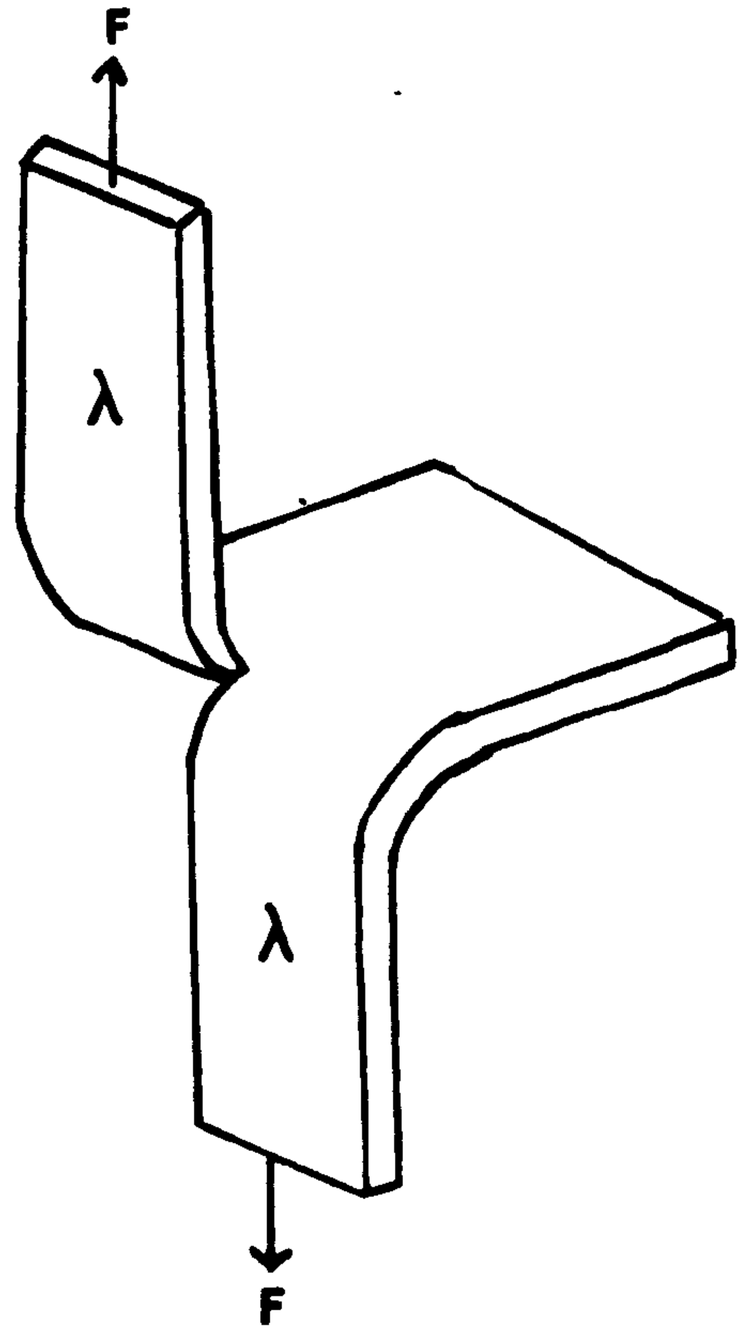

(b)

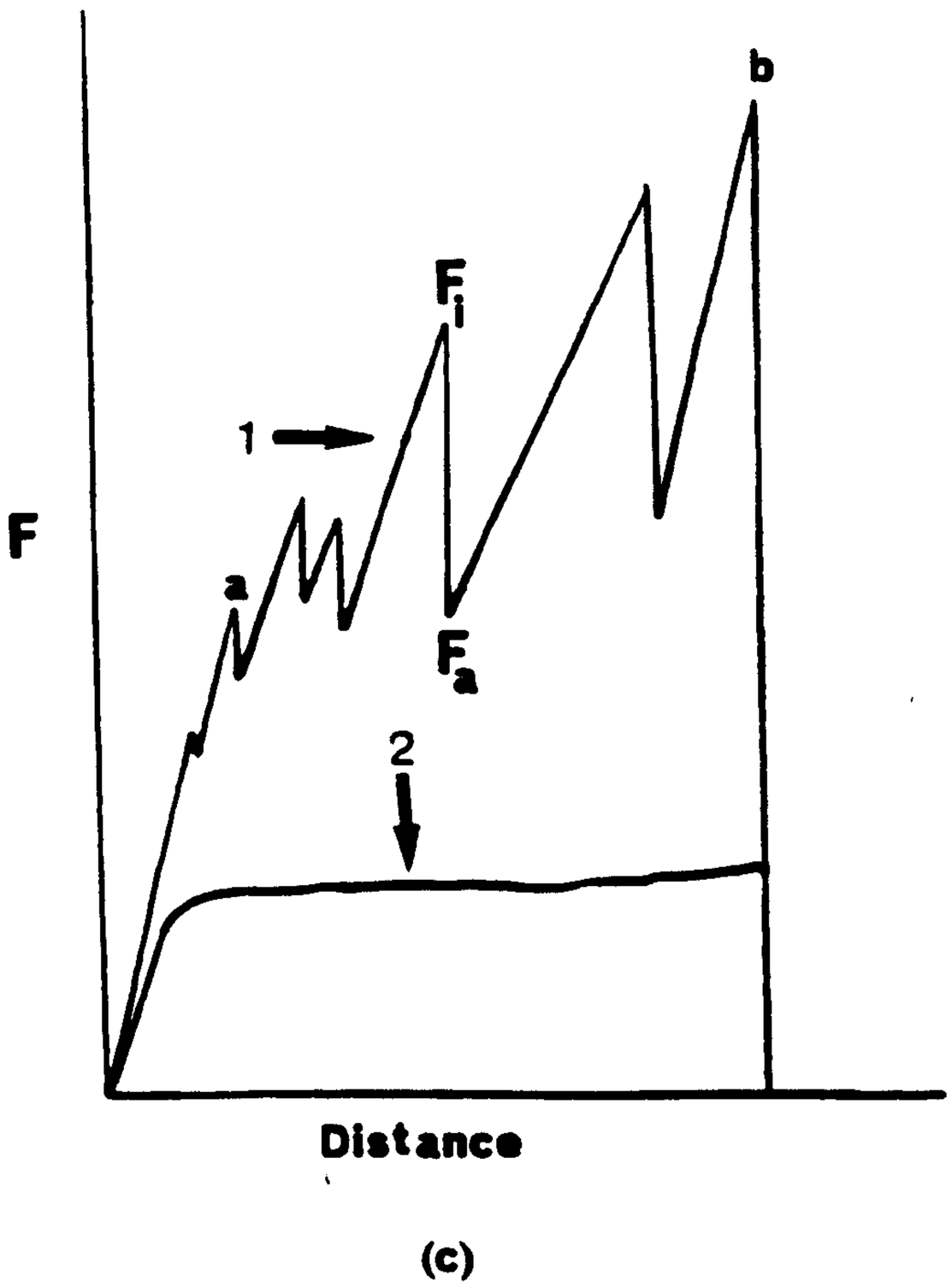

(c)

Figure 4.2: Schematic diagrams of trouser test-piece.
(a) Undeformed state: total length, ℓ = 100 mm,
crack length, c = 37 mm, total width, w = 15 mm,
and thickness, h = 2 mm. (b) Deformed state.
(c) Tearing force-distance chart: (1) stick-slip tearing
(2) steady tearing. ab= 'steady state' region, F_i is the
force at tear initiation and F_a is the force at tear arrest.

uniform rate in an Instron testing machine (Model 1122). This testing machine comprises a loading frame and a moving crosshead operated at a constant rate by two vertical drive screws. A strain-gauge load cell was mounted on its crosshead and was calibrated each time before the start of the experiment. The crosshead speed ranges from 0.05 mm per minute to 1000 mm per minute, thus providing a wide range of tear rates from which to choose. For tear measurement at other than room temperature (23°C), a thermostatic temperature cabinet was fitted to the machine. The whole assembly is as shown in Figure 4.3. Before tearing, the test-piece was first pre-warmed in the cabinet for 15 minutes to allow it to reach to the equilibrium temperature.

4.3 Tensile stress-strain measurements

Tensile measurements were done on dumbbell test-pieces at a rate of extension 100 mm per minute at 23°C in an Instron testing machine. The nominal stress, σ, i.e., force per unit cross-sectional area referred to the unstrained state, was plotted against extension ratio, λ, as shown in Figure 4.4a (curve (i)). From curve (i), strain energy density, U, at each extension ratio, λ, of interest could be determined. The area under the stress, σ, versus extension ratio, λ, plot, determined by tracing and weighing techniques, gave the strain energy density, U. Strain energy density, U, was then plotted against the extension ratio, λ. Figure 4.4a (curve (ii)) shows a typical curve for strain energy density, U, versus extension ratio, λ, up to the breaking extension. Figure 4.4b shows curves for σ, and U versus λ up to 200% extension which are required for the calculation of tearing energy.

4.4 Determination of tear strength

The tear strength was assessed in terms of the elastic stored strain energy released to create unit area of crack, defined as the tearing energy, T. For a trouser test piece it is given by

$$T = \frac{2F\lambda}{h} - wU \qquad (4.1)$$

where F is the tearing force, λ and U are the extension ratio and

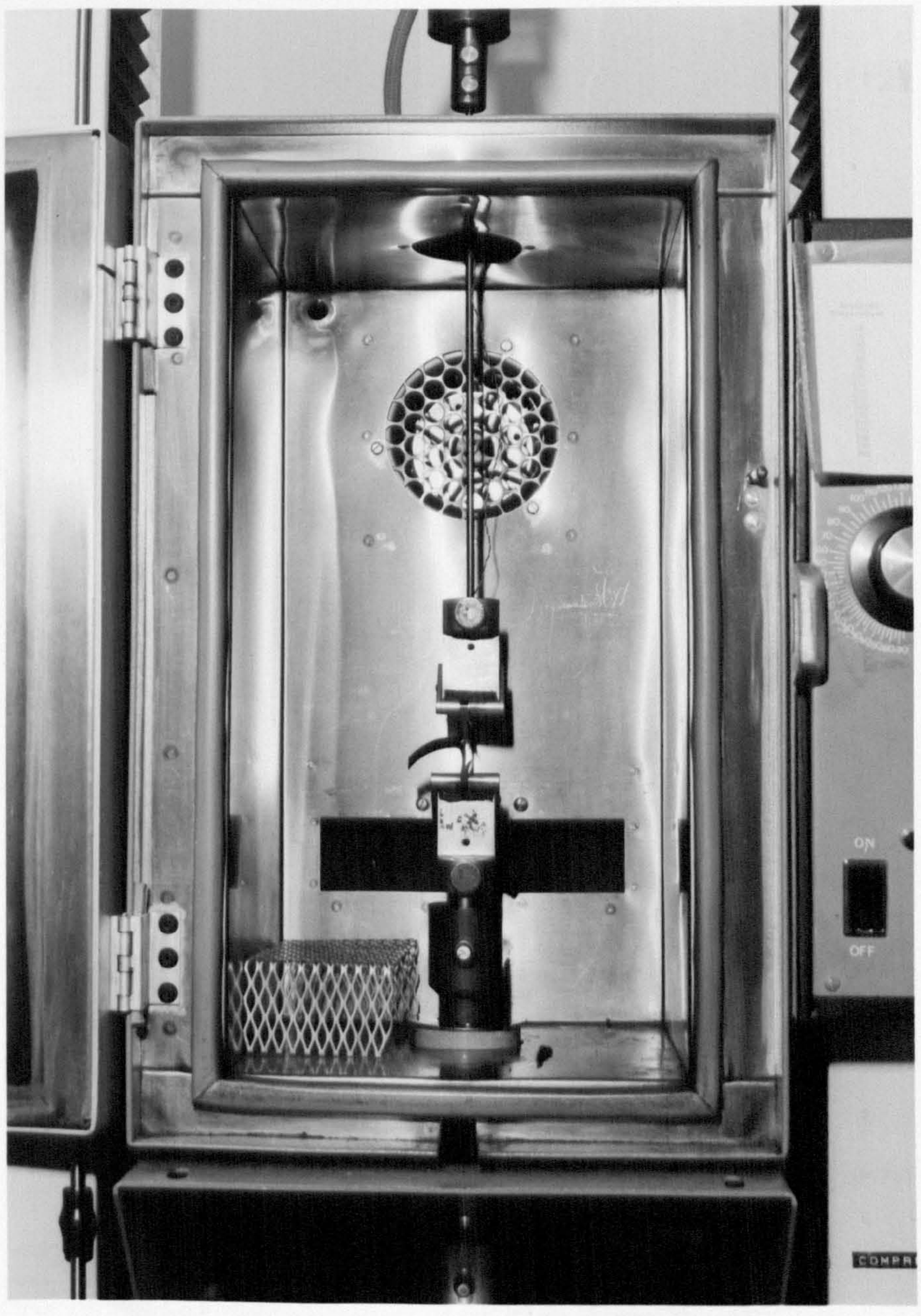

Figure 4.3: Temperature cabinet for tear testing at other than room temperature.

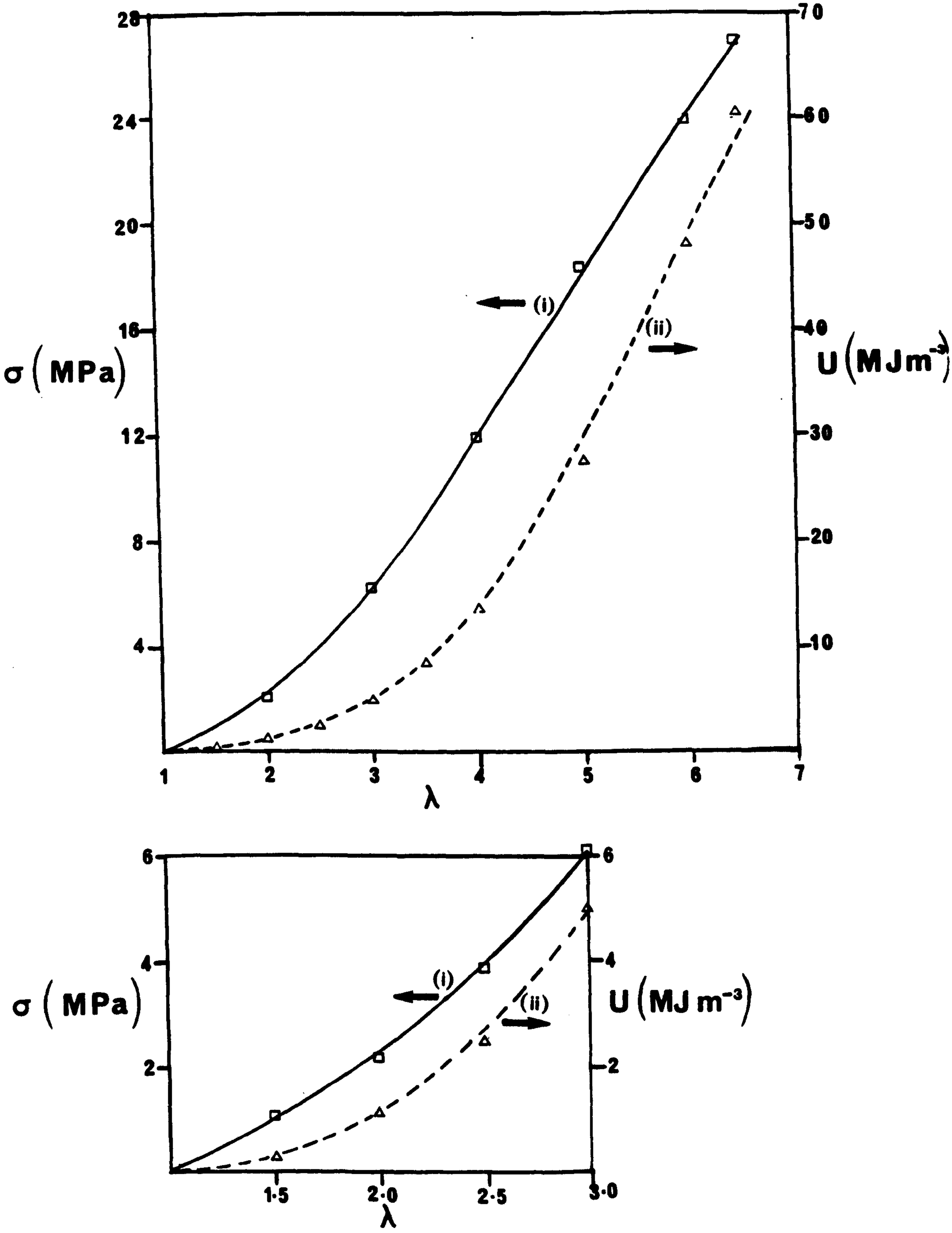

Figure 4.4: Stress, σ, and stored energy density, U, vs extension ratio, λ, black-filled (50 pphr HAF) NR vulcanizate (mix no. H1).

Curve (i) represents the stress and curve (ii) represents the stored energy density. (a) up to breaking extension (b) up to 200% strain.

Rate of extension 100 mm per minute, temperature 23°C.

the elastic strain energy density stored in the legs of the test-piece respectively, h is the thickness of the test-piece referred to the unstrained state, and w is the total width of the test piece. At small strain, that is when λ is not much greater than unity, the stress-strain relation is linear. In this region, equation 4.1 can be reduced to

$$T = \frac{F}{h}(\lambda + 1) \qquad (4.2)$$

as is shown in Appendix 4.1. When the legs of the test-piece are inextensible $\lambda \cong 1$, and equation 4.2 further reduces to

$$T = \frac{2F}{h} \qquad (4.3)$$

In this investigation, equation 4.2 was used throughout because of its accuracy and also its computation does not require a knowledge of strain energy density, U. The tearing force, F, was taken as the mean value of tear at initiation in the 'steady state' region, as shown schematically in Figure 4.2c, consistent with the approach suggested by Greensmith (16). The nominal stress in the legs of the test-piece was calculated, and the corresponding extension ratio, λ, was obtained from Figure 4.4b rather than from Figure 4.4a, because the former gave better descrimination than the latter. The average nominal thickness, h, was used unless the test piece tore at an angle. In cases like this, the actual torn zone was measured.

The reproducibility and accuracy of equation 4.2 was checked and compared with equations 4.1 and 4.3. The results are shown in Table 4.5. There are two important observations emerged from the results. First, the agreement between equations 4.2 and 4.1 was excellent. Furthermore, it shows that equation 4.2 still works satisfactorily even in the moderately high strain regions, where the stress-strain relationship was no more linear. Secondly, equation 4.3 gave tearing energies consistently lower by about 40% than did equations 4.1 and 4.2. This was attributed to extension ratio in the legs of the test-piece which was not taken into consideration in equation 4.3. Thus this gives good evidence that equation 4.3 is applicable only to situations where extension in the legs are absent which is consistent with the theory (19,29). The tearing energies

Table 4.5: Comparison of methods of calculating tearing energy
Tearing conditions: tear rate 830 µm s^{-1},
temperature 23°C. Data obtained from HAF black-filled NR vulcanizates (mix H1)

Av. force, F (N)	40.5	44.5	55.0	39.4	49.5	50.0	44.0	
Thickness, h (mm)	2.05	2.08	2.04	2.04	2.15	2.12	2.05	
Total width, w (mm)	15	15	15	15	15	15	15	
*σ (MPa)	2.63	2.85	3.60	2.58	3.07	3.14	2.86	
*λ	2.1	2.2	2.4	2.1	2.25	2.27	2.2	
*U (MJ m^{-3})	1.4	1.7	2.3	1.4	1.8	1.85	1.7	
								Mean
$T = \frac{2F\lambda}{h} - wU$ (kJ m^{-2})	61.97	68.63	95.15	60.18	76.60	79.32	68.94	72.97
$T = \frac{F}{h}(\lambda+1)$ (kJ m^{-2})	61.24	68.46	89.13	59.92	74.83	77.12	68.68	71.34
$T = \frac{2F}{h}$ (kJ m^{-2})	39.51	42.79	54.02	38.66	46.05	47.17	42.93	44.45

Footnote:

* The average tensile stress, σ, strain energy density, U, and the extension ratio, λ, refer to the simple extension region in the legs of the test piece. U and λ were determined from U vs. λ and σ vs λ plots respectively shown in Figure 4.4b.

quoted in this thesis are the average values obtained from four or five test-pieces calculated according to equation 4.2.

4.5 Determination of crack propagation rate

The rate of crack propagation, r, is given by the relation

$$r = \frac{s}{2\lambda} \qquad (4.4)$$

where s is the rate of extension. When the legs are inextensible λ becomes unity and the crack propagation rate, r, is half the cross-head speed (extension rate), that is

$$r = 0.5s \qquad (4.5)$$

Equation 4.5 was used to evaluate the rate, r, irrespective of the type of tear failure. Thus this gives an average value for the rate. Although it is not quantitatively valid for stick-slip tearing where the rate fluctuates with the tearing force, nevertheless it can still be considered as a parameter which gives some indication of the dependence of tear strength on rate. The same approach was used by Greensmith et al (16,29,32).

4.6 Measurement of the knot diameter

As discussed earlier in Section 2.3, tearing energy, T, is given approximately by

$$T \cong U_b d \qquad (4.6)$$

where U_b is the strain energy density at break and d is the diameter of the tip referred in the unstrain state. Thomas (22) and Greensmith (23) verified the relationship between tearing energy and diameter of the tear tip by making semi-circular tear tip model. There are no attempts yet, as far as the author is aware, to correlate tearing energy with the actual size of the diameter of the knot produced by vulcanizates that failed by knotty tearing. However, Greensmith (16) did observed that the knots were approximately semi-circular, and the size of the knots formed was about 2mm, which was of the same order of magnitude predicted by equation 4.6.

In this investigation, an attempt was made to correlate the tearing energy with the actual diameter of the knot formed by knotty tearing at different tear rate and temperature of measurements. The diameter of knot so measured at each tear rate and temperature would reflect the degree of blunting of tear tip. The smaller the knot diameter, the sharper the tear tip. Conversely, the larger the knot diameter, the blunter the tear tip. In this aspect of investigation, d was referred to the knot diameter formed by knotty tearing. d was estimated by measuring directly the knot diameter in the unstrained state, by means of an eye-piece lens scale. The scale had 150 divisions, each corresponding to 0.1 mm. The knot diameter can be read with an accuracy of about ±0.25 scale division. The measurement was possible because the knots were approximately semi-circular as shown schematically in Figure 4.5, and thus allowed the knot diameter to be measured with a fair accuracy. The corresponding tearing energy at each knot was noted from the tearing force chart. The measured knot diameter from the test-piece could then be compared with the value estimated from equation 4.6, since T and U_b were known. For example, if d_1 was the diameter of the first knot measured from the test-piece, then the corresponding value of d_1 estimated from the tearing force-chart was $d_1 = T_1/U_b$. T_1 was calculated using equation 4.2. The rest of the knots were measured and the corresponding theoretical values were calculated from the tearing force recorded in the chart in exactly the same manner. This was done on other test-pieces produced by tearing at other tear rates.

In this investigation, the value of U_b obtained by the method described above in Section 4.3 was used to estimate d from equation 4.6. Strictly speaking, it would be appropriate to determine U_b at similar rate at which the rubber at tear tip was brought to breaking point, using similar approach suggested by Greensmith (23). Because of time constraint, this was not done.

4.7 Methods of characterizing the type of tear failure

In steady tearing, the tear propagates steadily along the intended path. The tearing force does not fluctuate with the tear rate. In stick-slip tearing, the tear does not propagate at a steady rate, but rather, arrests and reinitiates (hence, stick-slip)

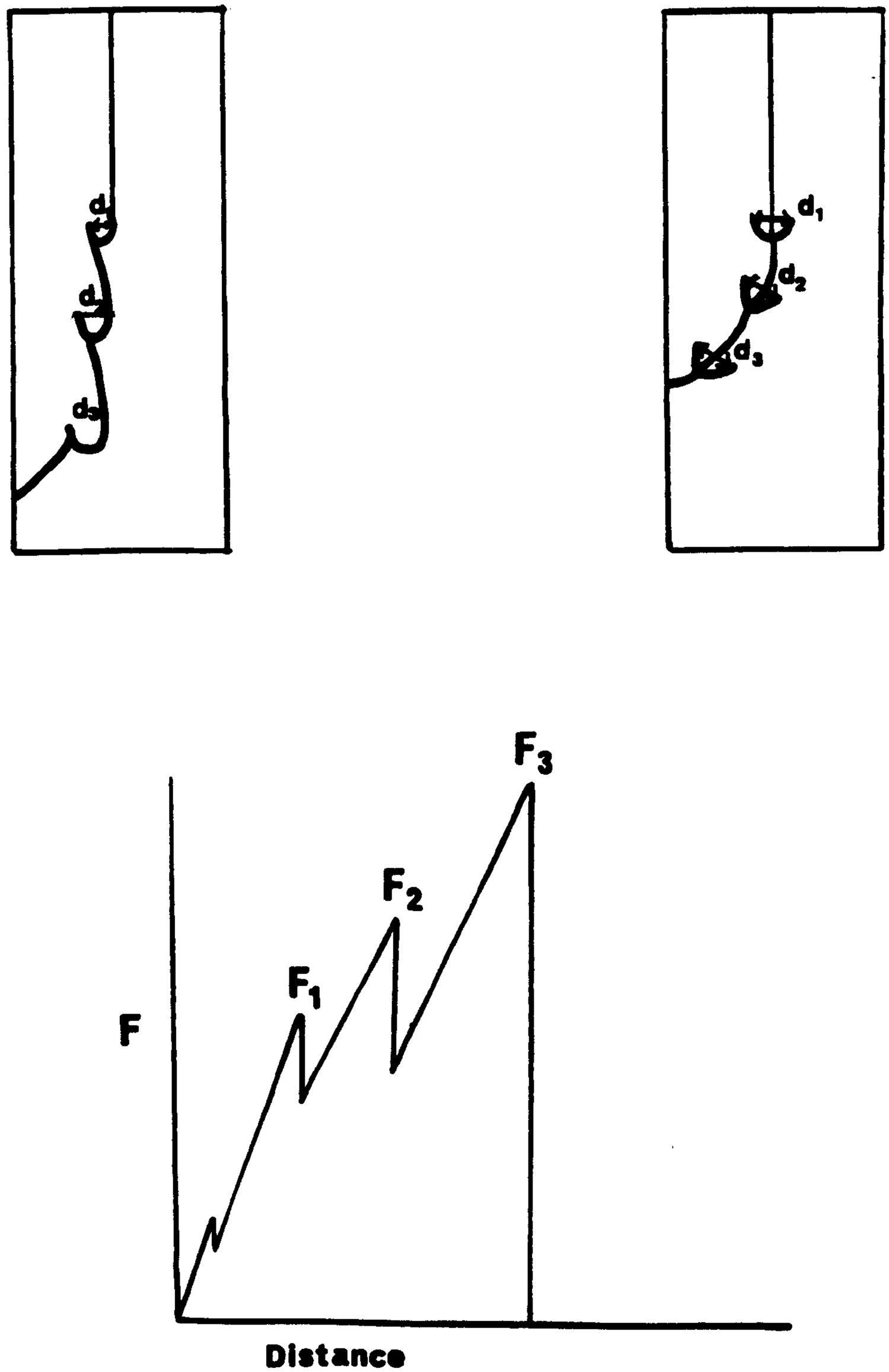

Figure 4.5: Schematic diagram showing shape of knots. The knot diameters d_1, d_2 and d_3 can be measured directly using an eye-piece lens scale. The values obtained can be checked against the calculated values: $d_1 = T_1/U_b$, $d_2 = T_2/U_b$ and $d_3 = T_3/U_b$. T_1, T_2 and T_3 can be calculated by substituting F_1, F_2 and F_3 respectively into $T = F(\lambda+1)h^{-1}$.

at fairly regular intervals. Correspondingly, the force necessary to propagate the tear varies widely from a maximum at tear initiation to a minimum at tear arrest. Figure 4.2c shows a schematic diagram of a tearing force-distance chart for a typical stick-slip tearing. The force, F_i, denotes the force to initiate tearing. In knotty tearing, the force, F_i, gradually increases with distance until a maximum is reached. As the force, F_i, builds up, the tear path deviates away from its original course, creating the knot. The tear tip broadens against the direction of tear propagation. When the maximum force is reached, the growth of the knot ceases and a new sharp tear tip is initiated. This new tear propagates forward very rapidly until the force minimum, F_a, is reached, then its growth is arrested. This cycle then repeats itself throughout the remainder of the test. According to Stacer, Yanyo and Kelly (44), the arrest force value is very significant since it apparently represents a minimum energy below which tear growth cannot proceed.

A method was introduced to classify the type of tear failure by means of calculating the tearing energy ratio, T_R. Tearing energy ratio was defined by the relationship

$$T_R = \frac{\text{Tearing energy at tear initiation}}{\text{Tearing energy at tear arrest}} \qquad (4.7)$$

Table 4.6 shows the tearing energy ratio for unfilled NR vulcanizates that failed by stick-slip tearing. Tearing energy at at tear initiation and tearing energy at tear arrest in Table 4.6 were plotted against tear rate on logarithmic scales because of the wide range of tear rate and tearing energy investigated. The plot is as shown in Figure 4.6 (curve a). The tearing energy ratio for stick-slip tearing ranging from 1.33 to 2.33. Table 4.7 shows the tearing energy ratio for NR vulcanizates filled with 30 phr of HAF black. Figure 4.6 (curve b) shows tearing energy at tear initiation and tearing energy at tear arrest plotted against tear rate, for the results shown in Table 4.7. The results show clearly that knotty tearing gave higher tearing energy ratio than that produced by stick-slip tearing. Tearing became less knotty with increasing rate as reflected by the decrease in knot diameter measured directly on the test-pieces. Correspondingly, the tearing energy ratio decreased. The results also show that, tearing energy at tear

Table 4.6: The ratio of tear initiation energy to tear arrest energy of unfilled NR vulcanizates (1 pphr dicumyl peroxide). Temperature of test 23°C.

Tear rate ($\mu m\ s^{-1}$)	4.2	42	170	420	830	4200	8300
T (initiation) ($kJ\ m^{-2}$)	6.65	8.8	9.7	13.4	12.1	8.28	8.1
T (arrest) ($kJ\ m^{-2}$)	5.0	6.0	6.0	6.0	6.0	5.6	5.8
T_R	1.33	1.47	1.62	2.23	2.02	1.48	1.40
Type of tear failure	s.s	s.s	s.s	s.s	s.s	s.s	s.s

Footnotes:

$T_R = \frac{\text{Tearing energy at tear initiation}}{\text{Tearing energy at tear arrest}}$

s.s - stick-slip tearing.

Table 4.7: The ratio of tear initiation energy to tear arrest energy of NR vulcanizates filled with 30 pphr HAF black (semi-EV vulcanization system). Base mix formulations as shown in Table 4.2. Temperature of test 23°C

Tear rate ($\mu m\ s^{-1}$)	4.2	42	170	420	830	4200	8300
T (initiation) ($kJ\ m^{-2}$)	146	113.88	60.17	65.32	60.61	36.74	41.39
T (arrest) ($kJ\ m^{-2}$)	41.71	29.97	18.23	17.19	20.2	16.70	24.35
T_R	3.5	3.8	3.3	3.8	3.0	2.2	1.7
Type of tear failure	k	k	k	k	k	k	k
"knot" diameter (mm)	2.0	2.9	1.0	1.1	1.03	0.4	0.8

Footnotes:

$T_R = \frac{\text{Tearing energy at tear initiation}}{\text{Tearing energy at tear arrest}}$

k - knotty tearing.

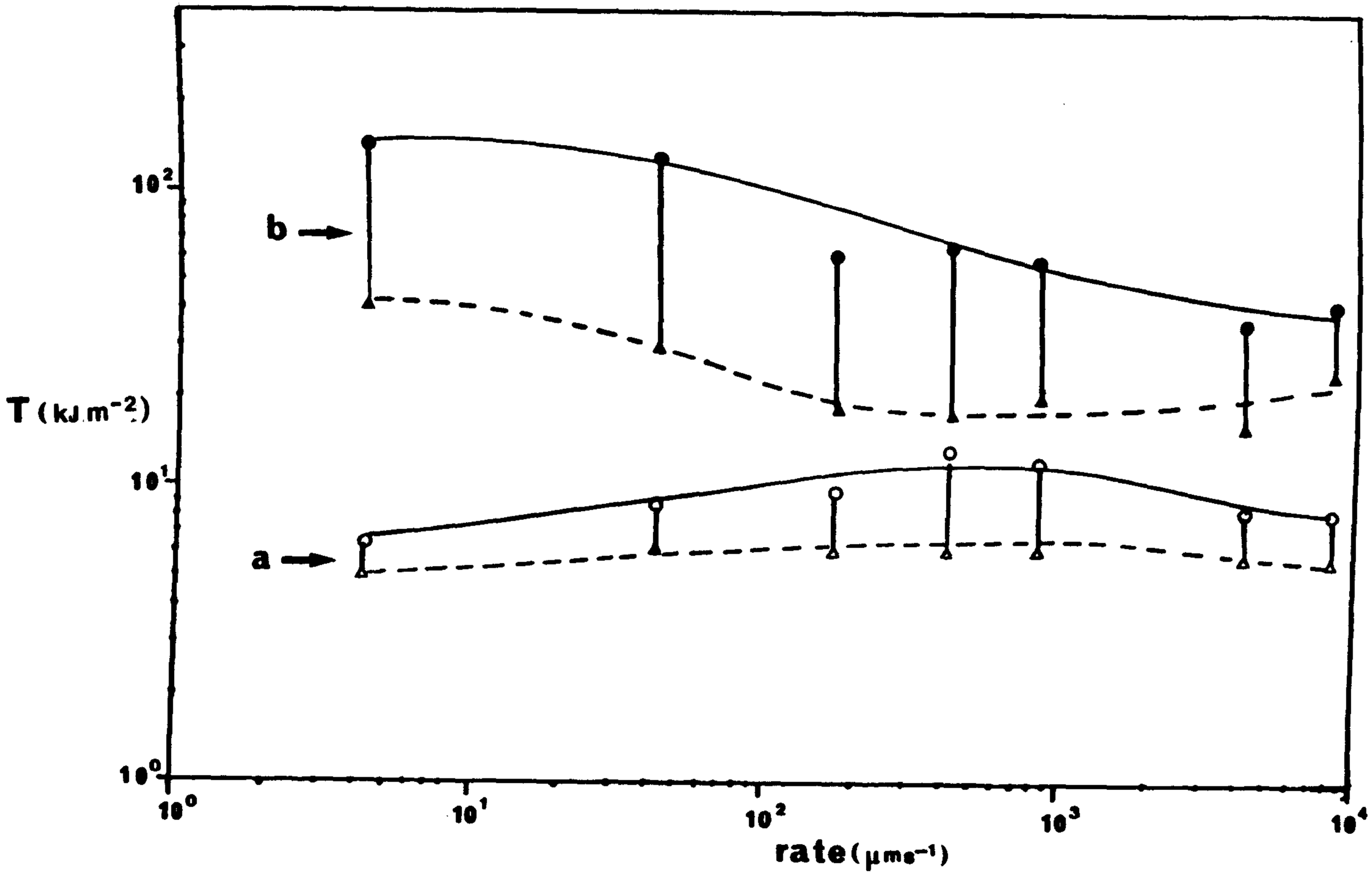

Figure 4.6: Tearing energy at tear initiation (full lines) and at tear arrest (broken lines) vs tear rate at 23°C. The vertical lines in (a) and (b) denote the magnitude of the difference between tearing force at tear initiation and tear arrest. Curves (a) denote stick-slip tearing obtained from unfilled NR peroxide vulcanizate. Curves (b) denote knotty tearing obtained from black-filled (30 pphr HAF) NR vulcanizate (semi-EV).

initiation fluctuates more than the tearing energy at tear arrest, which is consistent with the observations made by Stacer et al (44). They found that the standard deviations of the initiation values were significantly greater than those for the arrest. The tearing energies at tear initiation fluctuates more than those for the arrest probably because of the variations of tear-tip diameter at tear initiation is greater than those at tear arrest. According to Stacer, Yanyo and Kelly (44), stick-slip tearing can be viewed as a process alternating between a blunt tear tip at initiation and a sharp tip at arrest. The ratio of tearing energy at tear initiation to tearing energy at tear arrest was calculated and used to characterize the mode of tear failure as described below.

(i) knotty tearing: tearing was classified as knotty when (a) the tear propagated in stick-slip manner, (b) there was evidence of knots on the torn test-pieces. If the knots were not clearly defined, tearing energy ratio was used to charaterize the tear failure. In cases like this, tearing was classified as knotty if $T_R \geq 2.5$.

(ii) stick-slip tearing: tearing was classified as stick-slip when (a) the tear did not propagate at a steady rate, and (b) when tearing energy ratio was within the range from 1.05 to 2.5.

(iii) steady tearing: tearing was classified as steady when (a) the tear propagated at a steady rate, with minimum fluctuations of tearing force with tear rates, (b) tearing energy ratio did not exceed 1.05.

4.8 Measurement of relative crosslink concentration

The evaluation of crosslink concentration can be done by means of stress-strain measurements in simple extension or by means of measurements of equilibrium swelling. Both methods work satisfactorily for unfilled rubbers. In the case of black-filled rubbers, it has been suggested that the swelling method is more reliable than simple extension method (52), because the latter method is affected by complications associated with stiffening due

to 'black structure', non-affine deformation, and other factors. It has been suggested also that fillers appear to have less drastic effects on swelling properties (52). For these reasons, the crosslink concentration was assessed by the swelling method as suggested by Porter (52).

Samples were weighed accurately using an Oetling electronic analytical balance (model LA 164). They were then swollen in n-decane at 25°C for five days to attain the equilibrium state (i.e., when the swollen weight became constant). n-Decane has a molecular weight of 142.29, its density at 25°C is about 0.7264 gm cm^{-3} (54). Fresh n-decane was used after 48 hours to remove the sol materials (52). The equilibrium swollen weight was determined first, before drying the samples in a vacuum oven at 50°C until the weight was constant. The final weight of the dried samples were then noted. The volume of solvent absorbed, V_s, was calculated from the difference of the weights of the swollen and dried samples. The volume fraction of rubber in the swollen sample, υ_r, was calculated and corrected for the volume occupied by the carbon black and zinc oxide particles, using the relationship (52,54)

$$\upsilon_r = \frac{V_{RN}}{V_{RN} + V_s} \qquad (4.8)$$

where V_{RN} is volume of rubber network. The rubber network (RN) refers to the network formed from the rubber hydrocarbon and the curative by the vulcanization process, including any atoms or groups introduced in crosslinks or as modifications of the main rubber chains (53). V_{RN} was calculated from the initial weights of the samples and the mix compositions, using the relationship (54)

$$V_{RN} = \frac{(M_{RN})(M_O)}{(M_m)(\rho_{RH})} \qquad (4.9)$$

where M_{RN} is the weight of rubber network, i.e., the weight of rubber hydrocarbon (RH) and sulphur combined (54), M_m is the total weight of mix composition, M_o is the initial weight of the sample and ρ_{RH} is the density of rubber hydrocarbon. The calculation was based on the assumption that all the acetone insoluble material present in the raw rubber was present in the network, i.e., that there was no sol rubber (52,54). According to Porter (52), the assumption is justified provided that $\upsilon_r > 0.22$.

The results in Tables 4.4a, 4.4b, 4.4c and 4.4d, show that all the networks had values $\upsilon_r > 0.22$, consistent with the suggestion of Porter (52). The mean value of υ_r obtained from three samples was then substituted into the Flory-Rehner equation for the equilibrium swelling of rubber networks (55).

$$-\ln(1-\upsilon_r)-\upsilon_r-\Psi\upsilon_r^2 = 2\rho V_o[X]_{phys}(\upsilon_r)^{1/3} \qquad (4\cdot10)$$

where Ψ is the rubber-solvent interaction parameter, and has a value of 0.42 for NR in n-decane (57,62), and 0.639 for SBR in n-decane, V_o is the molar volume of solvent, and has a value of $195.88cm^3$ for n-decane, ρ is the density of rubber hydrocarbon, and has a value of 0.92 gm per cm^3 for NR (60) and 0.94 gm per cm^3 for SBR (60), and $[X]_{phys}$ is the physically manifested crosslink concentration. For a network containing tetrafunctional crosslinks only, the number of network chains is twice the number of crosslinks (58). Hence the number of crosslinks per unit weight of rubber is $N/2M_c$, where N is Avogadro's number, and M_c is the average molecular weight between crosslinks. The crosslink concentration expressed in ``gram molecules'' per gram of rubber is thus

$$[X]_{phys} = \frac{1}{2M_c} \qquad (4.11)$$

Equation 4.10 was later modified by Flory (56) to give

$$-\ln(1-\upsilon_r)-\upsilon_r-\Psi\upsilon_r^2 = 2\rho V_o[X]_{phys}(\upsilon_r^{\frac{1}{3}}-\frac{\upsilon_r}{2}) \qquad (4\cdot12)$$

There is no experimental evidence to justify the use of equation 4.12 in preference to equation 4.10 or vice versa and both of these equations are currently used. While there is preference for the modified equation 4.12, in the absence of experimental verification some workers, notably at MRPRA prefer to use the simpler original form, equation 4.10, until the question of the validity $-\upsilon_r/2$ term has been settled (52,53,54,57,58). It was beyond the scope of this thesis to debate this issue any further.

The determination of $[X]_{phys}$ from equation 4.10 or 4.12 is critically dependent on the value of the polymer-solvent interaction parameter, Ψ. Ψ must first be determined accurately, by substituting C_1 into either equations 4.13 or 4.14 (57). C_1 can

be determined by an independent method, for example, by equilibrium stress-strain measurement.

$$-\ln (1-\upsilon_r)-\upsilon_r-\Psi\upsilon_r^2 = 2C_1V_o\,\upsilon_r^{\frac{1}{3}} \qquad (4.13)$$

$$-\ln (1-\upsilon_r)-\upsilon_r-\Psi\upsilon_r^2 = 2C_1V_o\,(\upsilon_r^{\frac{1}{3}}-\frac{\upsilon_r}{2}) \qquad (4.14)$$

A Ψ value of 0.42, for NR swollen in n-decane was used in this investigation. This Ψ value was determined by Bristow (57) who determined C_1 by stress-strain measurement, and substituted the C_1 value which he obtained into the unmodified Flory-Rehner equation, i.e., equation 4.13. For this reason, the unmodified Flory-Rehner equation for equilibrium swelling, i.e., equation 4.10 was used in the present investigation. Furthermore equation 4.10 is simpler than equation 4.12 and adequate for the present purpose.

According to Porter (52), black-filled vulcanizates give larger values of $[X]_{phys}$ than the actual values of $[X]_{phys}$ observed for the corresponding unfilled vulcanizates. This apparent enhancement of crosslink concentration observed in black-filled vulcanizates may result from one or more of four causes:

(i) the filler may cause an increase in crosslinking efficiency of the vulcanizing agent, thus leading to additional polymer to polymer crosslinks.

(ii) the presence of the filler may enhance (by some unspecified mechanism) the degree to which existing polymer to polymer crosslinks or physical chain entanglements (or both) restrict swelling of the rubber.

(iii) the filler may restrict the swelling of the rubber because of adhesion of the rubber to the filler surface either by physical adsorption or through the formation of rubber to filler bond.

(iv) the filler may alter the affinity of the swelling agent for rubbers as reflected in the magnitude of the parameter Ψ.

By assuming that the polymer solvent interaction parameter, Ψ

and the molecular weight of the rubber in the mix are little altered by the presence of the carbon black, Porter (52) developed an empirical formula which allows the actual concentration of crosslinks in any natural rubber vulcanizate containing a known volume of HAF black to be determined. He found that there was a simple ~~linear~~ relationship between the apparent and actual crosslink concentratios, i.e.,

$$[X]_{act.} = \frac{[X]_{phys}}{1 + k\phi} \qquad (4.15)$$

where $[X]_{phys}$ is the <u>apparent</u> physically manifested crosslink concentration calculated from equation 4.10, k is a constant characteristic of the filler and has a value of 2.6 for HAF black, and Φ is the volume fraction of carbon black in the vulcanizate. For NR vulcanizates containing 50 pphr of HAF black, Φ is 0.2036, and Φ is 0.1355 for SBR filled with 30 pphr of HAF black. Equation 4.15 implies an apparent increase in physical crosslinking of 50% at a black concentration of 50 pphr (52). Equation 4.15 was used to estimate the <u>actual</u> concentration of physical crosslinks in the vulcanizate network.

APPENDIX 4.1

Derivation of equation 4.2

For a perfectly elastic body, the stress-strain relationship is linear and is said to obey Hooke's Law, ie.,

$$\sigma = Ee$$

where E is the Young's modulus of the material. Strain energy can be defined as the energy which is stored within a material when work has been done on the material. For a perfectly elastic body, the material remains elastic whilst work is done on it so that all the energy is recoverable. Thus strain energy U is the work done, W, on the body. The strain energy per unit volume (resilience) is given by the area under the stress-strain graph as shown schematically below

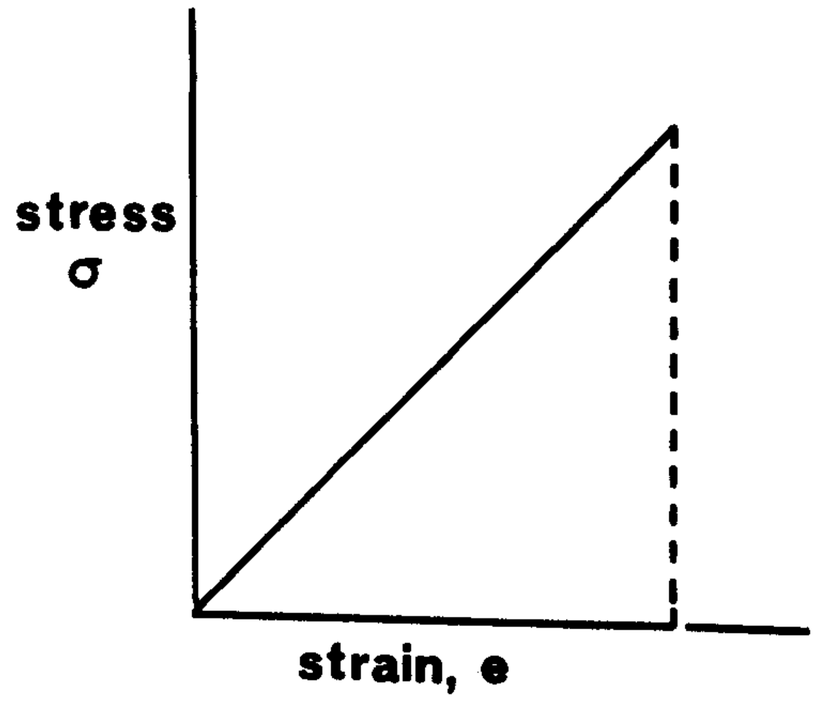

$$U = \frac{1}{2}\sigma e \qquad \text{(i)}$$

We have

$$T = \frac{2F\lambda}{h} - wU \qquad \text{(ii)}$$

The stress in the legs of the trouser test-piece is given by

$$\sigma = \frac{2F}{wh} \qquad \text{(iii)}$$

The strain e in the legs of the trouser test-piece is given by

$$e = \lambda - 1 \qquad \text{(iv)}$$

Substituting (iii) and (iv) into (i) gives

$$U = \frac{F}{wh}(\lambda - 1) \qquad \text{(v)}$$

Substituting (v) into (ii) gives

$$T = \frac{F}{h}(\lambda + 1) \qquad \text{(vi)}$$

Equation (vi) is the tearing energy equation for a trouser test-piece which takes account of the extension ratio in the legs of the test-piece.

CHAPTER FIVE

FACTORS WHICH AFFECT THE DEVELOPMENT OF KNOTTY TEARING
RESULTS AND DISCUSSIONS

5.1 What are the factors?

The range of tear rates and temperatures where knotty tearing can occur provides a relative measure of the reinforcing action of carbon black in a particular rubber vulcanizate. Some of the factors which affect the development of knotty tearing have been identified. These include the degree of strain-crystallization, the molecular mobility, filler loading, nature of carbon black particles, nature and concentration of crosslinks, and, most important of all, the strength anisotropy. All these factors are discussed here except the strength anisotropy, which will be discussed separately later in Chapter Seven.

5.2 Effect of strain-crystallization

The effect of strain-crystallization on the development of knotty tearing is clearly noticeable by considering the results shown in Figure 5.1. Here, the tearing energy of three rubbers (NR, ENR25, and ENR50) which strain-crystallize to different extents is plotted against tear rate using logarithmic scales because of the wide range of tearing energy and rate covered. The tear behaviours of these rubbers were compared with those of two non-strain-crystallizing rubbers (SBR and INR). All the rubbers were filled with 50 pphr HAF black, and a semi-EV vulcanization system was employed in each case. The full formulations were given in Table 4.3b of Chapter Four. Tearing measurements were carried out at 23°C using trouser tear test-pieces. The results are also presented in tabulated form as shown in Table 5.1A.

The readiness of each rubber to produce knotty tearing can be judged from the range of tear rates where knotty tearing occurred at this particular temperature. NR and ENR25, which readily strain-crystallize, produced knotty tearing over the whole range of tear rates investigated here. Figures 5.2a and b show the type of knotty

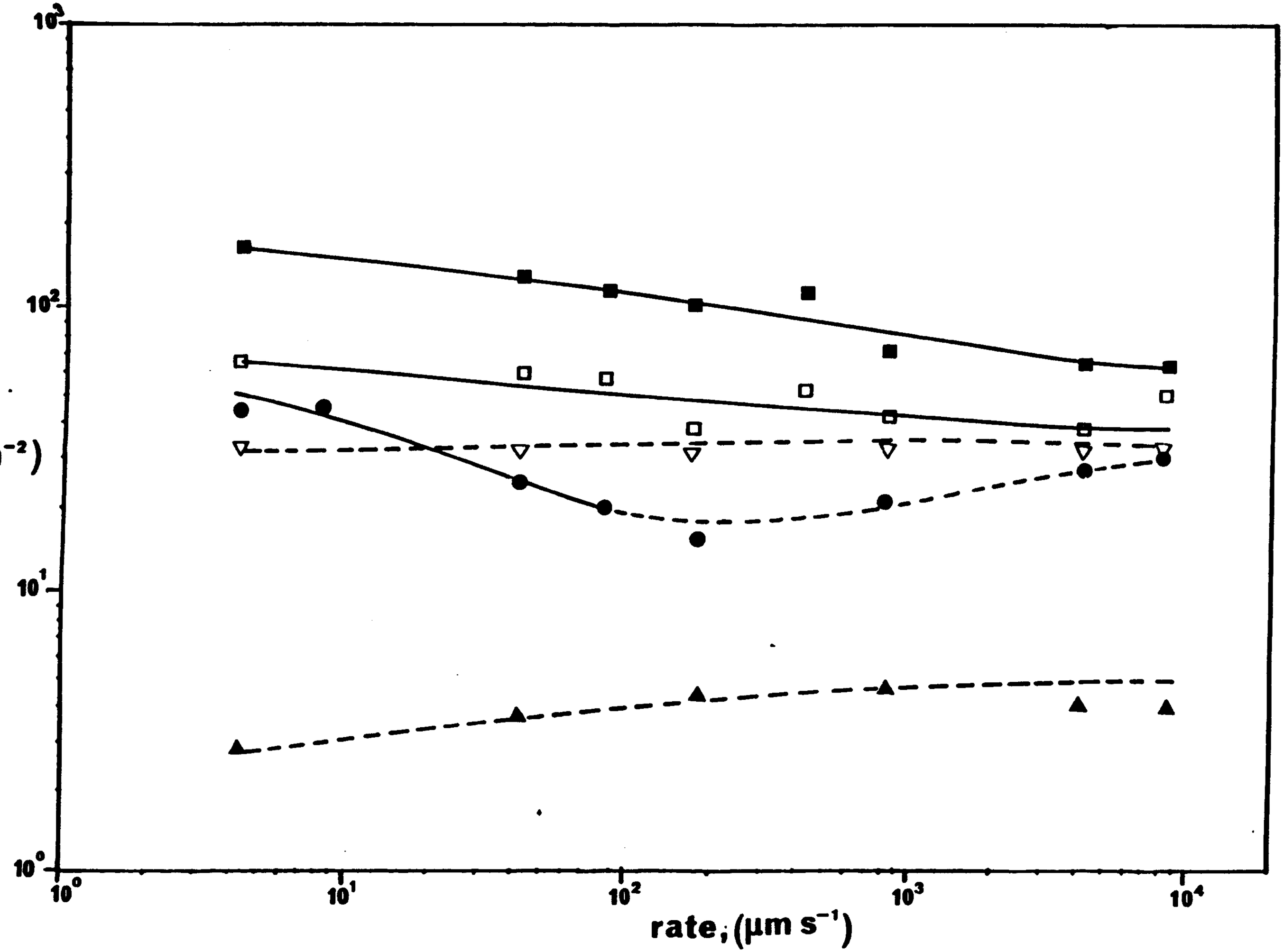

Figure 5.1: Tearing energy vs tear rate, showing effect of strain-crystallization on development of knotty tearing. Temperature 23°C. Formulations shown in Table 4.3b.

Table 5.1A: Comparison between tearing energy of strain-crystallizing and non-strain-crystallizing rubber vulcanizates at 23°C. Full formulations are shown in shown in Table 4.3b in Chapter Four.

Tear rate ($\mu m\ s^{-1}$)	4.2	42	170	420	830	4200	8300
NR, T ($kJ\ m^{-2}$)	165	133	100	110	70	64	62
Type of tear failure	k	k	k	k	k	k	k
ENR 25, T ($kJ\ m^{-2}$)	66	66	38	54	43	38	50
Type of tear failure	k	k	k	k	k	k	k
ENR-50, T ($kJ\ m^{-2}$)	44	24	15	18	21	27	32
Type of tear failure	k	k	s	s	s	s	s
SBR, T ($kJ\ m^{-2}$)	34	34	33	-	33	35	34
Type of tear failure	s	s	s	-	s	s	s
INR, T ($kJ\ m^{-2}$)	2.7	3.6	4.2	-	4.6	4.0	4.0
Type of tear failure	s	s	s	-	s	s	s

k - knotting tearing s - steady tearing

Table 5.1B: Comparison between tearing energy of strain-crystallizing and non-strain crystallizing rubber vulcanizates at the same molecular mobility to that of NR at 23°C. Full formulations are shown in Tables 4.3b in Chapter Four.

Tear rate ($\mu m\ s^{-1}$)	8.3	42	170	420	830	1700	4200	8300
ENR-25, T ($kJ\ m^{-2}$)	95	63	72.4	55	62	37.3	37	51
Type of tear failure	k	k	k	k	k	k	k	k
ENR-50, T ($kJ\ m^{-2}$)	80	52	52	45	32	41	36	31
Type of tear failure	k	k	k	k	k	k	k	k
SBR, T ($kJ\ m^{-2}$)	20	21	22	22	22.5	-	23	20
Type of tear failure	s	s	s	s	s	-	s	s

k - knotty tearing s - steady tearing

Temperature: ENR-25 47°C, ENR-50 68°C, SBR 32°C

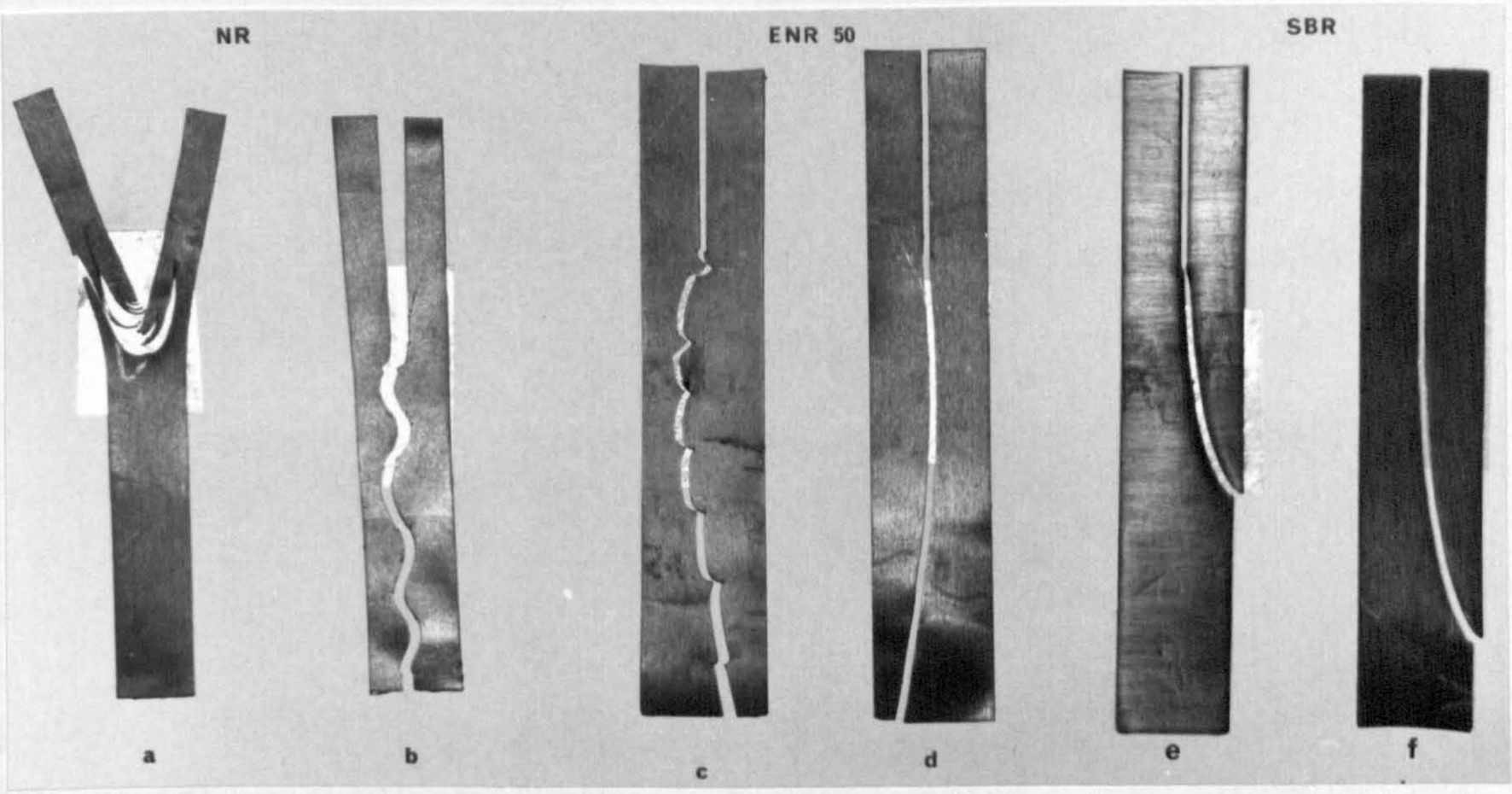

Figure 5.2: Photographs showing the types of tear failure at 23°C at (a) 4.2 μm s^{-1} (b) 830 μm s^{-1} (c) 83 μm s^{-1} (d) 830 μm s^{-1} (e) 4.2 μm s^{-1} (f) 8300 μm s^{-1}

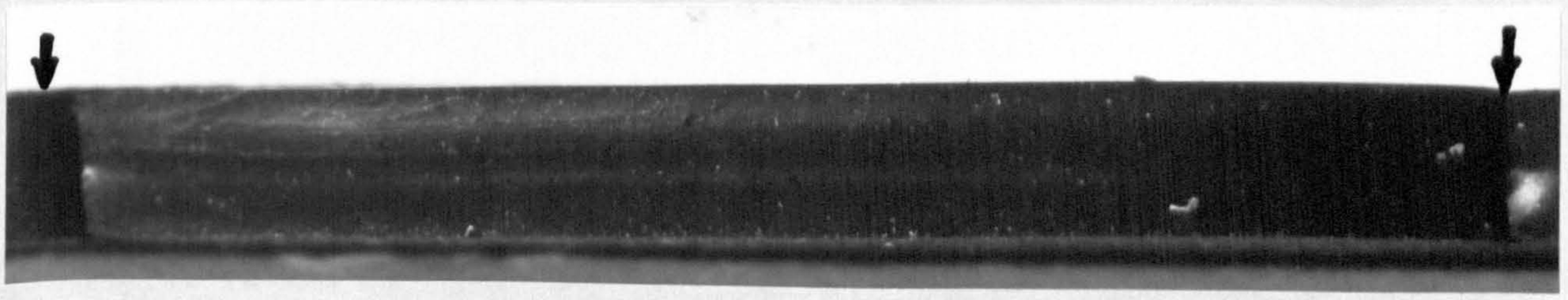

(a) Fractured surface of knotty tearing of ENR 25 (8x magnification)

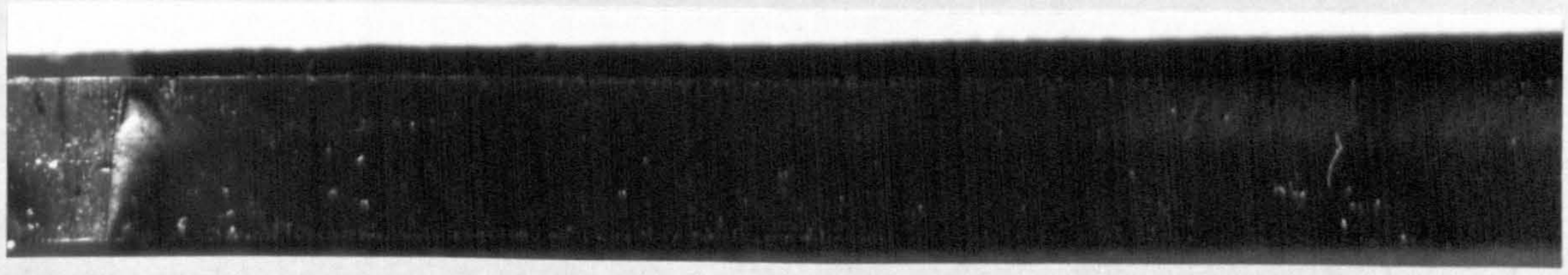

(b) Fractured surface of steady tearing of ENR 50 (8x magnification)

(c) Fractured surface of steady tearing of SBR (8x magnification)

Figure 5.3: Photographs showing fractured surfaces of black-filled rubber vulcanizates (50 pphr of HAF) at 23°C

tearing produced by NR at tear rates of 4.2 μm s^{-1} and 830 μm s^{-1} respectively, and Figure 5.3a shows the fractured surface of ENR 25 at tear rate of 830 μm s^{-1}. The arrows in Figure 5.3a indicate the deviated crack, perpendicular to the fracture plane. In the case of ENR50 which strain crystallizes less readily than NR and ENR 25, and also has lower molecular mobility than NR and ENR 25, (since the θ_g of ENR 50 is higher than the θ_g of NR and ENR 25), knotty tearing occurred over a narrow range of tear rates. At this particular temperature, knotty tearing occurred at slow tear rates ranging from 4.2 μm s^{-1} to 83 μm s^{-1}, and the type of knotty tearing produced is shown in Figure 5.2c. At tear rates greater than 83 μm s^{-1}, the lower molecular mobility may not allow the strengthening structures to develop rapidly enough around the tip to produce the strength anisotropy necessary for the occurrence of knotty tearing. Thus tearing proceeded steadily as shown in Figure 5.2d producing the smooth fractured surface shown in Figure 5.3b.

In the case of SBR and INR, although the molecular mobility is higher than that of ENR50, they are non-strain-crystallizing rubbers, and so knotty tearing was not observed. At this particular temperature, they produced the steady type of tearing shown in Figure 5.2 (e and f) at all tear rates investigated, with the relatively smooth fractured surfaces shown in Figure 5.3c.

From Table 5.1A, it is rather surprising to see that in steady tearing regions, tearing energies of black-filled SBR vulcanizates were higher than the tearing energies of black-filled ENR 50 vulcanizates. It was expected that a ENR 50 black-filled vulcanizate would produce higher tearing energy than that produced by an SBR material because the former is more hysteresial than the latter. ENR 50 is more hysteresial than SBR because the former can strain-crystallize and has higher glass-transition temperature than SBR. It is not entirely clear why the tearing energy of black-filled ENR 50 in steady tearing regions is lower than the tearing energy of black-filled SBR. According to Andrews and Walsh (11), the strength of filler-rubber interaction appears to be an important parameter in promoting high hysteresis and hence high tear strength. Poorly-adhering filler which separates at low stresses exerts no influence on tear strength. It may be that the filler-rubber interaction in ENR 50 is lower than the filler-rubber

interaction in SBR. Experiments along the lines described by Andrews and Walsh (11) to check the strength of filler-rubber interaction might be used to shed some light on the matter.

The tearing energies of isomerised NR over a wide range of tear rates were very low. The tearing energies of the black-filled isomerised NR was a factor of about 2 higher than the corresponding unfilled vulcanizates. The tear behaviour of unfilled vulcanizates will be discussed later, in Section 5.5. As far as the author is aware, there is no previous published work on the tear strength of black-filled isomerised NR for comparison with the values obtained in the present investigation.

Greensmith (16) also investigated the effect of temperature and tear rate on the development of knotty tearing of NR and SBR (GR-S then known as) vulcanizates filled with 50 pphr of HAF black. Table 5.2a shows the comparison between the results of Greensmith and those obtained in the present investigation for NR vulcanizates filled with 50 pphr of HAF black. Table 5.2b shows a similar comparison for SBR vulcanizates filled with 50 pphr of HAF black. Considering the results shown in Table 5.2a, there is no conflicting evidence with regard to the mode of tear failure. Both Greensmith's results and the results obtained from the present investigation indicate that knotty tearing occurred in black-filled NR vulcanizates at tear rates ranging from 4.2 $\mu m\ s^{-1}$ to 8300 $\mu m\ s^{-1}$, at 23°C. There appears be a descrepancy with respect to the magnitude of tearing energy which can be attributed to the method of calculation. Greensmith (16) calculated the tearing energy of a trouser tear test-piece using the relationship,

$$T = 2Fh^{-1} \qquad (5.1)$$

whereas the tearing energy of a trouser tear test-piece in the present investigation was calculated using the relationship,

$$T = F(\lambda + 1)h^{-1} \qquad (5.2)$$

where F is the tearing force at tear initiation, h is the nominal thickness and λ is the extension ratio in the legs of the test-piece. Equation 5.2 reduces to equation 5.1 when λ=1, i.e.,

Table 5.2a: Comparison between tearing energy results of Greensmith (16) with tearing energy results obtained from the present investigation

Temperature 23°C, NR filled with 50 pphr of HAF black

Tear rate ($\mu m\ s^{-1}$)	4.2	42	170	420	830	4200	8300
T($kJ\ m^{-2}$),Greensmith (16)	63	63	45	44	42	25	11
Type of tear failure	k	k	k	k	k	k	k
*$T=F\ h^{-1}(\lambda+1)(kJ\ m^{-2})$	165	133	100	110	70	64	62
Type of tear failure	k	k	k	k	k	k	k
*$T= 2F\ h^{-1}(kJ\ m^{-2})$	84	67	52	44	43	25	21

* - present investigation

k – knotty tearing **s – steady tearing**

TABLE 5.2b

Comparison of tearing energy results of Greensmith (16) with tearing energy results obtianed from the present investigation

Temperature 23°C SBR fulled with 50pphr of HAF black

Tear rate ($\mu m\ s^{-1}$)	4.2	42	170	830	4200	8300
T ($kJ\ m^{-2}$), Greensmith (16)	**63**	**16**	**17**	**18**	**18**	**18**
Type of tear failure	k	s	s	s	s	s
*$T=F\ h^{-1}(\lambda+1)\ (kJ\ m^{-2})$	34	34	33	34	34	34
Type of tear failure	s	s	s	s	s	s
*$T=2F\ h^{-1}(kJ\ m^{-2})$	**24**	**24**	**23**	**24**	**25**	**25**

* - present investigation

when there is no extension in the legs of the test-piece. In order to eliminate such extension, Greensmith (16) used trouser tear test-pieces having wider legs (total width of 4 cm) than the trouser tear test-pieces used in the present investigation (total width of 1.5 cm). However, the approach used by Greensmith (16) was suitable only for weak rubber vulcanizates such as unfilled SBR (29). In the case of strong rubber vulcanizates, particularly black-filled vulcanizates, extension in the legs of the test-piece cannot be eliminated simply by using wide trouser tear test-piece. Earlier investigation by the author using a trouser tear test-piece having dimensions similar to that used by Greensmith, indicated that extension in the legs of the test-piece was still considerable and significant. In cases like this, equation 5.2 is more appropriate than equation 5.1. This aspect was discussed earlier in Section 4.4 in Chapter Four.

When the tearing energy results of Greensmith are compared with the tearing energy results obtained from the present investigation calculated using equation 5.1, the agreement between the two is very good. Thus this indicates clearly that the apparent descrepancy discussed above is to be attributed to the method of calculating the tearing energy. Thus it is important that the extension in the legs of the test-piece is taken into account when calculating tearing energy of a trouser tear test-piece. Otherwise the results obtained will be somewhat misleading.

Similarly, the magnitude of tearing energy of black-filled SBR obtained by Greensmith was about 50% lower than the tearing energy obtained from the present investigation. However, if the tearing energy in the present investigation is calculated using equation 5.1, the results obtained are of the same order of magnitude obtained by Greensmith, as shown in Table 5.2b. However, there is a minor disagreement with respect to the range of tear rate over which smooth tearing can occur. Greensmith (16) found that, at 25°C steady tearing occurred in black-filled SBR vulcanizates at tear rates ranging from 42 $\mu m\ s^{-1}$ to 8300 $\mu m\ s^{-1}$, and at tear rate of 4.2 $\mu m\ s^{-1}$, knotty tearing occurred. The present investigation shows that at 23°C, steady tearing occurred in black-filled SBR at tear rate ranging from 4.2 $\mu m\ s^{-1}$ to 8300 $\mu m\ s^{-1}$. Thus overall the results obtained from the present investigation, agree very well with those of Greensmith (16).

The results so far seem to indicate that strain-crystallization effectively increases the range of tear rates over which knotty tearing can occur. It may be that crystallization helps to promote knotty tearing, presumably by enhancing further the strength anisotropy already induced by the carbon black. Comparison between NR and INR provides convincing evidence on the role of strain-crystallization in promoting knotty tearing. This is because the issue of molecular mobility can be avoided, because both NR and INR have approximately the same glass-transition temperature. The comparison also shows that knotty tearing is an effective way by which carbon black enhances the tear strength. For examples, at tear rates of 4.2 μm s^{-1} and 8300 μm s^{-1}, the tearing energy of the NR vulcanizate was about 60 times and 15 times respectively higher than that of INR vulcanizate.

The results shown in Figure 5.1 do not discriminate between the effects attributable to strain-crystallization and those attributable to molecular mobility, except for the case of NR and INR. In order to match the molecular mobility to that of NR at 23°C, the test temperatures for the ENR 25, ENR50 and SBR vulcanizates were raised appropriately by the difference between the θ_g of the rubber and that of NR according to the relationship

$$\theta = (\theta_g - \theta_{gNR}) + 23°C \qquad (5.3)$$

where θ_g is the glass-transition temperature of the rubber, θ_{gNR} is the glass-transition temperature of NR, and θ is the test temperature required to match the molecular mobility to that of NR at 23°C. The results are shown in Figure 5.4, where tearing energy is again plotted against tear rate using logarithmic scales. The table at the top right-hand side of the plot shows the temperature, θ, which was calculated to be necessary to match the molecular mobility to that of NR at 23°C, and also the mode of tear failure. It is interesting to see that ENR50 produced knotty tearing over the whole range of tear rates, if its molecular mobility was increased sufficiently to allow rapid development of strengthening structures around the tip to produce the necessary strength anisotropy. This indicates that molecular mobility also plays an important role in promoting knotty tearing. It should be noted also that the amount of

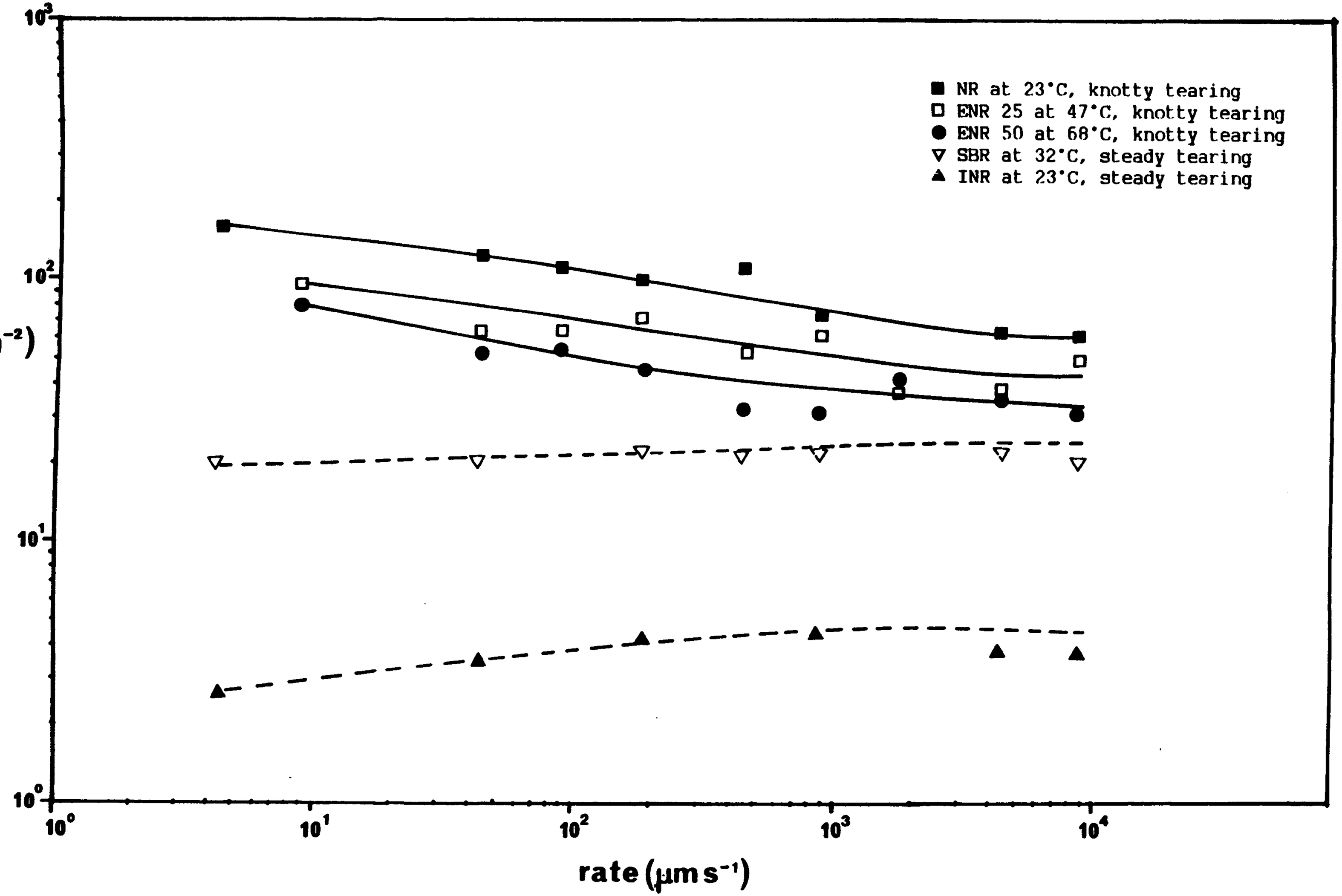

Figure 5.4: Tearing energy vs tear rate, showing effect of strain-crystallization at the same molecular mobility as NR on development of knotty tearing.

strain-crystallization which occurs may be reduced as the temperature of testing was raised. However, it has been suggested that the crystals are not completely melted and that residual crystals still remain around the tear tip, even at high temperatures up to 150°C (63). The results shown in Table 5.1B and in Figure 5.4 still show that the tearing energy increases with increasing degree of strain-crystallisability of the rubber.

In the case of black-filled SBR vulcanizates, raising the test temperature still did not produce knotty tearing. Perhaps the molecular mobility was still not sufficient to promote rapid development of strengthening structures around the tip and thus to produce strength anisotropy. Thus the findings so far indicate that the readiness of the vulcanizate to produce knotty tearing, as reflected by the range of tear rates where knotty tearing occurs, follows the order of the degree of strain-crystallization of the rubber. According to Greensmith (16), the mechanism by which crystallization helps to promote knotty tearing might be associated with the strengthening effect of crystallization, ensuring that the stress at the tip is always sufficiently high for the carbon black structure to form around the tip there. Furthermore, the crystallites themselves may be regarded as providing strengthening structures, additional to those associated with the carbon black. In the case of black-filled non-strain-crystallizing rubber vulcanizates, Medalia (49) suggested that the strengthening structures could be formed by alignment of carbon black aggregates and their linkage into chains or strands.

Thus there are three important points that can be learned from the results shown in Figures 5.1 and 5.4 respectively.

(i) The range of tear rate over which knotty tearing can occur increases with increasing degree of strain-crystallization.

(ii) The magnitude of tearing energy also increases with increasing degree of strain-crystallization.

(iii) The internal viscosity of the rubber also plays an important role in promoting knotty tearing.

5.2.1 Variation of tearing energy with tear rate

Referring to Figure 5.1 again, it is evident that the tearing energy varies with the tear rate. In smooth tearing regions, the tearing energy increases slightly with increasing tear rate. In contrast, in knotty tearing regions, the tearing energy decreases with increasing tear rate. In the former case, the increase in tearing energy is associated with the increase in energy dissipation (hysteresis) with rate. In the latter case, the variation in tearing energy is associated with the strengthening structures which require an appreciable time to form (16). At low tear rates, the degree of anisotropy increases and causes large tear deviations as reflected by the large knot diameter shown in Figure 5.2a. At a higher tear rate, the time scale is shorter, the black structure has less time to develop, and the degree of anisotropy developed may not be great. This is reflected in the small-scale tear deviations as shown in Figure 5.2b. Greensmith (16) also suggested that both the stress and extension at the tip could influence the development of strengthening structures, for the amount of structures might be expected to increase with extension (or stress) at the tip. According to Stacer, Yanyo and Kelly (44), the tearing energy at tear initiation is also affected by the volume of the material near the tear tip which is allowed to deform, and the energy stored in deforming this region. The volume of material deformed near the tear tip is higher at a low tear rate than at a high tear rate.

5.2.2 Correlation between tearing energy and knot diameter

An attempt was made to correlate the tearing energy with the knot diameter produced by test-pieces that tore in knotty manner, at each tear rate investigated. The size of each knot diameter at a particular tear rate was measured, and the corresponding tearing energy was calculated from the tearing force chart using equation 5.2. Knowing the tearing energy, T, and the stored energy density at break, U_b, the knot diameter can be estimated using the relationship (22)

$$d \cong TU_b^{-1} \qquad (5.4)$$

since

$$T \cong U_b d \qquad (5.5)$$

Tables 5.3a, b, c, d and e show the quantitative comparison between the measured knot diameter (referred to the unstrained state) with the estimated values calculated from equation 5.4. Each table gives results at a particular tear rate. The agreement between the measured and the estimated values calculated from equation 5.4 was fortitously good. Figure 5.5 shows tearing energy calculated from equation 5.2, plotted against knot diameter for NR vulcanizates. The points were obtained from the results shown in Tables 5.3a, b, c, d and e, and with other results not shown in the table. The points with different symbols denote the actual measured knot diameter produced at a particular tear rate. The straight line which passes through the origin, was obtained by plotting T calculated from equation 5.2 against d calculated from equation 5.4. In calculating d from equation 5.4 it was assumed that the stored energy density at break, U_b, was constant. Strictly speaking, this is not true since Greensmith (23) found that U_b determined from tensile stress-strain measurements, varied with rate of extension.

According to equation 5.5, the slope of the straight line gives the value of U_b; in this case 57 MJ m^{-3}. It is interesting to see that the tearing energy, T, increased with increasing knot diameter in accordance to the approximate relationship given by equation 5.5 above. On the whole, the quantitative agreement between the knot diameter measured directly from the test-pieces with the values estimated from equation 5.4, can be considered fortitously good, although at low tear rates the descrepancy became very marked. This descrepancy is of course to be expected in view of the work done to break per unit volume of rubber not having been determined at the equivalent crack propagation rate to the tear measurement, and also in view of the difficulty in measuring the size of the knot diameter.

The most important message that can be learned from Figure 5.5 is that blunting of the tear tip appears to be the principal mechanism by which knotty tearing enhances the tear strength. The

Table 5.3: Correlation between tearing energy and the knot diameter of black-filled NR vulcanizate. Full formulations shown in Table 4.3b (mix H1) in Chapter Four. Temperature of test 23°C.

(a) Tear rate = 42 μm s^{-1} U_b = 57.0 MJ m^{-3}

T (kJ m^{-2})	116	149	212	178	152	163	120
d, measured (mm)	2.0	2.6	6.2	4.7	2.5	2.5	1.8
d = T/U_b (mm)	2.0	2.6	3.7	3.1	2.7	2.9	2.1

(b) Tear rate = 170 μm s^{-1} U_b = 57.0 MJ m^{-3}

T (kJ m^{-2})	68	92	113	167	45	55	67
d, measured (mm)	1.0	1.3	1.3	4.2	0.6	1.0	1.2
d = T/U_b (mm)	1.2	1.6	1.9	3.0	0.8	1.0	1.2

(c) Tear rate = 830 μm s^{-1} U_b = 47.0 MJ m^{-3}

T (kJ m^{-2})	51	79	123	59	61	30	42
d, measured (mm)	1.5	1.6	1.8	0.9	1.0	0.5	1.0
d = T/U_b (mm)	0.9	1.4	2.1	1.0	1.1	0.5	0.74

(d) Tear rate = 4200 μm s^{-1} U_b = 57.0 MJ m^{-3}

T (kJ m^{-2})	31	46	66	31	72	51	70
d, measured (mm)	0.5	0.8	1.0	0.5	1.5	0.7	1.1
d = T/U_b (mm)	0.5	0.8	1.2	0.5	1.2	0.9	1.2

(e) Tear rate = 8300 μm s^{-1} U_b = 57.0 MJ m^{-3}

T (kJ m^{-2})	40	43	52	67	58	30	40
d, measured (mm)	1.1	1.0	0.8	1.2	1.0	0.6	0.5
d = T/U_b (mm)	0.7	0.7	0.9	1.2	1.0	0.5	0.7

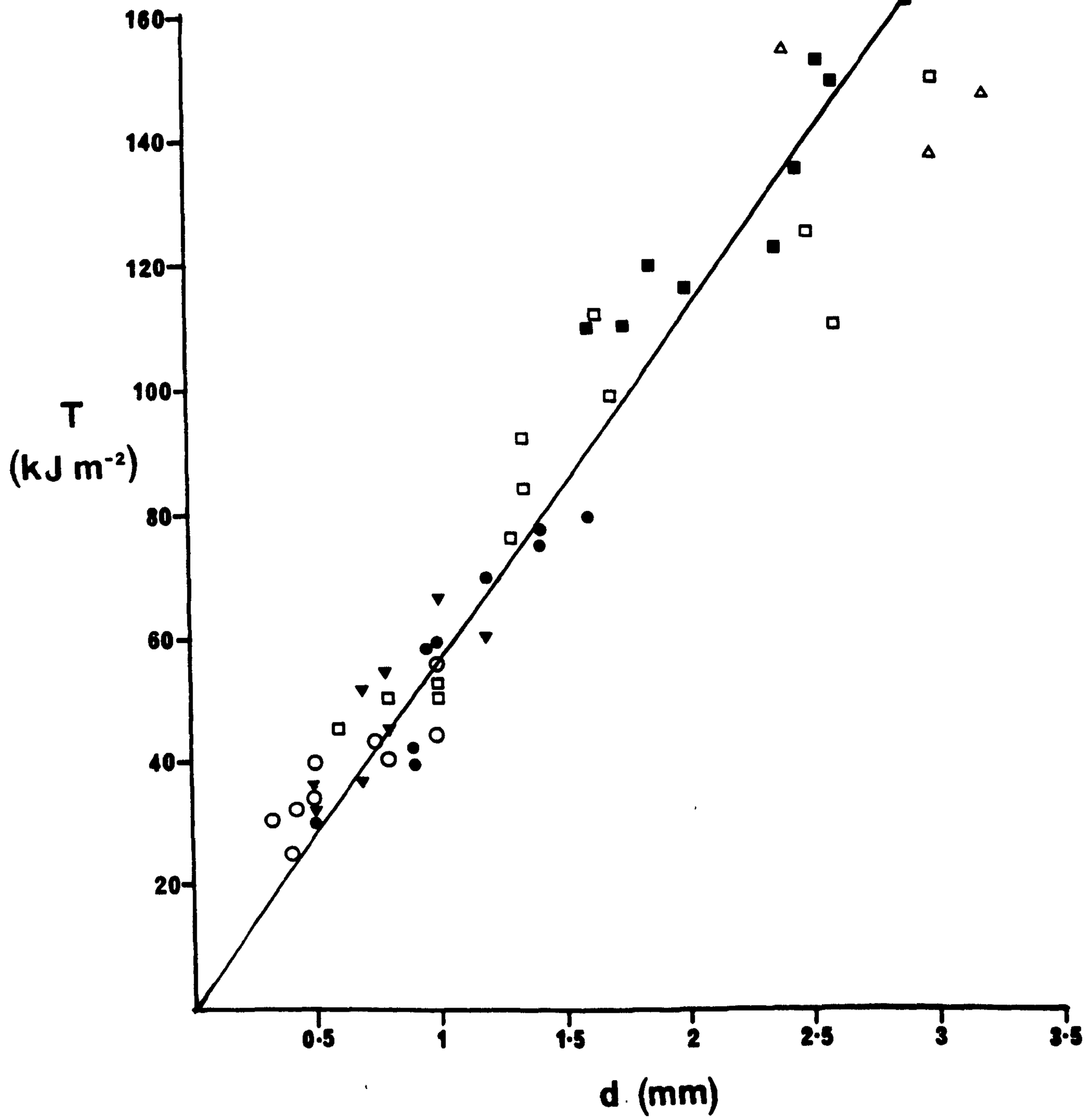

Figure 5.5: Tearing energy, T, vs knot diameter, d, showing correlation between tearing energy and knot diameter in the unstrained state. The straight line shows the tearing energy-tip diameter relationship obtained from equation 5.5. The points indicate the measured knot diameter at tear rate △4.2 μm s^{-1} ■42 μm s^{-1} □170 μm s^{-1}, ● 830 μm s^{-1} ▼4200 μm s^{-1} ○8300 μm s^{-1}.
Temperature at 23°C. Mix no. H1 in Table 4.3b.

magnitude of the knot diameter reflects the degree of blunting of the tear-tip. The larger the knot diameter, the blunter the tear tip. The blunting of the tear-tip is very significant in enhancing the tear strength because it helps to reduce the stress concentration at the tear-tip. Therefore a large knot diameter reduced the stress concentration more effectively than a small knot diameter. Consequently, a large knot diameter gave higher tearing energy than did the small knot diameter. Thus the results shown in Figure 5.5 provide a useful indication of the dependence of tearing energy on the diameter of the tear-tip.

Another interesting observation was the effect of tear rate on the diameter of the knot. A low rate of tearing produced a large knot diameter, d, and a high rate of tearing produced a small knot diameter. For example, reducing the tear rate from 8,300 $\mu m\ s^{-1}$ to 42 $\mu m\ s^{-1}$ increased both the diameter, d, and tearing energy, T, by a factor of about 4. In order to explain this observation, it is necessary to invoke the formation of strengthening structures at the tip of the tear, parallel to the direction of the applied force, and perpendicular to the direction of tear growth as suggested by Busse (15) and Greensmith (16). Also, the strengthening structures require an appreciable time to form as suggested by Greensmith (16).

In knotty tearing, additional energy must be applied to propagate the tear either through or around the strengthening structures. Thus a large knot diameter reflects large regions of strengthening structures forming at the tip of the tear. At a low tear rate, the strengthening structures could probably develop over large regions around the tip of the tear because they had sufficient time to form. Large knot diameters were produced at low tear rate because the tear had to circle around over large regions of strengthening structures. At a high tear rate, probably the strengthening structures could develop over small regions around the tip of the tear because they had insufficient time to form. Small knot diameters were produced at high tear rate because the tear had to circle around small regions of strengthening structures. This is consistent with Greensmith's (16) results where knotty tearing did not occur in black-filled NR vulcanizates at tear rates higher than 25,000 $\mu m\ s^{-1}$, since according to Greensmith at

this rate of tearing, the strengthening structures had insufficient time to develop. Thus the variations of the tearing energy with tear rate, in knotty tearing regions, are associated with the variations of the degree of strengthening structures developed at the tip of the tear at a particular tear rate.

The results shown in Figure 5.5 indicate a strong correlation between tearing energy and the unstrained diameter of the tear-tip, d. Although equation 5.5 is only an approximate relationship, in principle it can be used to predict the tearing energy, T, if the unstrained tip diameter,d, and the work to break per unit volume rubber, U_b, are known. Greensmith (23) found that the values of U_b obtained from tensile measurements at various rates of extension, agreed very well with U_b determined from the energy to initiate tearing at an incission with a tip of a semi-circular form. The present investigation extends further the work of Greensmith (23) and shows that the relationship given by equation 5.5 can be applied to tearing initiated from a sharp tear tip. The results in Figure 5.5 seem to imply that in principle, the effect of tear rate upon T can be predicted with fair accuracy provided the values of d and U_b upon rates are known.

The main conclusion of Section 5.2.2, is that knotty tearing enhances the tear strength by increasing the effective diameter of the tear-tip.

5.3 Effect of molecular mobility

The effect of molecular mobility was investigated further by using a non-strain-crystallizing rubber, SBR, so that the issue of strain-crystallization could be avoided. The results are shown in Figure 5.6 where tearing energy at four further temperatures is plotted against tear rate on logarithmic scales. The points in Figure 5.6 were obtained from Table 5.4 which represented the average tearing energy of five test-pieces at each tear rate and temperature of measurements. Figures 5.7a, b, c, d, e, f and g show photographs of the types of tear failure and fractured surfaces of the test-pieces. It is interesting to note from Figure 5.6 that the range of tear rates where knotty tearing occurred increased as the molecular mobility increased with increasing temperature. At 23°C

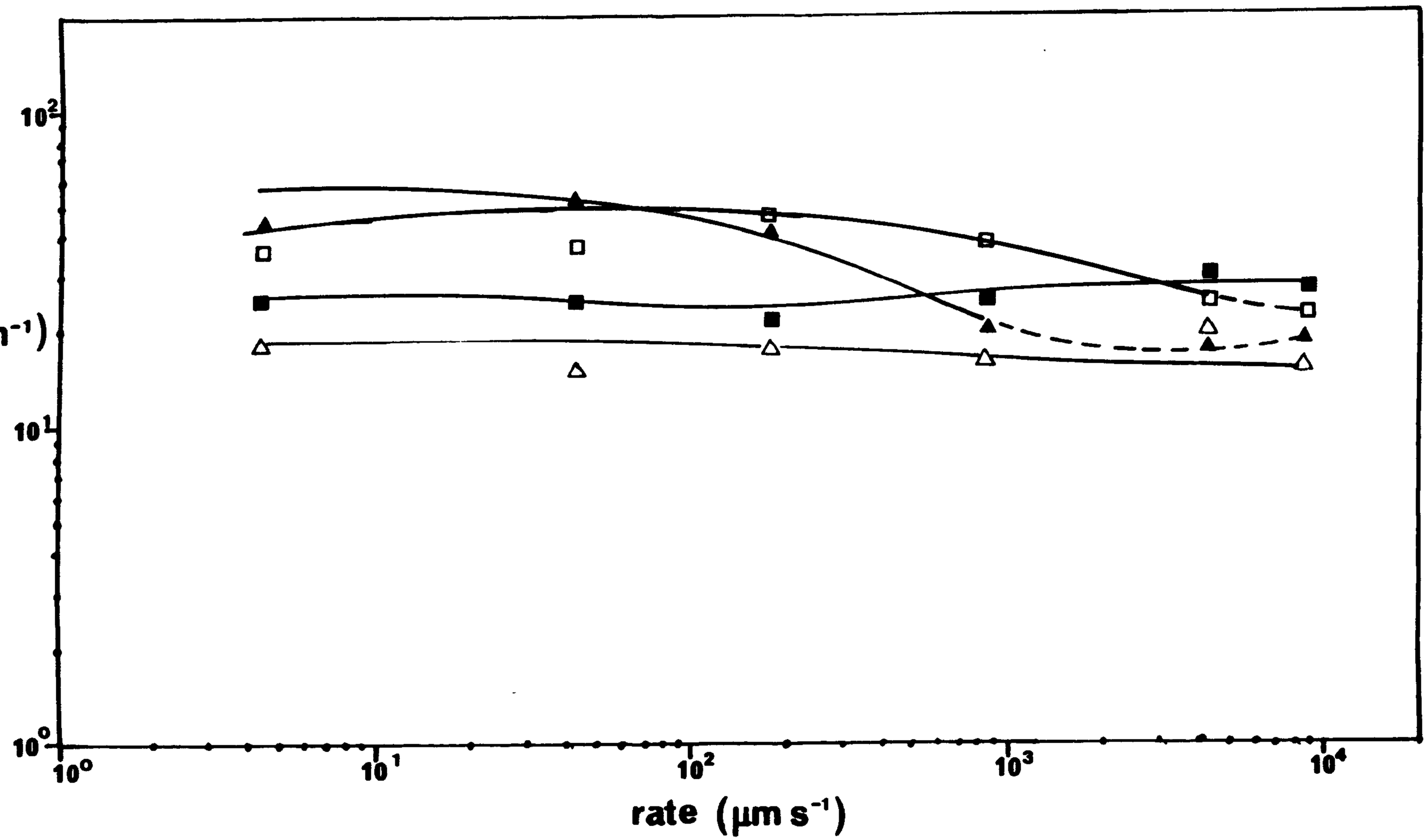

Figure 5.6: Tearing energy, T, vs tear rate, showing effect of molecular mobility on development of knotty tearing of black-filled SBR vulcanizate, (mix no. H4 in Table 4.3b)
▲ 50°C, □ 70°C, ■ 90°C, △ 120°C.

Table 5.4: Effect of tear rate and temperature on tearing energy of black-filled SBR vulcanizates. Full formulations shown in Table 4.3b (mix H4) in Chapter Four.

Tear rate (μms^{-1})	4.2	42	170	830	4200	8300
T at 23°C (kJ m^{-2})	34	34	33	33	34	34
T_R	1.0	1.04	1.05	1.0	1.0	1.0
Type of tear failure	s	s	s	s	s	s
T at 50°C (kJ m^{-2})	46	54	42	21	18	20
T_R	1.6	2.8	2.6	1.5	1.0	1.0
Type of tear failure	k	k	k	s.s	s	s
T at 70°C (kJ m^{-2})	44	40	47	40	27	23
T_R	1.74	2.24	7.61	3.72	2.39	1.0
Type of tear failure	k	k	k	k	k	s
T at 90°C (kJ m^{-2})	43	34	29	31	30	27
T_R	1.9	2.57	3.78	4.25	2.85	2.63
Type of tear failure	k	k	k	k	k	k
T at 120°C (kJ m^{-2})	15	15.0	18	16	20	16
T_R	2.1	2.11	6.07	4.77	2.85	3.29
Type of tear failure	k	k	k	k	k	k

Footnotes:

s - steady tearing k - knotty tearing

$$T_R = \frac{\text{Tearing energy at tear initiation}}{\text{Tearing energy at tear arrest}}$$

a b c d

e

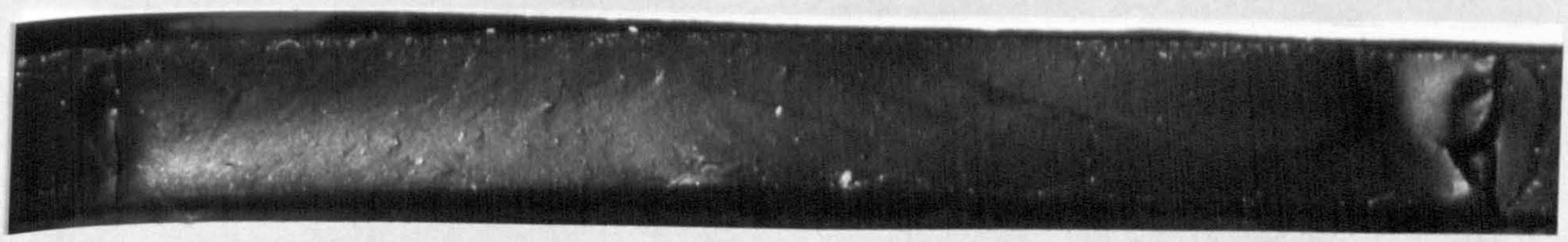

f

g

Figure 5.7: Photographs showing the type of tear failure of black-filled SBR vulcanizate (mix no. H4 in Table 4.3b)
a) 23°C, r = 4.2 μm s^{-1} b) 50°C, r = 830 μm s^{-1}
c) 70°C, r = 170 μm s^{-1} e) 120°C, r = 4.2 μm s^{-1}
e) Fractured surface at 23°C, r = 4.2 μm s^{-1} (8x magnification)
f) Fractured surface at 70°C, r = 170 μm s^{-1} (8x magnification)
g) Fractured surface at 120°C, r = 4.2 μm s^{-1} (8x magnification)

(Table 5.4), tearing proceeded steadily even at the very lowest tear rate, producing a relatively smooth torn surface as shown in Figure 5.7e. Even at the lowest tear rate investigated here, the tearing energy ratio, T_R, was still giving a value of one, implying that the tear propagated at a steady rate along the intended tear path, without fluctuations in the tearing force with tear rate. In contrast, at the lowest tear rate i.e., 4.2 μm s^{-1}, Greensmith (16) found that HAF black-filled SBR underwent knotty tearing. The descrepancy here may partly be attributed to the difference in the grade of styrene butadiene copolymer, and the actual formulations of the vulcanizates used. Greensmith (16) used styrene butadiene copolymer (GR-S) prepared by a hot polymerization. In contrast, styrene butadiene copolymer (SBR) used in the present investigation was prepared by cold polymerization (65). Generally, GR-S gives better processing and finished product improvements than SBR. Furthermore, GR-S can accept higher filler loadings than SBR. It has been claimed that generally SBR gives better all round physical properties than GR-S (65).

At 50°C, tearing occurred in a knotty manner, at least at tear rates ranging from 4.2 μm s^{-1} to about 830 μm s^{-1}. At 50°C, Greensmith found that knotty tearing occurred at tear rates ranging from 4.2 μm s^{-1} to 420 μm s^{-1}, which is consistent with the range of tear rates over which knotty tearing can occur in the present investigation. At 70°C, knotty tearing occurred at tear rates ranged from 4.2 μm s^{-1} to 4200 μm s^{-1}. Greensmith (16) did not report tear measurements at this temperature.

At 90°C, knotty tearing occurred at all tear rates used here. This observation is also consistent with Greensmith's results. Greensmith (16) found that at 90°C, knotty tearing still occurred even at a tear rate of 25,000 μm s^{-1}. At tear rates higher than 25,000 μm s^{-1}, the tear reverted to steady tearing. At 120°C, knotty tearing occurred over the whole range of tear rates investigated here. However, the temperature also affected the magnitude of the tearing energy. For example, at 120°C the tearing energy was about one third of that obtained at 50°C, even though knotty tearing occurred at 120°C and steady tearing occurred at 50°C. The decrease in tearing energy might be attributed to lower energy dissipation associated with the decrease in the internal viscosity of the vulcanizate at high temperature.

In unfilled SBR vulcanizates, tear failure occurs by steady tearing. In steady tearing, the tearing energy at any given tear rate always decreases with increasing temperature (16,32,64). The decrease in tearing energy with increasing temperature is attributed to a decrease in hysteresis because the internal viscosity of the vulcanizate decreases with increasing temperature. In black-filled SBR vulcanizates, the situation is complicated by the variations of the tear-tip diameter with tear rate and temperature. The results shown in Figure 5.6, indicate that at the lowest tear rate, i.e., 4.2 $\mu m\ s^{-1}$ where knotty tearing occurred, tearing energy decreased with increasing temperature. At the highest tear rate, i.e., 8300 $\mu m\ s^{-1}$, tearing energy can increase with increasing temperature. For example, tearing energy at 90°C was higher than tearing energies at 50°C and 70°C respectively. The reason for this is because at 90°C, knotty tearing could occur and thus giving high tearing energy. In contrast, at 50°C and 70°C, knotty tearing did not occur at this tear rate, and thus tearing energies were slightly lower than obtained at 90°C. Similar observations were noted from Greensmith's results (16).

The main inference that can be obtained from Section 5.3 is that in the absence of strain-crystallization, knotty tearing still can occur if the molecular mobility of the vulcanizate is adequate to allow the black structure to form at the tip of the tear.

5.3.1 Variation of tearing energy with temperature

The increase in molecular mobility with increasing temperature may affect the magnitude of the tearing energy in two ways. It may increase the tearing energy by allowing rapid development of knotty tearing, and it may reduce the tearing energy by reducing the internal viscosity and hence the hysteresis associated with the increase in the thermal energy. The effect of temperature on tearing energy is shown in Figures 5.8(a),(b),(c) and (d), where tearing energy is plotted against temperature for various elastomers. Both NR and ENR25, which readily strain-crystallize, produce knotty tearing over the whole range of temperatures. In the case of ENR50, at this particular tear rate knotty tearing occurred at 40°C and above, whereas in the case of SBR it occurred at 60°C

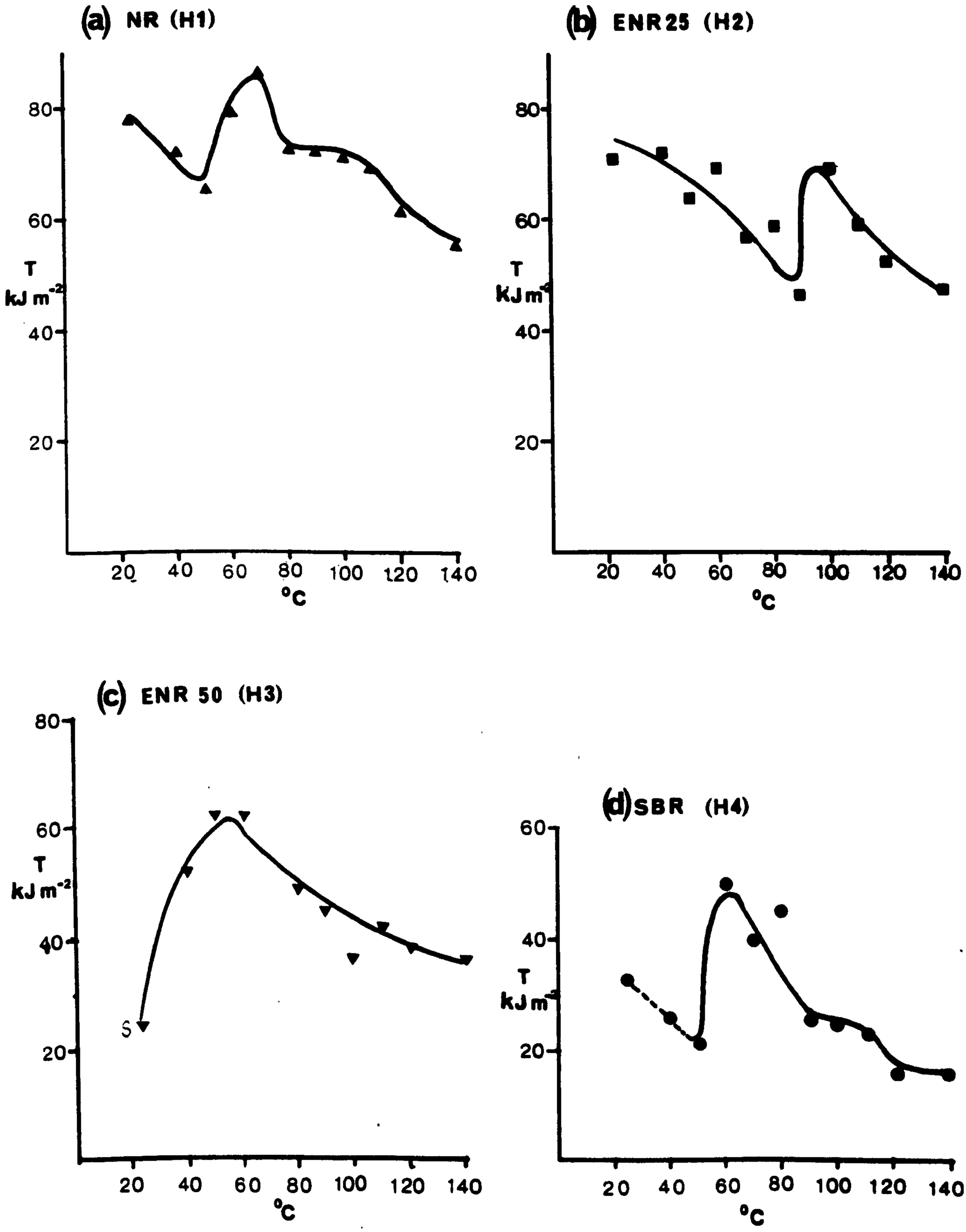

Figure 5.8: Tearing energy, T, vs temperature, showing effect of temperature on tearing energy. Tear rate 830 μm s^{-1} Mixes no. H1, H2, H3 and H4 in Table 4.3b.
——— knotty tearing - - - - steady tearing

and above. Each rubber displayed perculiar variations of tearing energy with temperature. The variations can to be attributed to the size of the knot diameter formed at a particular temperature, as is shown by the photographs in Figures 5.9(a),(b),(c) and (d).

Histograms were constructed showing the relative frequency of the size of knot diameter formed at a particular temperature. Such histograms for ENR 25 are shown in Figure 5.10. At 23°C, the average knot diameter predicted from equation 5.4 was about 1.2mm, and the experimental values show that about 60% were in the range of 0.6 mm to 1.0 mm, and 20% in the range of 1.4 mm to 1.6 mm. At 50°C and 70°C, the knot diameter decreased (ca. 50% being less than 0.5 mm). Parallel to this, there was a decrease in the tearing energy. Further rise in temperature increased the size of the knot diameter, and parallel to this there was an increase in the tearing energy. However, at 120°C and above, inspite of the observed increase in knot diameter, the tearing energy decreased. This may have been a consequence of a lowering of the energy dissipation.

Referring again to Figure 5.8, it is interesting to see that, over a wide range of temperatures, the magnitude of the tearing energy still follows the same order as does the amount of crystallinity of the rubber induced by straining, ie., NR > ENR25 > ENR50 > SBR. For example at 140°C, the tearing energy of ENR25 was about 85%, ENR50 was about 66% and SBR was about 28%, respectively, of that of NR. This suggests that the crystals are not completely melted, but apparently some still remain at the tear tip to enhance the tear resistance.

5.4 Effect of nature and concentration of crosslinks

Three vulcanizing systems, namely, a conventional, an efficient vulcanization (EV) and a peroxide were employed for this part of the investigation. The details of the formulations, and the tensile and swelling properties of the vulcanizates are given in Tables 4.4a,b, and c respectively. The tear measurements were carried out at 23°C by separating the legs of the trouser test-piece at a tear rate of 830 μm s^{-1}. The results are presented in tabulated form, shown in Tables 5.5A, B and C, as well as in graphical form, shown in Figure 5.11a, where tearing energy is

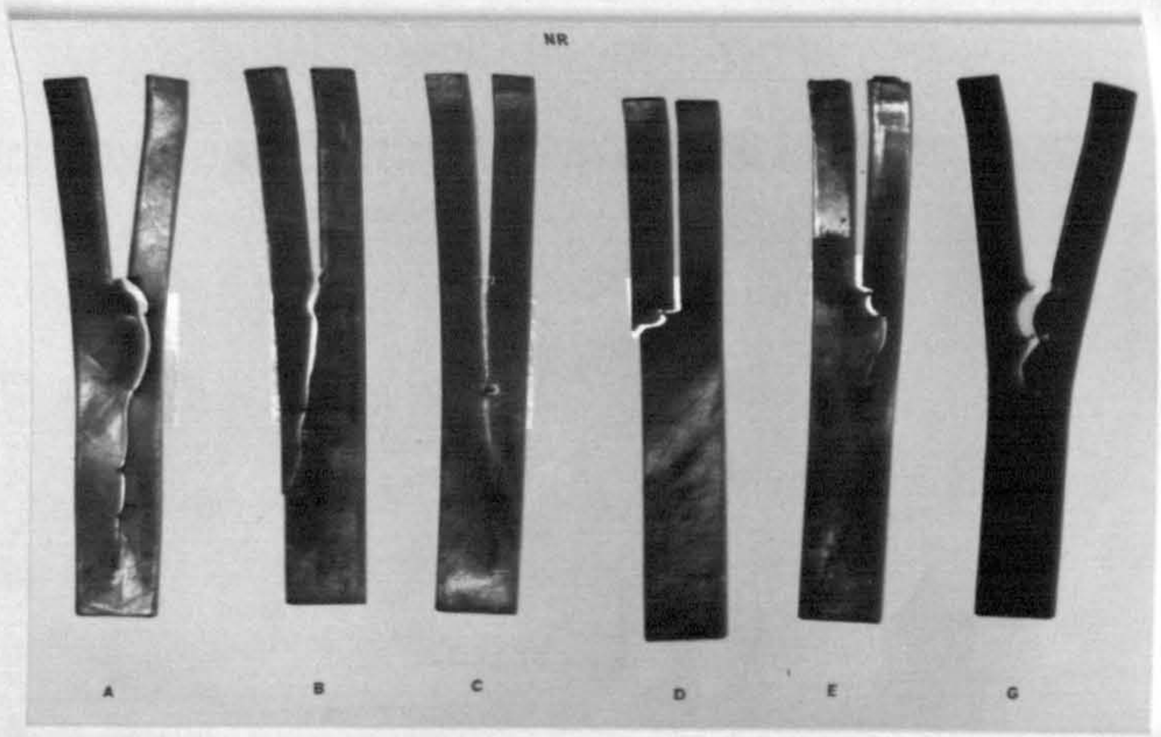

NR

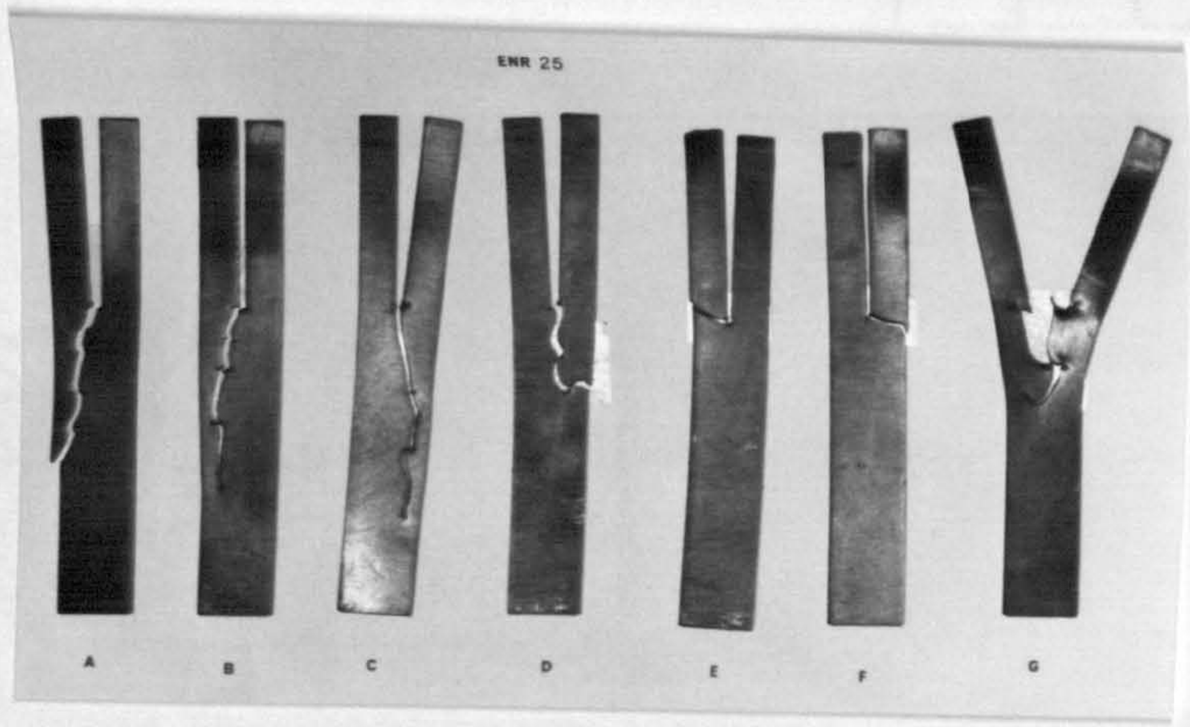

ENR 25

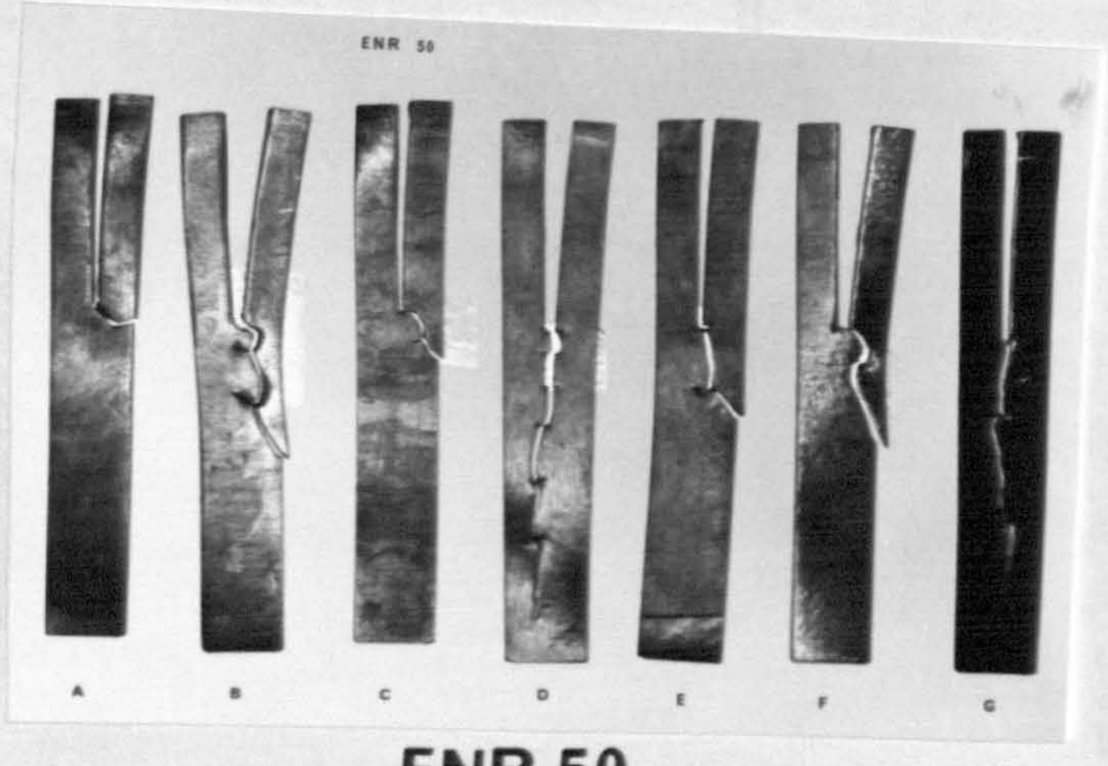

ENR 50

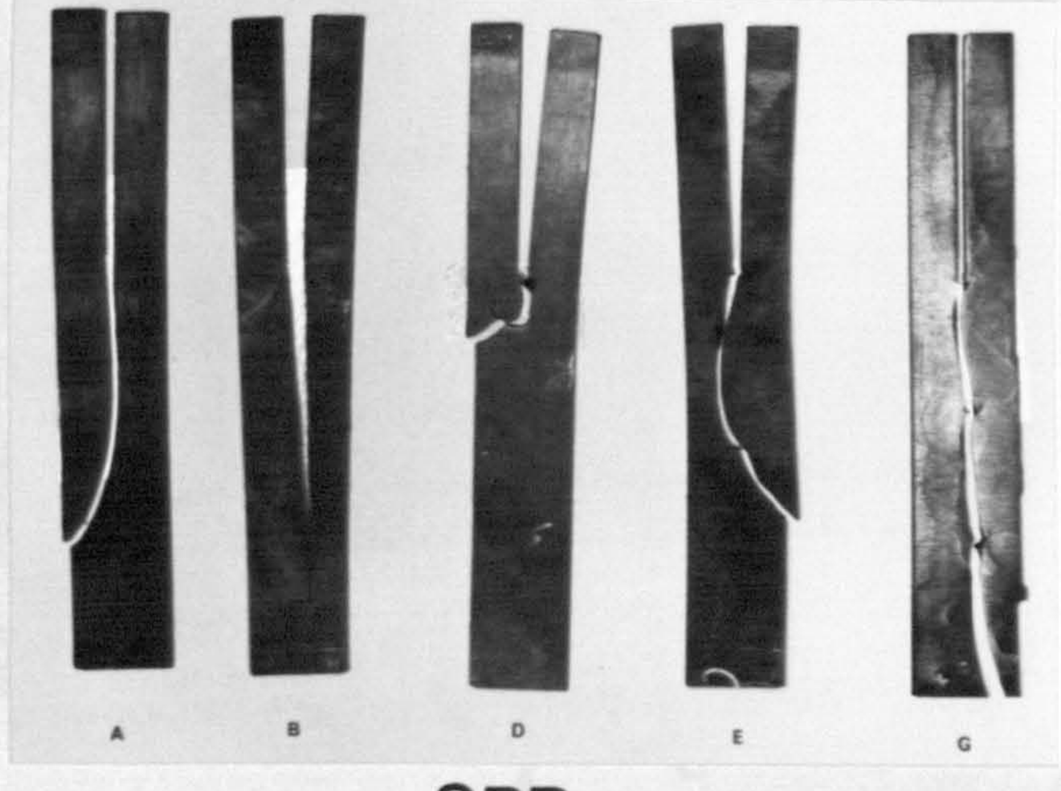

SBR

Figure 5.9: Photographs showing the type of tear failure at different temperatures of tear test. Tear rate 830 μm s^{-1}.
A 23°C, B 40°C, C 50°C, D 60°C, E 80°C, F 90°C, G 100°C.
(a) NR (b) ENR 25 (c) ENR 50 (d) SBR.

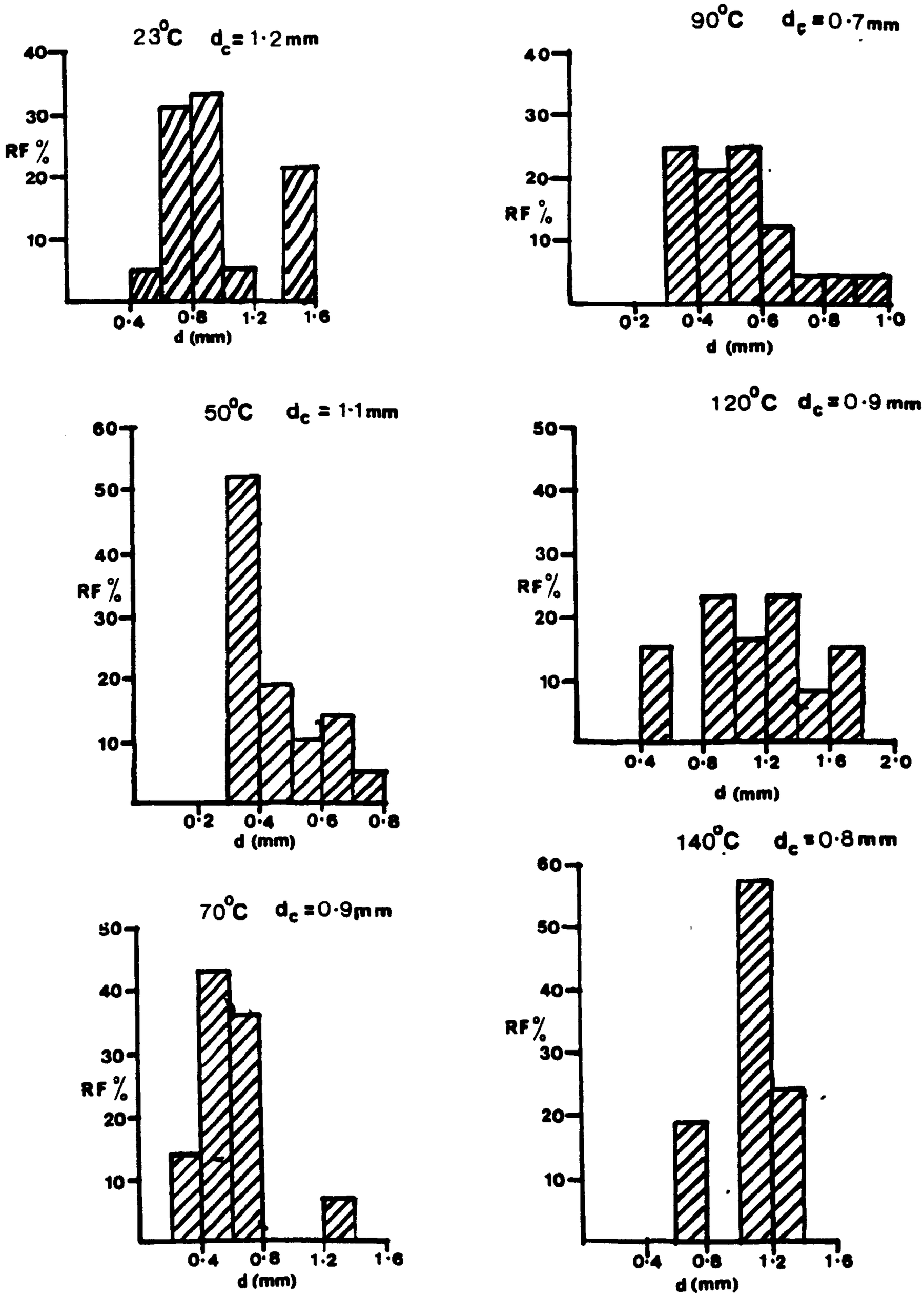

Figure 5.10: Relative frequency, FR, vs knot diameter, d, showing the variations of strength anisotropy at different temperatures for ENR 25. Mix no. H2 in Table 4.3b. Tear rate 830 μm s^{-1}. $d_c = TU^{-1}$

Table 5.5: Effect of nature and concentration of crosslinks on tearing energy of black-filled (50pphr HAF) NR vulcanizates
Temperature 23°C Tear rate 830 μm s^{-1}

(A) Conventional vulcanization system

Mix number	A1	A2	A3	A4	A5	A6	A7	A8
[X] $_{phys}$ actual $\times 10^{-2}$ mol/kg RH	2.38	2.47	3.93	4.95	5.50	6.39	9.57	9.61
U_b (MJ m^{-3})	42.9	43.0	44.8	57.6	63.3	54.5	55.4	59.0
T (kJ m^{-2})	6.41	5.9	12.45	67.64	50.09	35.06	34.87	33.62
$d = T/U_b$ (mm)	0.1	0.1	0.3	1.2	0.8	0.6	0.6	0.6
$\bar{d}$ (mm)	-	-	-	2.0	0.8	0.6	0.5	0.5
Type of tear failure	s	s	s	k	k	k	k	k

s - steady tearing k - knotty tearing

(B) EV vulcanization system

Mix number	B1	B2	B3	B4	B5	B6	B7
[X] $_{phys}$ actual, $\times 10^{-2}$ mol/kg RH	2.31	3.40	4.74	4.98	6.62	10.78	12.67
U_b (MJ m^{-3})	40.6	52.4	62.7	55.3	45.9	26.7	8.86
T (kJ m^{-2})	6.23	65.14	59.25	59.7	35.92	5.0	5.32
$d = T/U_b$ (mm)	0.1	1.2	0.9	1.1	0.8	0.2	0.6
$\bar{d}$ (mm)	-	2.5	2.0	1.6	1.5	0.1	0.1
Type of tear failure	s	k	k	k	k	s	s

s - steady tearing k - knotty tearing

(C) Peroxide vulcanization system

Mix number	C1	C2	C3	C4	C5	C6	C7	C8	C9
[X]phys actual, $\times 10^{-2}$ mol/kg RH	1.85	2.75	3.26	3.86	4.23	5.72	5.72	7.41	9.14
U_b (MJ m^{-3})	30	40	33	36	41	37.3	34.4	23	19.3
T (kJ m^{-2})	4.87	5.16	8.05	8.6	50.1	45.69	42.43	4.87	4.63
$d = T/U_b$ (mm)	0.1	0.1	0.2	0.2	1.2	1.2	1.2	0.2	0.2
$\bar{d}$ (mm)	-	-	-	-	2.5	1.5	1.5	0.1	0.1
Type of tear failure	s	s	s	s	k	k	k	s	s

s - Steady tearing k - Knotty tearing

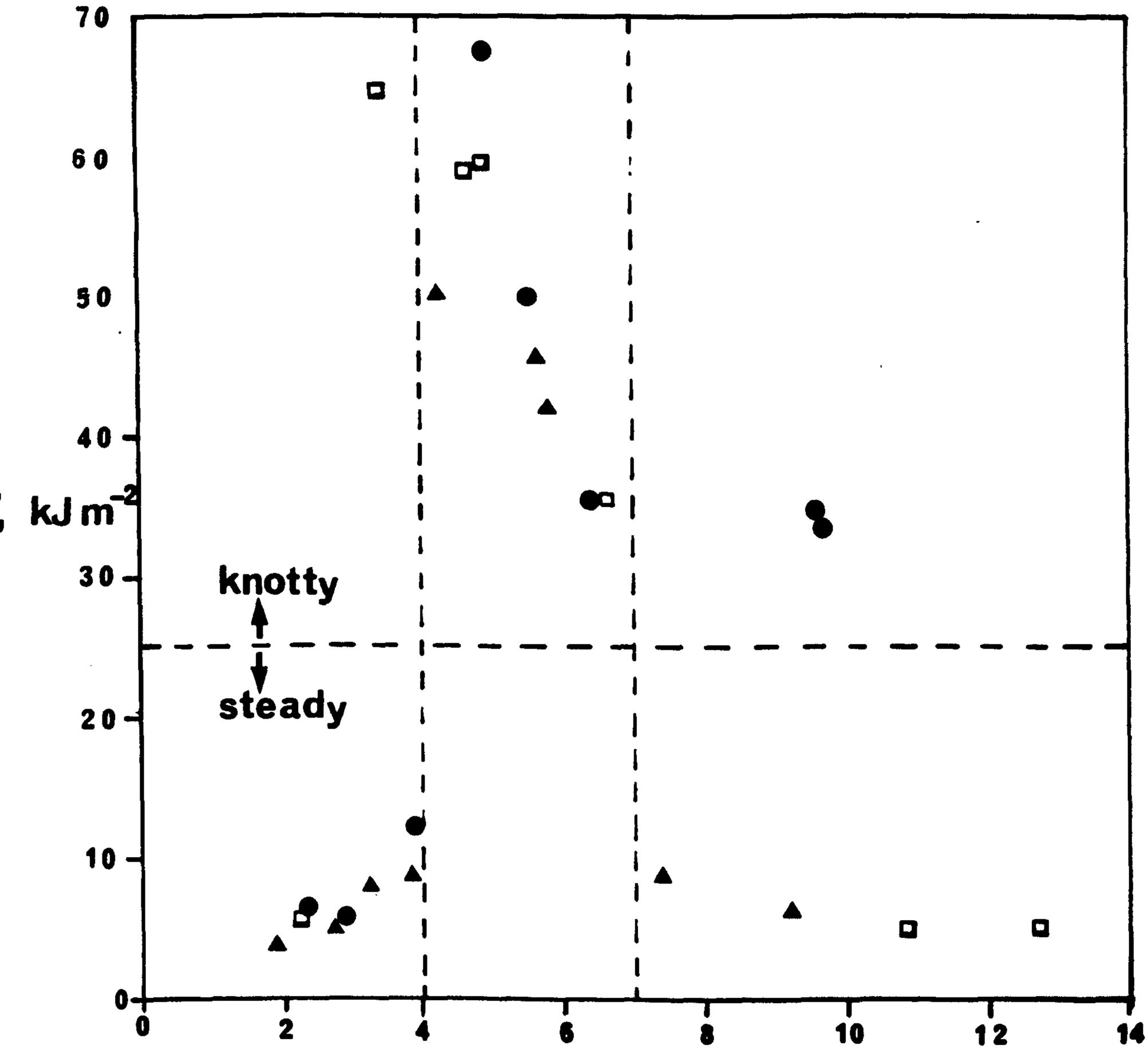

Figure 5.11a: Tearing energy, T, vs crosslink concentration, showing influence of crosslink concentration on development of knotty tearing in NR black-filled vulcanizates produced by ● conventional, □ EV, and ▲ peroxide vulcanization systems. Tear rate 830 μm s^{-1} Full formulations are given in Tables 4.4a, b and c.

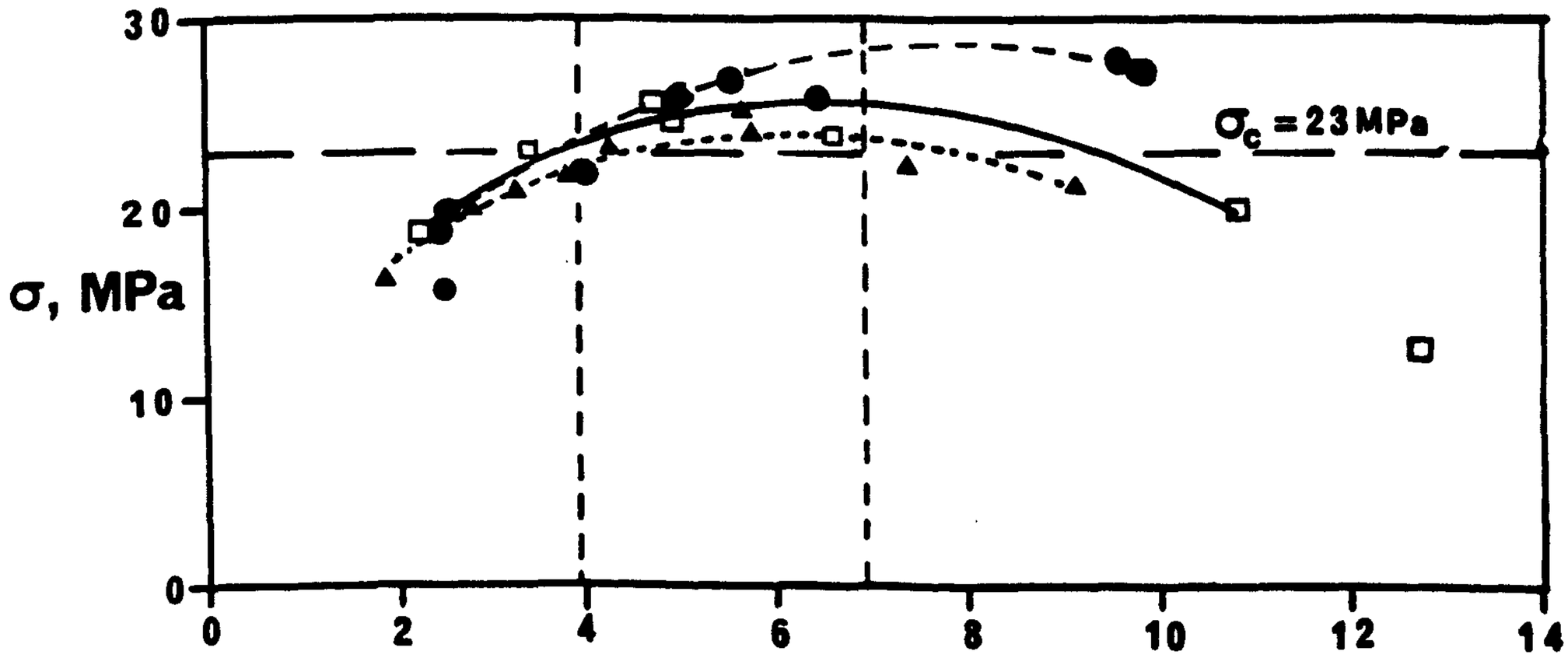

Figure 5.11b: Nominal tensile strength, σ, vs crosslink concentration, produced by ● conventional, □ EV, and ▲ peroxide vulcanization systems. Full formulations are given in Tables 4.4a, b and c.

plotted against crosslink concentration. To facilitate the discussions, the plot is divided into three regions. Region 1 is the region of low crosslink concentration, ranging from 1.8×10^{-2} to 4.0×10^{-2} mol per kilogram of rubber hydrocarbon. Region 2 is the region of moderate crosslink concentration, ranging from 4×10^{-2} to 7.0×10^{-2} mol per kilogram of rubber hydrocarbon, and Region 3 is the region of high crosslink concentration, greater than 7.0×10^{-2} mol per kilogram of rubber hydrocarbon.

In Region 1, the three cure systems all produced steady tearing, as shown in Figure 5.12 for vulcanizates A1, B1 and C1. The letter and the number correspond to the mix number as shown in Tables 4.4a,b, and c in Chapter Four. Figure 5.13 shows the fractured surface of each vulcanizate (A1,B1 and C1). The actual torn surface was as smooth as glass. In Region 1, the tearing energy increases with increasing crosslink concentration. This increase is attributed to an increase in the stored energy density at break U_b, as shown in Table 5.5. This suggests that in the steady tearing region, U_b, is the dominant factor affecting the tear strength rather than the tip-diameter. In this region, the effect of the nature of crosslink on the tearing energy is small.

In Region 2, knotty tearing was observed for vulcanizates produced by all three vulcanizing systems, as shown in Figure 5.12 for vulcanizates A4, B3 and C5. The fractured surfaces of the vulcanizates are shown in Figure 5.13. In this region the tearing energy decreases with increasing crosslink concentration, and also depends upon the nature of the crosslink. The magnitude of the tearing energy given by the three types of crosslink decreases in the following order polysulphidic > monosulphidic > carbon-carbon.

In Region 3, the influence of crosslink concentration on the tearing energy becomes very marked. The conventional cure system produced vulcanizates having high tearing energy associated with knotty tearing, as shown in Figure 5.12 for vulcanizate A8. The corresponding fractured surface is shown in Figure 5.13. In contrast, the EV and peroxide systems produced vulcanizates having low tearing energy with steady tearing, as shown in Figure 5.12 for vulcanizates B7 and C9. The corresponding fractured surfaces are shown in Figure 5.13. Although vulcanizates B6, B7, C8 and C9

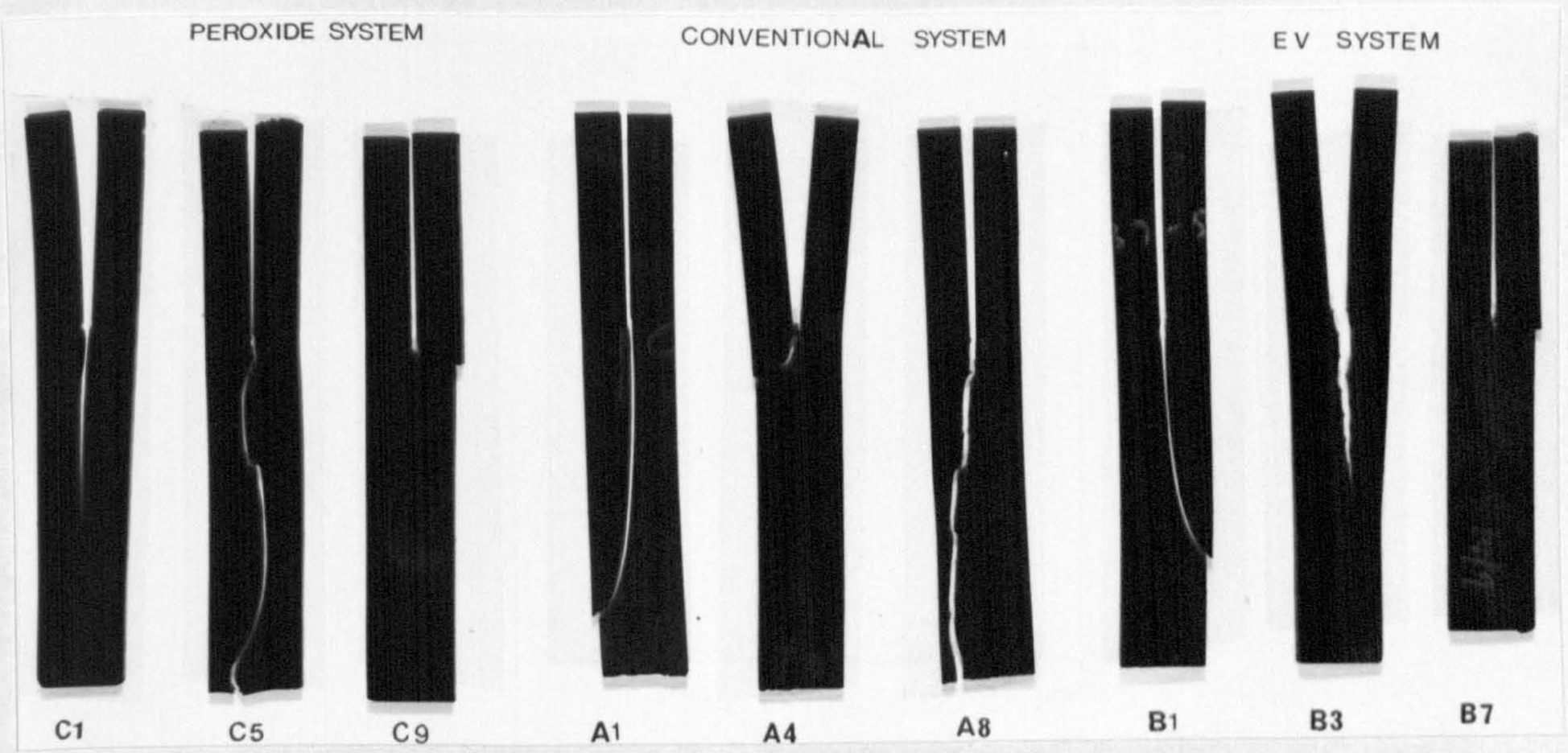

Figure 5.12: Photographs showing the types of tear failure observed in vulcanizates produced by different vulcanization systems. Full formulations are given in Tables 4.4a, b and c.

(a) Fractured surfaces of conventional sulphur vulcanizates

(b) Fractured surfaces of EV sulphur vulcanizates

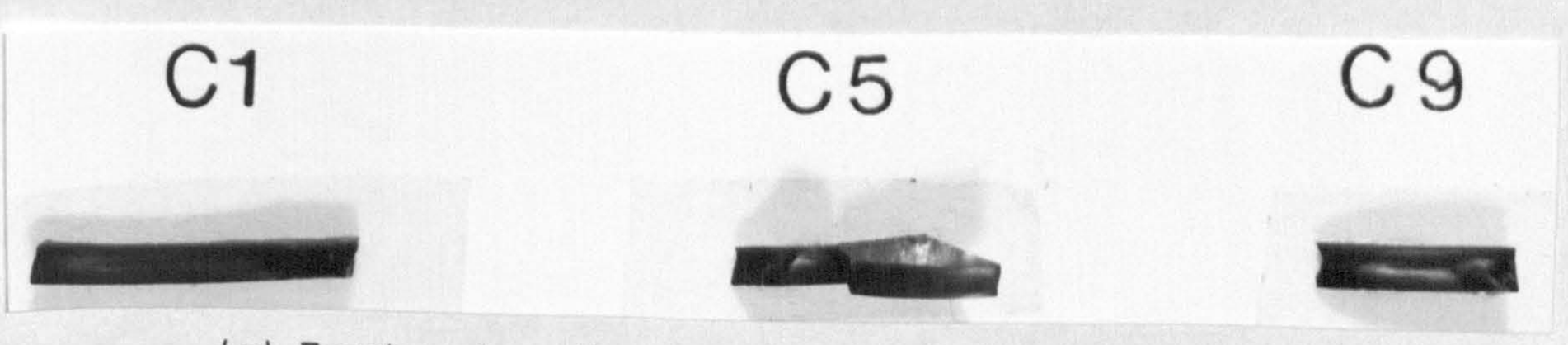

(c) Fractured surfaces of peroxide vulcanizates

Figure 5.13: Photographs showing fractured surfaces of NR black-filled vulcanizates produced by different vulcanization systems.

produced steady tearing, the actual torn surface appeared to be rougher than the torn surface produced by vulcanizates in Region 1. The roughness of the torn surface was of the order 0.1 mm to 0.2 mm. The difference in tearing energy for the vulcanizates produced by the conventional and the other two curing systems is substantial. The tearing energy of vulcanizates produced by the conventional system was approximately 7 times the tearing energy of vulcanizates produced by the other two curing systems.

Comparing the results for tensile strength versus crosslink concentration shown in Figure 5.11b with those for tearing energy versus crosslink concentration shown in Figure 5.11a, there appears to be a critical tensile stress (ca. 23 MPa) below which steady tearing occurs and above which knotty tearing occurs. The stress and extension at the tip of the tear can influence the development of strengthening structures and hence the occurrence of knotty tearing. According to Greensmith (16), the amount of strengthening structures developed eg., crystallization, is affected by the stress or extension at the tip. The amount of structures is expected to increase with increasing stress or extension at the tip of the tear (16). The extent of strain-crystallization occurring at the tip of the tear is very significant in promoting knotty tearing. As discussed in Section 5.2 above, Greensmith (16) suggested that the local strain-crystallization at the tip of the tear, could help to promote knotty tearing, by ensuring that the stress at the tip is always sufficiently high for the carbon black structure to form around the tip, to induce the strength anisotropy necessary for the occurrence of knotty tearing. It is known that in an unfilled NR vulcanizate, the extent of crystallization induced by straining is affected by the crosslink concentration of the network in the vulcanizate (66). The variations of tearing energy with crosslink concentration may be associated with the degree of strain-crystallization occurring at the tip of the tear which can affect the degree of strength anisotropy developed around the tip of the tear.

The dependence of the development of knotty tearing on crosslink concentration will now be discussed in the light of the explanation put forward by Gee (66) for the dependence of the tensile strength of gum natural rubber upon crosslink concentration.

In Region 1, where the degree of crosslinking is very low, portions of the uncrosslinked molecular chains can flow during extension. It is easy for the system to response to the deforming stress by flow. As a result, the stress is dissipated before the critical stress necessary to effect reorientation and crystallization is attained. This results in steady tearing, because the stress is not high enough to induce the strength anisotropy required for knotty tearing to occur. In Region 2, where the crosslink concentration is moderately high, flow associated with molecular slippage is no longer feasible. Over this region, appreciable molecular orientation occurs during extension. This results in substantial degrees of crystallization which greatly enhance the strength. In Region 2, the stress is high enough to induce the strength anisotropy necessary to produce knotty tearing. Any further insertion of crosslinks can only result in a tightening of the network. This would impose an increasing number of restrictions on any molecular segment which are attempting to align with a neighbouring segment. The overall effect is that the degree of orientated crystallization decreases, and so in consequence does the strength anisotropy.

As discussed in Section 5.2.2, the knot diameter reflects the extent of strengthening structures developed at the tip of the tear. A large knot diameter reflects large regions of strengthening structures forming at the tip of the tear, and a small knot diameter reflects small regions of strengthening structures forming at the tip of the tear. The knot diameter of the vulcanizates that failed by knotty tearing was measured, and the average value obtained was compared with the value calculated from equation 5.4. The results in Tables 5.5A, B and C show that, the mean knot diameter, $\bar{d}$, decreased with increasing crosslink concentration. The decrease in knot diameter with crosslink concentration might be attributed to low extent of strengthening structure forming at the tip of tear, as a consequence of low extent of local strain-crystallization developed at the tip of the tear for reasons explained above. The decrease in tearing energy with increasing crosslink concentration is consistent with the decrease in knot diameter with increasing crosslink concentration. This explains the very obvious decrease in tearing energy which is observed in Region 3.

It can be argued that the application of a sufficiently high stress would eventually produce orientation and hence crystallization no matter how tight the network is. However, the network reaches its finite extensibility limit, and breaks before the stress required to produce orientation is reached. This is clearly reflected by both the EV and peroxide vulcanizates in Region 3. In the case of conventional sulphur vulcanizates, the network can sustain high stress because of the ability of the crosslinks to yield and thus relieve the local stress concentration. This gives larger regions of high stress around the tip in which orientation is sufficient to produce the strength anisotropy necessary for knotty tearing.

The effect of crosslink concentration on the tearing energy of black-filled rubber was further investigated using SBR filled with 30 pphr of HAF black, and cured with the conventional vulcanizing system shown in Table 4.4d. At this level of carbon black loading, SBR did not produce knotty tearing. Instead it produced stick-slip tearing with rough fractured surfaces. The effective tear-tip diameter will be of the order of the roughness of the torn surface. In stick-slip and steady tearing, hysteresis is the dominant factor which enhances the tear strength. Thus it is interesting to see how the tear strength is affected by the crosslink concentration.

Figure 5.14 shows the results. The tearing energy for vulcanizates having five different levels of crosslink concentration is plotted against tear rate on logarithmic scales. In the absence of knotty tearing, the tearing energy decreased as the crosslink concentration increased. This indicates that, when variation in the size of tear tip is minimised, energy dissipation plays an important role in determining the tear strength of the vulcanizate. It is known that vulcanizates having lower crosslink concentration dissipate higher energy than do those having higher crosslink concentration, and hence give high tearing energy over a broad time scale (40). This parallels the results shown in Figure 5.14. For example, at a tear rate of 100 $\mu m\ s^{-1}$, the tearing energy of the the vulcanizate having a crosslink concentration 2.03×10^{-2} mol per kilogram of rubber hydrocarbon was about 6 times that of the vulcanizate having a crosslink concentration of 10.37×10^{-2} mol per kilogram of rubber hydrocarbon.

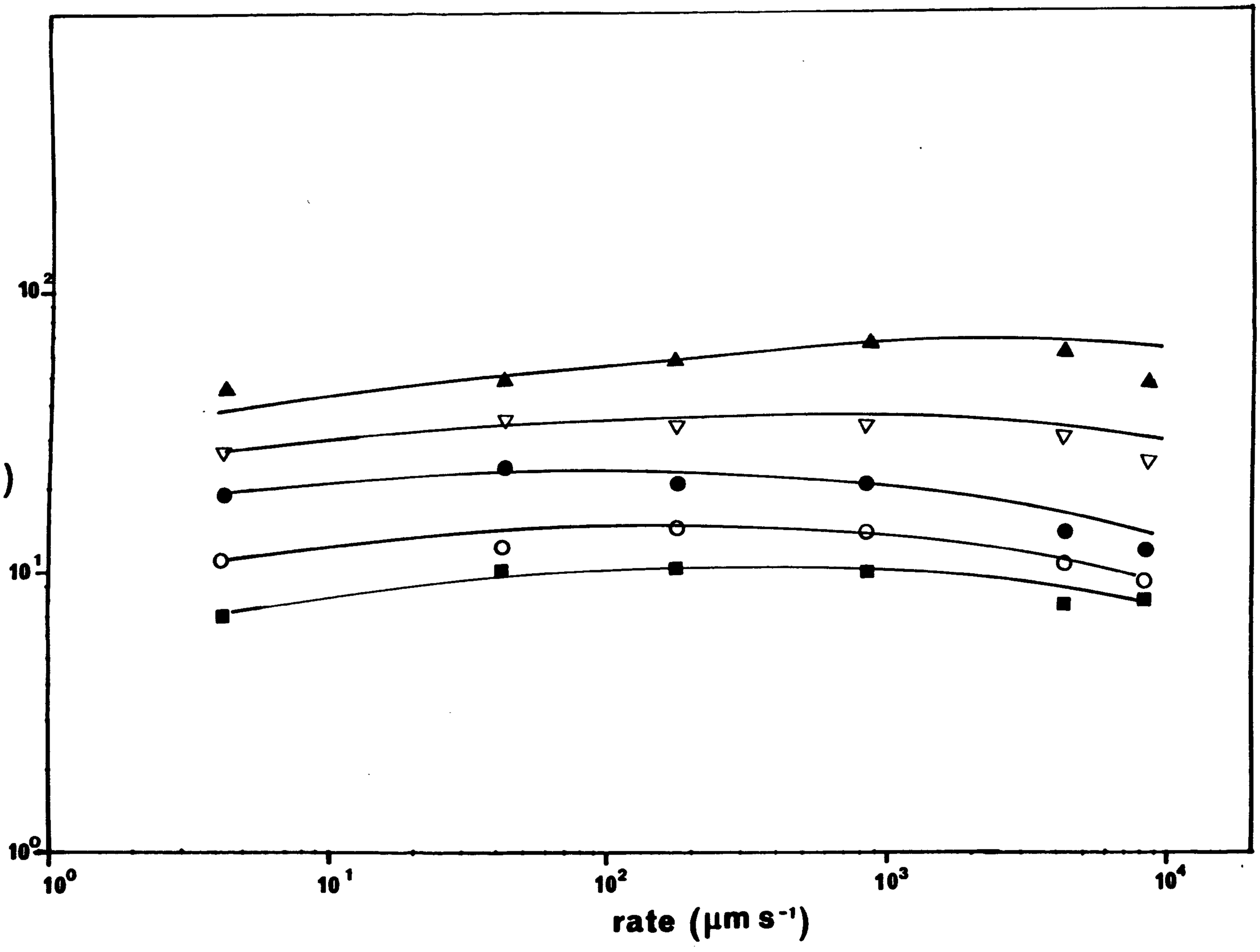

Figure 5.14: Tearing energy, T, vs tear rate at 23°C, showing effect of crosslink concentration on tearing energy of SBR filled with 30 pphr of HAF and cured with a conventional sulphur vulcanization system. ▲ 2.03×10^{-2}, ▽ 4.38×10^{-2}, ● 6.61×10^{-2} ○ 8.75×10^{-2}, ■ 10.37×10^{-2} mol per kg of RH.

The dependence of tearing energy on crosslink concentration shown in Figure 5.14 is consistent with the dependence of tearing energy of unfilled isomerized NR on crosslink concentration investigated by Brown, Porter and Thomas (40). This indicates that the variation of the tearing energy of a black-filled NR vulcanizate with crosslink concentration is associated with the variation of tear tip diameter. This suggests that in knotty tearing the magnitude of the tear-tip diameter associated with tear deviation is the major factor which influences the tear strength, and that this factor outweighs the effect of hysteresis. In the absence of knotty tearing, hysteresis becomes the major factor in determining the tear strength.

5.5 Effect of filler loading

In Section 5.2, the tear behaviour of rubbers filled with 50 pphr of HAF black was discussed. Figure 5.15 gives further results for the tear behaviour of the same rubbers but, at lower filler loadings than 50 pphr. Results are also given for unfilled vulcanizates. Consider the tear behaviour of the unfilled vulcanizates. This gives some indication of the inherent tear strength of the vulcanizates in the absence of added fillers. The results are presented in tabulated and in graphical form. Table 5.6A and Figure 5.15a compare the tear behaviour of NR, ENR25, ENR50, SBR and INR at 23°C. The results show that the tearing energy is affected by both the degree of crystallinity and the glass-transition temperature of the rubber. This is reflected by the fact that the tearing energy decreases in the order of decreasing degree of strain crystallisability, i.e., NR > ENR25 > ENR50. It is also noted that in the absence of strain-crystallization, the magnitude of the tearing energy is influenced by the glass-transition temperature of the rubber.

In the absence of strain-crystallization, rubbers with high glass-transition temperature dissipates more energy than rubbers having low glass-transition temperature. Thus rubbers having high glass-transition temperature give higher tearing energy than rubbers having low glass-transition temperature. For this reason, the tearing energy of unfilled SBR is higher than the tearing energy of

TABLE 5.6: Effect of filler loading on tearing energy

(A) Unfilled vulcanizates (Full formulations shown in Table 4.3a, Chapter Four) Temperature 23°C

Tear rate ($\mu m\ s^{-1}$)	8.3	42	83	170	420	830	1700	4200	8300
NR, T ($kJ\ m^{-2}$)	16	27	24	26	42	33	30	33	32
Type of tear failure	s.s	s.s	s.s	s.s	s.s	s.s	s.s	s.s	s.s
ENR 25, T ($kJ\ M^{-2}$)	35	30	31	30	33	27	30	26	23
Type of tear failure	s.s	s.s	s.s	s.s	s.s	s.s	s.s	s.s	s.s
ENR 50, T ($kJ\ m^{-2}$)	19	19	18	19	20	17	18	19	20
Type of tear failure	s.s	s.s	s.s	s.s	s.s	s.s	s.s	s.s	s.s
SBR, T ($kJ\ m^{-2}$)	2.1	3	3	4	4	4.5	5.0	4.6	5.1
Type of tear failure	s	s	s	s	s	s	s	s	s
INR, T ($kJ\ m^{-2}$)	0.9	1.4	1.6	1.9	2.1	2.2	2.4	2.4	2.4
Type of tear failure	s	s	s	s	s	s	s	s	s

s - steady tearing s.s - stick-slip tearing

(B) Unfilled vulcanizates (Formulations shown in Table 4.3a, Chapter Four) Comparison at the same molecular mobility with that of NR at 23°C

Tear rate ($\mu m\ s^{-1}$)	8.3	42	83	170	420	830	1700	4200	8300
ENR 25, T ($kJ\ m^{-2}$)	18.5	20	20	22	20	19.5	21	21	17
Type of tear failure	s.s	s.s	s.s	s.s	s.s	s.s	s.s	s.s	s.s
ENR 50, T ($kJ\ m^{-2}$)	8.3	6.4	6.6	6.8	8.5	8.5	9.5	10	10
Type of tear failure	s.s	s.s	s.s	s.s	s.s	s.s	s.s	s.s	s.s
SBR, T ($kJ\ m^{-2}$)	1.85	1.95	2.3	2.9	2.7	3.3	3.3	3.8	3.3
Type of tear failure	s	s	s	s	s	s	s	s	s

Temperature: ENR 25 47°C, ENR 50 68°C, SBR 32°C

s - steady tearing s.s - stick-slip tearing

TABLE 5.6: Effect of filler loading on tearing energy. Base mix formulations shown in Table 4.2. Semi-EV cure system was used in each case.

(c) 10 pphr of HAF

Tear rate, ($\mu m\ s^{-1}$)	42	83	170	420	830	1700	4200	8300
NR, T ($kJ\ m^{-2}$)	27	22	19	18	17	19	18	17
Type of tear failure	k	k	s.s	s.s	s.s	s.s	s.s	s.s
ENR 25, T ($kJ\ m^{-2}$)	15	19	19	18	19	20	20	19
Type of tear failure	s.s	s.s	s.s	s.s	s.s	s.s	s.s	s.s
ENR 50, T ($kJ\ m^{-2}$)	16	16	17	16	18	18.5	19	22
Type of tear failure	s.s	s.s	s.s	s.s	s.s	s.s	s.s	s.s
SBR, T ($kJ\ m^{-2}$)	9	9.7	10	10.5	10	11	11.5	11
Type of tear failure	s.s	s.s	s.s	s.s	s.s	s.s	s.s	s.s

Temperature: NR 23°C, ENR 25 47°C, ENR 50 68°C, SBR 32°C

s.s - stick-slip tearing s - knotty tearing

(D) 25 pphr of HAF

Tear rate, ($\mu m\ s^{-1}$)	42	83	170	420	830	1700	4200	8300
NR, T ($kJ\ m^{-2}$)	82	67	39	49	39	38	38	28
Type of tear failure	k	k	k	k	k	k	k	k
ENR 25, T ($kJ\ m^{-2}$)	59	59	57	38	26	25	31	15.5
Type of tear failure	k	k	k	k	k	k	k	s
ENR 50, T ($kJ\ m^{-2}$)	40	38	39	39	35	25	25	18
Type of tear failure	k	k	k	k	k	k	k	s.s
SBR, T ($kJ\ m^{-2}$)	27	28	30	30	29	24	24	22
Type of tear failure	s.s	s.s	s.s	s.s	s.s	s.s	s.s	s.s

Temperature: NR 23°C, ENR 25 47°C, ENR 50 68°C, SBR 32°C

k - knotty tearing s.s - stick-slip tearing
s - smooth tearing

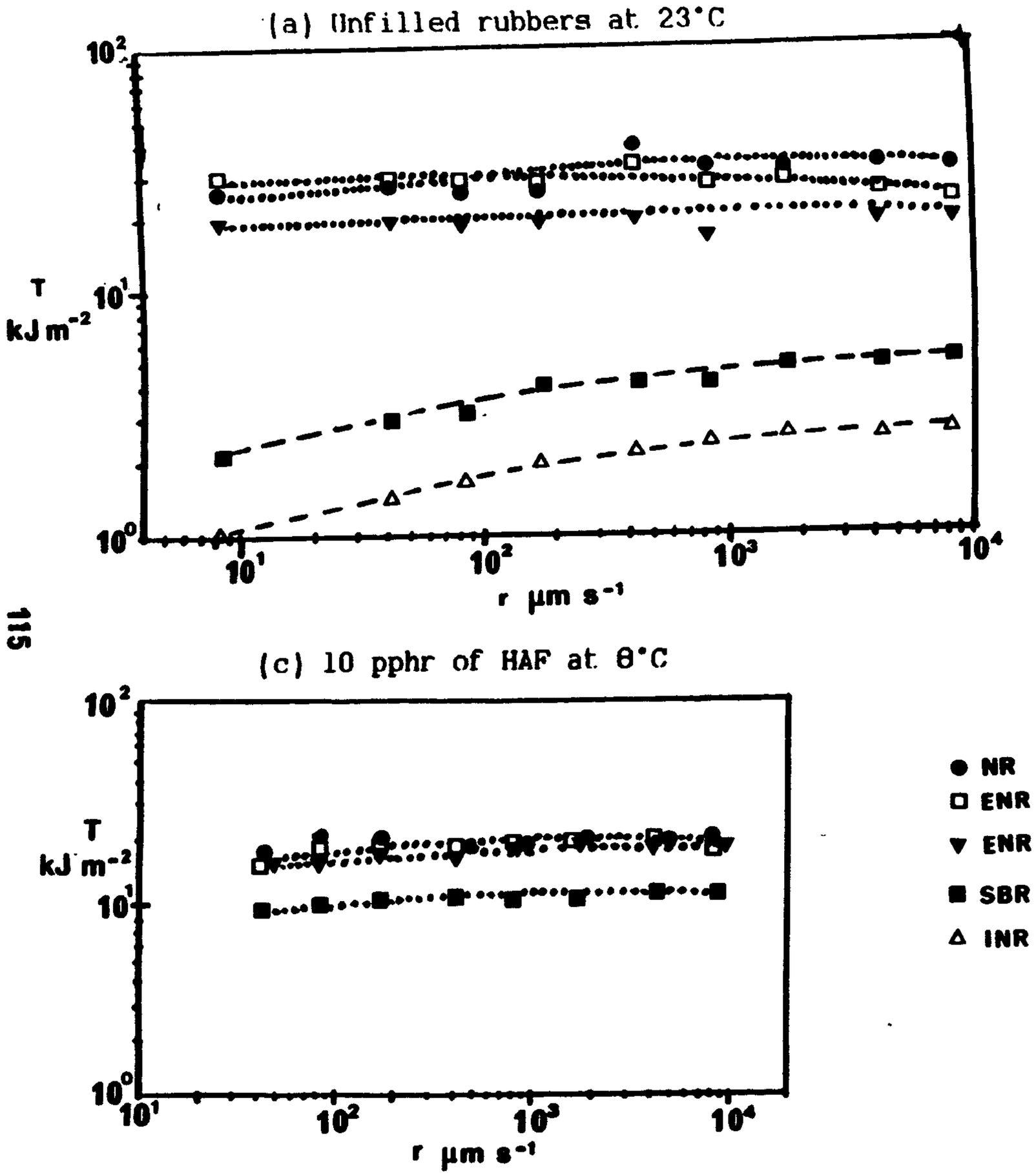

Figure 5.15: Tearing energy, T, vs tear rate, showing effect of HAF black loading on tear failure.
Cure system: semi-EV vulcanization system. Base mix formulations shown in Figure Table 4.2 in Chapter Four.
---- steady, ... stick-slip, and ——— knotty tearing

unfilled isomerised NR. The results shown in Table 5.6A and in Figure 5.15a clearly demonstrate the role of crystallization in enhancing tear strength. In fact, the comparison between natural and isomerised natural rubbers is particularly interesting because it gives some indication of the contribution to tearing energy strength made by crystallization relative to that made by internal viscosity of the material. For example, at a tear rate of 8.3 μm s^{-1} the tearing energy of NR was about 17 times greater than that of INR, indicating that the contribution made to tear by strain-crystallization is substantial.

When rubbers crystallize on stretching, they exibit more hysteresis energy loss than expected from viscoelastic considerations (67). It has been suggested, that the additional hysteresis energy loss when crystallization occurs could result from the formation and melting of crystalline regions upon extension and retraction of the material (68). The manner by which mechanical hysteresis influences the tear strength has been explained by Andrews (28). He suggested that, if a crack propagates into a hysteretic material, the strain concentration at the tip of the crack is substantially less than would be the case if the material were perfectly elastic. This arises because the strains ahead of the crack tip are 'frozen', that is, the rubber around the tip is prevented from deforming, and this results in a correspondingly lower stress concentration.

Table 5.6B and Figure 5.16b show the tear behaviour of these rubbers at the same relative molecular mobility as that of natural rubber at 23°C. This was achieved by raising the temperature appropriately according to equation 5.3 discussed earlier in Section 5.2. The variations of tearing energy with tear rate still show the same general trend as observed at 23°C, and the tearing energy still increases in the order of increasing degree of strain crystallisability. On raising the temperature to 47°C, there was a decrease of about 30% in the tearing energy of ENR25 over the whole range of tear rates, when compared with the tearing energy obtained at 23°C. In the case of unfilled ENR50 vulcanizates, raising the temperature to 68°C, the tearing energy decreased by about one half compared to the tearing energy obtained at 23°C. These decreases in the tearing energy may be associated with some melting of the crystalline phase.

The results in Table 5.6B show that, the tearing energy of SBR was at least 50% higher than the tearing energy of isomerised natural rubber over a wide range of tear rate. It was expected that the SBR vulcanizates would have the same tearing energy as that of INR vulcanizates because the vulcanizates were compared at the same molecular mobility. According to Mullins (35), the tearing energy is the same for all unfilled amorphous rubbers under conditions of equal segmental mobility. Mullins (35) arrived at this conclusion when he found that, the tearing energies of unfilled non-strain-crystallizing vulcanizates of SBR and NBR, having widely different glass-transition temperatures, were all seen to fall on a single mastercurve. Furthermore, he noticed that the tearing energy increased with increasing rate of tearing in accordance with the dissipation of energy by a viscous process. However, the tearing energies of unfilled SBR and unfilled INR vulcanizates were not the same when the vulcanizates were torn under condition of the same molecular mobility. The descrepancy may be a consequence of differences in the nature of the chemical crosslinks and the concentration at which they are present in the rubber.

A further interesting observation is the effect of tear rate on tearing energy. Figures 5.15a and 5.15b indicate little or no dependence of the tearing energy of NR and ENR25 vulcanizates on tear rate presumably because strain-crystallization outweighs viscoelastic effects. In the case of ENR50, there was no dependence of tearing energy on tear rate at 23°C, but there appeared to be a slight dependence of tearing energy on tear rate at 68°C. This may be a consequence of lowering of the degree of crystallinity associated with melting. The results obtained here are in agreement with the earlier work by the author (64).

The non-strain-crystallizing rubbers SBR and INR, showed a strong dependence of tearing energy on tear rate. For example, at 23°C increasing the tear rate from 8.3 $\mu m\ s^{-1}$ to 8300 $\mu m\ s^{-1}$, increased the tearing energy by factors of 2 and 2.5 for INR and SBR respectively, as shown in Figure 5.15a. In amorphous rubber, the dependence of tearing energy on tear rate is a consequence of the hysteresis associated with the internal viscosity of the material (29,32,42,64). The internal friction, or internal

viscosity, arises from the molecular chains rearranging their conformations requiring segments to slide past one another. The hysteresis arising from internal friction depends on the rate and temperature of deformation. At low temperatures or high tear rates, hysteresis increases because the internal viscosity increases. In contrast, the hysteresis arising from crystallization is not highly dependent upon rate and temperature. This explains why the tearing energy of strain-crystallizing rubbers is relatively unaffected by the tear rate. Apparently at tear rates greater than 10 m s^{-1}, NR does not strain-crystallize and the effect of tear rate on tearing energy becomes significant (30).

Another interesting observation associated with the tearing of unfilled rubbers was the type of tear failure. All the strain-cystallizing rubbers produced stick-slip tearing, whilst the two non-strain-crystallizing rubbers produced steady tearing with little fluctuations of tearing force with rates of tearing. The fractured surface associated with stick-slip failure appeared to be slightly rougher than steady failure as shown in Figure 5.17 (first row). Roughening of the crack tip can also increase the tear strength.

When fillers such as carbon black are incorporated into a rubber matrix, both the type of tear failure and the magnitude of tearing energy are affected. The effect is more pronounced in the case of a non-strain-crystallizing rubber, such as SBR. Figures 5.16a,b,c and d, show the effect of HAF black at various loadings. Generally, the tearing energy increases as the black loading increases, particularly in the case of SBR which does not strain-crystallize. At 10phr and 25phr of HAF black, the tearing energy increased by factors of 3 and 10 respectively compared to the corresponding unfilled vulcanizates. In the case of strain-crystallizing rubbers the effect was very pronounced at 25phr and above, where knotty tearing can occur. However, the magnitude of the tearing energy depends on the degree of the knottiness and roughness of the fractured surface at each filler loading. Figure 5.17 shows photographs of the fractured surface at different filler loadings. At each level of filler, the magnitude of the tearing energy still follows the order of the strain-crystallisability of the rubbers, as is evident from Figures 5.15c and 5.15d.

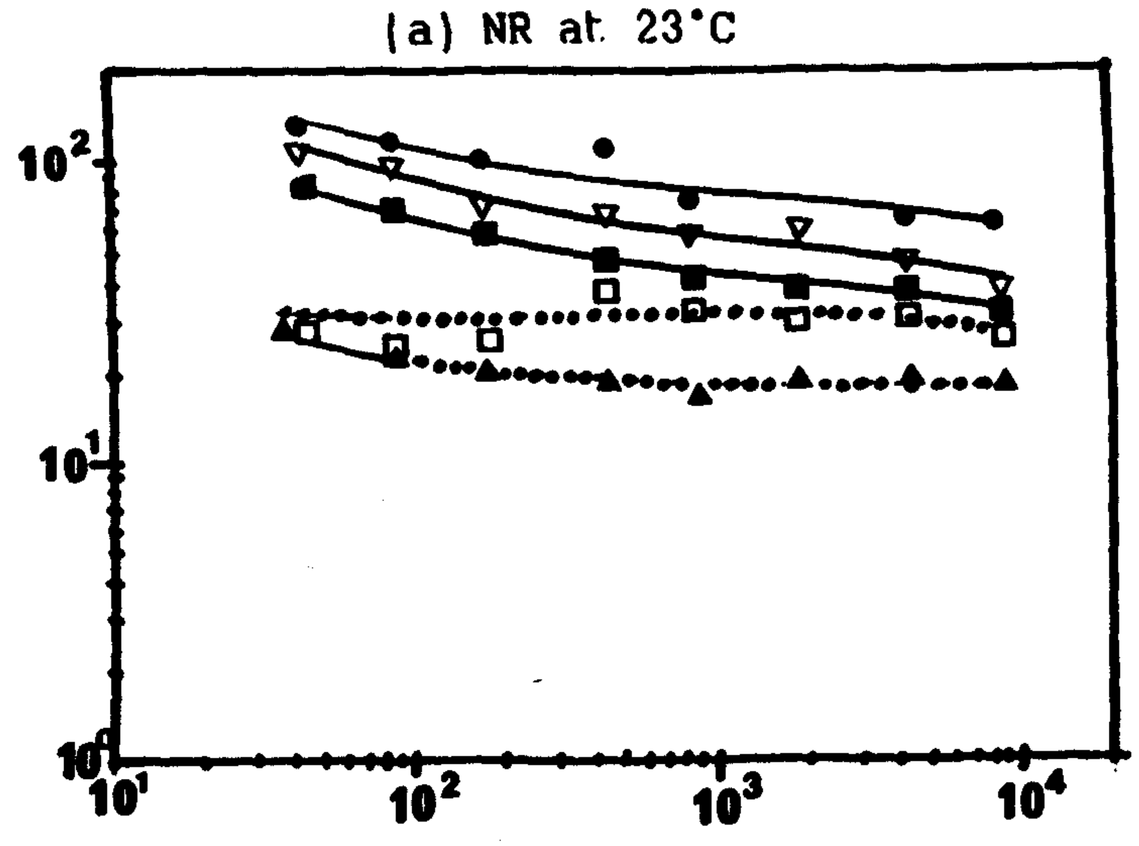

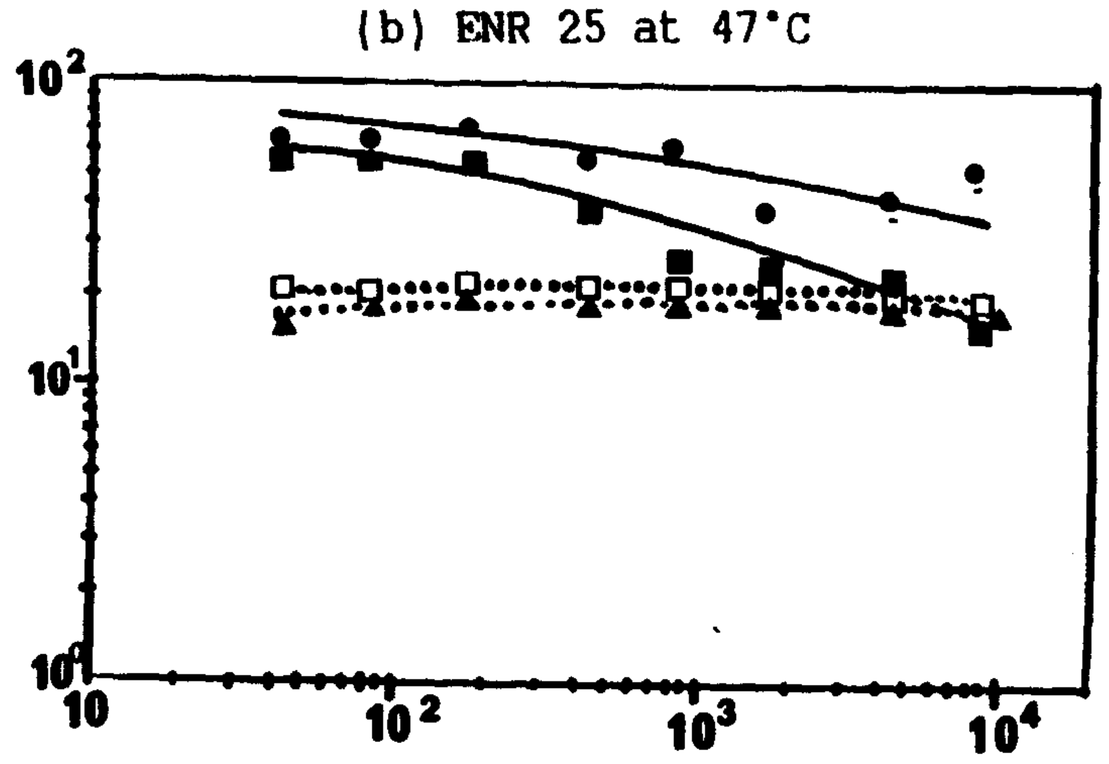

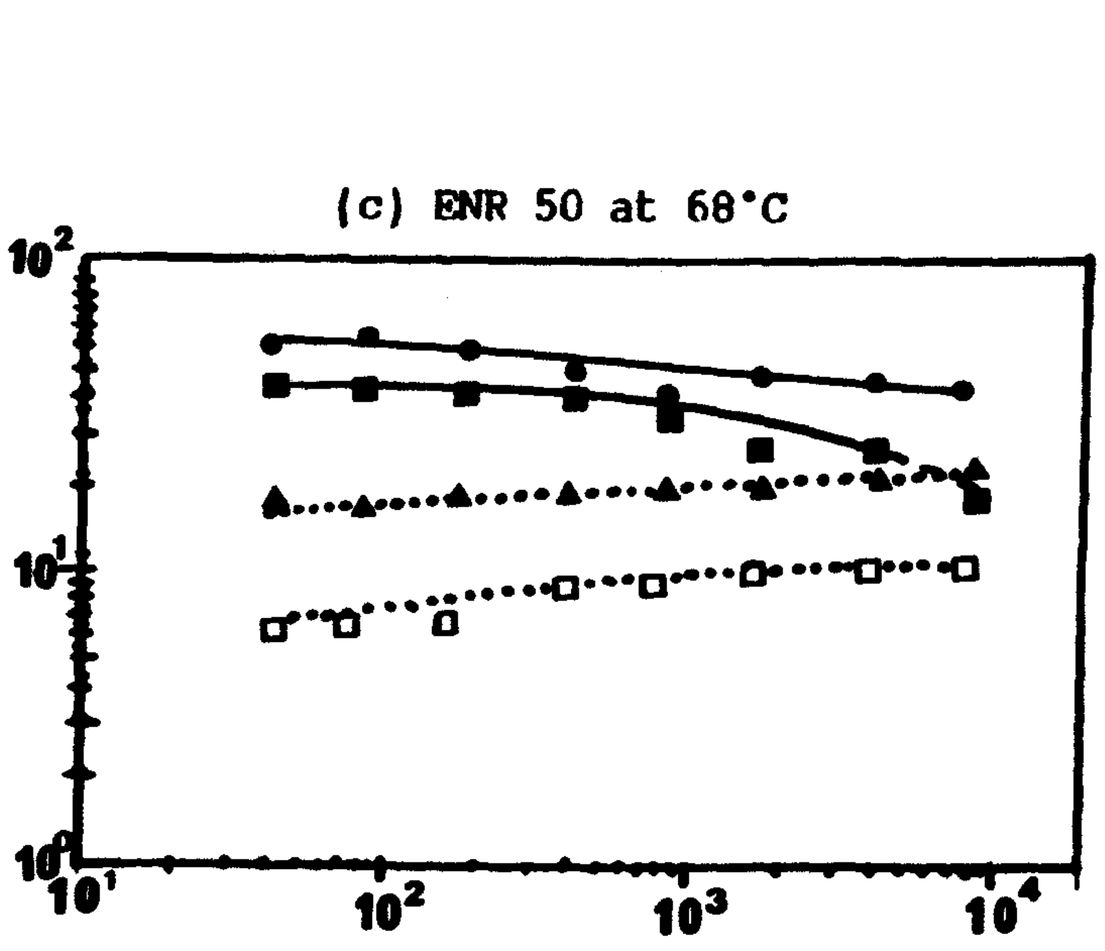

- ● 50 pphr HAF
- ▽ 40 pphr HAF
- ■ 25 pphr HAF
- ▲ 10 pphr HAF
- □ unfilled

Types of tearing
- ——— Knotty
- ····· Stick-slip
- – – – Steady

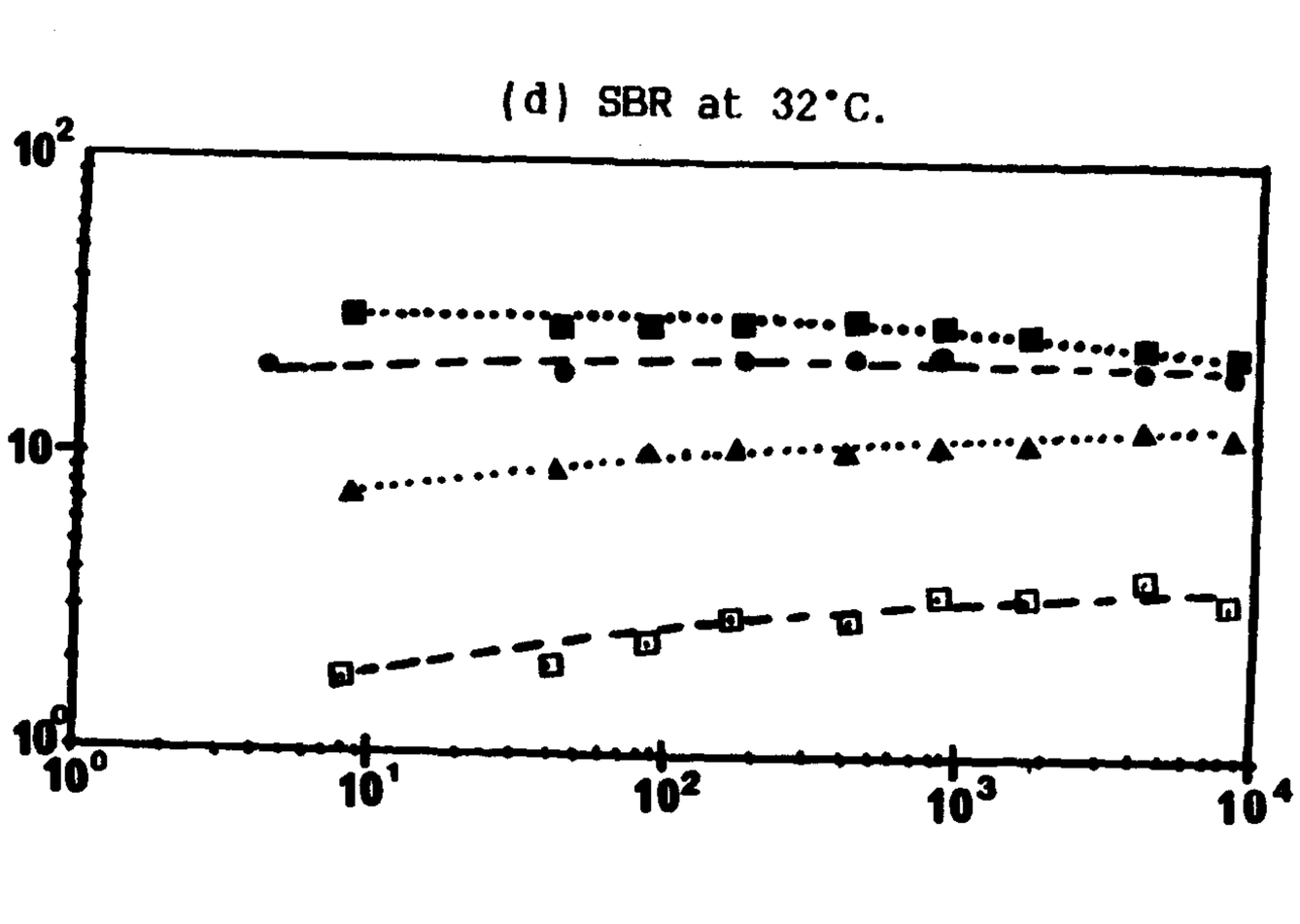

Figure 5.16: Effect of HAF black loading on tearing energy. Base mix formulations shown in Table 4.2 in Chapter Four.

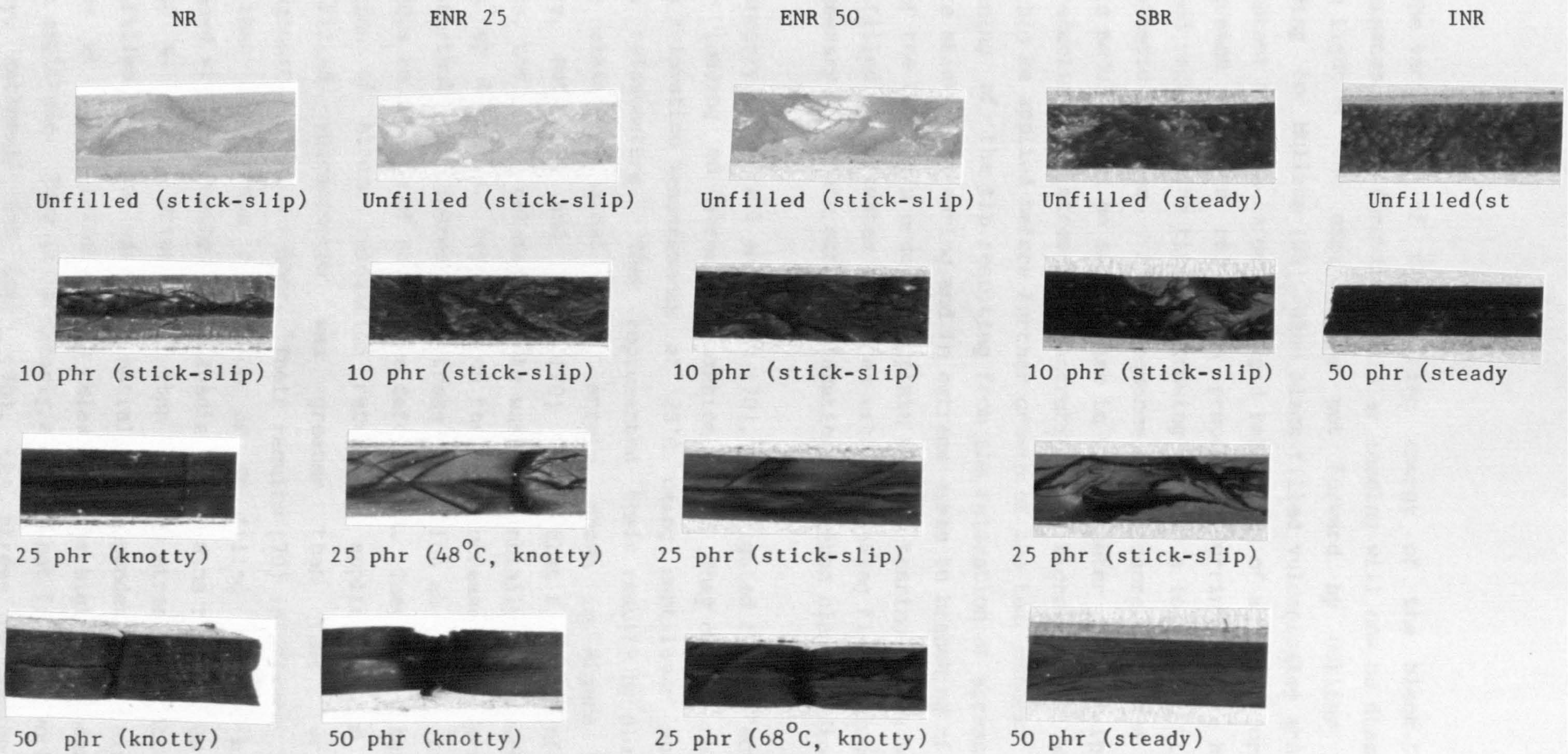

Figure 5.17: Photographs showing fractured surfaces at different HAF loadings at tear rate of 830 μm s^{-1}.

The variations of the tearing energy of the black-filled vulcanizates as a function of filler loading will now be discussed in the light of the explanations put forward by Mullins (69). According to Mullins (69), when black-filled vulcanizates are held at constant strain a large and rapid relaxation of stress occurs. A consequence of this relaxation process occurring in the highly strained region at the tip of a growing tear is a local reduction in the elastic modulus. A consequence of the decrease in the local elastic modulus will be an increase in the diameter of the tip and the reduction in stress concentrations. A higher overall stress must then be applied before further growth of the tear occurs. This broadening of the tip resulting from the relaxation of stress will lead to stick-slip tearing and in extreme cases to branching of the tip of the tear. In order to explain why the tearing energy of the black-filled vulcanizates increases with increasing filler loading, it necessary to relate stress relaxation to carbon black loading.

Gregory, Metherell and Smith (70), investigated the effect of filler loading on stress relaxation of NR. They carried out the stress relaxation measurements at 23°C using cantilever spring stress relaxometers. They represented their results by plotting stress relaxation against tensile strain, shown in Figure 5.18. Gregory, Metherell and Smith (70) found that for many unfilled rubbers, the stress relaxation rate was substantially independent of strain up to 200%, beyond which the rate increased considerably. They attributed the increase in stress relaxation at strains higher than 200% to effects of non-affine deformation. They found that the variation of stress relaxation rate with applied strain for black-filled vulcanizates was greater than that for the corresponding unfilled rubber. Their results (70) in Figure 5.18, show that the stress relaxation of NR filled with SRF black, increased with increasing filler loading at strains ranged from 30% to 400 %. At a strain lower than 30%, the stress relaxation of black-filled rubbers was substantially independent of strain, whereas at high strains, stress relaxation was highly dependent on strain amplitude. Thus it is clearly evident that from the work of Gregory, Metherell and Smith (70), the stress relaxation rate increases with increasing filler loading. The significance of stress relaxation ahead of the tear tip on the tear resistance was discussed above.

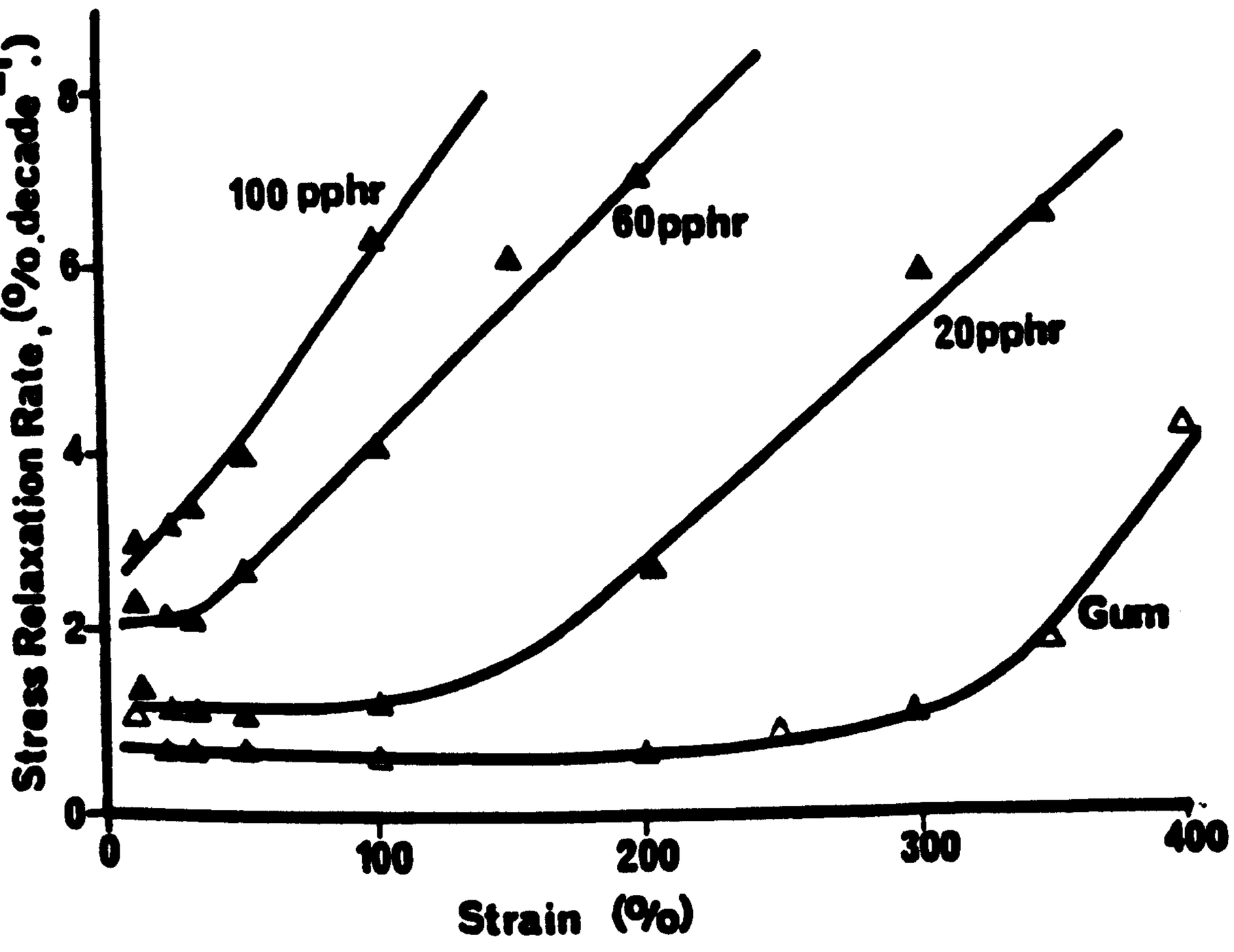

Figure 5.18: Variation of stress relaxation rates with applied strain for SRF-black-filled vulcanizates (Ref. 70)

Putting together Mullins's suggestion (69) and the experimental data of Gregory, Metherell and Smith (70), the reason for the increase in the tearing energy with increasing filler loading can be explained as follows: The increase in the tearing energy with increasing filler loading, may be attributed to an increase in the diameter of the tear-tip and reduction in stress concentrations as a consequence of the relaxation of stress ahead of the rupture tip, and that the stress relaxation rate increases as the filler loading increases.

The effect of filler loading on the size of knot diameter was investigated, to see if there was any evidence of increase in the knot diameter with increasing filler loading. Tearing measurements were carried out at a tear rate of 830 μm s^{-1} at temperatures ranging from 50°C to 120°C, using ENR 25 vulcanizates filled with HAF black. The HAF black loading was varied from 25, 40, 50 to 60 parts per hundred of rubber. The knot diameter, d, was measured by means of an eye-piece lens scale. The results are shown in Tables 5.7 A,B,C and D. The value of d shown in each table represents the average value measured from five test-pieces. The value was compared with that estimated from equation 5.4. The value of U_b referred to stored energy density at break determined by integrating the area under the stress-strain curve at break, produced by straining the dumbbell test-pieces at an extension rate of 100mm per minute at 23°C. No attempts were made to make stress-strain measurements at temperatures and rates corresponding to the tear measurement. The values of d shown in each table are an approximate only. The agreement between the measured value of d and the value of d estimated from equation 5.4 is reasonably good, in view of the uncertainty of the actual value of U_b. In general, the tearing energy increased with increasing filler concentration, although at 50°C and 90°C, ENR 25 vulcanizates having low black loading gave higher tearing energy than that of the vulcanizates having high black loading. The values of d shown in Tables 5.7 A,B,C and D, were plotted against HAF black loading. The results are shown in Figures 5.19A, B, C and D. The results show that the knot diameter increased with increasing filler loading, which is consistent with the increase in tearing energy with increasing filler loading.

TABLE 5.7: Effect of filler concentration and temperature on tearing energy of black-filled ENR 25 vulcanizates using semi-EV cure system. Base mix formulations shown in Table 4.2 in Chapter Four. Tear rate: 830 μm s^{-1}

(A) Temperature 50°C

HAF black	25	40	50	60
T (kJ m^{-2})	29.0	38.5	64.5	46.4
U_b (MJ m^{-3})	51	53	59	57
$d^b = T/U_b$ (mm)	0.6	0.7	1.1	0.8
d (mm)	0.5	0.6	0.9	0.8

(B) Temperature 70°C

HAF Black	25	40	50	60
T (kJ m^{-2})	36.0	52.0	56.1	59.3
U_b (MJ m^{-3})	51	53	59	57
$d^b = T/U_b$ (mm)	0.7	1.0	0.95	1.0
d (mm)	0.6	0.7	0.7	0.8

(C) Temperature 90°C

HAF Black	25	40	50	60
T (kJ m^{-2})	39.7	61.0	46.4	71.0
U_b (MJ m^{-3})	51	53	59	57
$d^b = T/U_b$ (mm)	0.8	1.1	0.8	1.2
d (mm)	0.9	1.3	0.7	1.5

(D) Temperature 120°C

HAF Black	25	40	50	60
T (kJ m^{-2})	22.0	43.0	58.0	75.0
U_b (MJ m^{-3})	51	53	59	57
$d^b = T/U_b$ (mm)	0.4	0.8	1.0	1.3
d (mm)	0.6	1.2	2.0	2.4

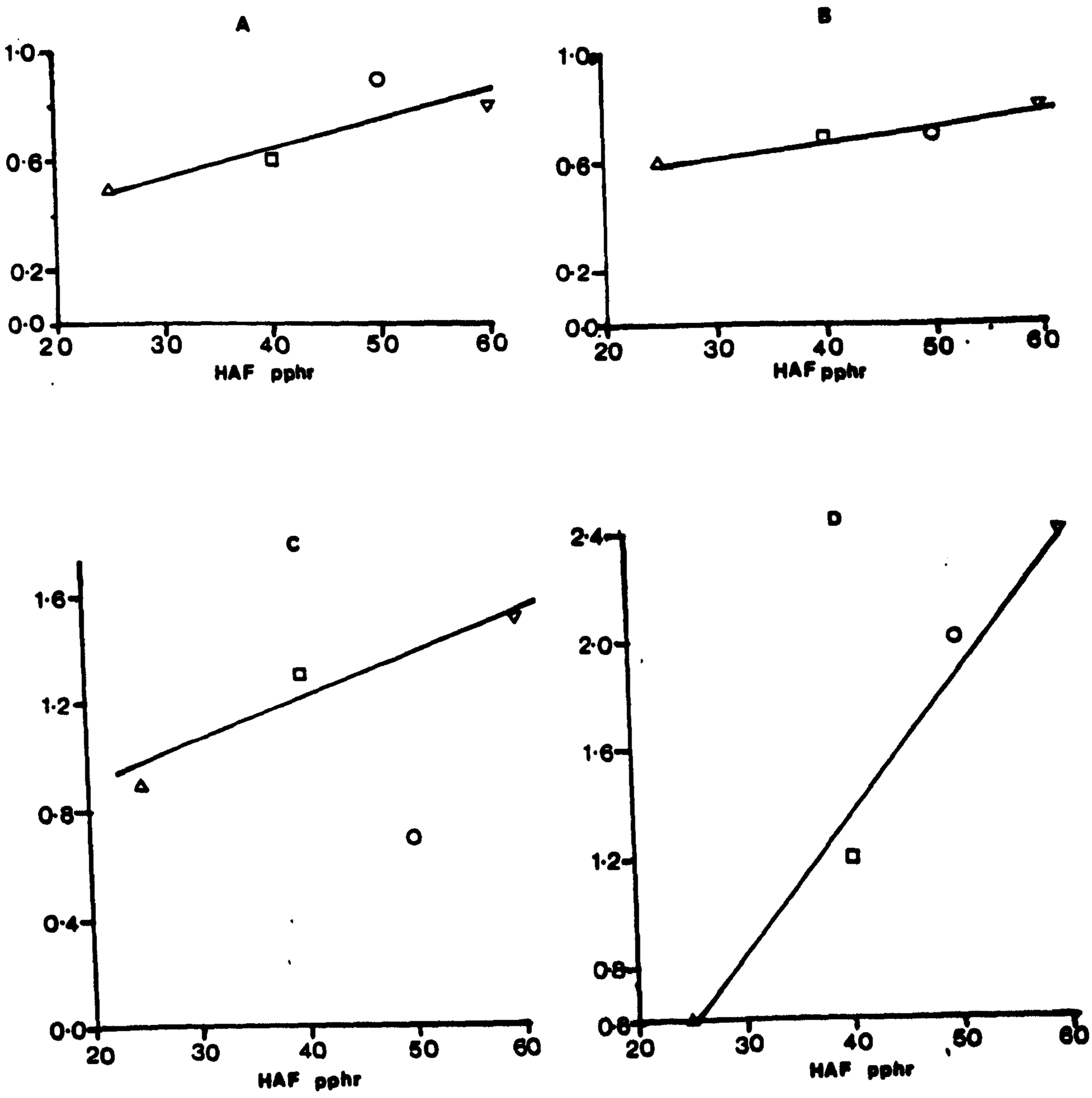

Figure 5.19: Knot diameter, d, vs HAF black loading, showing variation of d with filler loading. △ 25 pphr, □ 40 pphr ○ 50 pphr, and ▽ 60 pphr of HAF black.
(A) 50°C (B) 70°C (C) 90°C (D) 120°C
at tear rate of 830 μm s^{-1}, using ENR 25 vulcanizate cured with semi-EV vulcanization system.

The effect of filler loading on the size of knot diameter was investigated further by making tear measurements on SBR vulcanizates filled with 40 pphr, 50 pphr and 60 pphr of HAF black, so that the issue of strain-crystallization could be avoided. The tear measurements were carried out at 90°C because earlier work had shown that knotty tearing could occur in black-filled SBR at 90°C (refer to Section 5.3). The rate of tearing was varied by separating the legs of the trouser test-piece at a rate of extension ranging from 0.5 mm per minute to 1000 mm per minute. The tear rate was taken as half the rate of extension. The results are shown in Table 5.8. Generally, the tearing energy at each tear rate increased with increasing filler loading, which is consistent with the results shown in Table 5.7. The mean knot diameter shown in Table 5.8 was plotted against tear rate. Figure 5.20 shows the result of the plot. Linear scale was used for the mean knot diameter and logarithmic scale was used for the tear rate because of the wide range of tear rates investigated. The knot diameter decreased with increasing rate of tearing which is consistent at each level of black loading. The results shown in Figure 5.20 are in a good agreement with the results discussed in Section 5.2.2. The most interesting point about the results shown in Figure 5.20, is that the knot diameter increased with increasing filler loading, which is in good agreement with the results shown in Figure 5.19.

The main conclusion that can be drawn from the results here, is that the increase in tearing energy with increasing carbon black concentration can be attributed to an increase in the effective diameter of the tear tip.

5.6 Effect of the nature of filler

All the results so far were obtained using vulcanizates containing an HAF black. This black has a mean diameter of about 0.04 microns, but is present in the rubber compound in a flocculated condition with aggregates up to about 0.3 microns in diameter (71). The tear behaviour of vulcanizates which contained an MT black was also investigated. MT black consists of substantially spherical particles of mean diameter about 0.4 microns. Another significant difference between an MT and an HAF black is that the former has

TABLE 5.8: Effect of HAF black concentration on tearing energy of SBR Full formulations shown in Table 4.3b for mix H4 in Chapter Four. Temperature 90°C.

Tear rate ($\mu m\ s^{-1}$)	4.2	42	170	830	4200	8300
(a) 40 pphr HAF, T ($kJ\ m^{-2}$)	32	31	24	22	26	29
d (mm)	4.0	2.2	2.0	1.2	1.4	1.5
(b) 50 pphr HAF, T ($kJ\ m^{-3}$)	43	34	29	30	30	27
d (mm)	4.1	2.4	2.0	1.6	1.6	1.2
(c) 60 pphr HAF, T ($kJ\ m^{-1}$)	42	34	40	38	35	36
d (mm)	4.0	2.6	2.2	1.8	1.5	1.7

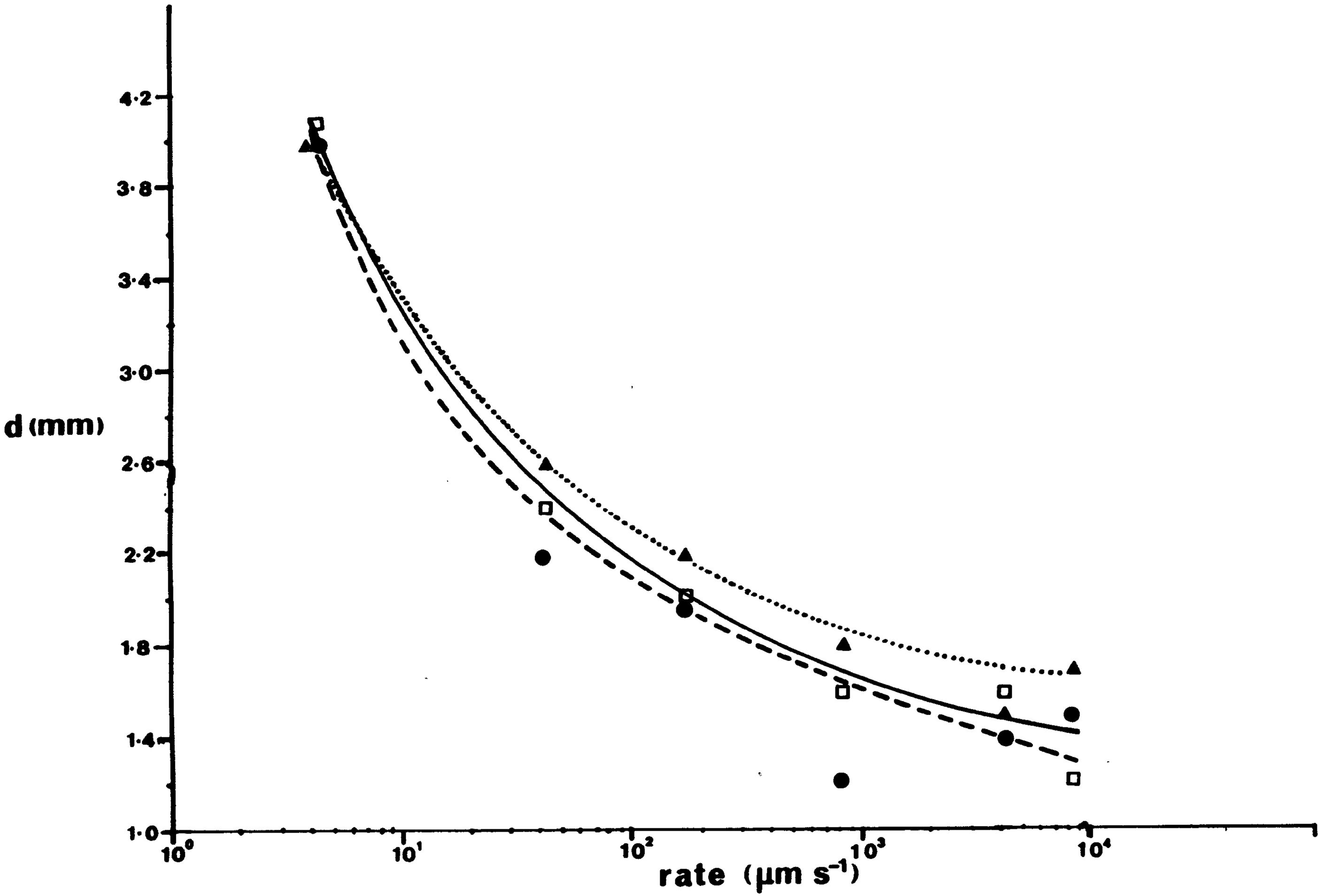

Figure 5.20: Knot diameter, d, vs tear rate, showing variation of knot diameter with filler loading at various tear rates at 90°C. Rubber sample: SBR cured with semi-EV vulcanization system.
● 40 pphr, □50 pphr, and ▲60 pphr of HAF.

little or no ``structure'' (7), whereas the latter has ``structure'' (7). The term ``structure'' refers to the joining together of carbon particles into long chains and tangled three-dimensional aggregates (7), which takes place in the flame during the manufacture of carbon black. The term ``black structure'' has also been used by Greensmith (16) and Medalia (49) to denote the alignment of carbon black aggregates and their linkage into chains or strands. Thus, ``black structure'' occurs at the tip of the tear as a consequence of large local deformation around the tip of the tear. The formation of ``black structure'' at the tip of tear is very significant in inducing the strength anisotropy necessary for knotty tearing to occur (15,16).

Another important characteristic of carbon black particles is the surface activity which is believed to affect the extent of rubber-filler interaction (8,72). Carbon blacks consist of 90% to 99% elemental carbon (7). The other major constituents are combined hydrogen and oxygen. The principle groups present are phenolic, ketonic and carboxylic, together with lactones (7). The surface groups are not physically absorbed but are chemically combined. MT and HAF blacks also differ significantly in term of surface activity because the former is produced by thermal process whereas the latter is produced by furnace process. MT black has lower surface activity than HAF black and the former does not give ``bound rubber'' while the latter gives considerable ``bound rubber'' (73). ``Bound rubber'' reflects the extent of rubber-filler interaction. High ``bound rubber'' indicates strong rubber-filler interaction. It would be of interest to see how the differences in the characteristic of the carbon blacks will affect the tear behaviour of the rubber.

Vulcanizates containing 50 pphr of MT black were prepared using the formulations given in Table 4.3c of Chapter Four. The formulations shown in Table 4.3c are different from Table 4.3b only in the type of black. The former used an MT black and the latter used an HAF black, otherwise the cure system (semi-EV) and other basic ingredients were the same. Thus any differences observed between the tear behaviour of vulcanizates produced by an MT black and the tear behaviour of vulcanizates produced by an HAF black, reflected the effect of the differences of the characteristic of the two blacks.

Tearing measurements were carried out using trouser tear test-pieces in an Instron machine, at temperature of 23°C, at various tear rates. The results are shown in Table 5.9 and in Figure 5.21, where tearing energy is plotted against tear rate using logarithmic scales. Natural rubber gave knotty tearing at tear rates ranging from 8.3 μm s^{-1} to 83 μm s^{-1}. At tear rates greater than 83 μm s^{-1}, NR gave steady tearing with smooth fractured surfaces. The results obtained from the present investigation are more-or-less in agreement with the results of Greensmith (16) who found that, with 50 pphr of MT black, NR gave knotty tearing at tear rates ranging from 4.2 μm s^{-1} to 42 μm s^{-1} at temperatures ranging from -20°C to 25°C. At tear faster than 42 μm s^{-1}, it reverted to either stick-slip or steady tearing. No attempts were made to investigate the effect of tear rate on the tear behaviour of MT black-filled NR, and other rubbers used in the present investigation, at temperatures other than at 23°C. However, Greensmith (16) found that, at 90°C, knotty tearing occurred at tear rates ranging from 4.2 μm s^{-1} to about 8300 μm s^{-1}, and at a tear rate higher than 8300 μm s^{-1}, tearing reverted to the steady type.

In the case of ENR25, steady tearing occurred over the whole range of tear rates investigated. The tearing energy was about one fifth of that of a similar vulcanizate reinforced with HAF black, and about one half that of the corresponding unfilled vulcanizate. This suggests that crystallization is more effective in enhancing tear strength than is the presence of large particles of MT black. The same conclusion applies to ENR50.

In the case of SBR, the tearing energy was about 5 times higher than that of the corresponding unfilled vulcanizate, but one half or less than that of the corresponding HAF black-filled vulcanizate. Greensmith (16) found that SBR, when filled with 50 pphr of MT black, did not produce knotty tearing at any tear rate (0.1 μm s^{-1} to 10^6 μm s^{-1}) and temperature (-20°C to 90°C) which he investigated. Thus on the whole, HAF blacks were more effective in enhancing the tear strength than the corresponding MT black. The results for NR and SBR obtained in the present investigation are more-or-less in agreement with those of Greensmith (16).

TABLE 5.9: Tearing energy produced by MT black vulcanizates at various tear rates at 23°C. Full formulations shown in Table 4.3c in Chapter Four.

Tear rate ($\mu m\ s^{-1}$)	8.3	42	83	170	420	830	1700	4200	8300
NR, T ($kJ\ m^{-2}$)	25	24	27	9.6	11	12	12	11	11
Type of tear failure	k	k	k	s.s	s.s	s	s	s	s
ENR 25, T ($kJ\ m^{-2}$)	7.4	11	9.7	8.5	9.5	8.5	8.5	8.2	10
Type of tear failure	s	s	s	s	s	s	s	s	s
ENR 50, T ($kJ\ m^{-2}$)	7	12	13	13	14.5	15	13	16	17
Type of tear failure	s	s.s	s.s	s.s	s.s	s.s	s	s	s
SBR, T ($kJ\ m^{-2}$)	11	14	16	16	16	13	15	11	10
Type of tear failure	s.s	s.s	s.s	s.s	s.s	s	s	s	s

k - knotty tearing s.s - stick-slip tearing s - steady tearing

Table 5.10: Effect of carbon black type on stress relaxation (Ref. 70)

Filler type (ASTM number)	Av. particle size (nm)	Stress relaxation rate at 100% strain (% per decade)
SAF (N110)	20 - 25	5.1
HAF (N330)	28 - 36	4.7
SRF (N762)	70 - 96	4.1
MT (990)	250 - 350	2.1

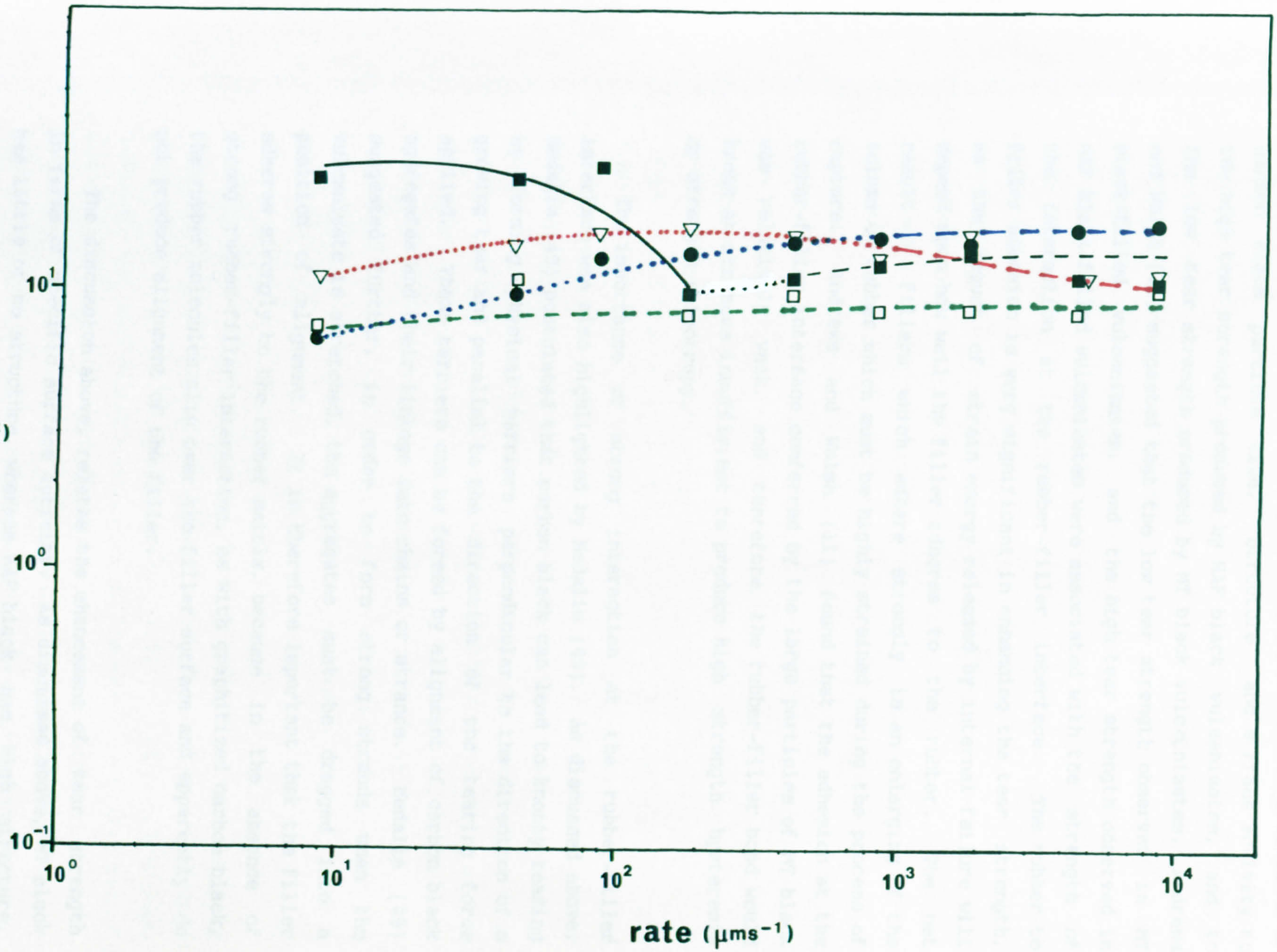

Figure 5.21: Tearing energy, T, vs tear rate at 23°C,
showing effect of MT black on tearing energy.
Full formulations are given in Table 4.3c in Chapter Four.

It is very difficult to determine the relative contributions of carbon black particle size, ``structure'' and surface activity to the high tear strength produced by HAF black vulcanizates, and to the low tear strength produced by MT black vulcanizates. Andrews and Walsh (11) suggested that the low tear strength observed in MT black-filled vulcanizates, and the high tear strength observed in HAF black-filled vulcanizates were associated with the strength of the interaction at the rubber-filler interface. The rubber to filler adhesion is very significant in enhancing the tear strength, as the amount of strain energy released by internal failure will depend upon how well the filler adheres to the rubber. The net result of fillers which adhere strongly is an enlarging of the volume of rubber which must be highly strained during the process of rupture. Andrews and Walsh (11) found that the adhesion at the rubber-filler interface conferred by the large particles of MT black was relatively weak, and therefore the rubber-filler bond would break at stresses insufficient to produce high strength hysteresis or strength anisotropy.

The importance of strong interaction at the rubber-filler interface was also highlighted by Medalia (49). As discussed above, Medalia (49) postulated that carbon black can lead to knotty tearing by forming physical barriers perpendicular to the direction of a growing tear and parallel to the direction of the tearing force applied. These barriers can be formed by alignment of carbon black aggregates and their linkage into chains or strands. Medalia (49) suggested further, in order to form strong strands when the vulcanizate is stretched, the aggregates must be dragged into a position of alignment. It is therefore important that the filler adheres strongly to the rubber matrix, because in the absence of strong rubber-filler interaction, as with graphitized carbon black, the rubber molecules slip over the filler surface and apparently do not produce alignment of the filler.

The discussion above, relates the ehancement of tear strength in terms of specific surface activity. As discussed above, MT black has little or no structure, whereas HAF black has high structure. According to Brennan, Jerymyn and Boonstra (8), the specific surface activity and the structure effect of blacks on the physical

properties of the vulcanizates, vary simultaneously and are difficult to separate. One method of separation is to heat the carbon black to a temperature in excess of 1600°C. Heat treatment is known to change surface properties without altering structure properties to any important degree (72). As discussed above, Medalia (49) found that, in the absence of surface activity (eg., graphitized carbon black) ``strenghtening structure'' at the tip of the tear apparently does not develop, because the rubber molecules slip over the filler surface before molecular alignment and orientation can take place. Medalia's suggestion is also in accord with Dannenberg's observations (72). Dannenberg (72) found that, the tensile modulus at 300% tensile strain (M 300) decreased progressively with increasing temperature when carbon black was subjected to heat treatment. Dannenberg (72) suggested that the decrease in the M 300 was a consequence of a decrease in rubber-filler interaction because of a decrease in surface activity, as a consequence of heat treatment. The decrease in the rubber-filler interaction allows greater chain segment mobility at the interface and decreases the energy requirements for molecular alignment. Boonstra (74) who investigated the effect of heat treatment of carbon black on the physical properties of the vulcanizates, came to conclusion that both specific surface activity and structure are necessary to provide reinforcement. High structure without surface activity does not result in high reinforcement. High surface activity without structure also does not impart a high degree of reinforcement. In the light of the findings of Dannenberg, Medalia and Boonstra, it appears that apparently carbon black structure plays little or no role in enhancing the tear strength in the absence of specific surface activity.

The effect of particle size on stress relaxation rate is very substantial according to the experimental evidence of Gregory, Metherell and Smith (70), shown in Table 5.10. Their results show that at the same filler concentration, the small size particles of carbon black gave higher stress relaxation rate than large size particles of carbon black, when comparison is made at the same tensile strain. In the light of the experimetal evidence of Gregory, Metherell and Smith (70), it is expected that small particles of HAF black will give higher tearing energy than large

particles of MT black, since Mullins (69) postulated that tearing energy increases with increasing rate of stress relaxation, as discussed above.

In conclusion, vulcanizates filled with HAF black give higher tearing energy than vulcanizates filled with MT black. The reasons for high tearing energy imparted by HAF black may possibly be related to its smaller particle size than that of MT black, higher structure and higher surface activity than MT black.

5.7 Summary of results and observations

The tear behaviour of black-filled rubbers is very complex. Lateral tear deviations or knotty tearing always appear to be the principal mechanism by which carbon black enhances tear strength. Knotty tearing increases the effective size of the diameter of the tear tip. This in turn helps to reduce the stress concentration at the tear tip. A good correlation between the tearing energy and the the knot diameter, measured in the unstrained state, has been observed. The tearing energy increases progressively with the knot diameter.

Some other factors which affect the development of knotty tearing have been investigated. These include the degree of strain-crystallization, molecular mobility, the nature of crosslink, the concentration of crosslinks, the amount of filler, and the nature of the filler. Strain-crystallizing rubbers give knotty tearing more readily than do non-strain-crystallizing rubbers. This is thought to be a consequence of an increase in the strength anisotropy because of extra molecular orientation and strengthening structures associated with strain-crystallization.

Molecular mobility affects the rate of development of the strengthening structures required to produce the strength anisotropy necessary for the occurrence of knotty tearing. Knotty tearing occurs readily at high temperatures or at slow tear rates, when the black structure has enough time to develop.

Conventional sulphur vulcanizing systems produce vulcanizates which show knotty tearing over a wider range of crosslink

concentration than do vulcanizates produced by EV and peroxide vulcanizing systems. This is attributed to an ability to relieve local stress concentrations through yielding, thus giving large regions of high stresses where orientation is substantial.

For strain-crystallizing rubbers, at least 25 pphr of HAF black is required to produce knotty tearing. At 50 pphr of black loading, HAF black-filled vulcanizates give higher tearing energy than MT black-filled vulcanizates. This is attributable to HAF black having smaller particle size than MT black; the higher surface activity and ``structure'' of HAF black than MT black, also promote knotty tearing.

CHAPTER SIX

TEAR BEHAVIOUR OF A PRE-STRAINED VULCANIZATE THEORETICAL ANALYSIS AND EXPERIMENTAL WORK

6.1 ``Hammer head'' crack model

Figure 6.1a shows a photograph of a simple extension test piece which tore in a knotty manner. It can be seen clearly that the crack deviated sideways almost at right angles to the intended path. It has been suggested that the tear deviation is associated with the development of local strength anisotropy around the tip, perpendicular to the intended path (15,16). The longitudinal splitting of the tear along the grain of an oriented structure is typical of the failure of a highly anisotropic material such as fibres and wood. Indeed, the 'hairs' which protruded out as shown in the photograph (a), provide supporting evidence that failure had occured in a fibrous manner, and thus substantiating the existence of a local anisotropic zone. In any material that exhibits strength anisotropy, the strengths along and transverse to the direction of molecular orientation are not the same.

A model crack which simulates the crack tip shown in Figure 6.1a is first considered. Such a model can in principle be used to evaluate the strain energy release rate, $\partial W/\partial A$, both in parallel and transverse to the direction of the applied force. It is of interest to compare the elastic strain energy release to propagate tearing in the direction parallel to the applied force, with the elastic strain energy release to propagate tearing in the direction transverse to the applied force. Such a model crack is called a ``hammer head''.

6.2 Mathematical analysis

Let c be the initial crack length at the edge of a tensile strip transverse to the direction of extension, E, as shown in Figure 6.2a. Let c' be the length of an initial crack parallel to the direction of extension E as shown. Figure 6.2b shows the ``hammer head'' crack tip in the deformed state, which resembles the crack tip which forms during knotty tearing, as shown in Figure

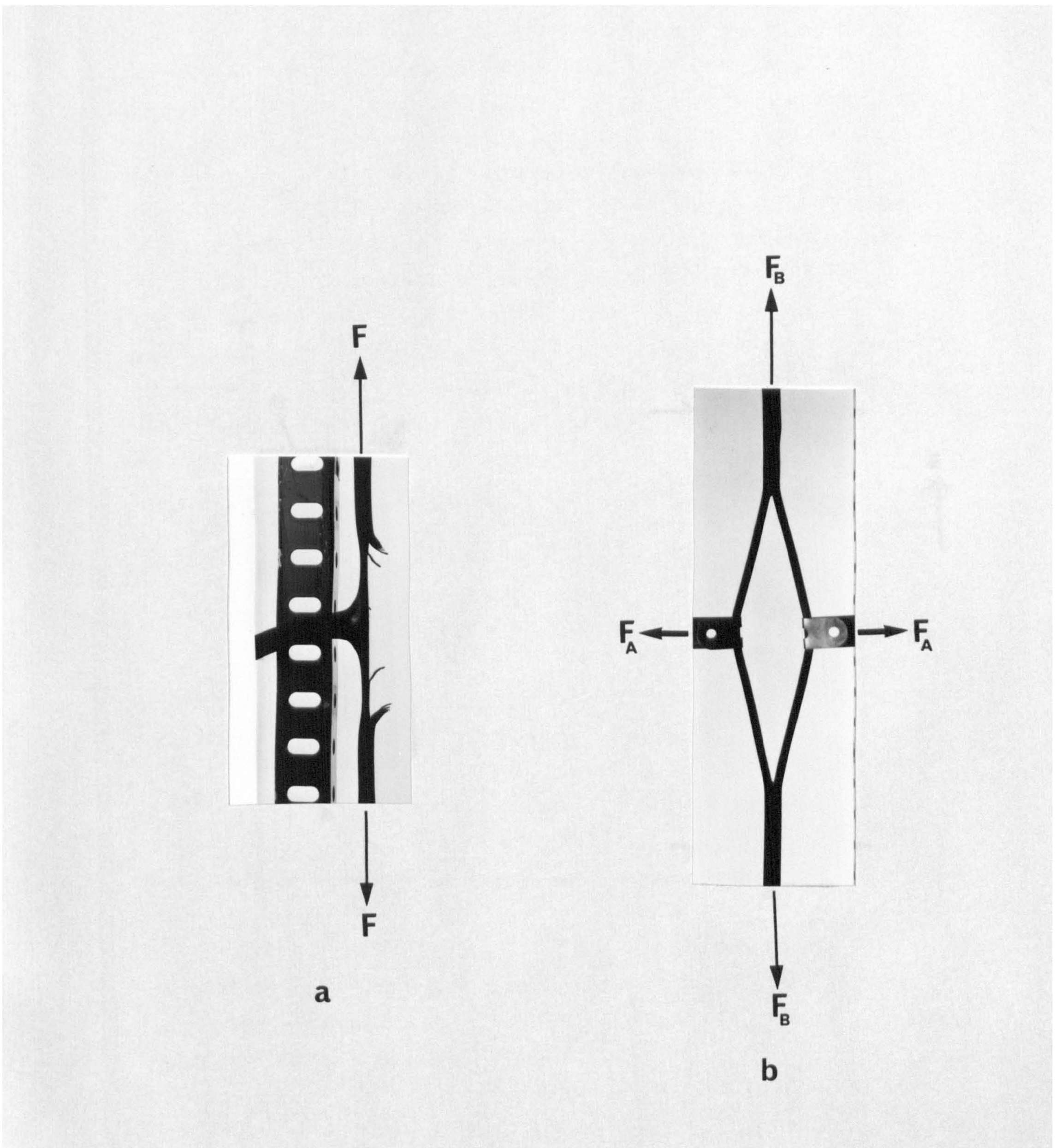

Figure 6.1: Photographs showing (a) knotty tearing in a simple extension (trouser tear) test-piece (b) split tearing in a split test-piece geometry.

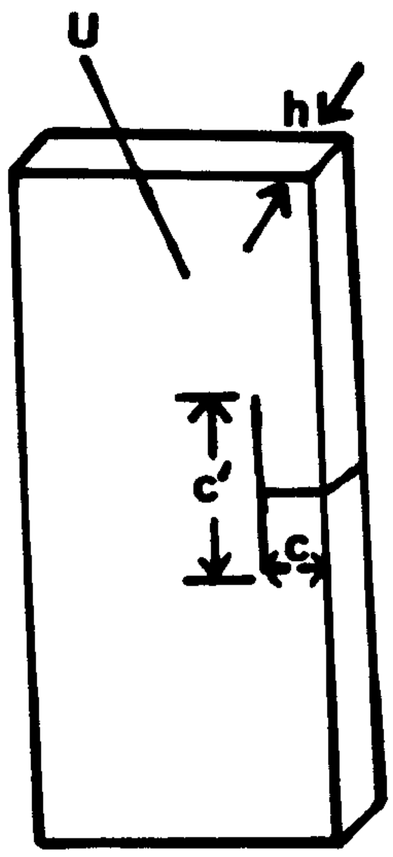

a

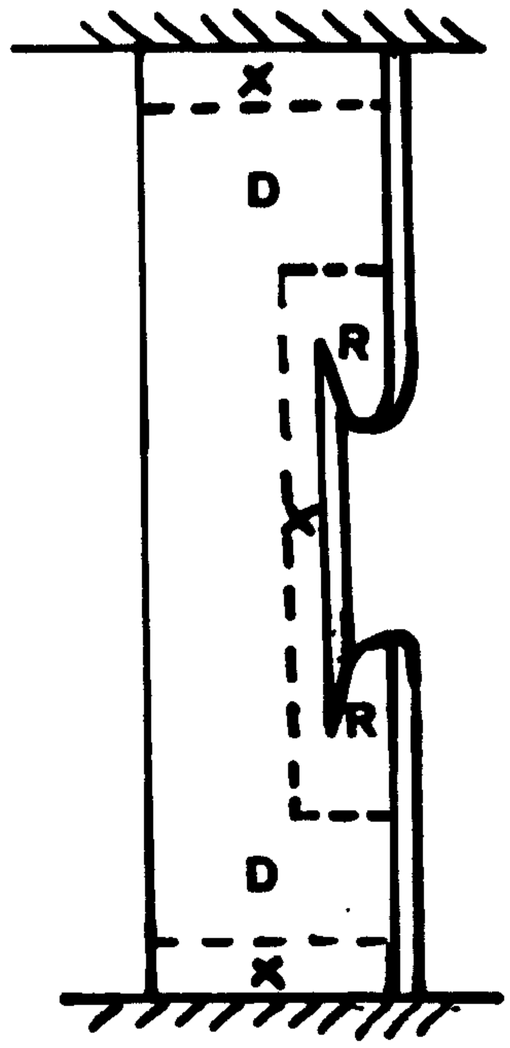

b

Figure 6.2: Schematic diagram showing a ''hammer head'' crack-tip model.
(a) in unstrained state (b) in a deformed state.
c'- initial crack length parallel to direction of extension, E
c - initial crack length transverse to direction of extension E
D - simple extension region, X - region of complexed strain
R - relaxed region.

6.1a. The test-piece should be sufficiently long for there to exist regions of simple extension, D, remote from the crack tip. The strains around the neighbourhood, X, of the crack tip and clamps are very complex. There are also relaxed regions, denoted by R. Provided that the overall separation between the clamps is unchanged, an increase in the crack length of amount δc' (measured in the unstrained state of the test-piece) does not alter the state of strain in the region X but merely shifts this region parallel to the direction of the crack c', causing the regions R to grow at the expense of the region D. Thus if the crack c' grows by a small amount δc', the volume of rubber transferred from simple extension region D into the relaxed regions R, is given by chδc' where, h is the nominal (unstrained) thickness.

The change in the elastic stored energy, δW, when a crack grows by δc' is given by

$$\delta W = -chU\delta c' \qquad (6.1)$$

where U is the strain energy density of the bulk vulcanizate containing no cut. From equation 6.1, it follows that

$$-\frac{1}{h}\left(\frac{\partial W}{\partial c'}\right)_l = T_{ff} = cU \qquad (6.2)$$

This then gives the tearing energy as cU, for crack propagating in the direction parallel to the extension applied.

The strain energy release rate, ∂W/∂A, for a-parallel-sided test piece containing a single edge crack, c, referred to the unstrained state is given by (19)

$$-\frac{1}{h}\left(\frac{\partial W}{\partial c}\right)_l = T_{tr} = 2kcU \qquad (6.3)$$

where k is a varying function of strain and has an average value of of about 2 (75). Equation 6.3 gives the tearing energy transverse to the direction of extension. Thus, the ratio of tearing energy in the transverse direction T_{tr}, to tearing energy in the parallel direction, T_{ff}, is given by

$$\frac{T_{tr}}{T_{ff}} = 2k \qquad (6.4)$$

Equation 6.4 indicates that $T_{b'}$ is higher than $T_{f'f'}$ only if $2k > 1$. If $2k < 1$, then $T_{b'}$ is lower than $T_{f'f'}$. Since k varies from unity to π (75), thus 2k is always greater than unity. Thus it follows that crack propagation transverse to the direction of extension requires higher tearing energy by a factor of 2k than does crack propagation in the direction parallel to the applied extension. The final solution agrees with the more detailed mathematical analysis of Rivlin and Thomas (76), who suggested that, for equation 6.4 to be valid some elements of anisotropy must exist around the crack tip, so that the elastic stored strain energy release to propagate tearing in the direction parallel to extension is different from that to propagate tearing in the direction perpendicular to the applied extension.

6.3 Split tear test-piece

The most suitable test piece to investigate the effect of strength anisotropy on the tearing energy is a split tear test-piece shown in Figure 6.1b. This is one of the test-pieces introduced by Thomas (20) to check the tearing energy concept. The reasons why it is preferred to other common test-pieces are as follows:

(i) In this-test piece (Figure 6.1b), a pre-strain is applied in the direction of F_B, so that when tearing is induced under the action of forces F_A, the tear progresses in the direction of F_B. Thus if anisotropy is introduced by the application of F_B, the observed tearing energy gives a quantitative measure of the consequences of this anisotropy.

(ii) The development of a `knot' at the tip of a more conventional tear test-piece involves crack propagation in the direction of the major strain ahead of the tip, so that the split tear test-piece may give some insight into the knotty tear phenomenon.

(iii) The computation of tearing energy does not require the knowledge of strain energy density, U, (see later in Section 6.6). In contrast, both a pure shear and edge-cut test-pieces require an independent measurement of U.

Furthermore, unlike an edge-cut test-piece (where tearing energy is a function of cut length, c) the tearing energy of a split tear test-piece is independent of the size of the cut length. This enables evaluation of the time-dependent crack growth at a particular tearing energy.

(iv) The geometry of the test-piece enables better control of crack propagation along the pre-strained direction without any necessity to score the test-piece, provided, of course, that sufficient anisotropy is introduced in the material. With other test-pieces, it may be required to stabilise crack propagation by scoring.

6.4 Experimental procedure

6.4.1 Preparation of split tear test-piece

The test-pieces were prepared by stamping a die on a uniformly flat 15 cm x 13 cm x 0.5 mm moulded vulcanized sheet. The dimensions of the test-piece in the undeformed state are shown in Figure 6.3. In cases where the crack propagation was found to be unstable, the surface of the test-piece was scored on both sides using the method described by Thomas (20). Four bench-marks were drawn on the surface of the test-piece to facilitate the measurement of the extension ratio, λ.

6.4.2 Constant-load tearing method

Tearing was done using the framework shown in Figure 6.4. The test-piece was first pre-strained to an elongation defined by an extension ratio λ_B by winding up the ratchet system. The force, F_B, necessary to maintain the test-piece in the pre-strained state was noted 30 minutes later after allowing for stress relaxation. Independent measurements on stress relaxation were carried out, and it was found that the stress decayed rapidly for the first 20 minutes by as much as 30%, and became relatively stable after 30 minutes. Then a pair of forces F_A were applied by hanging dead loads via pulley systems. The pulleys were designed to give minimum friction by having a 'U'-shaped groove and by installing a double shielded ball race. Thus the frictional forces encountered here were negligible relative to forces F_A and F_B, and were neglected.

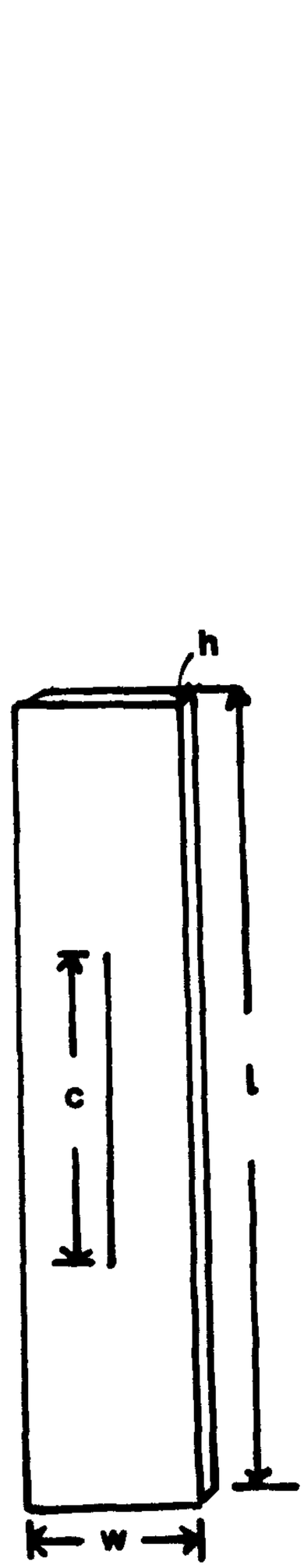

a) Unstrained

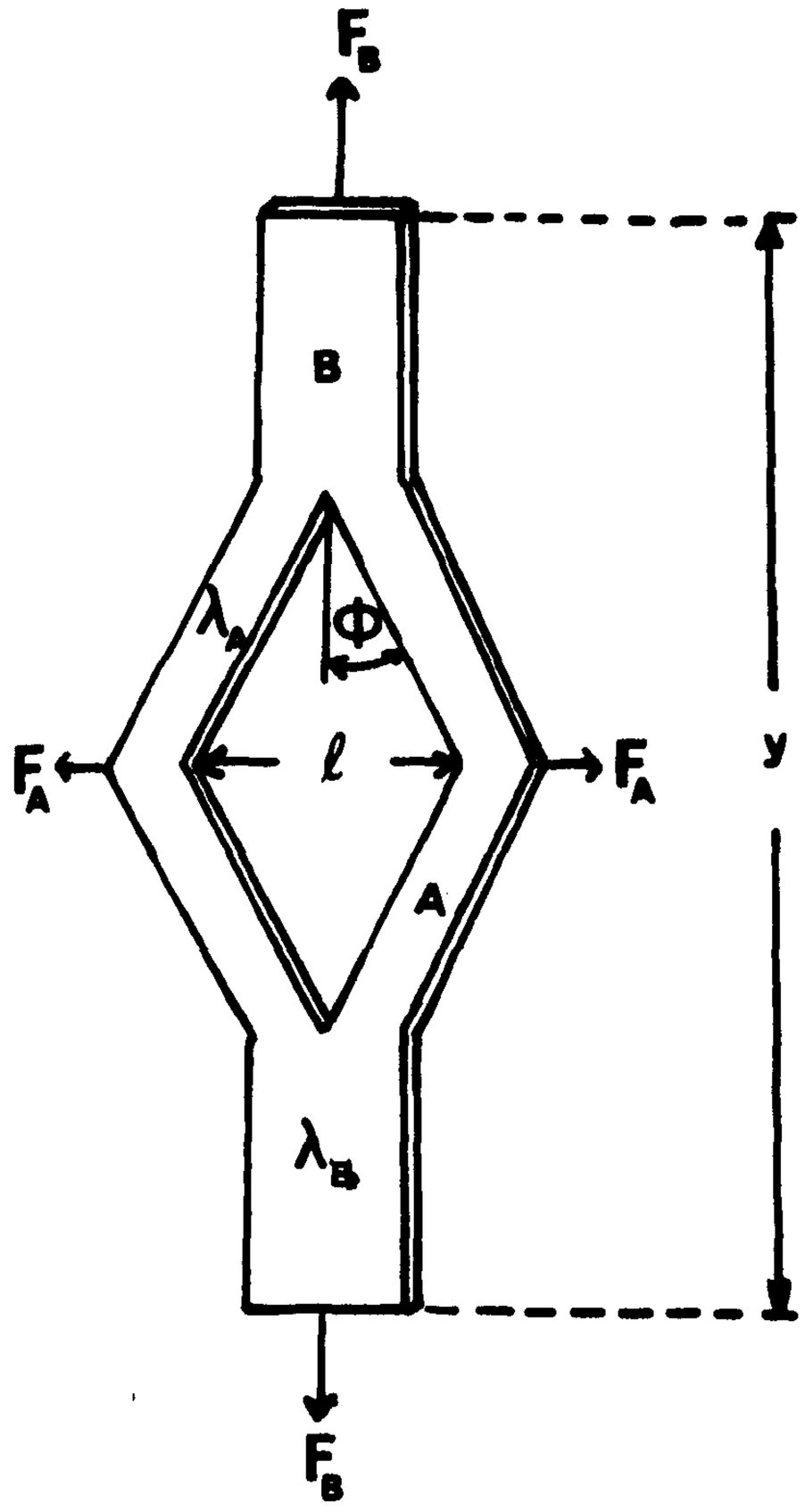

b) Strained

Figure 6.3: Schematic diagram showing split tear test-piece geometry
(a) unstrained state: l = 120 mm, w = 10 mm, h = 0.5 mm, c = 50 mm.
(b) strained state: F_B - pre-straining force, F_A - tearing force
λ_B - extension ratio in simple extension region B,
λ_A - extension ratio in simple extension region A.

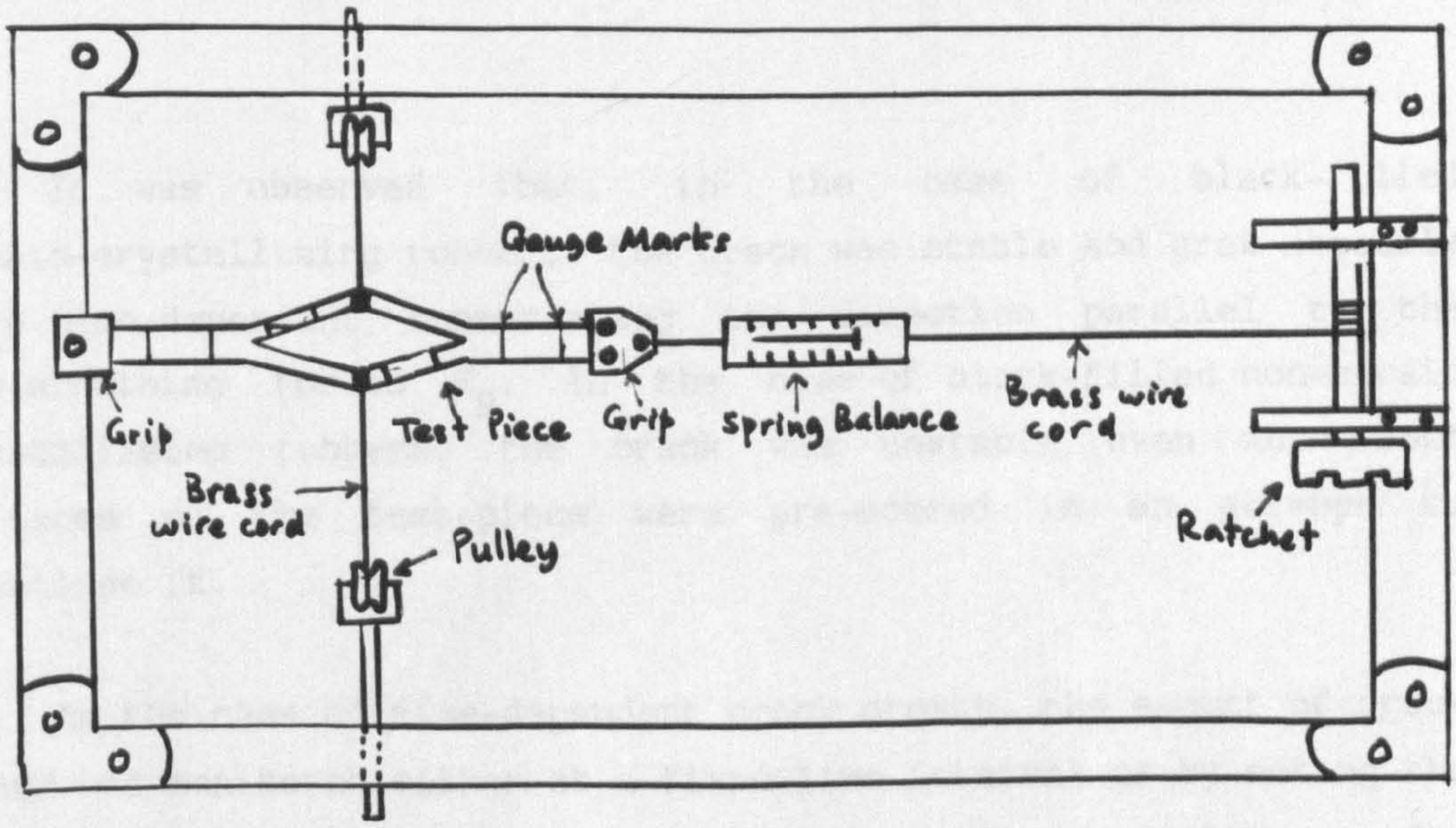

Figure 6.4: Apparatus for constant load tearing method.

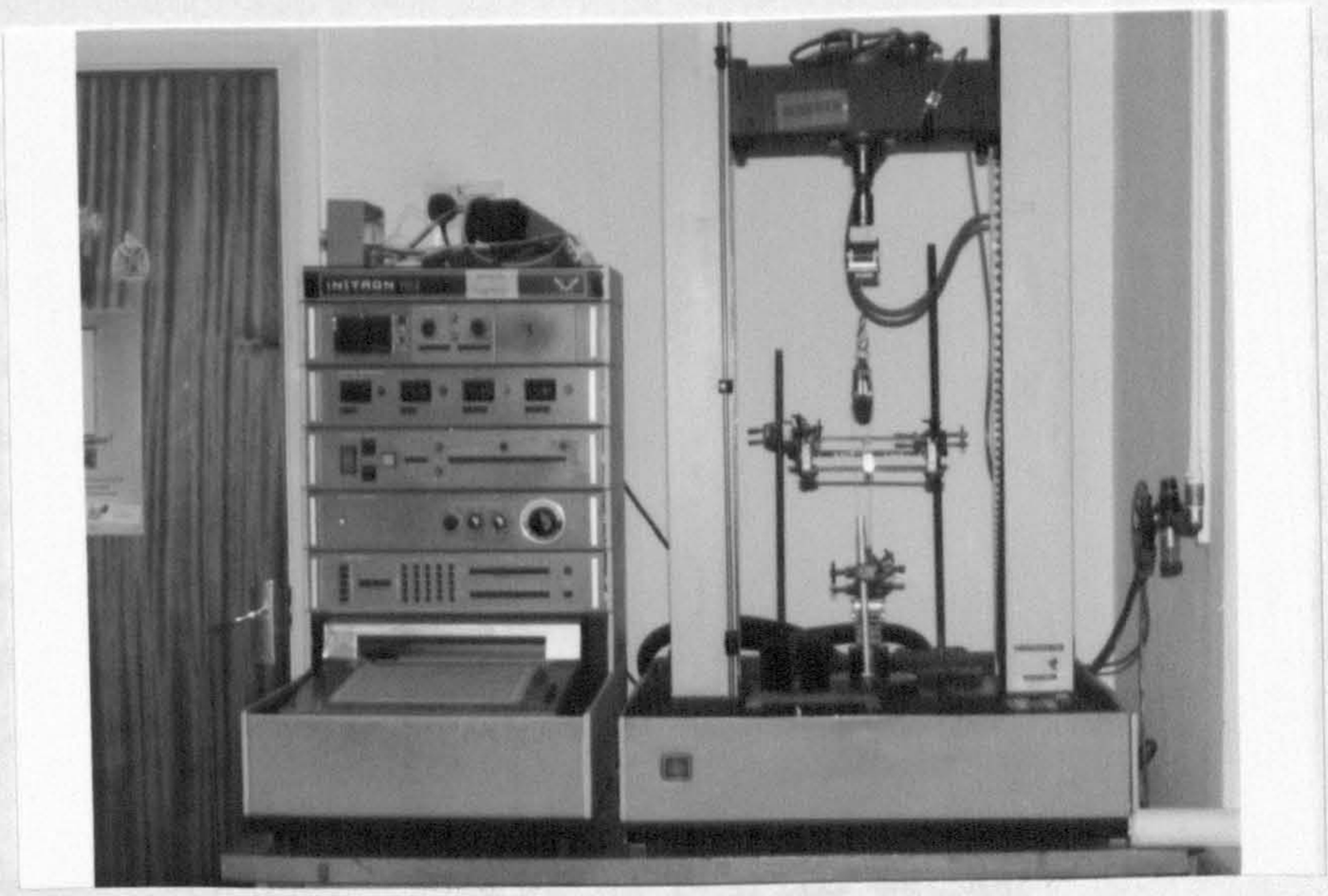

a

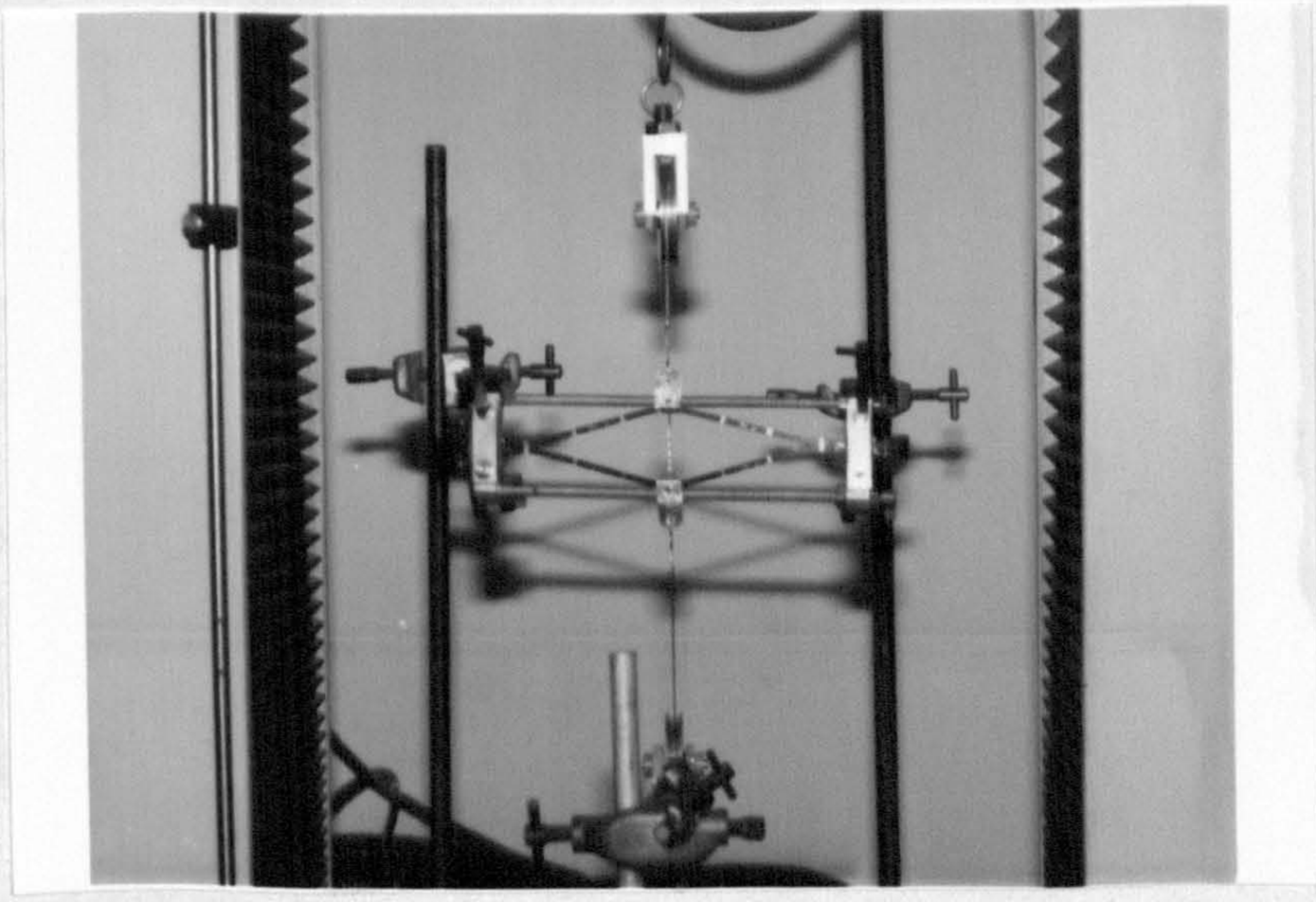

b

Figure 6.5: Experimental set-up for constant-rate-of-separation tearing method
a - initial set up, b - actual tearing process.

It was observed that, in the case of black-filled strain-crystallizing rubbers, the crack was stable and grew steadily in a time-dependent manner along the direction parallel to the pre-straining forces F_B. In the case of black-filled non-strain crystallizing rubbers, the crack was unstable even when both surfaces of the test-piece were pre-scored in an attempt to stabilise it.

In the case of time-dependent crack growth, the amount of crack grown was monitored either at a fixed time interval or by noting the time at which the tip of a crack reached a fixed distance. The former method was useful for slow and moderate crack propagation. Here, the crack length, c, in the strained state was measured by means of an eye-piece lens scale. The scale consisted of 150 divisions, each corresponding to 0.1 mm. The crack length could be read with an accuracy of about ±0.25 scale division. When taking measurements, the dead loads were removed, and the tip of the crack was slightly strained to facilitate the measurement. In the case of rapid crack propagation, several grid lines 5 mm apart were drawn on the surface of the pre-strained test-piece. The time the tip of the crack crossed each line was noted using a stop watch. The angle, ϕ, was measured using a protector.

6.4.3 Constant-rate-of-separation tearing method

The test-piece was pre-strained to an extension ratio, λ_B, by extending it at a rate of 100 mm per minute in an Instron machine. The stress was allowed to relax for 30 minutes, after which the test-piece was clamped with a suitable jig. The load cell carrying the pulleys was calibrated first with a one-Newton load. Then the tearing force F_A was applied by separating the arms of the test-piece via the pulleys at a uniform rate (100 mm per minute), as shown in Figure 6.5.

6.5 Calculation of tearing energy from measurements on a split tear test-piece

The derivation of the tearing energy for a split tear test-piece has been published by Thomas (20). In view of the

complexity of the analysis, the basis of the derivation for the tearing energy of this test-piece is given below:

This test-piece shown in Figure 6.3b is deformed by two pairs of forces F_A and F_B. There are regions A and B which are in simple extension. The extension ratios in regions A and B are given by λ_A and λ_B respectively. The tension N in region A makes an angle ϕ with the test-piece axis.

The energy W stored elastically in the test-piece is a function of the cut length c, the distance l between the points of application of F_A and the distance y between the points of application of F_B. Thus if W = f(c,l,y), then

$$dW = \left(\frac{\partial W}{\partial c}\right)_{ly} dc + \left(\frac{\partial W}{\partial l}\right)_{cy} dl + \left(\frac{\partial W}{\partial y}\right)_{cl} dy \qquad (6.5)$$

and

$$F_A = \left(\frac{\partial W}{\partial l}\right)_{cy} \qquad (6.6)$$

$$F_B = \left(\frac{\partial W}{\partial y}\right)_{cl}$$

Substituting 6.6 into 6.5 gives

$$\left(\frac{\partial W}{\partial c}\right)_{F_A F_B} = \left(\frac{\partial W}{\partial c}\right)_{ly} + F_A\left(\frac{\partial l}{\partial c}\right)_{F_A F_B} + F_B\left(\frac{\partial y}{\partial c}\right)_{F_A F_B} \qquad (6.7)$$

The complex strains around the points of applications of F_A and around the ends of the cut will not vary with c, provided F_A and F_B are constant. If c increases by δc, the regions at the end of the cut will move outwards by δc but still have the same total stored energy, the net effect being for regions A to grow at the expense of regions B. The overall length l between the points of application of force F_A, will increase by an amount δl, given by $\lambda_A \delta c \sin\phi$. Therefore

$$\left(\frac{\partial l}{\partial c}\right)_{F_A F_B} = \lambda_A \sin\phi \qquad (6.8)$$

also

$$\left(\frac{\partial y}{\partial c}\right)_{F_A F_B} = \lambda_A \cos\phi - \lambda_B \qquad (6.9)$$

From the geometry of the test piece it can be shown that

$$F_A = 2N \sin \phi \qquad (6.10)$$
$$F_B = 2N \cos \phi$$

Since $\tan \phi = \sin\phi/\cos\phi$, therefore

$$\tan \phi = F_A/F_B \qquad (6.11)$$

Also when the external forces F_A and F_B are held constant, the volume of rubber transferred from regions B to regions A as the crack propagates by δc is given by $wh\delta c$. w and h are the nominal width and thickness of the test-piece. The elastic stored energy lost when the crack increases by δc is given by $wh(U_A - U_B)\delta c$, where U_A and U_B are the stored energy densities in regions A and B respectively. Thus,

$$\left(\frac{\partial W}{\partial c}\right)_{F_A F_B} = wh\left(U_A - U_B\right) \qquad (6.12)$$

Substituting equations 6.8., 6.9 and 6.12 into equation 6.7 gives tearing energy, T, for a split tear test-piece

$$T = -\frac{1}{h}\left(\frac{\partial W}{\partial c}\right)_{l_y} = \frac{F_A \lambda_A \sin\phi}{h} + \frac{F_B(\lambda_A \cos\phi - \lambda_B)}{h} - w(U_A - U_B) \qquad (6.13)$$

A split-tear test-piece is equivalent to two trouser tear test-pieces joined together. It can be proved such is the case when $F_B = 0$. When U_A is close to U_B, λ_A is not much greater than λ_B, by putting $\lambda_A = \lambda_B + \Delta\lambda$, it can be shown approximately that

$$wh(U_A - U_B) = \frac{\Delta\lambda(F_B + 2N)}{2} \qquad (6.14)$$

From equations 6.10,

Substitute $\cos\Phi = \dfrac{F_B}{\sqrt{F_A^2 + F_B^2}}$ into $2N = \dfrac{F_B}{\cos\Phi}$ gives

$$2N = \sqrt{F_A^2 + F_B^2} \qquad (6.15)$$

Substituting equations 6.11, 6.14 and 6.15 into 6.13, gives the

following useful approximation for tearing energy of a split tear test-piece.

$$T = -\frac{1}{h}\left(\frac{\partial W}{\partial c}\right)_{ly} = \frac{\bar{\lambda}}{h}\left(\sqrt{F_A^2 + F_B^2} - F_B\right) \qquad (6.16)$$

where $\bar{\lambda} = \frac{\lambda_A + \lambda_B}{2}$

Table 6.1 shows a typical set of results which compare the tearing energy computed using equation 6.13 with that using equation 6.16. The agreement between the two equations was excellent. In fact, the descrepancies between the two equations were very small, being about 0.2% on average, were far less than the uncertainties associated with the measurements.

In this investigation, equation 6.16 was used throughout to calculate the tearing energy, since it was easy to compute as it does not require the knowledge of other parameters such as the strain energy densities and the angle Φ. In the case of the constant-load method, shown schematically in Figure 6.6a, F_A was determined from the dead load applied, and F_B was determined from the spring balance 30 minutes after the test-piece was pre-strained to allow for stress-relaxation. The extension ratios λ_A and λ_B were determined by measuring the distance between the two bench marks by means of a vernier scale. In the case of the constant-rate-of-separation method, F_A was half the force required to split the test piece (Figure 6.6b). The latter force obtained from the chart of the test machine. The extension ratio λ_B was determined from the separation of the bench marks. The extension ratio λ_A was obtained from curves of stress versus extension ratio of the type shown in Figure 4.4b (in Chapter Four).

6.6 Determination of crack propagation rate

In a constant load tearing measurement, tearing occurred in a time-dependent manner, i.e., the length of the crack increased with time. The average rate of crack propagation, r, was determined from the slope of straight line of crack length versus time of the type shown in Figures 6.7a, b and c for black-filled (50 pphr HAF) NR vulcanizate. For example, Figure 6.7a gave an average r of 0.33 $\mu m\ s^{-1}$ at tearing energy of 1.92 $kJ\ m^{-2}$. The crack length, c_o, was referred

Table 6.1: Comparison between two methods of calculating tearing energy from measurements on split tear test-pieces, using constant-rate-of-separation method.

F_B (N)	40.8	37.5	34.2	37.5	37.0
F_A (N)	7.0	6.3	6.0	6.0	6.45
λ_B	2.90	2.97	2.93	2.90	2.87
λ_A	2.92	3.0	2.95	2.98	2.90
U_B (MJ m)	4.4	4.82	4.55	4.67	4.25
U_A (MJ m)	4.52	5.00	4.70	4.85	4.41
T_1 $kJ\,m^{-2}$	2.38	2.56	2.56	2.17	2.44
T_2 $kJ\,m^{-2}$	2.43	2.53	2.60	2.19	2.40

Mean T_1 = 2.43 $kJ\,m^{-2}$ Mean T_2 = 2.42 $kJ\,m^{-2}$
standard deviation of T_2 = 0.156.

$$T_1 = \frac{F_A \lambda_A \sin\phi}{h} + \frac{F_B(\lambda_A \cos\phi - \lambda_B)}{h} - w(U_A - U_B)$$

$$T_2 = \frac{\bar{\lambda}}{h}\left(\sqrt{F_A^2 + F_B^2} - F_B\right)$$

(a)

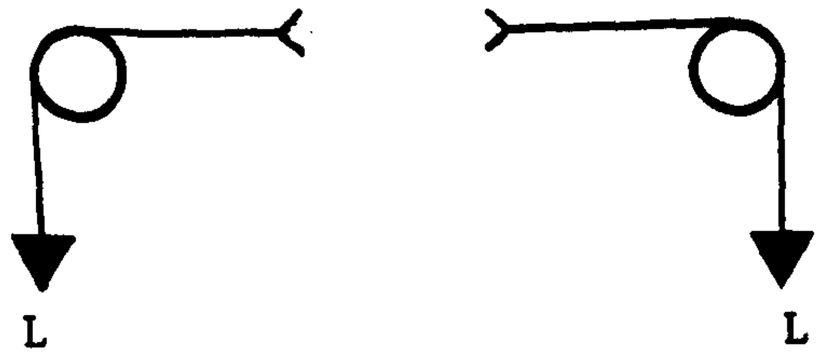

F =(9.81L) N
L is load in Kilogram

(b)

$F_. = F_t/2$

Figure 6.6: Schematic diagrams showing (a) constant-load and (b) constant-rate-separation methods.

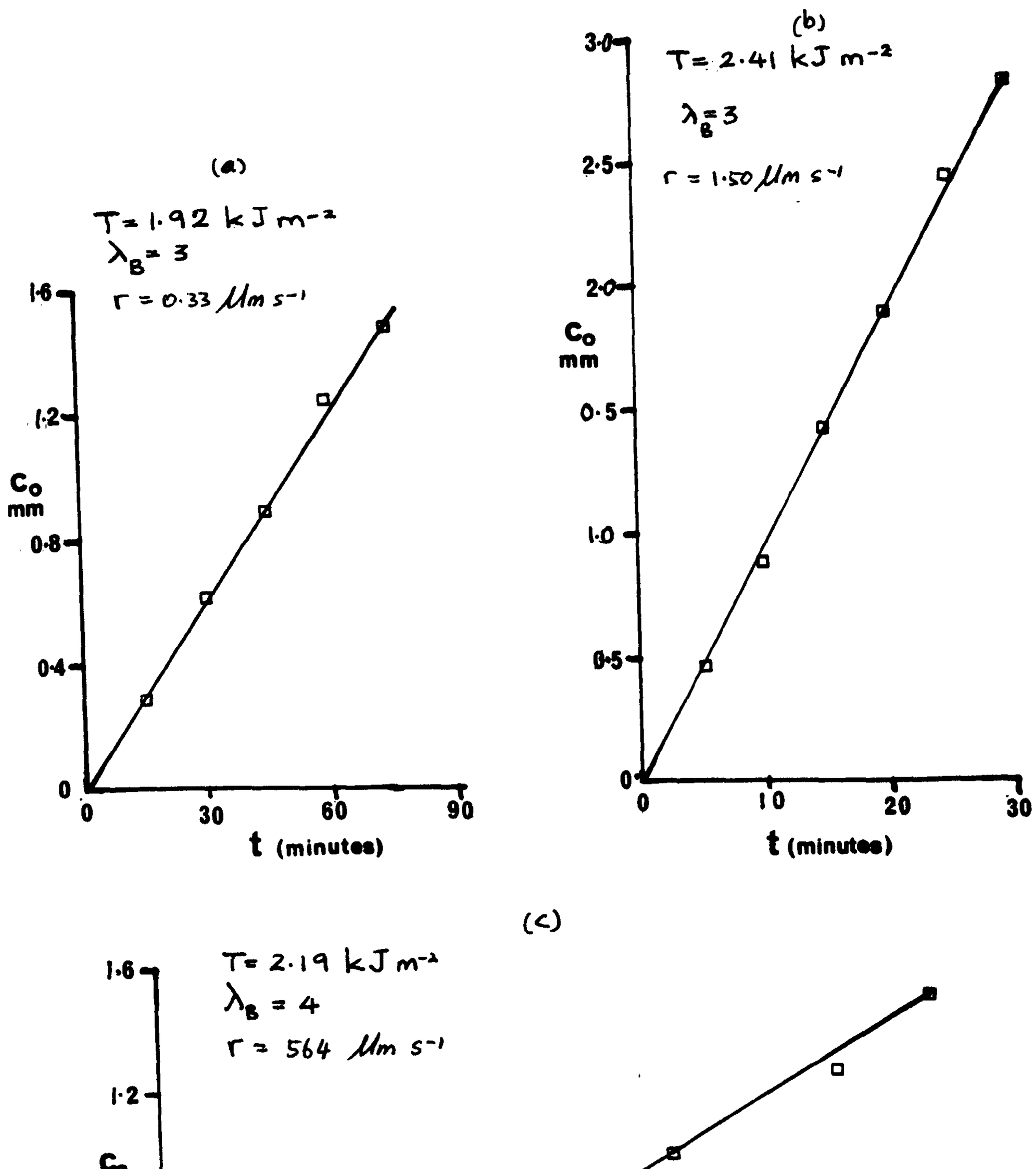

Figure 6.7: Crack length, c_o vs time plots obtained from constant-load tearing method. The slope of the straight line gives the rate of crack propagation, r. All tear measurements were carried out at 23°C, for black-filled NR vulcanizates. The full formulations are shown in Table 4.3b for mix H1.

to the unstrained state and it is given by

$$c_o = c\lambda_B^{-1} \qquad (6.17)$$

where c is the crack length measured in the extended state defined by the extension ratio λ_B. In a few cases, the measured slope were checked with slope obtained from data analysed using a linear regression method with the aid of a computer. In this regression the line was not constrained to go through the origin. The agreement between the two results was excellent. The regression coeficient for c upon t was always closed to 1 indicating the correlation between the two quantities was very good.

In a constant load measurement, the angle ϕ was also measured and was found to agree closely with the value obtained from equation 6.9. The angle was found to be relatively constant except if F_B decreased, in which case the angle would increase.

CHAPTER SEVEN

TEAR BEHAVIOUR OF PRE-STRAINED VULCANIZATES

RESULTS AND DISCUSSION

7.1 Time-dependent tearing

The term ``time-dependent tearing'' denotes the increase in crack length with time when tearing is carried out under constant load (29,32,64). This behaviour is usually displayed by unfilled non-strain-crystallizing rubber vulcanizates, for example, SBR vulcanizates. In contrast, unfilled vulcanizates which do strain-crystallize, for example, NR vulcanizates, do not display time-dependent tearing under constant load. There is a critical load above which tearing occurs catastrophically, and below which tearing does not occur (29,32,64). Thomas (77) suggested that, as long as the region of the tear-tip remains crystalline under this constant load, time-dependent tearing would not occur. However, if the load is removed and reapplied, crack growth occurs even although the load applied is below the critical value necessary to cause catastrophic tearing. This aspect of crack growth is term as ``dynamic crack growth'' (77). According to Thomas (77), under static loading, strain-crystallization at the tip of the tear prevents bond rupture continuing to its full extent. Under cyclic loading, when the load is relaxed to zero strain the crystals at the tear tip are melted away. As a consequence of the melting of these crystals, tearing takes place in a subsequent extension before strain-crystallization occurs again. In dynamic crack growth, the amount of crack growth depends primarily on the number of cycles rather than the period of cycling.

In the present investigation, time-dependent tearing in the direction of extension was observed when pre-strained black-filled strain-crystallizing vulcanized rubbers were subjected to constant load. As far as the author is aware, the time-dependent tearing observed in this aspect of investigation has never been reported or published previously. A further surprise was that pre-strained black-filled SBR vulcanizates which do not strain-crystallize did

not show similar time-dependent tearing under constant load. The findings here are in contrast to the tear behaviour normally observed in the unfilled vulcanizates as discussed above.

Some suggestions are now put forward to explain this unexpected behaviour. In split tearing experiments, the test-piece was first pre-strained to a predetermined extension. For a rubber which is amorphous but potentially crystallizable, such as NR, this mechanical stretching would induce some crystallization. The explanation for the time-dependent tearing observed in pre-strained black-filled NR, ENR 25 and ENR 50 vulcanizates may possibly be as follows: As discussed above, in strain-crystallizing rubbers the crystalline regions which form locally at the tip of the tear can prevent time-dependent tearing (32,64). In split tearing, crystallization occurs in the bulk of the vulcanizate when the test-piece is pre-strained. Since the stress giving the orientation was maintained during the test, the crystals would remain in the bulk and would not melt. When the tearing forces F_A were applied, possibly few crystallizable units were available to induce further crystallization at the tip of the tear. As a consequence of the absence of strain-crystallization at the tip of the tear, time-dependent tearing occurred. It was also observed that the tip of the tear of pre-strained black-filled strain-crystallizing rubber vulcanizates were generally very sharp as shown in Figure 7.1a. It was also observed that the fractured surface of pre-strained black-filled strain-crystallizing rubber vulcanizates was very smooth. Similar observations have been reported by Gent and Kim (47).

In contrast, pre-strained black-filled SBR vulcanizates did not show similar time-dependent tearing over the whole range of strain (100% to 400%) investigated. The crack did not even split in the direction of the molecular orientation, even when both surfaces of the test-piece were pre-scored to stabilise the crack propagation in this direction. Figure 7.1b shows that the crack tip of SBR (pre-strained to 270%) was very blunt; this might be attributed to instability of the crack. Because of the instability of crack propagation, no further investigations were carried out using black-filled SBR vulcanizates.

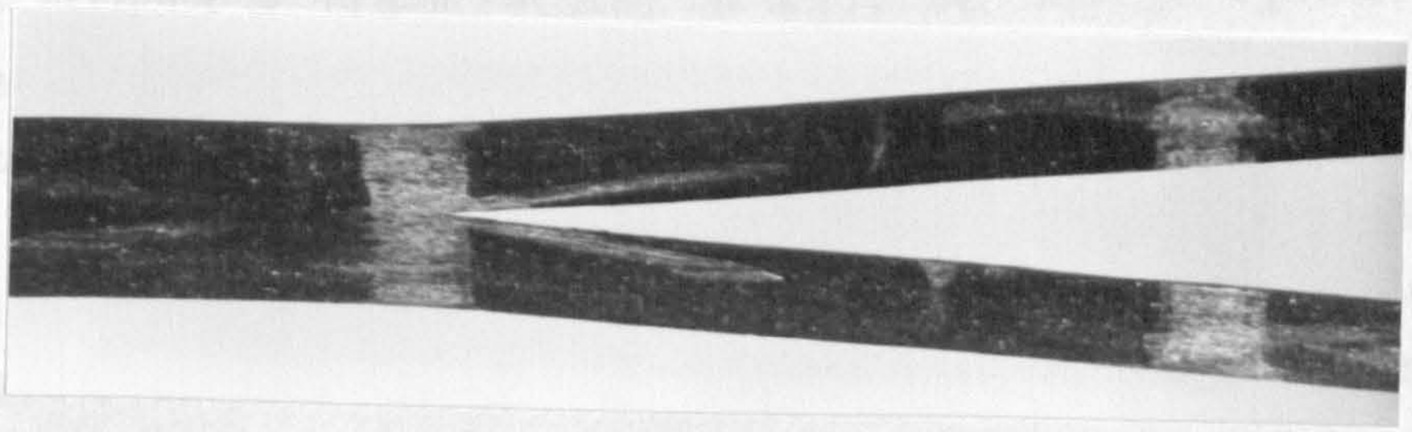

a

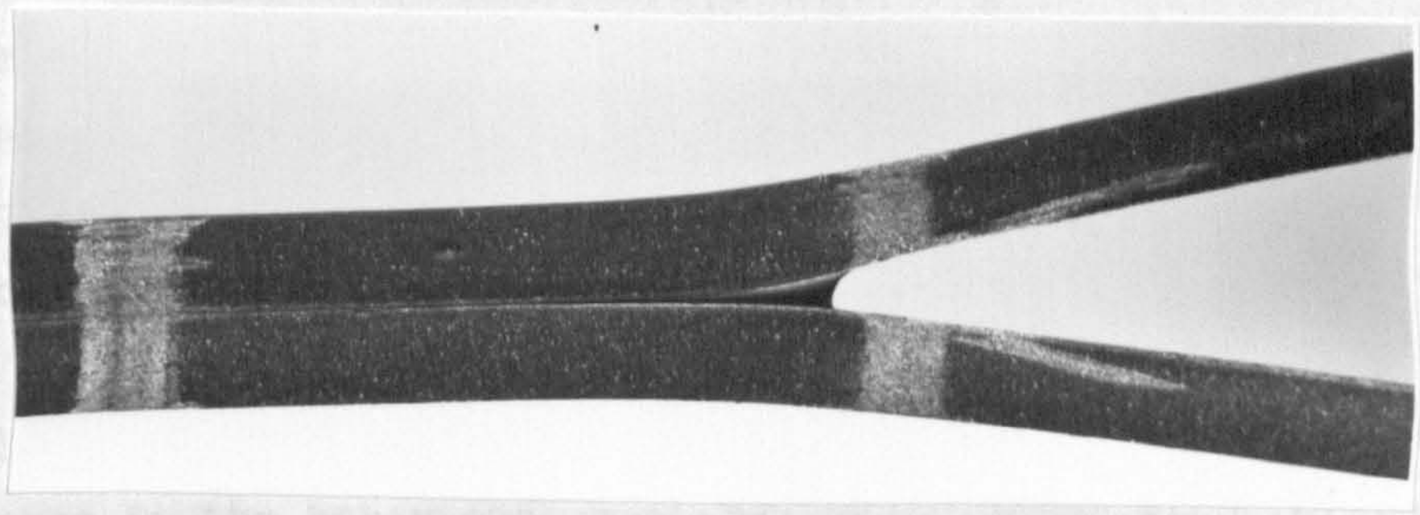

b

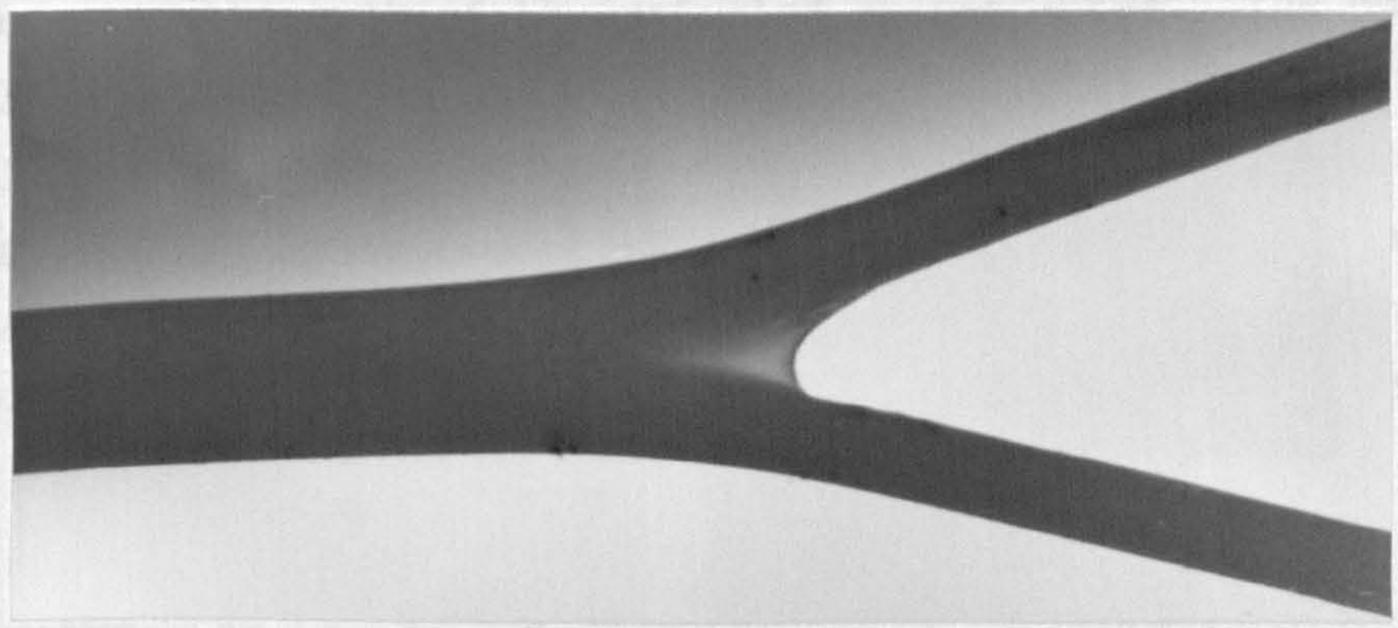

c

Figure 7.1: Photographs showing the crack-tip of a pre-strained split test-piece

(a) Black-filled NR, λ_B = 4.5, F_A = 4.29N, F_B = 78.48N.
(b) Black-filled SBR, λ_B = 3.7, F_A = 6.0N, F_B = 29.40N.
(c) Unfilled ENR 25, λ_B = 5.5, F_A = 3.9N, F_B = 9.80N.
Full formulations for NR and SBR are shown in Table 4.3b for mixes H1 and H4 respectively. Formulations for unfilled ENR 25 are shown in Table 4.2 for mix G2 in Chapter Four.

The effects of pre-straining on unfilled strain-crystallizing vulcanized rubbers were investigated to see if they exhibit time-dependent tearing. The experiment was carried out using unfilled NR and ENR 25 vulcanizates. The findings were that they did not exhibit time-dependent tearing, and also that the crack was found to be unstable even when the surfaces were scored. Figure 7.1c shows a typical crack tip of pre-strained strain-crystallizing unfilled ENR 25 vulcanizate. The white regions around the tip of of the tear indicate the occurrence of a local strain-crystallization there. The presence of crystalline regions at the tear tip suppressed time-dependent tearing. The reasons why pre-strained strain-crystallizing black-filled vulcanizates showed time-dependent tearing and pre-strained strain crystallizing unfilled vulcanizates did not are not entirely clear. In the author's opinion, the differences in the behaviour may be associated with differences between the extent of crystallization which developed in the bulk of black-filled vulcanizates and the extent of crystallization which developed in the bulk of the unfilled vulcanizates. The amount of crystallinity forming at the tear-tip would then depend on the crystallizable units available for further crystallization at the tip. Mullins and Tobin (78) found that the degree of crystallinity which developed in black-filled NR vulcanizates was higher than that which developed in unfilled NR vulcanizate when they were compared at the same strain. Mullins and Tobin determined the volume changes which accompanied the changes in the density of the rubber vulcanizates as a consequence of strain-crystallization which occurred during extension. They measured the volume changes by hydrostatic weighing technique. Basically this involved weighing the ring specimens and frame under distilled water, first in the unstretched position, and then with the specimens at a chosen extension. They then calculated the change in the volume from the mean of the difference in weight between the stretched and the unstrectched states (78). Mullins and Tobin (78) suggested that black-filled NR vulcanizates strain-crystallize more readily than do unfilled NR vulcanizates because of the strain amplification effect (78,79). According to Mullins and Tobin, black-filled vulcanizates are considered to consist of two phases; one is hard (the filler particles) and relatively inextensible, the other (the rubber phase) is soft and extensible. The strain in the soft regions is

considerably higher than that calculated from the measured extension as a consequence of the local strain amplification at or near the hard phase. As a result, crystallization will occur at much lower extensions than in a corresponding unfilled vulcanizate. Thus in the light of the findings of Mullins and Tobin, it can be envisaged that in black-filled NR vulcanizates the remaining cystallizable units available to cause further crystallization at the tear-tip would be less than the corresponding unfilled system. In the unfilled system, the remaining crystallizable units were therefore available for further local strain crystallization at the tip of the tear, where the local stress at the tip was much higher than the stress in the bulk of the vulcanizate. As a consequence of the development of local strain-crystallization at the tip of the tear, time-dependent tearing was not observed in the unfilled systems.

7.2 Tearing energy in direction of molecular orientation

This section discusses the effects of strength anisotropy on the tearing energy of pre-strained strain-crystallizing black-filled (50 pphr HAF) rubber vulcanizates prepared using a semi-EV vulcanizing system. All the investigation was carried out using the constant load method. The tearing energy in split tear test-pieces quantifies the energy required to propagate tearing in the direction of molecular orientation, parallel to direction of pre-strain which is applied. Thus the tearing energy in this direction gives a quantitative measure of the anisotropy induced in the vulcanizate as a consequence of pre-straining. Figure 7.2a shows a plot of tearing energy versus rate of crack propagation in the direction of molecular orientation, for a black-filled NR vulcanizate at 23°C, using the data shown in Tables 7.1. Logarithmic scales were used because of the wide range of tearing energies and rates investigated. Control samples (trouser test-pieces) of similar thickness were taken from the same vulcanized sheet and torn at different tear rates using an Instron machine. The results, which are shown in the same plot, provide a comparison between the magnitude of tearing energy of steady tearing in the direction of molecular orientation and that of the tearing energy of knotty tearing. The tearing energies obtained from trouser tear test-pieces which produced knotty tearing were substantially higher than the tearing energies obtained from split tear test-pieces which

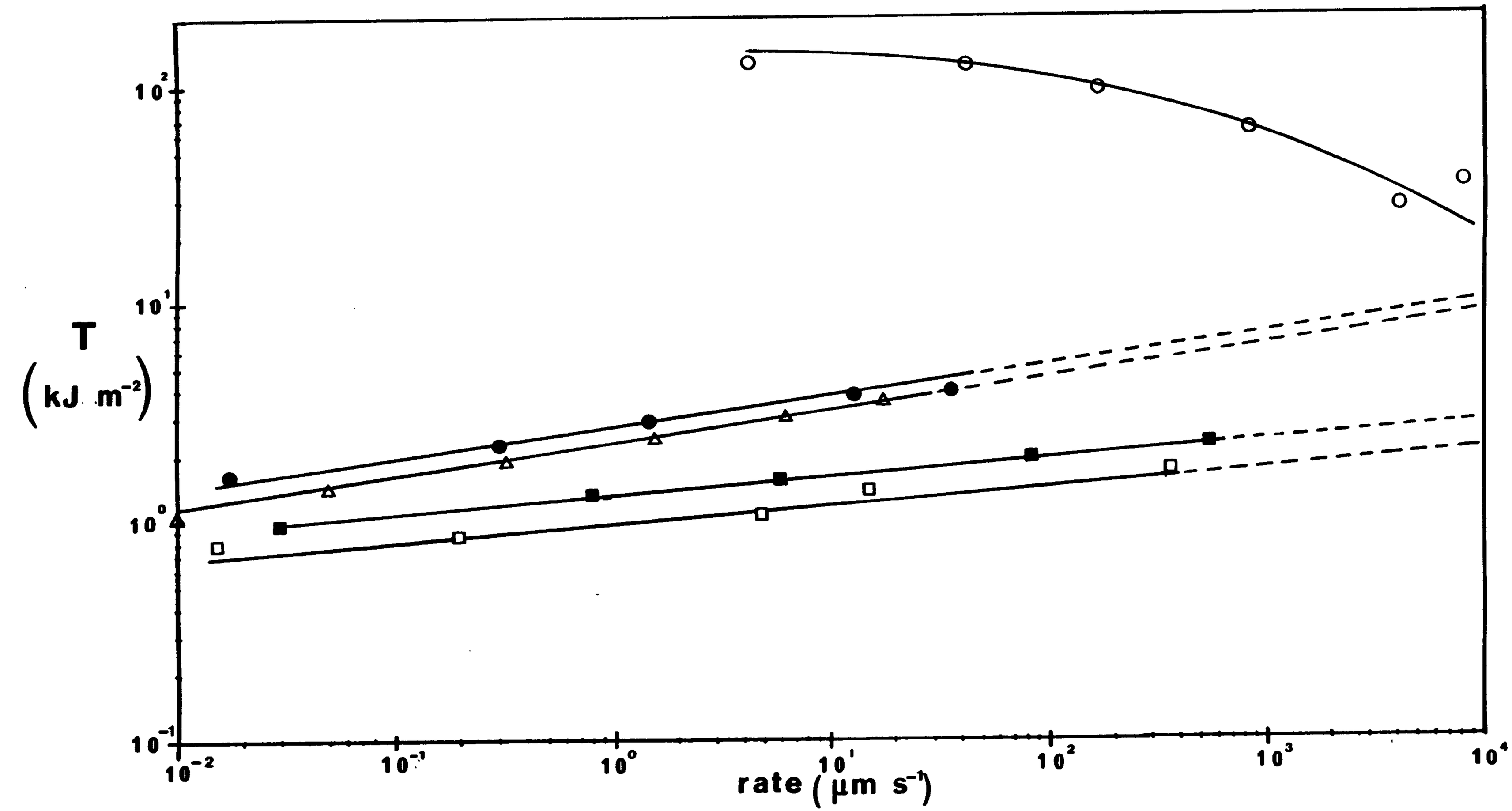

Figure 7.2a: Tearing energy, T vs rate of crack propagation, r, of black-filled NR vulcanizate at 23°C. Full formulations are shown in Table 4.3b for mix H1 in Chapter Four.
●λ = 2.5, △λ = 3.0, ■λ = 4.0, □λ = 4.5, O Control samples (trouser tear test-piece). Broken lines indicate extrapolation lines.

Table 7.1: Tearing energy of pre-strained black-filled (50pphr HAF) NR vulcanizates at 23°C using split-tear test-pieces

(a) Pre-strained at 150% strain

T (kJ m^{-2})	1.65	2.25	2.91	3.66	3.77
r (μm s^{-1})	0.02	0.30	1.45	13.0	37.8

(b) Pre-strained at 200% strain

T (kJ m^{-2})	1.08	1.47	1.92	2.42	2.99	3.60
r (μm s^{-1})	0.01	0.05	0.33	1.60	6.32	17.5

(c) Pre-strained at 300% strain

T (kJ m^{-2})	0.74	1.00	1.31	1.51	1.87	2.19
r (μm s^{-1})	0.002	0.03	0.80	5.97	86.5	564

(d) Pre-strained at 350% strain

T (kJ m^{-2})	0.80	0.86	1.02	1.40	1.74
r (μm s^{-1})	0.015	0.20	4.80	15.0	356

Full formulations of the vulcanizates are given in Table 4.3b (mix H1).

produced steady tearing. For example, at 150% pre-strain, the tearing energy for a crack propagating at a rate of 4.2 μm s^{-1} in the direction of molecular orientation was a factor of about 40 lower than the tearing energy of knotty tearing, when compared at the same tear rate. This indicates that the tear resistance in the direction of molecular orientation is very low as reflected by the low tearing energy for propagation of tearing in this direction. Similar observations were reported by Gent and Kim (47). The tearing energy at this particular pre-strain (150%) and tear rate (4.2 μm s^{-1}) was about 2.0 kJ m^{-2}. This value is of similar order of magnitude to that reported by Gent and Kim (47) who investigated the tear strength of stretched rubber using pure shear test-pieces. However, they did not report at what rate of tearing they obtained their results.

7.3 Effect of the extent of molecular orientation on strength anisotropy

This investigation was carried out by pre-straining the test-pieces to four different strain levels, ranging from 150% to 350% strain. The higher the pre-strain level, the greater the degree of molecular orientation, and hence the stronger the anisotropy which was expected to develop as a consequence of the pre-straining. The results are shown in Figure 7.2a. One of the interesting observations is that, at any particular tear rate the tearing energy decreased as the amount of pre-straining was increased. This observation agrees with the observations reported by Gent and Kim (47) and by Chasset and Thirion (48). This suggests that, as the degree of anisotropy increases, the tear resistance in the direction of molecular orientation decreases. For example, the tearing energy at 350% pre-strain was about one third the tearing energy at 150% pre-strain, when comparison was made at tear rate 4.2 μm s^{-1}. The tearing energy obtained in this investigation was of the same order of magnitude as that obtained by Gent and Kim (47). Thus this suggests the primary effect of pre-straining is to suppress crack diversion as suggested by Lake and Yeoh (31). Lake and Yeoh (31), who carried out an investigation of the resistance of vulcanized rubbers to cutting by sharp objects, found that the tearing energy iniatiated from a sharp crack tip formed by a sharp blade was about 0.3 kJ m^{-2} for black-filled NR vulcanizate (50

pphr HAF). The tearing energy that Lake and Yeoh obtained was of the same order of magnitude as that obtained in the present investigation and that obtained by Gent and Kim (47).

The low tear resistance in the direction of molecular orientation can be used to explain the tear diversion observed in knotty tearing. In knotty tearing, it is observed that the tear deviates almost at right angles to the intended path, and propagates in a new direction parallel to the anisotropic zone where molecular orientation is substantial. Tear diversion may be attributed for the tendency of the tear to propagate in the direction of molecular orientation because the tearing energy in this direction is comparatively low. Gent (79) put forward a suggestion that the easy splitting of highly-stretched rubber vulcanizates may be a direct source of strength by causing the tear-tip to become blunter. The results shown in Figure 7.2a give a good illustration how a given material can be strong when the tear-tip becomes blunt, and then become weak when the tear-tip is very sharp.

7.4 Effect of tear rate on tearing energy

The dependence of tearing energy on tear rate depends on the type of tear failure. In knotty tearing, the tearing energy decreases with increasing tear rate, the gradient of tearing energy-tear rate curve being negative (Figure 7.2a). In contrast, tearing energy in steady tearing increases with increasing tear rate, the gradient of the straight line being positive (Figure 7.2a). According to Greensmith and Thomas (29), the negative gradient in the tearing energy-tear rate relationship is associated with the presence at the tip of the tear of a strengthening structure that takes appreciable time to form. They postulated that the amount of strengthening structure would decrease at high rates of tear propagation where there was insufficient time for the structure to form. In contrast, tearing energy in steady tearing regions increases at high rates of tear propagation because of the high energy dissipation encountered at high tear rates. The tearing energy-tear rate relationship in steady tearing regions obtained from split-tear test-pieces was extrapolated to higher rates than those investigated. Table 7.2 shows the ratio of tearing energy of knotty tearing (T_k) to tearing energy of steady tearing (T_s)

Table 7.2: Dependence of tearing energy on tear rates at 23°C

rate ($\mu m\ s^{-1}$)	8300	4200	830	170	42	42
T_k ($kJ\ m^{-2}$)	25	28	60	90	120	130
T_s ($kJ\ m^{-2}$)	9	8.5	6.0	5.2	4.6	3.3
$\frac{T_k}{T_s}$	3.0	3.3	10	15	26.1	39.4

N.B. T_k - tearing energy produced by knotty tearing obtained from 'trouser' tear test-pieces

T_s - tearing energy produced by steady tearing obtained from split-tear test-pieces at 150% strain

Table 7.3: Effect of pre-straining on the tear strength

Pre-strain (%)	150	200	300	350
$T_s\ kJ\ m^{-2}$	9.0	8.0	2.5	2.0
$T_k\ kJ\ m^{-2}$ (control)	25	25	25	25
$\frac{T_k}{T_s}$	3.0	3.1	10.0	13

N.B. T_k - tearing energy produced by knotty tearing obtained from 'trouser' tear test-pieces

T_s - tearing energy produced by steady tearing obtained from split-tear test-pieces.

Tear test conditions : temperature 23°C, tear rate 8,300 μms^{-1}

obtained from split-tear test-pieces pre-strained at 150% strain. The tearing energies for split tear test-pieces at tear rates ranging from 83 μm s^{-1} to 8300 μm s^{-1} were obtained by extrapolation The ratio increases as the tear rate decreased.

Table 7.3 shows the ratio of tearing energy of knotty tearing to tearing energy of steady tearing at a tear rate of 8300 μm s^{-1}. The ratio increases as the amount of pre-straining increased. From Tables 7.2 and 7.3, it can be seen that the effect of slowing the tear rate was analogous to increasing the amount of pre-straining. For example, at tear rates of 830 μm s^{-1} and 170 μm s^{-1}, the ratios T_k/T_s shown in Table 7.2 were of the same orders of magnitude as the ratios obtained at 300% and 350% pre-strain and at a tear rate rate of 8300 μm s^{-1} shown in Table 7.3. This supports the suggestion that the strengthening structure can form more effectively at slow tear rates than at high tear rates.

7.5 Strength anisotropy in ENRs

Figures 7.2b and 7.2c show plots of tearing energy versus tear rate at 23°C for pre-strained black-filled ENR 25 and ENR 50 vulcanizates respectively, based on the data shown in Table 7.4 for ENR 25 and Table 7.5 for ENR 50. Logarithmic scales were used in each plot for the reason stated earlier. Just like pre-strained black-filled NR vulcanizates, the tearing energy of pre-strained black-filled ENR 25 and ENR 50 decreased as the amount of pre-straining increased. This shows that the tearing energy- tear rate relationship was consistent for the three black-filled rubber vulcanizates (NR, ENR 25, ENR 50) investigated. However, there is also an interesting observation. When the plots shown in Figure 7.2a were transposed on the plots shown in Figures 7.2b and 7.2c respectively using tracing paper, it was found that the tearing energy-tear rate (T-r) relationship for NR at 300% pre-strain was equivalent to the T-r relationship for ENR 25 at 350%. The T-r relationship for NR at 150% pre-strain was equivalent to the T-r relationship for ENR 50 at 250% pre-strain. These observations indicate that the amount of orientation produced at any given pre-strain increases as the strain-crystallisability of the rubber increases. The implications of this observations will be discussed in the next section.

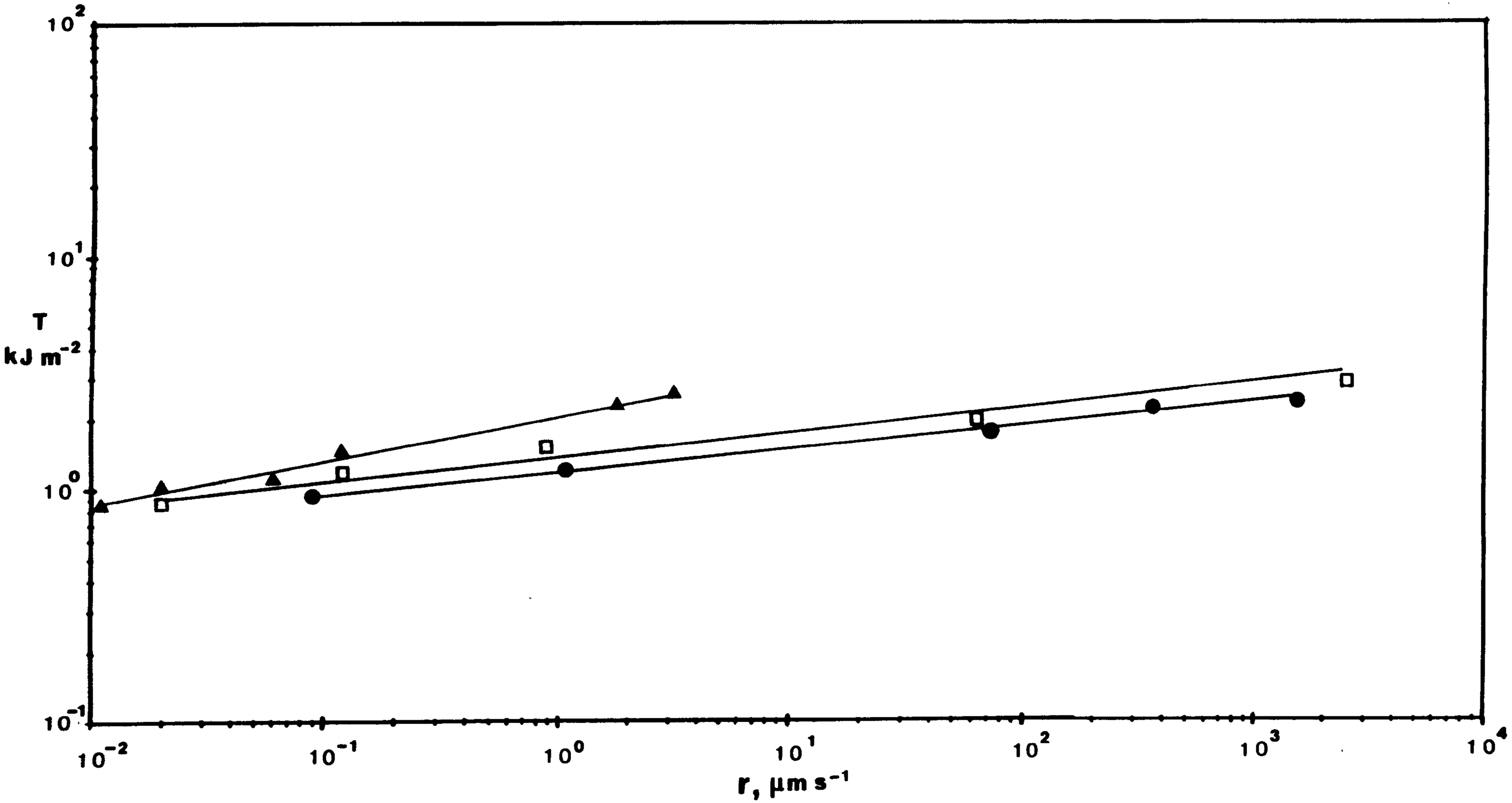

Figure 7.2b: Tearing energy, T vs rate of crack propagation, r, of black-filled ENR 25 vulcanizate at 23°C. Full formulations are shown in Table 4.3b for mix H2 in Chapter Four.
▲ λ = 3.5, □ λ = 4.0, ● λ = 4.5.

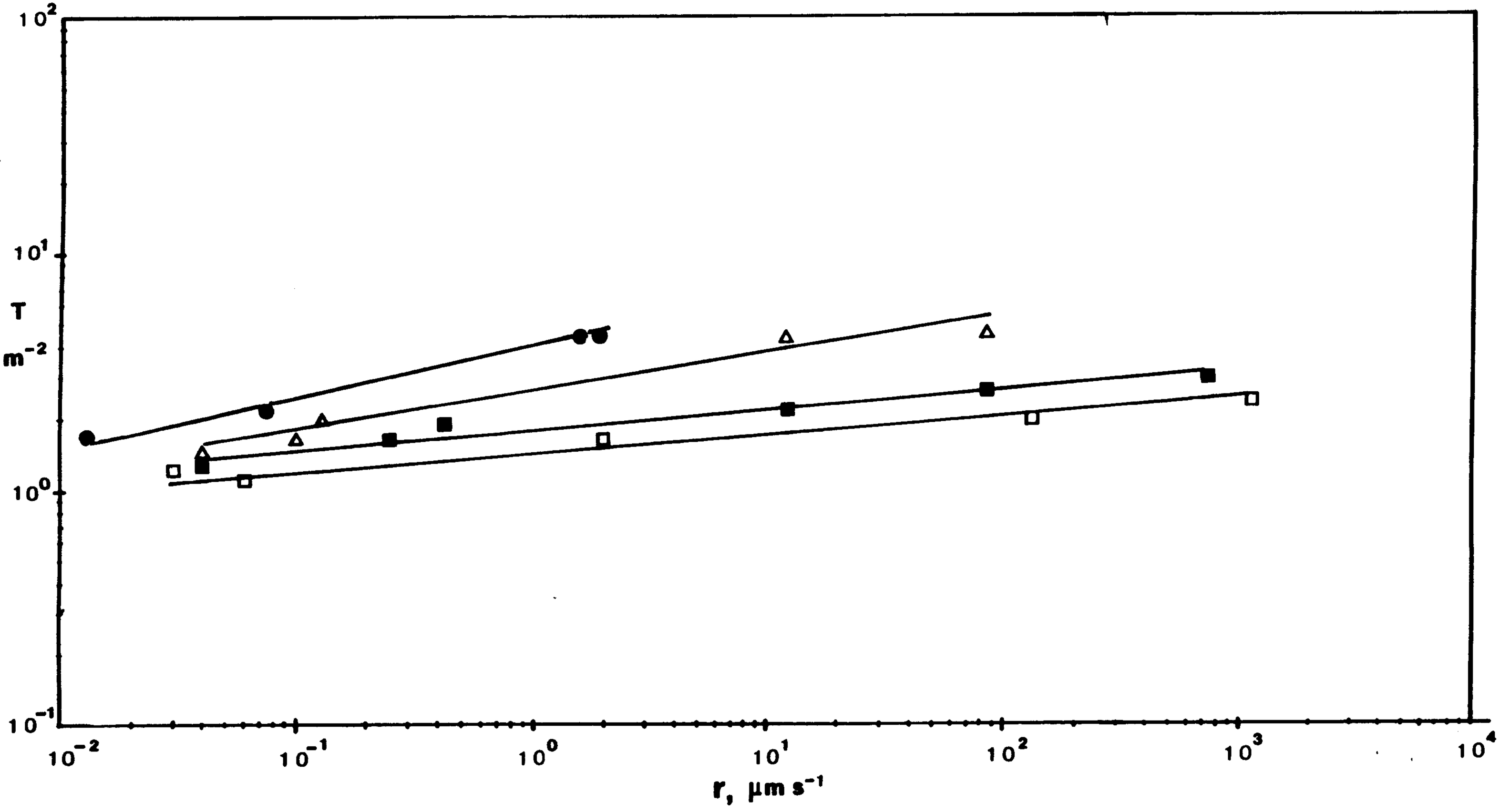

Figure 7.2c: Tearing energy, T vs rate of crack propagation, r, of black-filled ENr 50 vulcanizate at 23°C. Full formulations are shown in Table 4.3c for mix H3 in Chapter Four.
● λ = 3.0, △ λ = 3.5, ■ λ = 4.0, □ λ = 4.5.

Table 7.4: Tearing energy of pre-strained black-filled (50pphr HAF) ENR 25 vulcanizates at 23°C using split-tear test-pieces

(A) Pre-strained at 150% strain

T ($kJ\ m^{-2}$)	0.90	1.36	1.84	2.40	
r ($\mu m\ s^{-1}$)	0.02	0.13	0.85	9.40	

(B) Pre-strained at 200% strain

T ($kJ\ m^{-2}$)	0.89	1.05	1.14	1.46	2.26	2.42
r ($\mu m\ s^{-1}$)	0.01	0.02	0.06	0.12	0.80	3.01

(C) Pre-strained at 300% strain

T ($kJ\ m^{-2}$)	1.22	1.21	1.58	1.96	2.56
r ($\mu m\ s^{-1}$)	0.02	0.12	0.87	65.0	2500

Full formulations of the vulcanizates are given in Table 4.3b (mix H2).

Table 7.5: Tearing energy of pre-strained black-filled ENR 50 vulcanizates

(A) Pre-strained at 200% strain

T ($kJ\ m^{-2}$)	1.23	1.67	2.17	3.45	3.18
r ($\mu m\ s^{-1}$)	0.002	0.013	0.072	1.58	1.60

(B) Pre-strained at 250% strain

T ($kJ\ m^{-2}$)	1.28	1.43	1.63	3.16	3.40
r ($\mu m\ s^{-1}$)	0.01	0.04	0.10	12.2	85.0

(C) Pre-strained at 300% strain

T ($kJ\ m^{-2}$)	1.46	1.62	1.90	2.13	2.54	2.73
r ($\mu m\ s^{-1}$)	0.04	0.25	0.42	12.4	96.0	730

(D) Pre-strained at 350% strain

T ($kJ\ m^{-2}$)	1.31	1.10	1.66	1.98	2.32
r ($\mu m\ s^{-1}$)	0.03	0.06	2.0	135	1136.4

Full formulations of the vulcanizates are given in Table 4.3b (mix H3).

7.6 Effect of crystallization on strength anisotropy

Split tearing can occur in strain-crystallizing rubber vulcanizates, but not in a non-strain-crystallizing vulcanizate, such as SBR. This suggests that crystallization plays an important role in promoting strength anisotropy. The effect of the degree of strain-crystallization on strength anisotropy was investigated using black-filled NR, ENR 25 and ENR 50 vulcanizates. The test-pieces were pre-strained to 300%. The energy to propagate tearing in the direction of molecular orientation was plotted against rate of crack propagation using logarithmic scales. The results in Figure 7.3 show that, the tearing energy of pre-strained black-filled NR vulcanizates was about 20% and 40% lower than the tearing energy of pre-strained black-filled ENR 25 and ENR 50 vulcanizates respectively over the whole range of tear rates investigated. There are two possible reasons for the tearing energy to decrease in the order of increasing degree of strain-crystallizability of the rubber. The first reason can be associated with the differences in strength anisotropy developed in each vulcanizate. The second reason can be associated with the glass-transition temperature of the rubber.

The effect of strength anisotropy is considered first. According to Treloar (5), the effect of extension is to produce a degree of molecular alignment. The effect of molecular alignment is very significant in strain-crystallizing rubbers. A direct consequence of molecular alignment is to increase the rate of crystallization, and to some extent the amount of crystallization. The degree of alignment of the crystallites becoming more perfect with increasing extension. According to Treloar (5), anisotropy is a direct consequence of the high degree of molecular orientation in the stretched crystalline state. It is evident from the results shown in Figures 7.2a, b and c that the tearing energy for crack propagation along the molecular orientation i.e., parallel to the direction of extension decreases with increasing pre-straining. This implies that the higher the degree of molecular orientation the higher will be the strength anisotropy developed in the vulcanizate, and the lower will be the tearing energy for crack propagation in the direction of molecular orientation. The differences in the

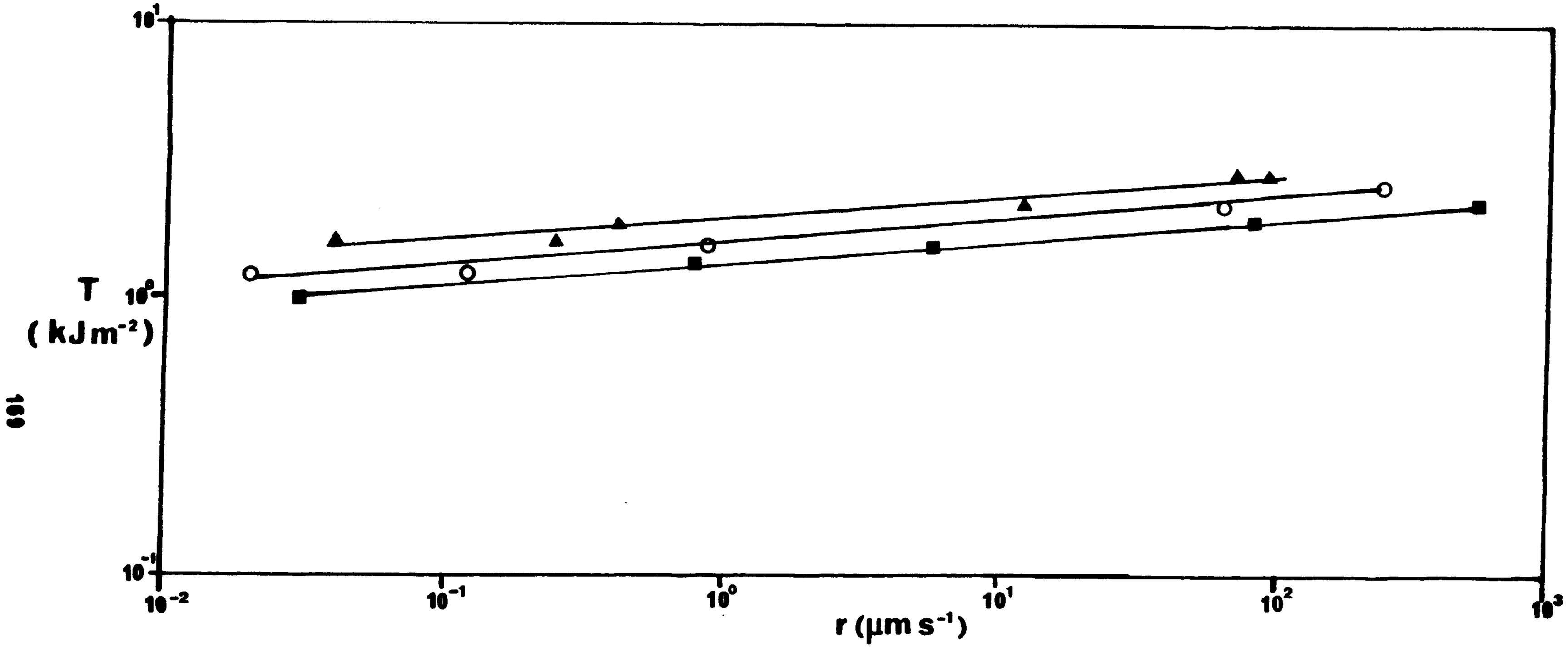

Figure 7.3: Tearing energy, T, vs rate of crack propagation, r, showing effect of strain-crystallization on the strength anisotropy developed as a consequence of pre-straining on black-filled (50 pphr of HAF) vulcanizates of ■ NR (mix H1), ○ ENR 25 (mix H2), and ▲ ENR 50 (mix H3). The full formulations are shown in Table 4.3b in Chapter Four.

tearing energy shown in Figure 7.3 can be attributed to the differences in the degree of strength anisotropy developed in each rubber. Although the rubbers (NR,ENR 25 and ENR 50) were pre-strained to the same strain, i.e., 300%, it is not necessary that the degree of strength anisotropy developed in each rubber was the same. As indicated in Section 7.5, the tearing energy-tear rate (T-r) relationship for NR vulcanizates at 150% pre-strain was equivalent to that developed in ENR 50 at 250% pre-strain. This observation is in line with the fact that ENR 50 strain-crystallizes less readily than NR because the ability of ENR 50 to strain-crystallize is affected to some extent by the epoxy groups adjacent to the main chain. Thus ENR 50 vulcanizates required 250% pre-strain whereas NR vulcanizates needed only 150% pre-strain to produce the same degree of strength anisotropy.

There is evidence suggesting that the polarity of the epoxy groups has slight effects on the rates of both nucleation and growth of crystallization, since the polar nature of the epoxy groups retards the molecular mobility of the rubber chains (80). Lee and Porter (80) exploited this observation to improve the resistance of hardening of raw (uncompounded) NR associated with crystallization at low temperatures. They investigated the effect of chemical groupings on the crystallization behaviour of raw NR at -26°C, the temperature at which the rate of crystallization of NR latex is highest. They found that the higher the polarity of the chemical groupings the higher the resistance to crystallization.

Further comparison shows that the T-r relationship of ENR 25 vulcanizates at 300% pre-strain is equivalent to the T-r relationship of ENR 50 at 350% pre-strain. Based on this evidence, the differences in the tearing energy of the rubber vulcanizates is associated with the differences in the degree of strength anisotropy. It is likely that the differences in the strength anisotopy developed in the vulcanizates may be associated with the degree of strain-crystallisability of the rubber. The higher the degree of strain-crystallization, the higher the degree of strength anisotropy developed in the vulcanizate because of extra molecular orientation associated with the crystalline regions.

The results shown in Figure 7.3 are in contrast to the results

obtained using trouser tear test-pieces where the tearing energy increased with increasing degree of strain-crystallisability of the rubber, as shown and discussed in Chapter Five. Although at first sight the results obtained from trouser tear test-pieces and those obtained from split-tear test-pieces appear to contradict each other, this is not the case. In actual fact, they compliment each other. The reasoning is as follows. In Chapter Five, it was shown that the occurrence of knotty tearing at a particular tear rate and temperature was affected by the degree of crystallinity of the rubber. The magnitude of the tearing energy and the range of tear rates over which knotty knotty tearing occurred was found to increase as the degree of strain-crystallisability of the rubber increases. It was suggested, that the readiness and the effectiveness of strain-crystallizing rubber vulcanizates to promote knotty tearing over a wide range of temperatures and tear rates was because crystallization enhanced further the strength anisotropy already induced by the carbon black. In fact, the results shown in Figure 7.3 provide quantitative evidence to substantiate this suggestion. This may explain why black-filled strain-crystallizing rubber vulcanizates promote knotty tearing far more effectively than black-filled non-strain-crystallizing rubber vulcanizates, over a wide range of temperatures and tear rates. This suggestion is also consistent with the experimental observations discussed in Chapter Five, and also with the work of Greensmith (16). Thus the suggestion that strain-crystallization gives further enhancement in strength anisotropy appears to be correct and the experimental results in Figure 7.3 bear out this view.

The differences in the tearing energy can also be interpreted in terms of the differences in the glass-transition temperature of the rubber. Kadir and Thomas (30) have shown that, in smooth tearing regions, the magnitude of the tearing energy of the rubber is ranked in the increasing order of the glass-transition temperature of the rubber. This implies that in steady tearing the tear strength is greatly influenced by the viscoelastic energy dissipation (hysteresis). In the present case, all the three black-filled rubber vulcanizates displayed time-dependent tearing. The tear propagated steadily in the direction of molecular orientation. The time-dependent tearing also suggests that local crystallization at the tear-tip did not occur. Apparently the the

tearing energy also increased in increasing order of the glass-transition temperature, θ_g, of the rubber. It is quite difficult to decide whether the differences in the tearing energy are associated with differences in strength anisotropy or with differences in the glass-transition temperature of the rubber. An alternative way to check this is to isomerize the three rubbers (NR, ENR 25, ENR50) to eliminate effects associated with strain-crystallization, and then repeat the experiment. Any differences in the tearing energy for propagation of tearing in the direction of molecular orientation will then be attributable to the glass-transition temperature of the rubber only, provided of course they are compared at the same crosslink concentration and are based on the same mix formulation. However, based on the tearing energy data of Kadir and Thomas (30), the tearing energy of unfilled nitrile (NBR, θ_g = -31°C) vulcanizates was about 4 times higher than unfilled NR vulcanizates when comparison is made in smooth tearing regions at tear rate of about 10 m s^{-1}. Since ENR 50 has a glass-transition temperature (θ_g= -27°C) near to NBR, its tearing energy should be higher than the tearing energy of NR, perhaps of the same order of magnitude shown by NBR. However, the ratio of the tearing energy of pre-strained ENR 50 to the tearing energy of pre-strained NR was small. It is not entirely clear why.

In general it can be concluded that the differences in the tearing energy shown in Figure 7.3 can be attributed in part with the differences in strength anisotropy and in part with the differences in the glass-transition temperature of the rubber.

7.7 The influence of nature and concentration of crosslink on tearing energy

Brown, Porter and Thomas (40) have found that the tearing energy of unfilled NR vulcanizates decreased with increasing crosslink concentration for each of the three vulcanizing systems (conventional, EV and peroxide) that they used. This observation is true when tearing proceeds in a steady and/or stick-slip manner, where the variation of the effective tip diameter is not too great. In the case of black-filled NR vulcanizates, the situation is complicated by the issue of knotty tearing, where there are variations in the effective tear-tip diameter. In cases like these,

it is difficult to isolate the contributions that come from the increase in tip diameter, the nature of the crosslinks, and that of the crosslinks concentration. In split tearing, the issue of the variation of tip diameter does not arise since the tear propagates steadily and producing very smooth fractured surface.

In the present investigation, all the test-pieces were pre-strained to 200% strain and tearing was carried out at 23°C by separating the arms of the test-piece at a crosshead speed of 100 mm per minute. The results are shown in Figure 7.4 where the tearing energy of black-filled (50 pphr HAF) NR vulcanizates based on the three vulcanizing systems (conventional, EV and peroxide) is plotted against crosslink concentration. The tearing energy of vulcanizates in each vulcanizing system decreased with increasing crosslink concentration. For example, in the case of the peroxide vulcanizates, the tearing energy of the vulcanizate having a crosslink concentration of 1.85×10^{-2} mol per kg of rubber hydrocarbon was about 3.5 times the tearing energy of a vulcanizate having a crosslink concentration of 7.4×10^{-2} mol per kg of rubber hydrocarbon. The progressive decrease of tearing energy with increasing crosslink concentration might be attributed to lower viscoelastic energy dissipation. Besides crosslink concentration, the magnitude of the tearing energy of the vulcanizates was also dependent upon the nature of the crosslink. At any crosslink concentration, the conventional cure system, which produced mainly polysulphidic crosslinks gave the highest tearing energy followed by the EV system which produced mainly monosulphidic crosslinks. The peroxide system, which produced essentially carbon-carbon crosslinks, gave the lowest tearing energy compared with the other two vulcanizing systems.

It has been suggested (40) that the ability of labile polysulphidic crosslink to relieve high local stresses by yielding is responsible for the observed high tearing energy in vulcanizates produced by the conventional system (40). The findings in the present investigation parallel with the findings of Brown, Porter and Thomas (40), who investigated the effects of the nature and concentration of crosslink on the tear strength of unfilled isomerized natural rubber. Thus, when knotty tearing is suppressed, the tearing energy-crosslink concentration relationship follow the expected trend, and is similar to that for the unfilled system.

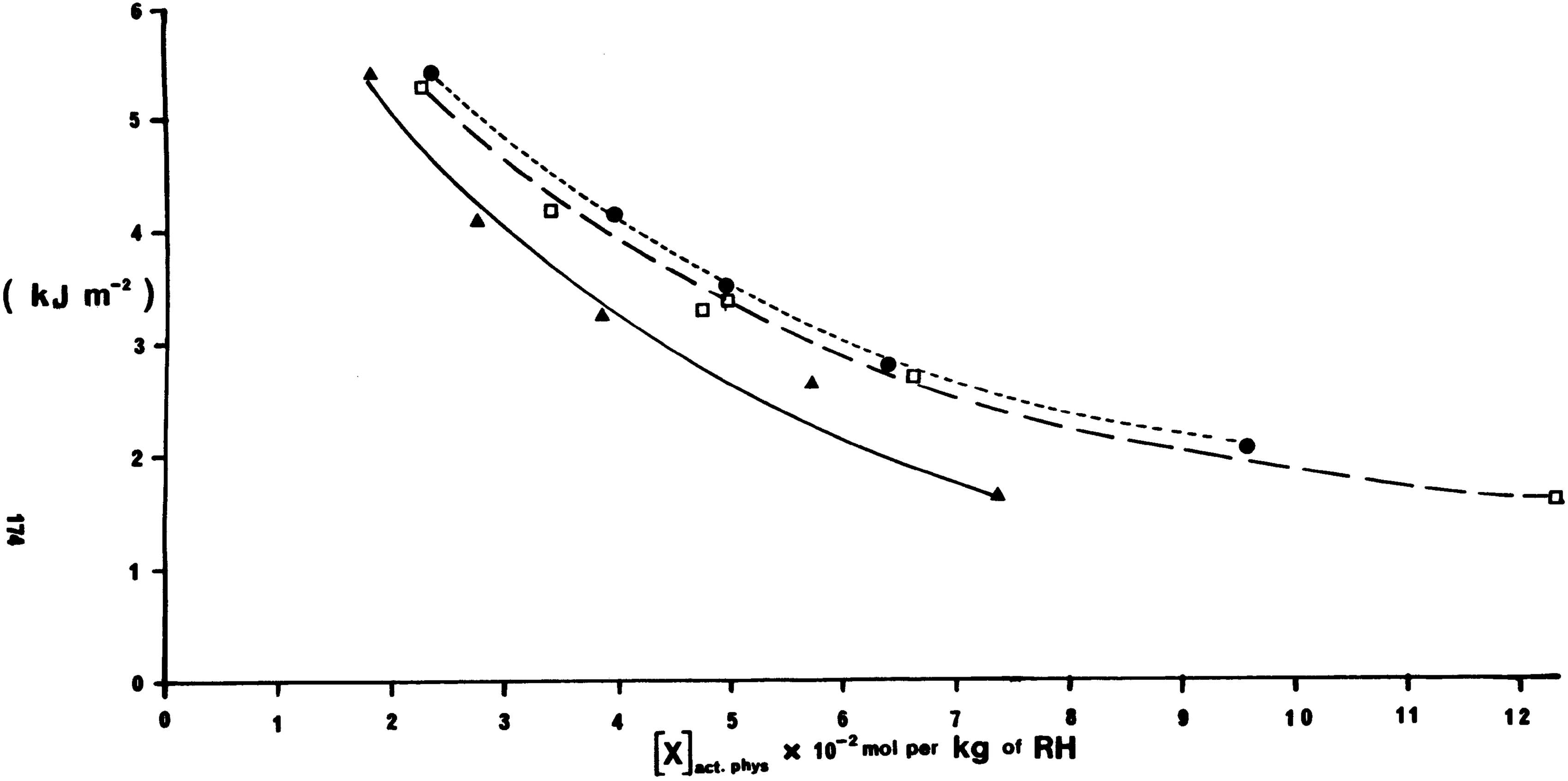

Figure 7.4: Tearing energy, T vs crosslink concentration of black-filled (50 pphr HAF) vulcanizates. ● conventional vulcanizate shown in Table 4.4a, □ EV vulcanizate shown in Table 4.4b, ▲ peroxide vulcanizate shown in Table 4.4c. Tear mesurements were carried out using constant-rate-of-separation method. Rate of extension 100 mm per minute at 23°C. $\lambda = 3$

When the tearing energy-crosslink concentration relationship obtained using trouser tear test-pieces (Figure 5.11a in Chapter Five) is compared with the tearing energy-crosslink concentration relationship obtained using split-tear test-pieces shown in Figure 7.4, two inferences can be drawn. First, in steady tearing regions the tearing energy obtained from trouser tear test-pieces was of the same order of magnitude as that using split-tear test-pieces, particularly if the crosslink concentration ranged from about 1.8×10^{-2} to 4.0×10^{-2} mol per kg of rubber hydrocarbon. Secondly, in knotty tearing regions the tearing energies obtained from trouser tear test-pieces were a factor of 10 or more higher than the tearing energies obtained from split tear test-pieces when compared at the same crosslink concentration. The first observation provides further experimental evidence that tearing energy gives a true measure of tear resistance independent of the test-piece geometry. However, this observation was only applicable in steady tearing where the tip diameter did not vary greatly. The second observation clearly indicates that the substantial difference in the magnitude of the tearing energy of vulcanizates obtained from trouser tear test-pieces and split-tear test-pieces was a consequence of differences in the tearing mechanisms. Trouser tear test-pieces produced knotty tearing which enhanced the tear strength by increasing the effective tear-tip diameter. The decrease in the tearing energy with increasing crosslink concentration was attributed to the tip diameter which decreased with increasing crosslink concentration. Split-tear test-pieces produced steady tearing, and the low tearing energy observed was attributed to the sharp tear-tip diameter where the local stress concentration at the tear tip is always high. The decrease in the tearing energy with increasing crosslink concentration was attributed to lower hysteresis at high crosslink concentration than at low crosslink concentration.

7.8 Effect of filler loading on tear strength

The tests were carried out by pre-straining the split-tear test-pieces to 200% strain and tearing by separating the arms at a rate of extension 100 mm per minute at 23°C using the Instron machine. The results are shown in Table 7.6. The tearing energy

Table 7.6: Effect of filler loading on split tearing at 200% pre-strain. Base mix for the HAF black-filled NR vulcanizates is shown in Table 4.2 in Chapter Four. The formulations for MT black-filled NR vulcanizate are shown in Table 4.3c (mix M1) in Chapter Four.

HAF (pphr)	25	40	50	60
T (kJ m^{-2})	1.52	2.52	2.56	2.62
MT (pphr)	-	-	50	-
T (kJ m^{-2})	-	-	1.75	-

increased progressively as the filler concentration increased. This increase in tearing energy was attributed to an increase in energy dissipation at higher filler loading (81).

7.9 Effect of particles size on tear strength

Split tearing on MT black vulcanizate was also investigated in exactly the same manner described above. The result is shown in Table 7.6 ~~(with star mark)~~. The degree of reinforcement obtained from large-sized MT black particles was very much less than that obtained from smaller size HAF black particles. The magnitude of the tearing energy of the vulcanizate contains 50 pphr MT black loading was more or less the same as that of the vulcanizate containing 25 pphr HAF black. This might be associated with lower energy dissipation of large-size black particles as suggested by Andrews and Walsh (11). Large-sized particles of MT black have lower surface area than small-sized particles of HAF black. Because of the high surface area of HAF black particles, the contact between the filler particles and the rubber phase is higher than that achieved with large-sized particles of MT black having low surface area. Consequently, the smaller-sized particles of HAF black interacted with the rubber more effectively than did the large-sized particles of MT black. According to Andrews and Walsh (11), a good interaction between the rubber and the black particles is necessary to give high hysteresis. Gregory (81) found that small-sized particles of carbon black gave higher tan δ than did large-sized particles of carbon black. Since tan δ gives a quantitative measure of hysteresis, thus this implies that small-sized black particles impart more hysteresis than do large-sized black particles. Thus the high tearing energy of HAF black-filled NR vulcanizates was attributed to high hysteresis which can improve the tear strength (11,23,35). The low tearing energy of MT black NR vulcanizates was attributed to their low hysteresis.

7.10 Summary of results

The use of split tear test-pieces has enabled the strength anisotropy to be assessed quantitatively. The tearing energy in the direction of molecular orientation was found to decrease (a) with increasing amount of pre-straining (b) with increasing amount of

crystallization, and (c) with decreasing rate of crack propagation. The first point may explain for the tear diversion observed in knotty tearing. When an advancing tear approaches the highly oriented anisotropic zone at the crack tip, the tear splits in the direction of molecular orientation because its tear resistance is very low as reflected by its low tearing energy for crack propagating in this direction. The second observation accords with the suggestion that crystallization can increase the strength anisotropy, presumably by giving extra molecular orientation. This helps to explain why strain-crystallizing rubber vulcanizates are more effective in producing knotty tearing over a wide range of tear rates and temperatures than are non-strain-crystallizing rubber vulcanizates. The third observation accords with the suggestion that knotty tearing occurs readily at low tear rate than at high tear rates since low tear rates allow more time for the strengthening structure to develop than do high tear rates, producing the strength anisotropy necessary for the occurrence of knotty tearing. Among other observations, it was found that, at the same molecular orientation, the tearing energy decreased with increasing crosslink concentration. The black-filled NR vulcanizates produced by the conventional vulcanizing system gave the highest tearing energy, followed by vulcanizates produced by the EV system, and finally by vulcanizates produced by the peroxide system, i.e., the order of tearing energy is the inverse of the order of the thermal stability of the crosslink. Furthermore, at the same level of molecular orientation, the tearing energy increased with increasing filler loading and decreased as the filler particle size increased.

CHAPTER EIGHT

EFFECTS OF PRE-STRESSING ON TEAR STRENGTH

EXPERIMENTAL

8.1 Introduction

In split tearing, the stress giving the orientation is maintained during the test. As discussed earlier in Chapter Two, there is evidence suggesting that when a large stress is imposed to a certain type of vulcanizate, some scission and subsequently recombination of crosslinks take place whilst in the strained state, thus giving a permanent set when the loading stress is removed (38, 39). Gent and Kim (47), have found that the tear strength of black-filled natural rubber after pre-stressing was affected by the anisotropy introduced during pre-stressing. They found a substantial difference in the tear strength for crack propagation in the parallel and transverse to the direction of molecular orientation. Rivlin and Thomas (76) had proposed a hypothesis based on a two-network model suggested by Green and Tobolsky (84). According to their hypothesis, tearing would take place preferentially on planes parallel to the direction of extension, if the number of links per chain segment in the second network introduced during pre-stressing is much less than that in the original unstrained network. It was of interest to check if this hypothesis can be used to explain the anisotropy introduced during pre-stressing. The method of approaching this aspect of the work was different from the methods described by Houwink and Janssen (33) and by Gent and Kim (34). In the present investigation, attempts were made to investigate the following aspects:

(a) To investigate if the anisotropy introduced by pre-stressing was affected by the length of time allowed for elastic and viscoelastic recovery. This was approached by making the tear measurements two minutes after the pre-stressing load was removed, and also by making tear measurements after having swollen and deswollen the pre-stressed vulcanizates. In this way, inferences could be made as to whether the anisotropy produced by pre-stressing was physical or chemical in nature. If it was physical, the

tear strength of pre-stressed vulcanizates after swelling and deswelling should be comparable with the tear strength of unstressed (control) vulcanizates. If it was chemical in nature, then the tear strength of pre-stressed vulcanizates after swelling and deswelling would be different to some extent from the tear strength of unstressed vulcanizates. This would then clarify the contradictions between the findings of Houwink and Janssen (46) and Gent and Kim (47). Houwink and Janssen claimed that the tear resistance of pre-stressed vulcanizates was recoverable after heating the pre-stressed vulcanizates for some hours (exact time not given) at 100°C. They found no significant different in the tear resistance when compared with the unstressed vulcanizates. In contrast, Gent and Kim (47) claimed that the anisotropy produced by pre-stressing was relatively permanent. They found that no recovery took place after storage at room temperature for several months or even after heating for one hour at 100°C. Gent and Kim (47) found that the tearing energy of pre-stressed vulcanizates after heat treatment was markedly lower than the tearing energy of unstressed control vulcanizates.

(b) To investigate the effect of crosslink type in sulphur vulcanizates by making measurements on pre-stressed samples based on sulphur vulcanizates produced by the conventional and soluble EV systems. These vulcanizates differ widely in their resistances towards permanent set. In this way it was possible to check whether if the anisotropy produced by pre-stressing was associated with the permanent set.

(c) To investigate the dependence of the tearing energy of pre-stressed vulcanizates on tear rates and temperatures. If tearing of pre-stressed vulcanizates occurred in a steady manner, tearing energy data at different temperatures and rates should then be transformable into a single mastercurve using the WLF equation.

8.2 Pre-stressing at large stress

The experimental procedure is shown schematically in Figure

8.1. A parallel-sided test-piece, measuring 75mm x 10mm x 0.5mm was prepared by stamping a die on a flat 150mm x 130mm x 0.5mm vulcanized sheet of uniform thickness. The distance l_o, referred to the unstrained state was measured accurately by means of a vernier scale. The test-piece was pulled at a rate of 100 mm per minute, to an elongation defined by an extension ratio, $\lambda, (=l_1/l_o)$. The corresponding stress was also noted. The test-piece was held in the extended state for one minute, before unloading the stress. The test-piece was allowed to relax for 24 four hours and the length between bench marks, l_2, was noted. The two ends of the test-piece were cut off since they were compressed by the grips. The uniformly pre-stressed portion of the test-piece was weighed and then swollen in toluene for 72 hours. This was done to ensure that any residual crystaline phase in the rubber was completely melted. Furthermore, it allowed rapid elastic recovery because it eliminated both the short-and-long term viscoelastic effects. The test-piece was then deswollen and dried by evaporation under a strong current of air in a fume chamber. The weight was regularly monitored until it was constant. Finally, a long cut of about 4 cm was introduced parallel to the direction of the extension previously applied. Tearing was carried out using an Instron machine by separating the legs of the test-piece at a uniform rate. Alternatively, for time-dependent tearing, the constant load method was used in which dead loads were applied to one of the legs of the test-piece (the other leg being fixed to a grip) and the rate of crack propagation was obtained from the slope of a plot of crack length versus time. For slow crack propagation, the crack length in the unstrained state was measured at a fixed time interval. In the case of rapid crack propagation, a video camera was used to facilitate the measurement. The time for the crack to propagate to a certain fixed distance was noted by counting the number of frames. For this particular case, one frame was equivalent to 0.04 second. Tearing measurements above room temperature were carried out in a thermostatic cabinet as described previously in Chapter Four.

In all cases, unstressed samples were also taken from the same vulcanized sheet to serve as controls. They were swollen under the same conditions as those used for the pre-stressed samples. This was done to avoid confusion concerning any effects which the solvent might have had upon the samples.

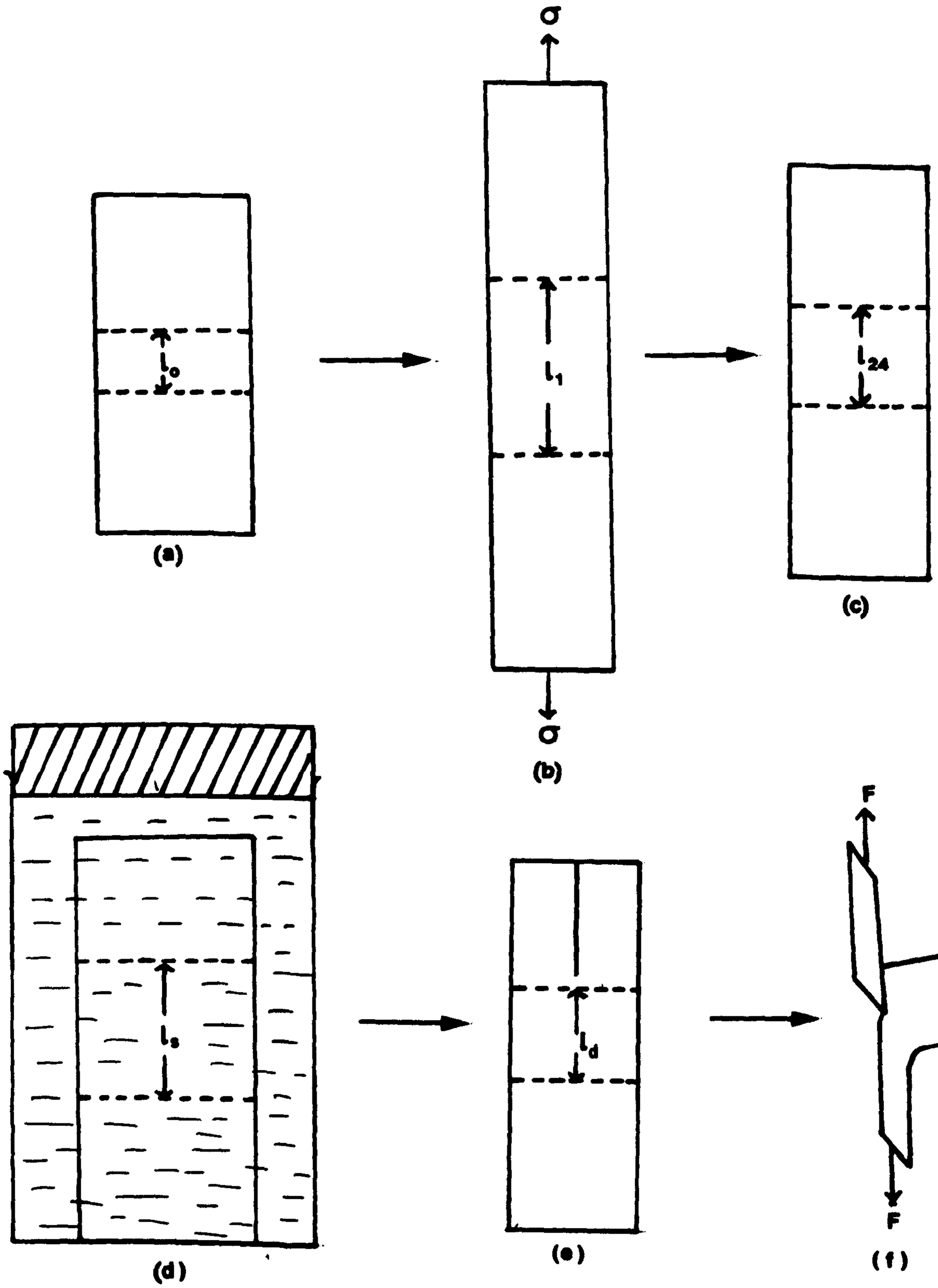

Figure 8.1: Schematic diagram showing the procedure for pre-stressing a vulcanizate. (a) unstressed sample (b) pre-stressed to an extension ratio, $\lambda = \frac{l_1}{l_o}$, by stress σ , for 1 minute (c) sample after 24 hours relaxation (d) sample swell to equilibrium (e) dried down sample, set $= \frac{l_d}{l_o} - 1$, (f) tearing in the direction of extension previously applied.

8.3 Pre-stressing at low stress

The method described in Section 8.2 introduces new crosslinks which form a second network through recombinations of the broken crosslinks produced by high mechanical deformation at large stresses. Alternatively, a new second network can also be introduced by means of a two-stage vulcanization. The final rubber mix was partially vulcanized in a mould in a steam-heated press. This is referred to the first-stage vulcanization. 24 hours later, the partially-vulcanized sheet was cut into several parallel strips measuring 75mm x 10mm x 0.5mm, and the individually strips strained to various extension in a framework contructed from Meccano. The strips were then put into an autoclave to complete the vulcanization. This is referred to as the second-stage vulcanization. The test-pieces were removed from the framework and allowed to relax for 7 days before making tear measurements in an Instron machine. As far as the author is aware, this method of investigation has not been attempted before; no reports on this method have been published before.

There are two differences between the method described in Section 8.2 and the method described here. The first is that, in the two-stage vulcanization method, the second network is formed by the introduction of crosslinks through the vulcanization process. In contrast, in the former method, the second network is formed through the recombination of the active sites of the broken crosslinks. In both cases, the second network is formed whilst the vulcanizates are in the deformed state. The second difference lies in the magnitude of the stress and the strain at which the second network is formed. The method described in Section 8.2 requires large stresses to produce sufficient crosslink rupture. In the two-stage vulcanization method, only a small stress is imposed in order to avoid breakage of the crosslink introduced during the first-stage vulcanization.

Stress-strain and equilibrium swelling measurements were carried out on samples after the first-stage vulcanization as well as after the second-stage vulcanization. The crosslink concentrations introduced in the first-stage and in the

second-stage vulcanizations were determined using the method described in Chapter Four. Also, tensile measurements were carried out on test-pieces vulcanized in the autoclave. The results showed that the tensile properties were the same as those of vulcanizates which had been vulcanized in the mould to the same final state of cure using a steam-heated press. This indicates that the vulcanizates which had been vulcanized in the autoclave were not affected by any oxidation which may have occurred as a consequence of exposure to air which might not have been completely removed before admitting steam to the autoclave.

8.4 Incorporation of di-n-butyl tetrasulphide (DBTS)

It has been suggested that it is possible to reduce the efficiency of the recombination process between broken crosslinks by incorporating a radical scavenger, di-n-butyl tetrasulphide (DBTS), through swelling (38,39,40). It is believed that DBTS would interfere with the recombination process, perhaps by terminating the active sites of the broken crosslinks. This is reflected in reductions in the set and the recombination efficiency (38,39). It was of interest to see to what extent DBTS has any effect on the tear behaviour of black-filled rubber.

In this investigation, a parallel-sided tensile strip was accurately weighed using an Oertling analytical balance. DBTS was dissolved in toluene in a suitable vessel, and the test-piece swollen in the solution for 7 days in the dark. It was assumed that DBTS was incorporated into the test-piece through a diffusion process. The swollen sample was weighed in a weighing bottle. It was then dried by evaporation in a fume chamber until its weight was constant. A similar test-piece was swollen in toluene not containing DBTS for the same length of time, to serve as a control. The amount of material extracted by toluene was calculated. The amount of DBTS incorporated was calculated by subtracting the final dried-down weight from the original unswollen weight after correction for the extracted material. This procedure was repeated for toluene solutions having various concentrations of DBTS. In each case, four test-pieces were used. The tear measurements were carried out using an Instron machine, and the average tearing energy was calculated. A similar experiment was carried out to investigate

the effect of DBTS on set. In this case, dumbbell shape test-pieces were used.

8.5 Measurement of tension set and volume fraction of rubber in swollen vulcanizates

The standard laboratory measurement of tension set according to ISO 2285 (BS 903: A5) specifications involves straining the test-piece, a tensile strip 38mm x 2mm x 2mm , to 100% extension and holding it there for at least 24 hours (or alternatively for the longer of periods 72 hrs. or 168 hrs.). After the recommended time, the test-piece is relaxed for 30 minutes and the residual extension is measured and the tension set calculated. This method was not suitable for the present investigation where the sample is pre-stressed to a large deformation. Furthermore, the standard laboratory tension set method does not descriminate between physical effects associated with viscoelasticity and chemical effect associated with any second network which forms through recombination processes which occurs during pre-stressing. The method of measuring the tension set adopted here was similar to that used by Brown, Porter and Thomas (39) which is described below. Dumbbell-shaped tensile test-pieces were used. The method of pre-stressing was similar to that shown schematically in Figure 8.1 and described in Section 8.2. Here, the bench marks were introduced in the centre portion of the test-piece, which is uniform. The test-piece was pre-stressed to a pre-determined stress for one minute before unloading. 24 hours later the distance between the two bench marks was measured and a section was cut from within the narrow portion (i.e., from within the highly-strained centre portion). The initial weight of this section, w_o, was determined before swelling in n-decane to determine the crosslink concentration and the volume fraction of rubber in swollen vulcanizate after pre-stressing. Fresh solvent was used after 48 hours to remove the sol material. The weight of the sample at equilibrium swelling, w_s, was determined. The sample was then dried in a vacuum oven at 40°C and weighed until its weight was constant. The dried-down weight, w_d, and the dried down length, l_d, were determined. The dried-down length was given by the distance between the bench marks which were retained even after swelling because the ink used for marking the bench marks did not dissolve in the solvent. The reason

for swelling and deswelling is that it allows rapid elastic recovery and eliminates the physical effects associated with viscoelasticity. Thus the permanent set observed should reflect only the chemical effect associated with any second network present in the final material. Unstressed control samples were prepared from the same vulcanized sheet and swollen for the same length of time and under the same conditions. Both the lengths and weights of these samples before and after swelling were determined. The volume fraction of rubber in swollen vulcanizate and the crosslink concentrations were calculated in the manner described in Chapter Four.

8.5.1 Calculation of tension set

The amount of permanent set was calculated from the relationship

$$\text{permanent set, } \zeta = \lambda_d - 1 \qquad (8.1)$$

where, $\lambda_d = \frac{l_f}{l_o}$, l_f being the final dried down length after correction had been made for the decrease in length associated with the extracted materials. l_f was calculated as

$$l_f = \frac{l_d \times l_{oc}}{l_{dc}} \qquad (8.2)$$

where l_{oc} is the length between the two bench marks of the control sample before swelling, and l_{dc} is the length between the two bench marks of the control sample after swelling, deswelling and drying.

8.6 Determination of tearing energy of pre-stressed samples

The tearing energy of a trouser tear test-piece was calculated using equation 4.2 as discussed in Chapter Four. However, there is a small point which should be clarified here. The thickness, h, which appears in equation 4.2 refers to the unstrained thickness, of the test-piece by definition of tearing energy (19). In a pre-stressed sample, the unstrained thickness refers to the original thickness before pre-stressing. If the unstrained thickness after pre-stressing were chosen, there is an apparent increase in tearing energy of about 20%, for example, when the samples were pre-stressed to 23 MPa. It should be noted that Gent and Kim (47) did their tear measurements on pre-scored trouser tear test-pieces to control the

crack propagation path either in the parallel or transverse to the direction of pre-stressing. However, no information concerning the tear rate and temperature of the tests was given. In the present investigation, all the tearing energies of the pre-stressed vulcanizates were referred to propagation of tearing in the direction of molecular orientation parallel to the direction of pre-stressing. No pre-scoring was required for this aspect of investigation. Tearing measurements were made at a cross-head speed (Instron Model 1122) of 100 mm per minute at 23°C, unless stated otherwise.

8.7 Dynamic measurements

Dynamic tests on NR black-filled (50 pphr HAF) vulcanizate were carried out at six different frequencies ranging from 0.1 Hz to 15 Hz. Tests were carried out at five different temperatures ranging from -20°C to 90°C. Double-shear test-pieces as shown schematically in Figure 8.2 were used. The test-piece consists of two rubber dics 25.4 mm in diameter with nominal thickness of about 5.73 mm bonded between three cylindrical metal pieces. The surface of the metal to be bonded was sandblasted first and then degreased in a suitable solvent for a few days to remove any rust and oil contamination on the metal surface. This procedure was necessary in order to obtain a good rubber metal bonding. The cleaned metal surface was painted with proprietary bonding agents, Chemlok 205 (primer coat) and Chemlok 220 (top coat). The rubber was then bonded to this surface by vulcanization carried out in a steam-heated press using a transfer moulding technique.

The dynamic testing was carried out using an Instron dynamic testing machine 1271 fitted with a temperature control cabinet and also with other ancillary equipment such as a Solatron 1250 frequency response analyser (FRA). The Solatron FRA displays results in terms of the shear stiffness i.e., the ratio of shear force to shear deflection, tan δ and the shear modulus G, i.e., the ratio of the stress amplitude to the strain amplitude. From this information the storage shear modulus G' and the loss shear modulus G" were calculated using the relations $G' = G\cos\delta$ and $G'' = G\sin\delta$ respectively. The loss modulus in tension, E", was calculated using the relation $E'' \cong 3G''$. All the tests were done

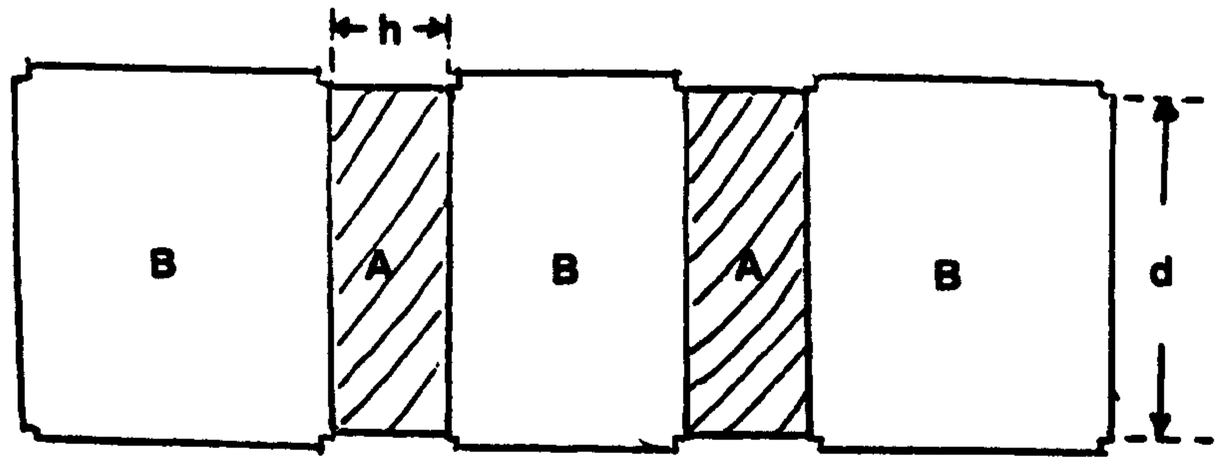

Figure 8.2: Schematic diagram showing a double shear test-piece.
A - rubber discs B - metal pieces.
Thickness, h = 5·73mm, Diameter d = 25·4mm

at 100% maximum strain amplitude. The objective of this investigation was to acertain if the dependence of the loss modulus (which gives a quantitative measure of energy loss) on frequency and temperature accords with the dependence of tearing energy on rate and temperature in the absence of knotty tearing.

CHAPTER NINE

EFFECTS OF PRE-STRESSING ON TEAR STRENGTH

RESULTS AND DISCUSSION

9.1 Effects of pre-stressing on the tearing energy

Effects of pre-stressing on the tearing energy of the conventional sulphur system NR black-filled vulcanizates (mix A6 Table 4.2a in Chapter Four) are shown in Figure 9.1, where tearing energy is plotted against strain. The data upon which this plot is based are shown in Table 9.1. Curve A represents data for pre-stressed samples that were not swollen, and curve B represents data for pre-stressed samples that were swollen, deswollen and dried down to a constant weight prior to the tear measurement.

The effect of pre-stressing on the tearing energy before swelling and deswelling is considered first. Here, tearing was carried out two minutes after the loading stress was removed from the test-piece. One of the most striking effects was the progressive decrease in the tearing energy with increasing strain. The decrease in the tearing energy is attributed to the decrease in the tip diameter, since tearing became less knotty as the strain was increased. In fact, at 350% strain and above, tearing changed from the knotty to the steady type. In the region of steady tearing, the tearing energy was less than that of the unstressed control samples by as much as a factor of 20 or more. This shows that, even when the stress giving the orientation was not maintained during the test, the anisotropy effect still persisted. A memory of previous stretching is therefore strongly evident in this material. This observation is not new, having been reported before by Gent and Kim (47) and by Houwink and Janssen (46). However, the reasons for its occurrence are still obscure.

The effect of the swelling treatment (curve B) is now considered. There are some interesting observations here. First, consider the effect of swelling and deswelling on the unstressed control samples. There was a slight decrease of about 10% in the tearing energy after the swelling treatment. The descrepancy here is attributed to the variations in the experimental results normally

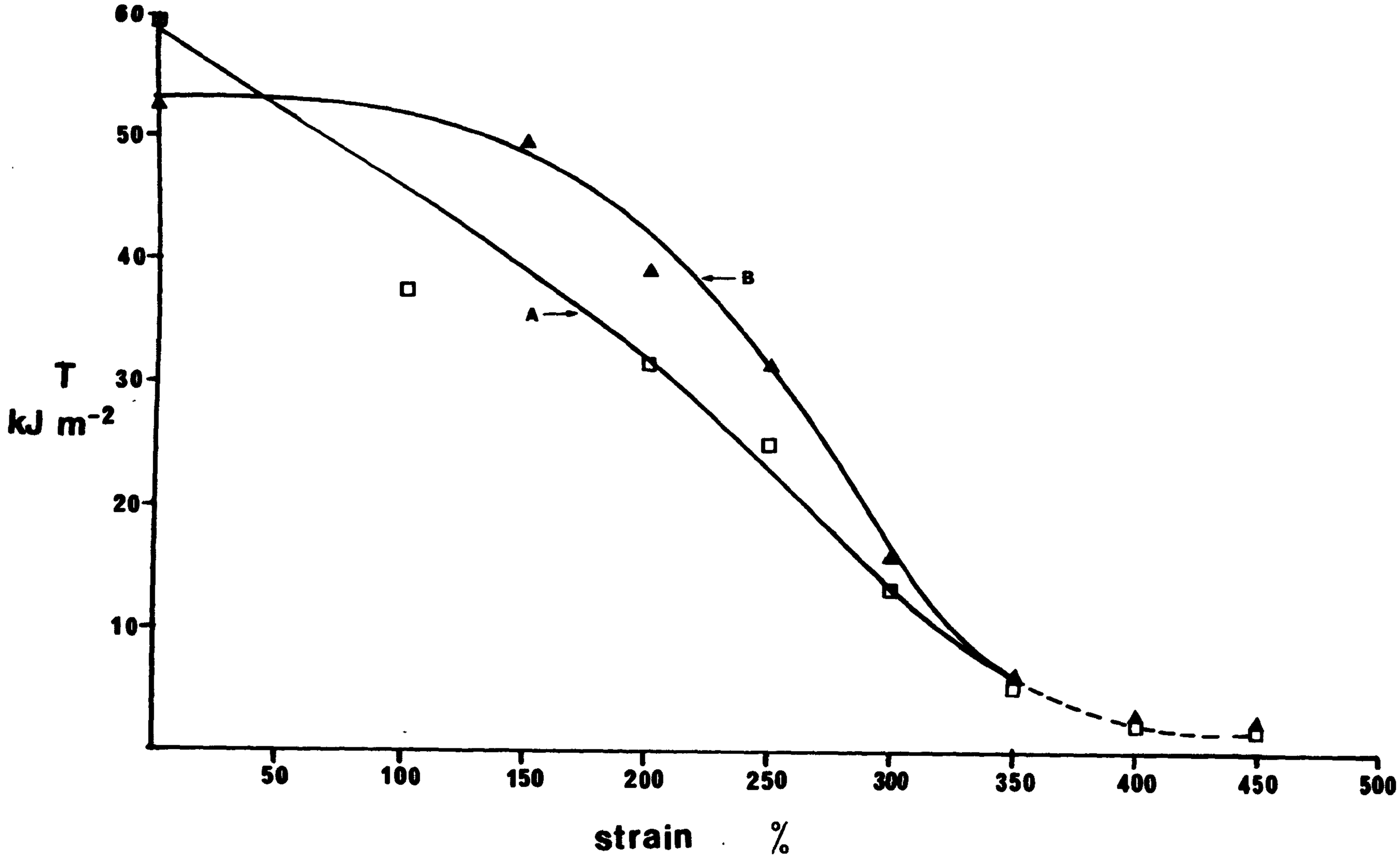

Figure 9.1: Tearing energy, T, vs strain, showing effects of pre-stressing on the tear strength of NR conventional system mix A6 in Table 4.4 black-filled (50 pphr HAF) vulcanizate. □ Unswollen samples (tearing 2 minute after pre-stressing), ▲ swollen, deswollen and dried down samples. Full line indicates knotty tearing, broken lines indicate steady tearing. Tearing at tear rate of 830 μm s^{-1} at 23°C, parallel to the direction of pre-stressing.

Table 9.1: Effects of viscoelastic recovery on the tearing energy of pre-stressed black-filled (50 pphr HAF) NR conventional sulphur vulcanizates for mix A6 shown in Table 4.4a in Chapter Four.

Tear rate 830 μm s^{-1} temperature 23°C

Strain (%)	0	100	150	200	250	300	350	400	450
* T (kJ m^{-2})	60.46	35.8	-	31.24	-	14.82	-	2.21	2.11
**T (kJ m^{-2})	52.02	-	49.2	39.35	31.24	16.14	5.3	+(2.83) 2.90	2.66
Types of tear	k	k	k	k	k	k	k+s	s	s

* Tearing energy of pre-stressed vulcanizates 2 minutes after removal of loading stress

** Tearing energy of pre-stressed vulcanizates after swelling and deswelling treatment

\+ Tearing energy of pre-stressed vulcanizates 10 days after removal of loading stress

k - knotty tearing, s - steady tearing.

Table 9.2: Tearing energy of pre-stressed black-filled (50 pphr HAF) soluble-EV NR vulcanizates after swelling and deswelling treatment. Full formulations are shown in Table 4.4b in Chapter Four.

Tear rate 830 μm s^{-1} temperature 23°C

Stress (MPa)	0	6	13	19	21	24
Strain (%)	-	150	260	340	370	400
T (kJ m^{-2})	51.11	45.5	34.09	30.00	35.79	26.55
Type of tear	k	k	k	k	k	k

k - knotty tearing.

observed in black-filled vulcanizates. Secondly, consider the effect of the swelling treatment on the pre-stressed samples. After swelling and deswelling, the tearing energy increases as reflected by the fact that curve B is above curve A. It appears that the anisotropy retained after pre-stressing was more pronounced before swelling than after swelling treatments. For examples, at 150% and 300% strain, the tearing energy was increased by about 33% and 16% respectively after swelling and deswelling. Five test-pieces were pre-stressed to 400% strain. After removing the pre-stressing stress, the test-pieces were left standing at 23°C for 10 days prior to making tear measurements. The average tearing energy of these pre-stressed vulcanizates is shown in Table 9.1. It is comparable to the average tearing energy after swelling and deswelling. This suggest that most of the viscoelastic recovery was completed after 10 days.

If it is assumed for the moment that the anisotropy retained after pre-stressing is associated with the set, then obviously the set after the swelling treatment is lower than the set before the swelling treatment because of the viscoelastic recovery brought about by swelling and deswelling. For example, the set measured one minute after the pre-stressing load was removed was about 43%; in comparison the set after the swelling treatment was 24%. The set measured after one minute is termed ``apparent set'', and the set after swelling and deswelling is termed ``permanent (real) set''. The observation that the anisotropy introduced by pre-stressing still existed even after swelling and deswelling suggests that the effect was permanent. This accords with the observations of Gent and Kim (47) discussed in Chapter Eight. Thus it appears that the effect was chemical in nature rather than physical in nature. In order to investigate this aspect further, tearing measurements were carried out on sulphur vulcanizates obtained using a soluble EV vulcanizing system. Such vulcanizates have high resistance to permanent set. The next section considers this aspect again and discusses the findings.

9.2 Correlation between tearing energy of pre-stressed vulcanizates and permanent set

Sulphur vulcanizates produced by two vulcanizing systems, viz,

the conventional and the soluble EV (see Tables 4.4a mix A6 and 4.4b in Chapter Four) systems were used because they displayed widely different degrees of resistance towards permanent set (36). The conventional system produces vulcanizates containing mainly polysulphidic crosslinks which are labile. They are easily broken and readily recombine when the vulcanizate is pre-stressed, thus giving high permanent set when the stress is removed. The soluble EV system produces vulcanizates containing predominantly monosulphidic crosslinks which are more stable than polysulphidic crosslinks. Such vulcanizates display the best resistance towards permanent set as far as sulphur vulcanizates are concerned. In each case, the samples were pre-stressed to varying degrees of strain, and both the tearing energy and the permanent set after swelling and deswelling were determined. The results are shown in Figure 9.2a where, tearing energy (on the LHS) and permanent set (on the RHS) are plotted against the strain. The tearing energies of the pre-stressed conventional vulcanizates were obtained from Table 9.1, and the tearing energies of the pre-stressed soluble EV vulcanizates were obtained from Table 9.2. The permanent set values were obtained from Table 9.4 for the conventional vulcanizates and from Table 9.6 for the soluble EV vulcanizates.

The effect of pre-stressing on the tearing energy of the vulcanizates is considered first. The effect of pre-stressing was greater in vulcanizates produced by the conventional system (curve A) than in vulcanizates produced by the soluble EV system (curve B). At 200% strain and above, the tearing energies of the vulcanizates produced by the conventional system were lower than the tearing energies of vulcanizates produced by the soluble EV system. For example, at 400% strain the tearing energy of the vulcanizate produced by the soluble EV system was about 10 times greater than the tearing energy of the vulcanizate produced by the conventional system. The large difference in the tearing energies of vulcanizates produced by the conventional and soluble EV system is attributed to the differences of tearing mechanism after pre-stressing. At 350% strain and above, pre-stressed vulcanizates produced by the conventional system tore in a steady manner. In contrast, at the same level of strain, pre-stressed vulcanizates produced by the soluble EV system still tore in a knotty manner. Although pre-stressed soluble EV vulcanizates produced knotty

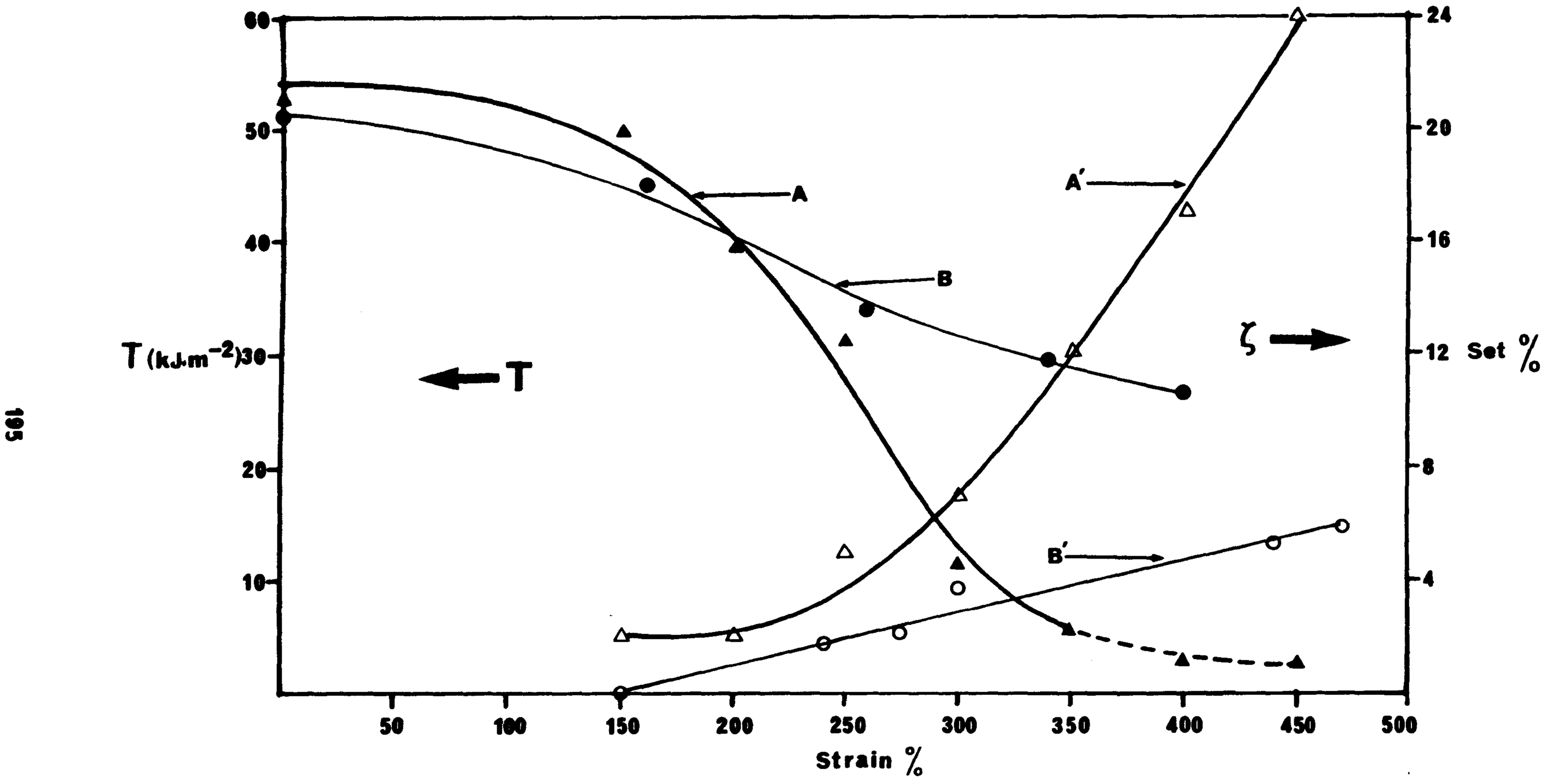

Figure 9.2a: Tearing energy, T, and permanent set vs strain, showing effect of nature of crosslink on tearing energy and permanent set. ▲ tearing energy and △ permanent set of black-filled (50 pphr HAF NR conventional vulcanizate (mix A6) shown in Table 4.4a. ● tearing energy and ○ permanent set of black-filled (50 pphr HAF) NR soluble EV vulcanizate shown in table 4.4b. Tear rate 830 μm s^{-1} at 23°C. Full line denotes knotty tearing, broken lines denote steady tearing.

tearing, the degree of knottiness was markedly less, as is indicated by their tearing energy being lower by a factor of about 2 than those of the corresponding unstressed control samples. This indicates that the anisotropy retained after pre-stressing is more pronounced in the conventional vulcanizates than in soluble EV vulcanizates. This observation may be attributed to the amount of permanent set, which was substantially higher in the conventional vulcanizates than in the soluble EV vulcanizates. According to the Rivlin and Thomas hypothesis (76), the introduction of a second network whilst in the deformed state may result in anisotropy. This secondary network forms during pre-stressing, perhaps through recombination of the active sites of the broken crosslinks. When the loading stress is removed, the original network tries to return to its original configuration but is prevented from doing so by this secondary network. Thus a small amount of permanent deformation is observed and this is what is known as permanent set. Permanent set can be used to assess the amount of anisotropy retained after pre-stressing, and the tearing energy for crack propagating in the direction of molecular orientation (i.e., parallel to the direction of extension previously applied) can be used as a quantitative measure of the strength anisotropy introduced. Thus the higher the set, the higher the degree of anisotropy retained, and the lower the tearing energy in the direction of molecular orientation, as is shown by the results in Figure 9.2a.

The correlation between tearing energy and set is shown in Figure 9.2b. The points were obtained from the results shown in Figure 9.2a. For the conventional sulphur system, the set was noted from curve A' and the corresponding tearing energy from curve A. For the soluble EV sulphur system, the set was noted from curve B' and the corresponding tearing energy from curve B. Figure 9.2b shows some interesting features. There is a critical set value of about 12%, above which the tearing energy is almost independent of the set. Between 0% to 12% set, the tearing energy decreases progressively as the amount of set increases. At 12% set, the tearing energy is about one tenth of the tearing energy of the control sample (0% set). It is also interesting to observe that the tearing energy-set correlation is independent of the vulcanizing system used for set values ranging from 2% to 12%. This is reflected by the fact that all the points lie satisfactorily around

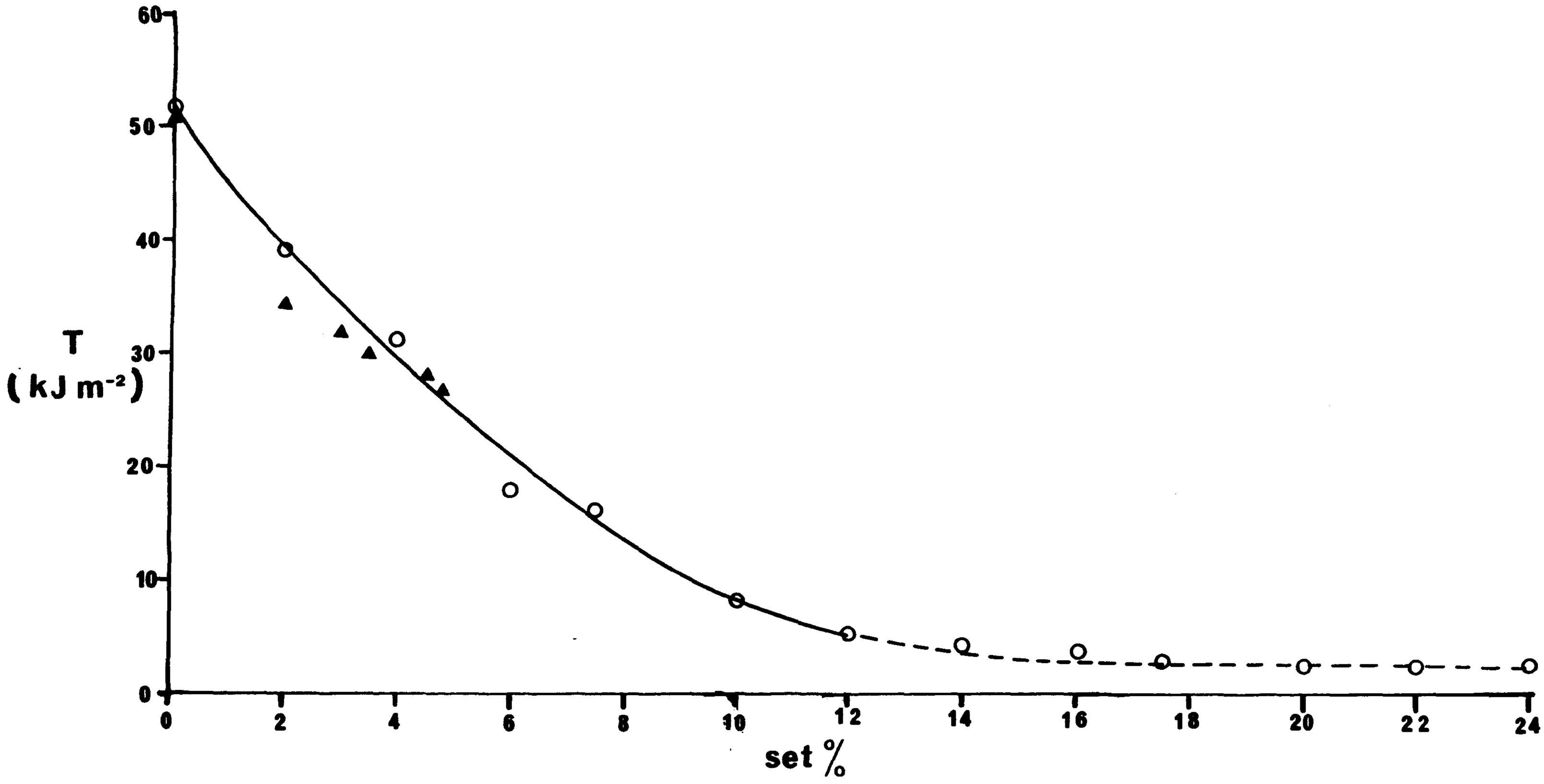

Figure 9.2b: Tearing energy, T, vs permanent set, showing the correlation between tearing energy and permanent set of black-filled (50 pphr HAF) NR vulcanizates. O conventional vulcanizate (mix A6) and ▲ soluble EV vulcanizate shown in Tables 4.4a and 4.4b respectively in chapter Four. Tear rate 830 μm s^{-1} at 23°C.

the tearing energy-set curve regardless of the vulcanizing system. Above the critical set value, the decrease in the tearing energy with increasing set is less pronounced than that observed below the critical value. Above the critical set value, steady tearing occurred producing a smooth fractured surface as is shown in Figure 9.3. Below the critical set value, knotty tearing occurred. It was also observed that above the critical set, time-dependent crack growth occurred in the direction of pre-stressing under constant stress. This suggests that the development of strain-crystallization at the tip of the tear was somewhat suppressed. Otherwise time-dependent crack growth did not occur. Below the critical set, no time-dependent crack growth in the direction of pre-stressing was observed. It appears that the amount of set affects the tear behaviour of black-filled conventional sulphur NR vulcanizate. No time-dependent crack growth was observed in pre-stressed black-filled EV NR vulcanizate.

To check further the relationship between permanent set and strength anisotropy, tearing measurements were made two minutes after the loading stress was removed from the pre-stressed vulcanizates so that there was not much time available for elastic recovery, hence giving additional set. It is of interest to check if pre-stressed soluble EV vulcanizates can produce steady tearing when the test is carried out under this condition. The samples were pre-stressed to 450% strain and held there for one minute before unloading the stress. One minute after unloading the stress, the apparent set was noted, and tear measurements were made one minute later at six different tear rates. The results are shown in Figure 9.4, where the tearing energies of pre-stressed sulphur vulcanizates produced by the conventional, semi-EV and the soluble EV systems are plotted against crack propagation rate in the direction of molecular orientation from the data shown in Table 9.3.

The effect of pre-stressing on soluble EV vulcanizate is considered first. The average apparent set after one minute was about 18%. At tear rates between 830 $\mu m\ s^{-1}$ and 8300 $\mu m\ s^{-1}$, steady tearing occurred, and at tear rates lower than 830 $\mu m\ s^{-1}$ knotty tearing occurred. This observation may be explained as follows: At fast tear rates the time was too short for significant elastic recovery to occur. As a result, the amount of

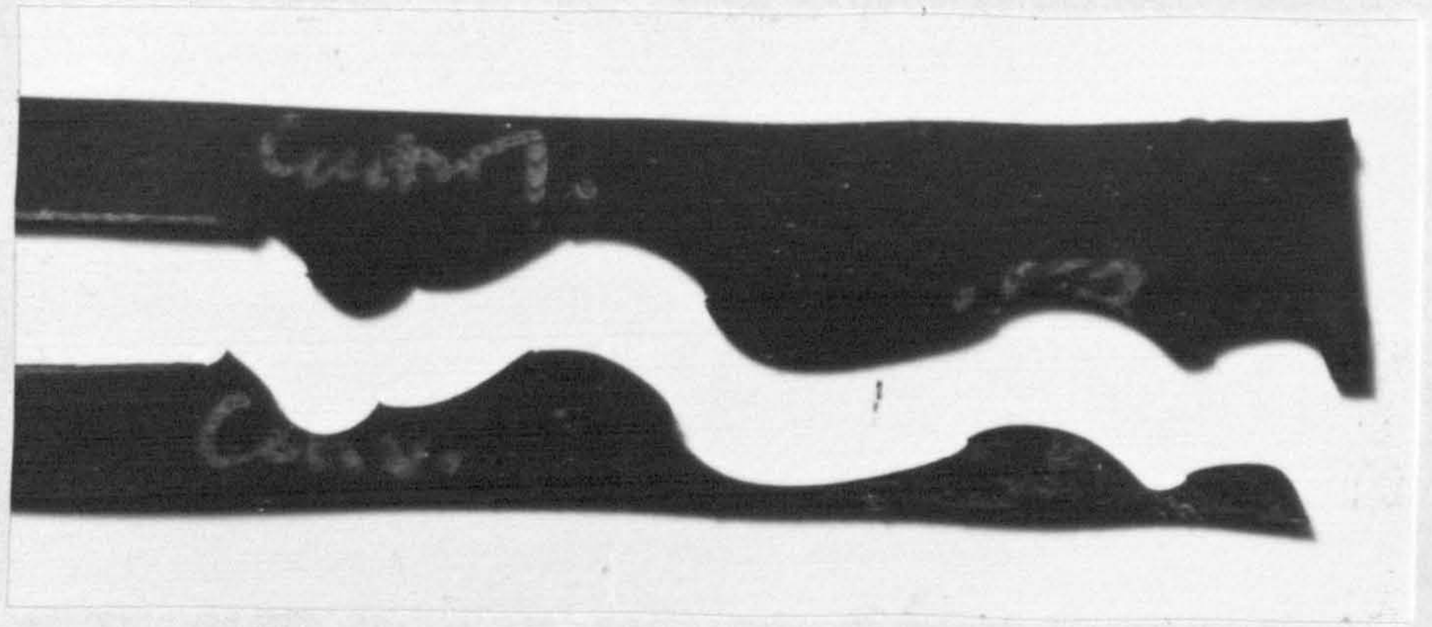

a

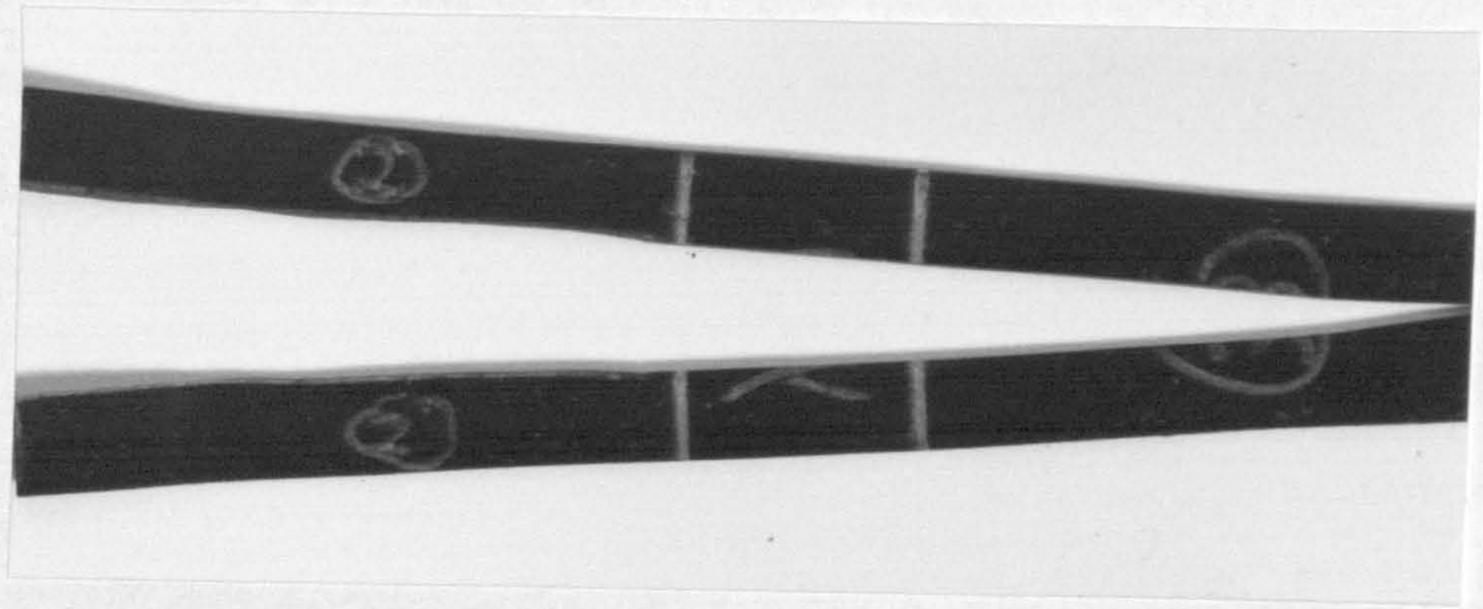

b

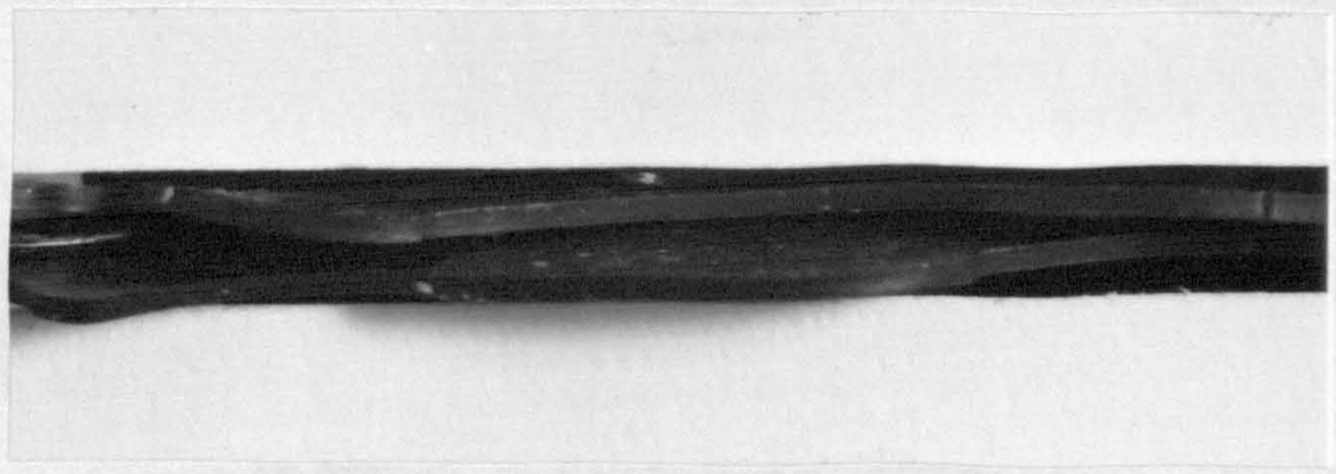

c

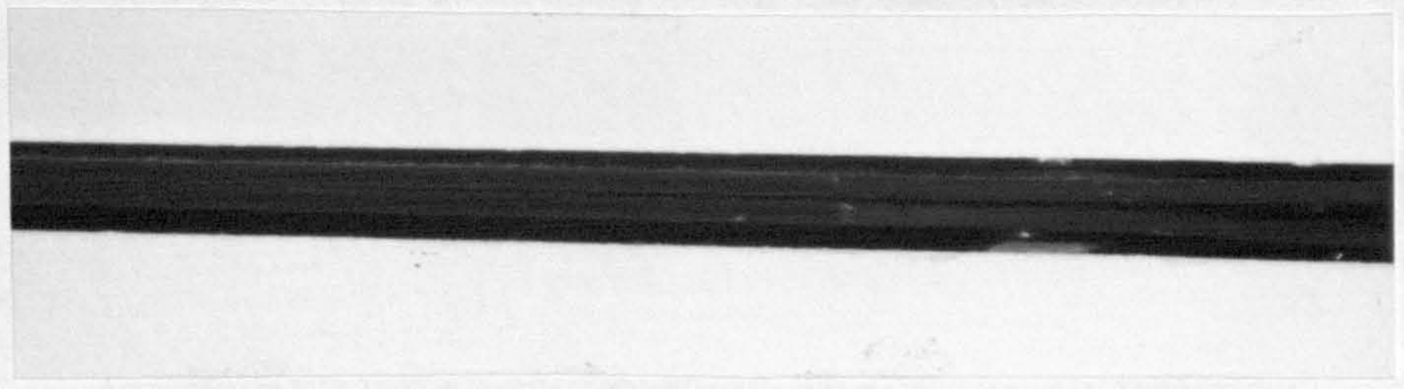

d

Figure 9.3: Photographs showing the types of tear failure before and after pre-stressing of black-filled NR vulcanizate. Tear rate 830 μm s^{-1} at 23°C. **a** unstressed control sample (knotty tearing), **b** pre-stressed sample (steady tearing), **c** fractured surface of control sample, **d** fractured surface of pre-stressed sample.

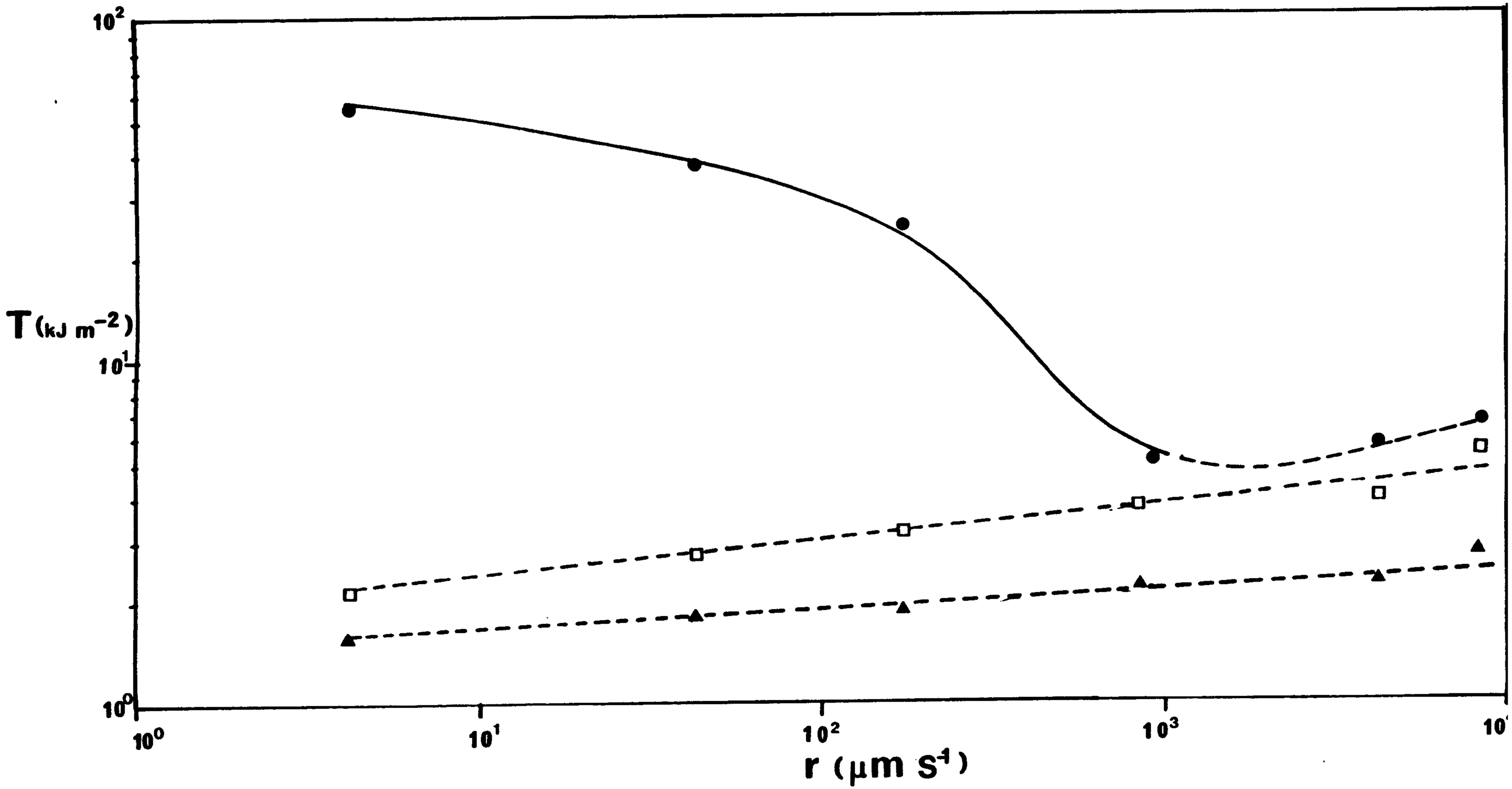

Figure 9.4: Tearing energy, T, vs tear rate, r, of conventional (▲), semi-EV □ and soluble EV (●) black-filled (50 pphr HAF) NR vulcanizates. Full formulations are shown in Tables 4.4a mix A6 (▲), 4.3b mix H1 (□), 4.4b (●). Samples were pre-stressed to 450% extension, tearing 2 minutes after the removal of pre-stressing load, at 23°C.
The apparent set after 1 minute (▲) 43%, (□) 29%, (●) 18%.
Full line denotes knotty tearing and broken lines denote steady tearing.

Table 9.3: Effect of tear rates on tearing energy of pre-stressed black-filled (50 pphr HAF) NR vulcnaizates at 23°C. All vulcanizates were pre-stressed to 450% strain.

Tear rate ($\mu m\ s^{-1}$)	4.2	4.2	170	830	4200	8300
* T ($kJ\ m^{-2}$)	1.54	1.69	1.85	2.17	2.21	2.68
Type of tear	s	s	s	s	s	s
** T ($kJ\ m^{-2}$)	2.10	2.71	3.14	3.75	3.80	4.29
Type of tear	s	s	s	s	s	s
***T ($kJ\ m^{-2}$)	58.21	36.73	24.57	7.40	5.58	6.42
Type of tear	k	k	k	k+s	s	s

* Set (%)	43
** Set (%)	29
***Set (%)	18

* Conventional cure system for mix A6 shown in Table 4.4a in Chapter Four.
** Semi-EV cure system for mix H1 shown in Table 4.3b in Chapter Four.
*** Soluble EV system shown in Table 4.4b in Chapter Four.

Tearing energy 2 minutes after the pre-stressing load was removed.
The apparent set was measured 1 minute after the pre-stressing load was removed.

s - steady tearing k - knotty tearing

set was still high and adequate to retain the anisotropy of strength, thus resulting in steady tearing. At slow tear rates, the crack propagated slowly, thus giving sufficient time for elastic recovery and hence reduced set. Once the set was below the minimum required, knotty tearing occurred, again probably because the set was not adequate to maintain the strength anisotropy in the direction of molecular orientation. In the cases of pre-stressed semi-EV and conventional vulcanizates, they tore steadily with smooth fractured surfaces at each tear rate investigated here. The fact that the crack still propagated in the direction of molecular orientation, even at the slowest crack propagation investigated here, suggests that the set was still high and adequate to retain the anisotropy in this direction. This observation also suggests that the set introduced by pre-stressing the vulcanizates produced by the conventional and semi-EV systems is attributable to chemical effects associated with the formation of a second network through the recombination process, this being the characteristic of polysulphidic crosslinks. In contrast, the set introduced by pre-stressing the soluble EV vulcanizates was predominantly physical in nature, being associated with viscoelastic effects. This may explain why pre-stressed soluble EV vulcanizates reverted to knotty tearing at slow crack propagation rates, because the set was physical in nature and continued to decrease as elastic recovery took place. In contrast, steady tearing did not revert to knotty tearing in the case of pre-stressed vulcanizates produced by the conventional system. This is because the set was predominantly chemical in nature and remained high even when elastic recovery was completed after swelling and deswelling, as shown earlier in Figure 9.1. Thus the results clearly show that the amount of set is an important factor in retaining the strength anisotropy after pre-stressing. The tearing energy-set correlation shown in Figure 9.2b bears out this view.

There are two other interesting observations. The first is concerned with the increase in the tearing energy with increasing tear rate observed here in steady tearing regions, irrespective of the vulcanizing system employed. This could well be associated with increase in the energy dissipation with increasing tear rate (35,68). The second concerns the effect of the vulcanizing system on the magnitude of the tearing energy. As discussed in Chapter

Seven, in steady tearing where the tip diameter is relatively constant, conventional sulphur vulcanizates gave the highest tearing energy, followed by EV and peroxide vulcanizates respectively, i.e., the tearing energy increases as the bond strength of the crosslink decreases. The polysulphidic crosslink (-C-S_x-C-) produced by the conventional system has a bond energy 64 kcal/mol, the monosulphidic crosslink (-C-S-C-) produced by the EV system has a bond energy 68 kcal/mol, and the carbon-carbon crosslink (-C-C-) produced by the peroxide system has a bond energy 84 kcal/mol (82). However, in the case of the pre-stressed samples used here, the tearing energy increased in the increasing order of the bond strength of the crosslink. The difference observed here could be associated with the degree of anisotropy. In split tearing discussed in Chapter Seven, the comparison was made at relatively the same molecular orientation, since they were all pre-strained to 200% extension. In the case of the pre-stressed samples, although they were pre-stressed to the same strain, however, it was the set that determined the strength anisotropy after pre-stressing. Since the set, and hence the anisotropy, increased in the reverse order of the bond strength of the crosslink, the tearing energy of pre-stressed vulcanizates decreases in the direction of increasing set.

The main conclusion that can be drawn from Section 9.2, is that the anisotropy retained after pre-stressing is a consequence of the set introduced during pre-stressing. This conclusion accords with Mullins's (83) view that anisotropic properties of filled vulcanizates, which are produced by stretching may be associated with the set. It is clearly evident from the results shown in Figures 9.2a and 9.4 where vulcanizates containing high proportions of polysulphidic crosslink which are known to give high set show substantially low tear strength after pre-stressing to large strain. In contrast vulcanizates containing high proportions of monosulphidic crosslink which are known to give low set still retain the high tear strength after pre-stressing to large strain. There are theoretical reasons for believing that network breakdown and formation under strain will produce anisotropy in crack propagation (76). According to hypothesis of Rivlin and Thomas (76), tearing will take place preferentially in planes parallel to the direction of extension, if the number of links per chain segment in the second network introduced during pre-stressing is much less than that in

the original network. The good correlation between tearing energy and set shown in Figure 9.2b is in accord with the hypothesis of Rivlin and Thomas (76). Gent and Kim (47) explained the anisotropy observed in pre-stressed vulcanizates on the basis of the Dannenberg hypothesis which states that crystallization brings about a segregation of filler particles. When the strain is released and the crystallites melt, weak paths are left in the elastomer thus allowing easy tearing along this direction. However, if this were the only mechanism, the anisotropy introduced by pre-stressing should not show a marked dependence on the nature of the crosslinks. Houwink and Janssen (46) suggested that the low tear resistance of pre-stressed vulcanizates in the direction of pre-stressing was associated with the splitting effect in this direction as a consequence of the orientation of particles. However, their suggestion does not provide any information on why the splitting effect is produced in pre-stressed conventional vulcanizates and not in the pre-stressed soluble EV vulcanizates. Thus as far as the present situation is concerned, the hypothesis of Rivlin and Thomas (76) appears to be the appropriate explanation for the anisotropy retain after pre-stressing.

9.3 Comparison between tearing energy of pre-strained with pre-stressed vulcanizates

Here, the term ``pre-strained'' refers to tear tests carried out using split-tear test-pieces, where the stress giving the orientation was maintained during the tear test. The term ``pre-stressed'' refers to tear tests carried out using trouser test-pieces where the stress giving the orientation was maintained for one minute only, and after that time the stress was removed. The pre-stressed vulcanizates were then swollen and deswollen and dried to constant weight prior to carrying out the tear test. The results are shown in Figure 9.5, where the tearing energies are plotted against crack propagation rate in the direction of molecular orientation, using logarithmic scales. In split tearing, the test-piece was pre-strained to 350% strain. In pre-stressed samples (trouser tear test-pieces), the strain applied during the one minute pre-stressing was 450%, and the associated permanent set was 24%. Both set of results are compared with the unstressed control samples (trouser tear test-pieces).

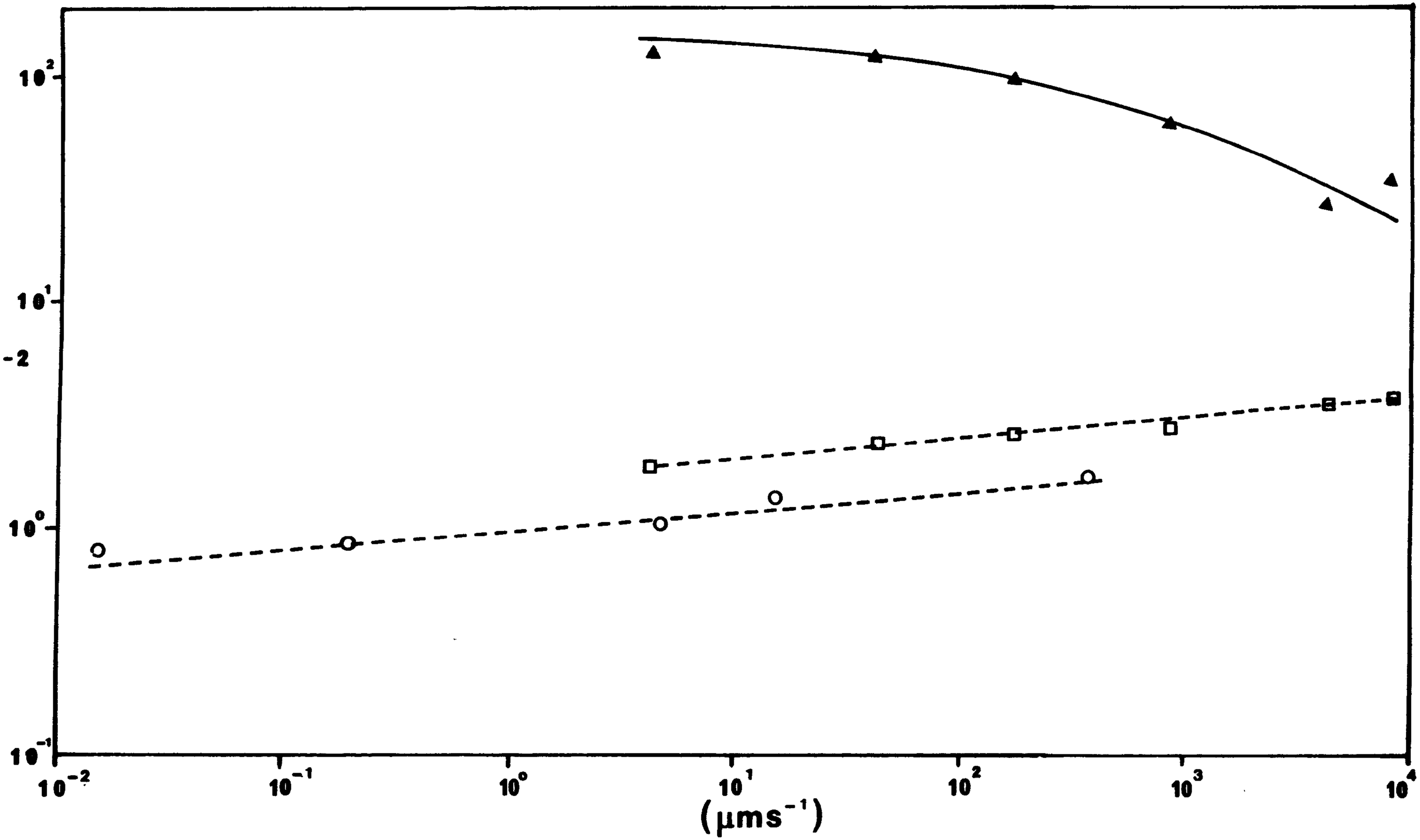

Figure 9.5: Tearing energy, T, vs tear rate, r, showing comparison between tear behaviour of unstressed (▲), pre-stressed (□) and pre-strained(O) black-filled NR vulcanizates. (▲) and (O) refer to mix H1 shown in Table 4.3b and (□) refers to mix A6 shown in Table 4.4a in Chapter Four. (□) pre-stressed to 450% strain and (O) pre-strained to 350 %. Pre-strained - split test-piece. Unstressed and pre-stressed - trouser test-pieces.

The effect of pre-stressing is considered first. At a crack propagation rate of 4.2 μm s^{-1}, the tearing energy of a pre-stressed conventional sulphur vulcanizate was a factor of about 60 lower than the unstressed (control) vulcanizates. When the stress giving the orientation was maintained during the test, the tearing energy decreased further by a factor of about 2. Thus this indicates that the anisotropy introduced by the set was very substantial, and not much different from the effect produced by pre-straining where molecular orientation was maintained during the test. This latter point is very significant because it implies that, in the vulcanizates produced by the conventional sulphur system, once the set has occurred during pre-stressing, it is no longer necessary to maintain the stress giving the molecular orientation since the anisotropy associated with the set is adequate to cause crack propagation in the direction of molecular orientation. In the case of an EV and a peroxide black-filled NR vulcanizates, it is necessary to maintain stress giving the molecular orientation in order for the crack to propagate in the direction of molecular orientation because the low set obtained from these vulcanizates is not adequate to retain the anisotropy after pre-stressing.

9.4 Effects of pre-stressing on equilibrium swelling and permanent set

The ease with which crosslinks can be broken when highly stressed and the ability of the broken crosslinks to recombine to form a second network whilst in the deformed state is greatly affected by the nature of the crosslinks (38,39,40). In black-filled vulcanizate, it appears that both the ease of breakage and the efficiency of recombination to form a second network are important factors contributing to the strength anisotropy which is necessary for the occurrence of knotty tearing. Equilibrium swelling and permanent set measurements were carried out on black-filled (50 pphr HAF) NR vulcanizates prepared using conventional, soluble EV and the peroxide vulcanizing systems. This investigation was approached in the way described by Thomas (38) and Brown, Porter and Thomas (39), for the unfilled NR system. The details of the experiments are discussed in Section 8.5 in Chapter Eight.

The results are given in Table 9.4 for the sulphur conventional system (black-filled NR), Table 9.5 for the sulphur conventional system (unfilled NR) and Table 9.6 for the soluble EV system (black-filled NR). The set after 24 hours refers to the residual extension which remained after a sample of rubber has been stretched for 1 minute to an extension ratio, λ, then released and allowed to recover for 24 hours. The permanent set refers to the residual extension which remained after a sample of rubber has been stretched for 1 minute to an extension ratio, λ, then released and allowed to recover by swelling, deswelling and drying to a constant weight. The set (24 hrs) is higher than the permanent (actual) set because the measured value of set (24 hrs) is a combination of both plastic flow and high-elastic deformation which has not completely recovered (83). In the present case, the permanent set is considered since it is this which reflects the two-networks formed during pre-stressing. $\Delta\upsilon_r$ denotes the difference between the volume fraction of rubber in a swollen vulcanizate after pre-stressing and the volume fraction of rubber in the swollen vulcanizate before pre-stressing (the unstressed control samples). The results obtained were expressed as a percentage of the volume fraction of rubber in swollen vulcanizate before pre-stressing, defined by equation 9.1.

$$\Delta\upsilon_r\ (\%) = \frac{\nu_r - \nu_{r,c}}{\nu_{r,c}} \times 100 \qquad 9.1$$

where υ_r is the volume fraction of rubber in the swollen vulcanizate after pre-stressing, and υ_{rc} is the volume fraction of rubber in the swollen vulcanizate before pre-stressing (unstressed control samples).

Figure 9.6a shows some interesting changes in the equilibrium swelling after the samples were pre-stressed. The plots were based on the data shown in Tables 9.4, 9.5, and 9.6. The changes in volume fraction of rubber in swollen samples, $\Delta\upsilon_r$ (%), are plotted against the nominal stress, σ, applied. The results show a marked difference in the $\Delta\upsilon_r$-σ relationship for vulcanizates produced by the conventional systems (both unfilled and filled) compared with the $\Delta\upsilon_r$-σ relationships for vulcanizates produced by the soluble EV and peroxide systems.

The soluble EV and peroxide vulcanizates show negative values

Table 9.4: Proportions of network breakdown (n_1/N) and recombination efficiency (n_2/n_1) as a functions of stress. Black-filled (50 pphr HAF) conventional NR vulcanizates. Full formulations shown in Table 4.4a for mix A6 in Chapter Four.

Stress (MPa)	6.4	9.67	12.73	16.4	19.6	22.42
λ	3	3.5	4.0	4.5	5	5.5
Set (24hrs)(%)	3.5	8	13	19.9	25.5	34.2
Permanent Set (%)	2.0	4	7.5	12.5	17.5	24
υ_r	0.3376	0.3425	0.3492	0.3596	0.3679	0.3808
$\Delta\upsilon_r$	-0.0088	-0.0039	0.0028	0.0132	0.0215	0.0344
$\Delta\upsilon_r$ (%)	-2.5	-1.1	0.81	3.81	6.21	9.93
n_1/N (%)	6.8	10.36	11.71	13.47	17.76	18.50
n_2/n_1 (%)	14.16	32.22	46.91	64.24	73.05	81.62

$\upsilon_{r,c}$ for unstressed control samples 0.3464.

Footnote:

$\frac{n_1}{N}$ and $\frac{n_2}{n_1}$ denote % of crosslinks broken and recombination efficiency (see Section 9.5).

$$\Delta\upsilon_r = \upsilon_r - \upsilon_{rc}$$

$$\Delta\upsilon_r\ (\%) = \frac{\nu_r - \nu_{r,c}}{\nu_{r,c}} \times 100$$

where υ_r is the volume fraction of rubber in the swollen vulcanizate for pre-stressed samples, υ_{rc} is the volume fraction of rubber in swollen vulcanizate for unstressed control samples.

The footnote above is also applicable to Tables 9.5 and 9.6.

Table 9.5: Proportions of network breakdown (n_1/N) and recombination efficiency (n_2/n_1) as a functions of stress. NR unfilled conventional vulcanizates. Base mix formulations shown in Table 4.2. Curatives sulphur 2.5 and MBS 0.5.

Stress (MPa)	5	10	13	16	19	22
λ	5.8	6.7	7.1	7.4	7.7	8.0
Set (24hrs)(%)	3.0	6.0	9.6	11.1	13.1	16.2
Permanent set (%)	1.3	4.8	7.0	8.5	12.1	15.6
υ_r	0.3006	0.3054	0.3100	0.3124	0.3170	0.3235
$\Delta\upsilon_r$	-0.0018	0.0030	0.0076	0.0100	0.0146	0.0211
$\Delta\upsilon_r$	-0.6	1.0	2.5	3.3	4.8	7.0
n_1/N (%)	6.85	9.15	9.65	9.9	11.03	11.65
n_2/n_1 (%)	20.39	28.86	37.11	40.4	43.6	45.5

$\upsilon_{r,c}$ for unstressed control samples is 0.3024.

Table 9.6: Proportions of network breakdown (n_1/N) and recombination efficiency (n_2/n_1) as a functions of stress. NR black-filled soluble EV vulcanizates. Full formulations shown in Table 4.4b in Chapter Four.

σ (MPa)	6	12	15	17	20	22	26
λ	2.55	3.4	3.8	4.1	4.45	4.7	5.2
Set 24hr (%)	2.0	4.1	5.53	7.58	9.0	11.11	13.64
Permanent Set (%)	0	1.51	2.02	3.66	5.36	5.94	8.29
υ_r	0.3337	0.3300	0.3306	0.3307	0.3334	0.3330	0.3358
$\Delta\upsilon_r$	-0.0012	-0.0158	-0.0152	-0.0151	-0.0124	-0.0128	-0.0100
$\Delta\upsilon_r$ (%)	-3.5	-4.6	-4.4	-4.4	-3.6	-3.7	-2.9
n_1/N (%)	9.0	14.05	15.3	17.2	18.4	21.0	22.4
n_2/n_1(%)	2.8	8.3	11.0	13.2	17.1	18.0	19.2

$\upsilon_{r,c}$ for unstressed control samples 0.3458

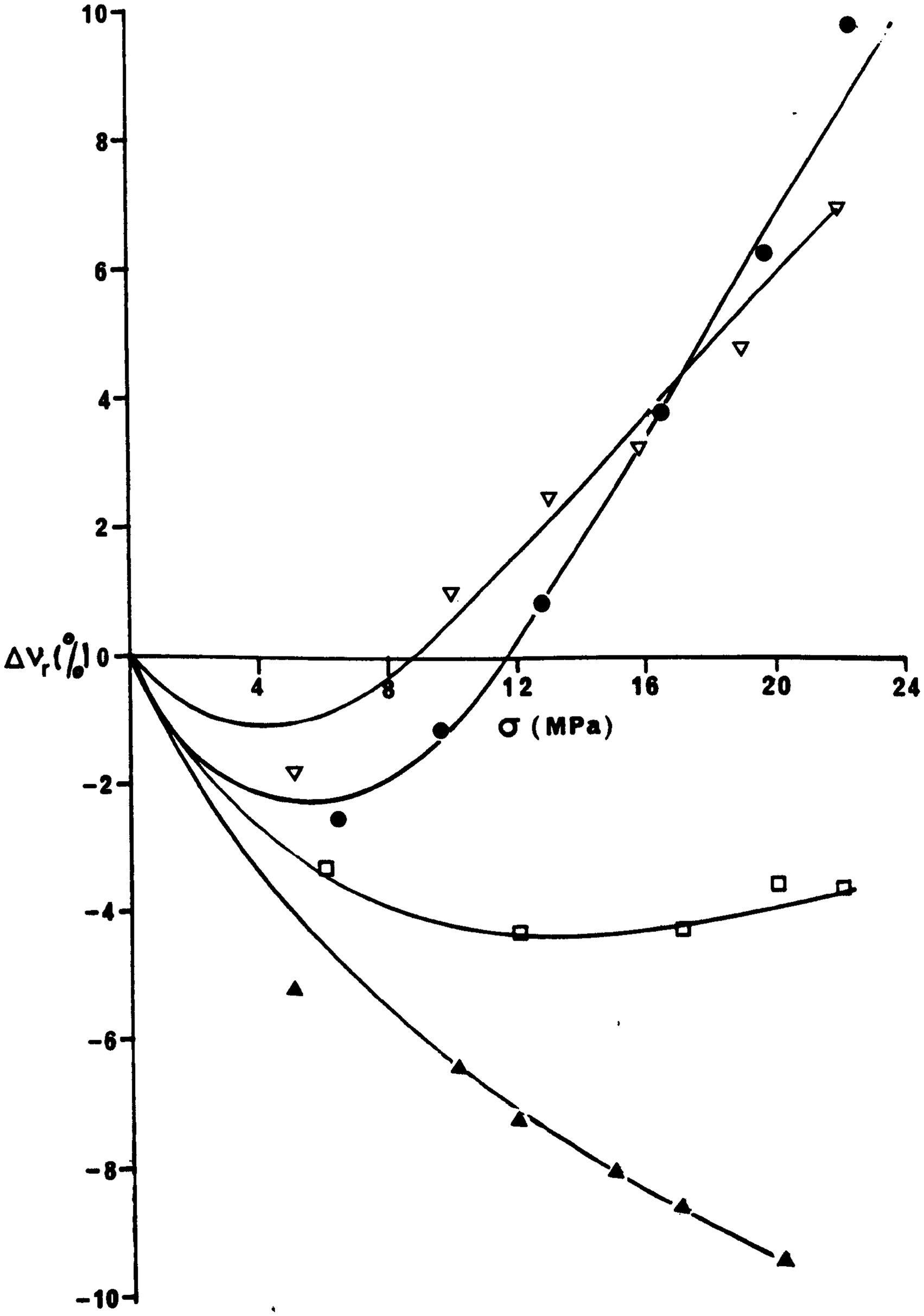

Figure 9.6a: Effect of stress, σ, upon % change in volume fraction, ΔV_r, of rubber in swollen vulcanizate with stress. ▽ Unfilled conventional NR vulcanizate (S-2.5pphr, MBS-0.5pphr), ● black-filled conventional NR vulcanizate (mix A6 shown in Table 4.4a), □ black-filled soluble EV NR vulcanizate (Table 4.4b), and ▲ black-filled peroxide NR vulcanizate (mix C3 shown in Table 4.4c

of $\Delta\upsilon_r$ over the whole range of stress applied. The observations here are consistent with those of Thomas (38) and of Brown, Porter and Thomas (39) for unfilled NR vulcanizates. These negative values of imply that the volume fraction of rubber in the swollen samples after pre-stressing was lower than the volume fraction of rubber in the swollen samples before pre-stressing (i.e., in the unstressed control samples). This is of course to be expected, because, when crosslinks are broken, the crosslink concentration remaining in the network will be less, and so the swelling of the network will be greater. The higher the stress level, the more crosslinks are broken and the lower the volume fraction of rubber in the swollen samples.

In contrast, both unfilled and black-filled conventional vulcanizates show an increase in $\Delta\upsilon_r$ at stresses greater than 12 MPa, i.e., the volume fraction of rubber in the swollen samples after pre-stressing was higher than the volume fraction of rubber in swollen samples before pre-stressing (i.e., in the unstressed control samples). An increase in volume fraction of rubber in the swollen samples indicates an increase in the number of crosslinks in the network. Before attempting to put forward any suggestion to explain this behaviour, it will be helpful first to consider the results shown in Figure 9.6b, where the permanent set is plotted against the stress. Both the unfilled and black-filled conventional vulcanizates produced higher set than did the soluble EV and the peroxide vulcanizates. For example, at 20 MPa, the set produced by unfilled conventional vulcanizates was about 4 times higher than the set produced by the peroxide black-filled vulcanizates. The set observed in the unfilled conventional NR vulcanizates was of the same order of magnitude to that observed by Thomas (38) and by Brown, Porter and Thomas (39). Apparently, a black-filled NR conventional vulcanizate showed an increase in set by about 19% when compared with the corresponding unfilled conventional vulcanizate. It is not clear whether this increase is attributable to interaction at the interface between the rubber matrix and the carbon black particles associated with the surface chemistry of the carbon black particles, or to some other unknown mechanisms. It was beyond the scope of the present work to investigate the nature of the linkages forming at the interface between the carbon black particles and the rubber matrix.

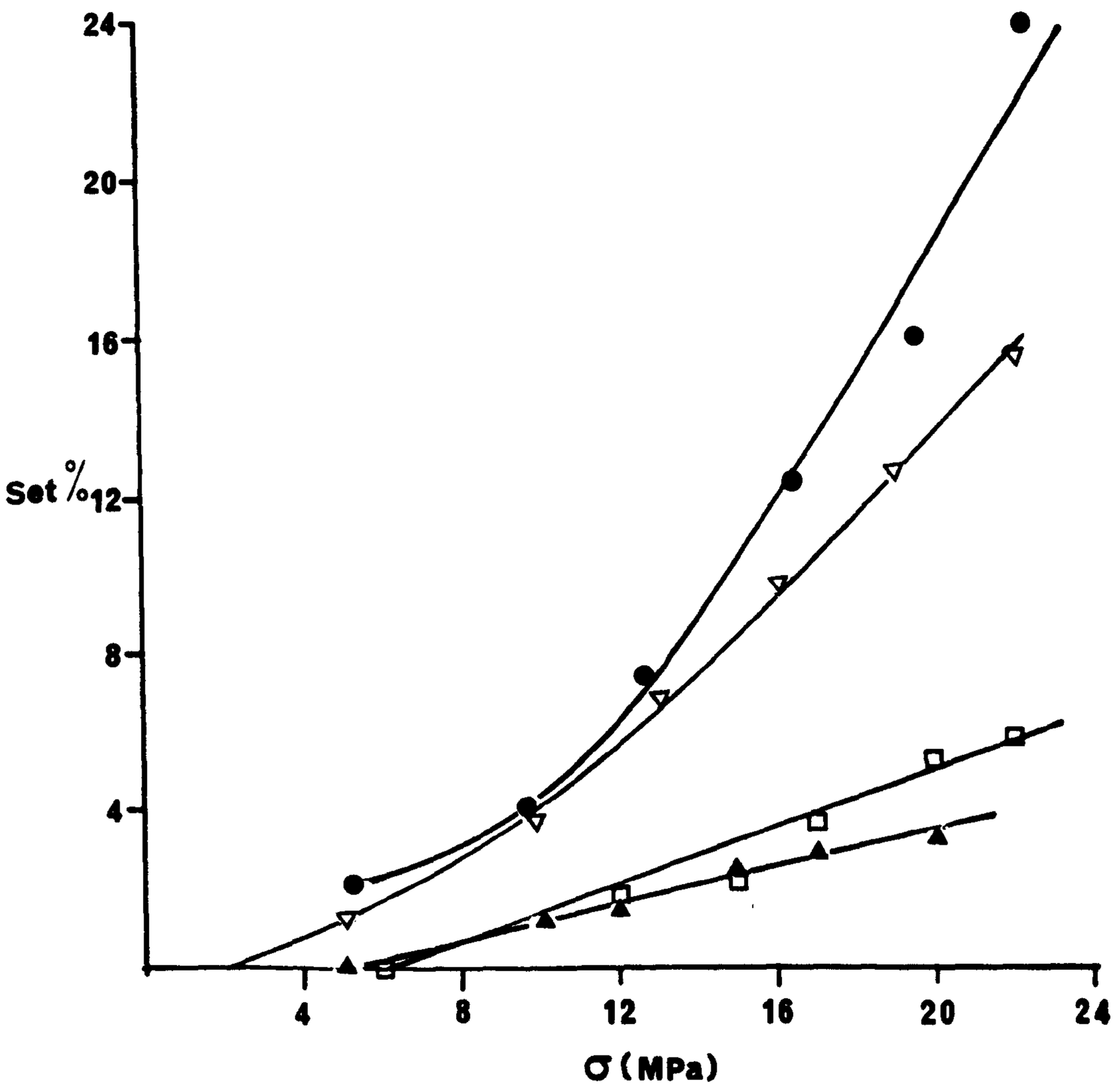

Figure 9.6b: Permanent set vs. stress, σ

▽ Unfilled conventional system (NR)

● Black-filled conventional system (NR+50 HAF)

□ Black-filled soluble EV system (NR+50 HAF)

▲ Black-filled peroxide system (NR+50 HAF)

See figure 9.6a for details of vulcanizate formulations.

Mullins (83) has made a comparative studies between the set of unfilled and black-filled (50 pphr MPC) NR conventional vulcanizates (S 3pphr, MBT 0.8pphr). Both unfilled and black-filled samples were extended to 200% extension at 20°C, for different periods ranging from 15 minutes to 7 days. Mullins (83) then measured the set remaining after 24 hours recovery at 120°C. He made some interesting observations. He observed that the set in black-filled vulcanizate was always higher than the set in the corresponding unfilled vulcanizate. The set increased with increasing period of extension. The rate of recovery of the unfilled vulcanizate was more rapid than that of the black-filled vulcanizate. According to Mullins (83), the difference between the set of a black-filled and an unfilled vulcanizate is attributed to the orientation of anisotropic filler particles or of chains of filler particles in the direction of stretch.

It was of interest to see if there was any correlation between $\Delta\upsilon_r$ and the permanent set. $\Delta\upsilon_r$ was plotted against permanent set for the conventional sulphur vulcanizates (unfilled and black-filled), soluble EV and the peroxide vulcanizates. The results are shown in Figure 9.7. For both unfilled and black-filled conventional vulcanizates $\Delta\upsilon_r$ increases linearly with increasing set. Since the set indicates the existence of two-networks in the pre-stressed vulcanizate, the increase in the volume fraction of the rubber in the swollen vulcanizate after pre-stressing may be associated with the two-networks formed during pre-stressing. In the case of soluble EV vulcanizate, between the range of 0% to 2% set there was an initial decrease of $\Delta\upsilon_r$ with set. Between the range of 2% to 8% set, $\Delta\upsilon_r$ increases with set. In the case of peroxide vulcanizate, $\Delta\upsilon_r$ decreases with increasing set. Thus it appears that like tearing energy, the volume fraction of the rubber in the swollen pre-stressed vulcanizate is also affected by the set.

9.5 Effects of large stresses on chain scissions and recombination of crosslinks

In order to interprete the changes in equilibrium swelling and the permanent set after pre-stressing, Thomas (38) and more recently

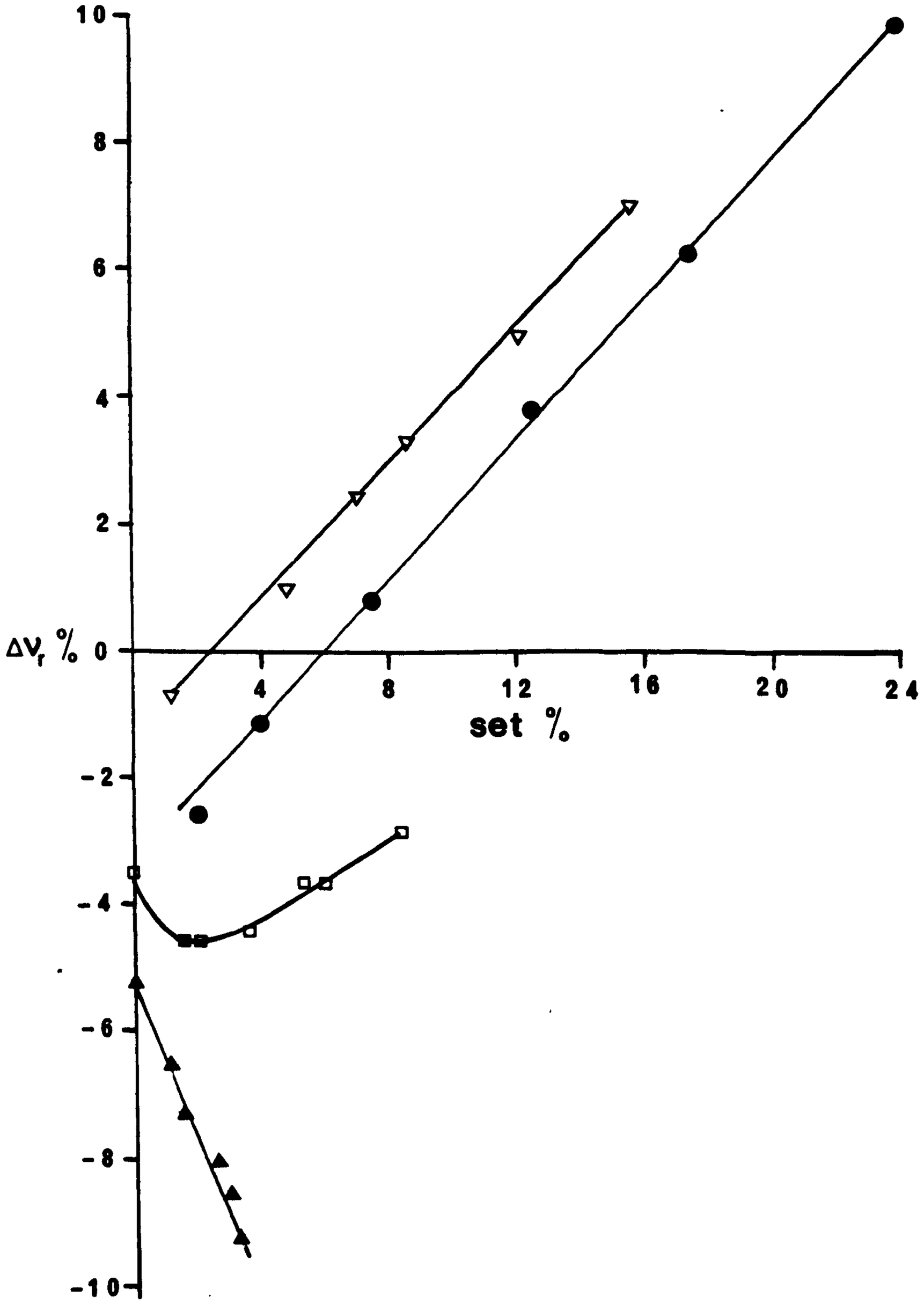

Figure 9.7: Δv_r vs permanent set (%), showing the relationship between percentage change in volume fraction of rubber in a swollen vulcanizate with permanent set for conventional sulphur unfilled (▽), black-filled (●) NR vulcanizate, and black-filled soluble EV (□), and black-filled peroxide (▲) NR vulcanizates. (▽) sulphur 2.5 pphr, MBS 0.5 pphr, base mix formulations as shown in Table 4.2. (●) mix A6 as shown in Table 4.4a, (□) as shown in Table 4.4b, (▲) mix C3 as shown in Table 4.4c. All black-filled vulcanizates contained 50 pphr HAF.

Brown, Porter and Thomas (39) have used the two-network theory of Green and Tobolsky (84) suitably modified to give the changes in equilibrium swelling (85). The application of such a theory gives a quantitative measure of the proportion of crosslinks which break and recombine under the influence of the applied stress. Suppose that there are initially N crosslinks per unit volume of rubber, and that on pre-stressing to an extension ratio λ, n_1 crosslinks break. Suppose also that, of these n_1 which break, n_2 recombine. Then the number of crosslinks which have broken, B, is

$$B = 1 - \frac{n_1}{N} \qquad (9.2)$$

Thomas (38), has shown that B is related to volume fraction of rubber in a swollen vulcanizate before and after pre-stressing and to the set by the relationship shown in equation 9.3.

$$B = \left(\frac{v_{r,c}}{v_r}\right)^{\frac{1}{3}} \left(\frac{\ln(1-v_r) + v_r + \psi v_r^2}{\ln(1-v_{r,c}) + v_{r,c} + \psi v_{r,c}^2}\right) \left[(1+\alpha\lambda)^2 \left(1+\frac{\alpha}{\lambda^2}\right)\right]^{-\frac{1}{3}} \qquad (9.3)$$

where $v_{r,c}$ is the volume fraction of rubber in the swollen unstressed vulcanizate, v_r is the volume fraction of rubber in the swollen pre-stressed vulcanizate. Ψ is the rubber-solvent interaction parameter, λ is the applied extension ratio and α is defined by equation 9.4.

$$\alpha = \frac{\lambda_d^3 - 1}{\lambda - \lambda_d^3 \lambda^{-2}} \qquad (9.4)$$

where λ_d-1 is the permanent set. According to Thomas (38) and Berry et al (85), equations 9.3 and 9.4 relate changes in modulus on bond formation in the stretched state to degree of crosslinking and to extension. According to Berry et al (85), in a two-network vulcanizate, the resultant network is considered to be equivalent to two interpenetrating networks, one unstrained at the original length and the other at the stretched length. The permanent set arises from the balancing of the retractive force of the first network and the extensive force of the second. Equations 9.3 and 9.4 were derived by Berry et al (85) by assuming that the bonds introduced did not contribute to the tension. In otherwords the chain segments in both networks are Gaussian so that the free-energy of deformation for the composite network is isotropic.

Also the recombination efficiency, RE, which is defined as the proportion of broken crosslinks recombine, is given by

$$RE = \frac{n_2}{n_1} = \frac{\alpha B}{1-B} \qquad (9.5)$$

The above theory has been applied successfully to account for the changes in the network during deformation occurring in unfilled vulcanizates. As far as the author is aware, the theory has not previously been applied to black-filled vulcanizates. In this present investigation, it is assumed that the theory is also applicable to black-filled vulcanizates.

The plots in Figure 9.8 show the dependence of the percentage of crosslinks broken (n_1/N) and the recombination efficiency (n_2/n_1), on tensile stress. The main point to note is that, there is no net gain in crosslinks resulting from pre-stressing in any of the vulcanizates produced by the three vulcanizing systems investigated. The recombination efficiencies are always below 100%. This observation accords with the findings of Thomas (38) and Brown, Porter and Thomas (39) for unfilled NR vulcanizates. Thus the increase in $\Delta\upsilon_r$ with increasing tensile stress observed in conventional vulcanizates for both unfilled and black-filled vulcanizates is not associated with a gain in crosslink concentration as might be suggested. The increase in $\Delta\upsilon_r$ may be attributable to some crosslink formation which occurs in the stressed state. The results in Figures 9.8 a and b show some evidence that crosslinks which have been broken by large mechanical deformation can recombine to form a second network whilst in the stressed state. Both the soluble EV and the peroxide vulcanizates showed low recombination efficiencies. In contrast, conventional vulcanizates showed high recombination efficiencies. For example, at a tensile stress of 22 MPa, about 18% of the crosslinks in the initial network of a conventional vulcanizate were broken, and of these 18% broken links about 80% recombined to form a second network. In contrast, in the case of the soluble EV vulcanizate, only 18% out of the 21% links which broke recombined. Thus in the conventional vulcanizate the recombination process was about 4 times more efficient than in the soluble EV vulcanizate.

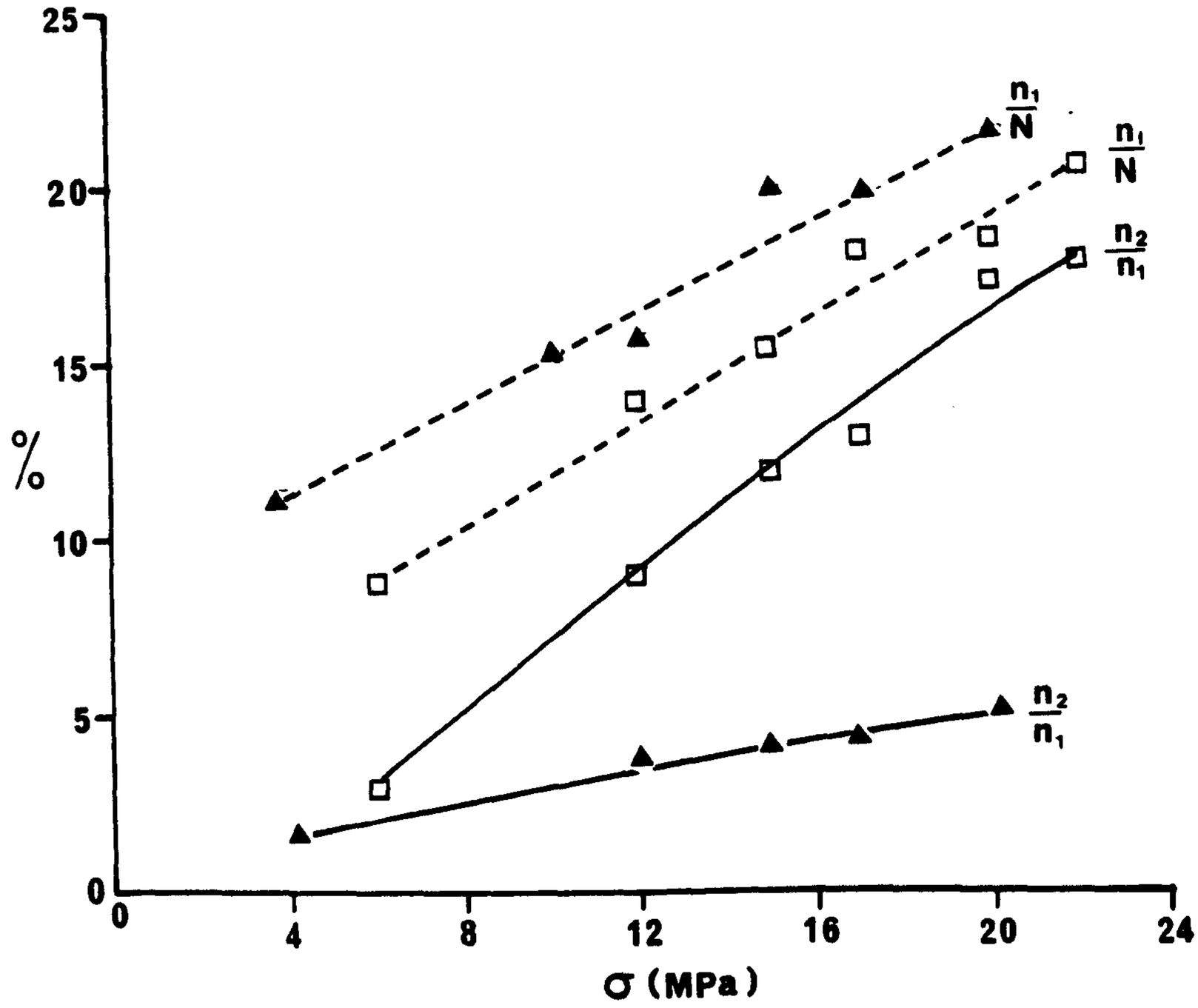

Figure 9.8a: Dependence of percentage of crosslinks broken, $\frac{n_1}{N}$, and recombination efficiency, $\frac{n_2}{n_1}$, on stress, σ, for black-filled (50 HAF) vulcanizates produced by soluble EV (□) shown in Table 4.4b and peroxide (▲) mix C3 shown in Table 4.4c.

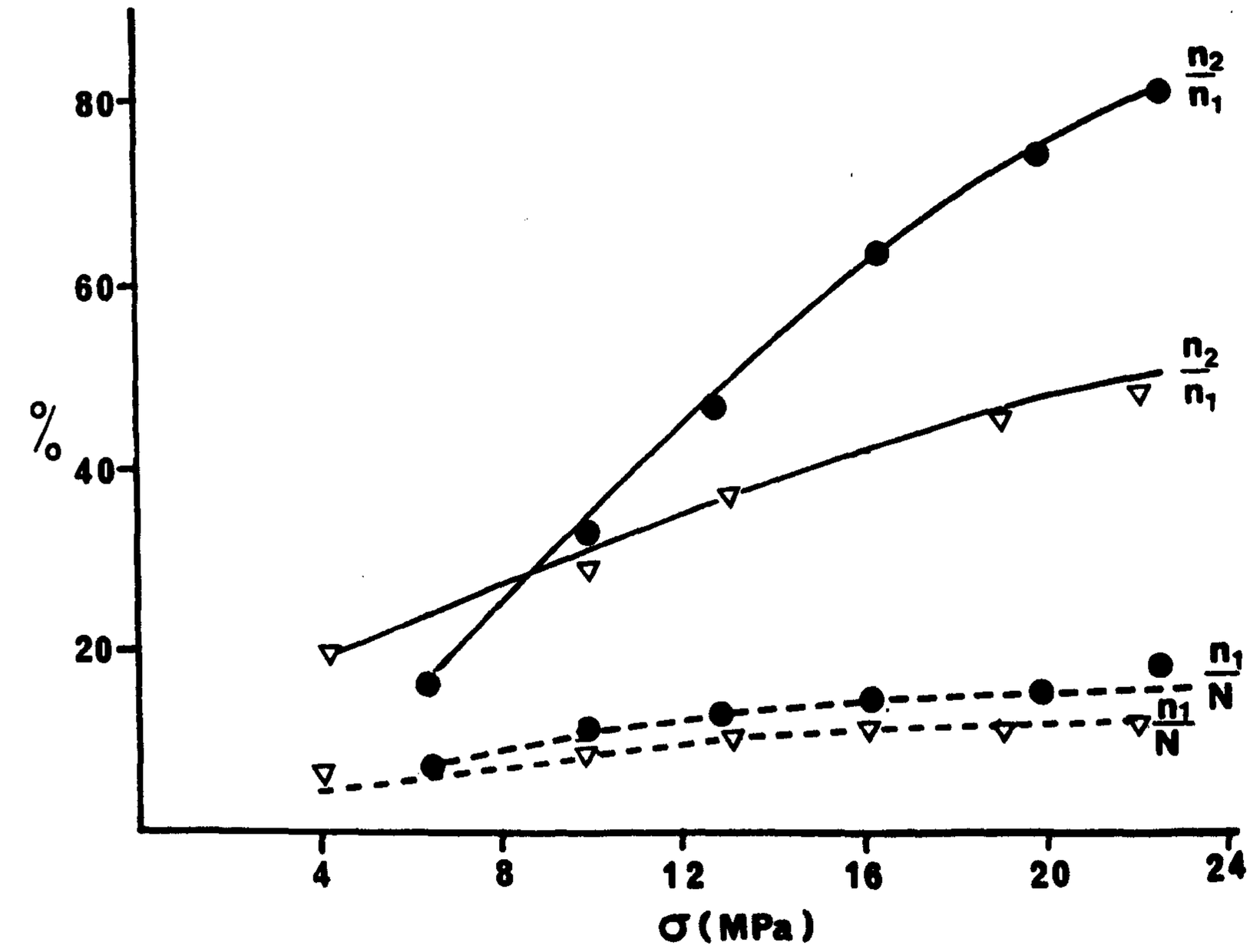

Figure 9.8b: Dependence of percentage of crosslinks broken, $\frac{n_1}{N}$, and recombination efficiency, $\frac{n_2}{n_1}$, on stress, σ, for unfilled (▽) and black-filled ● NR vulcanizates produced by conventional system for mix A6 shown in Table 4.4a.

Figure 9.9 shows a correlation between $\Delta\upsilon_r$ and the recombination efficciency n_2/n_1 for the conventional sulphur vulcanizates, soluble EV and the peroxide vulcanizates. Both unfilled and black-filled conventional sulphur vulcanizates showed an increase in $\Delta\upsilon_r$ as the recombination efficiency increased. In contrast, the soluble EV and peroxide vulcanizates showed a decrease of $\Delta\upsilon_r$. The results shown in Figure 9.9 are reminiscent of the results shown in Figure 9.7. It is evident that from the results that the increase in $\Delta\upsilon_r$ with increasing tensile stress observed only in conventional sulphur vulcanizates is a consequence of the effect of the two networks present in the final material.

Figure 9.10 shows the relation between the permanent set and the recombination efficiency n_2/n_1. It is evident that the set increases progressively as the recombination efficiency increases. The substantial difference in permanent set between conventional and both soluble EV and peroxide vulcanizates is also attributed to the presence of the two networks in the conventional vulcanizate after pre-stressing. Comparing the unfilled and the black-filled vulcanizates, the latter appears to show 60% increase in recombination efficiency. It is not clear whether this increase is associated with recombination of the two broken crosslinks or attachment of the broken croslinks to the carbon black particles, or both. It is known that the rubber can adhere to the surface of filler particles either by physical adsorption or through the formation of rubber-filler bonds that lead to the phenomenon of 'bound rubber'. Partial insolubilization of polymer due to adsorption of macromolecules on carbon black particles is commonly known as 'bound rubber' (8,10). It was beyond the scope of the present investigation to investigate this problem. Whatever the processes that might have occurred, the increase in the recombination efficiency parallels the observed higher permanent set observed in the black-filled vulcanizates as compared with unfilled vulcanizates.

Figures 9.8a and b, show that the proportion of crosslinks broken (n_1/N) and the recombination efficiency (n_2/n_1) increase with increasing stress. n_2/n_1 was plotted against

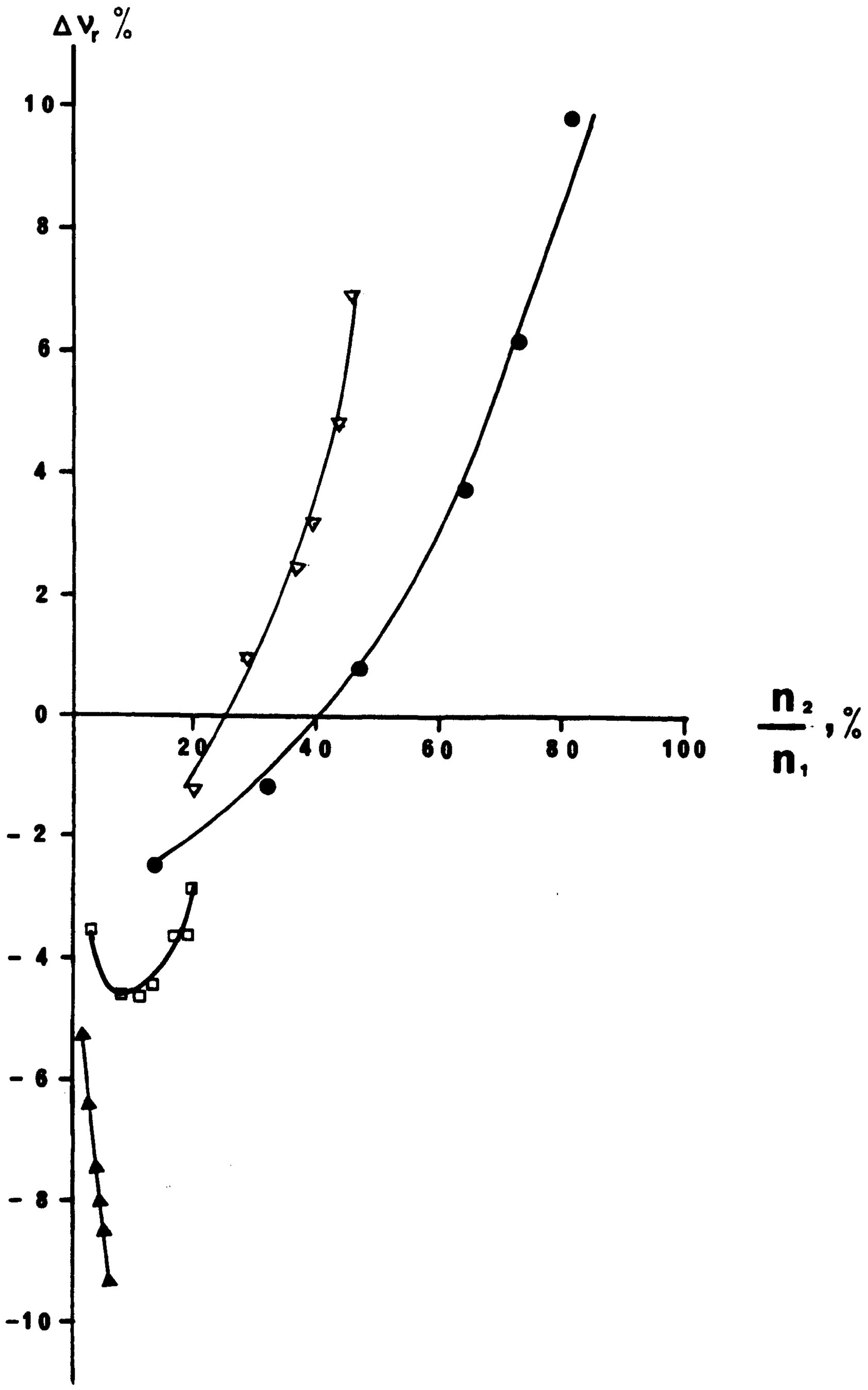

Figure 9.9: Δv_r % vs $\frac{n_2}{n_1}$ (%), showing the correlation between percentage change in volume fraction of rubber in a swollen vulcanizate with recombination efficiency. ▽ Conventional (unfilled) ● Conventional (black-filled) □ Soluble EV (black-filled) ▲ Peroxide (black-filled). Formulations as stated in Figures 9.8a and 9.8b.

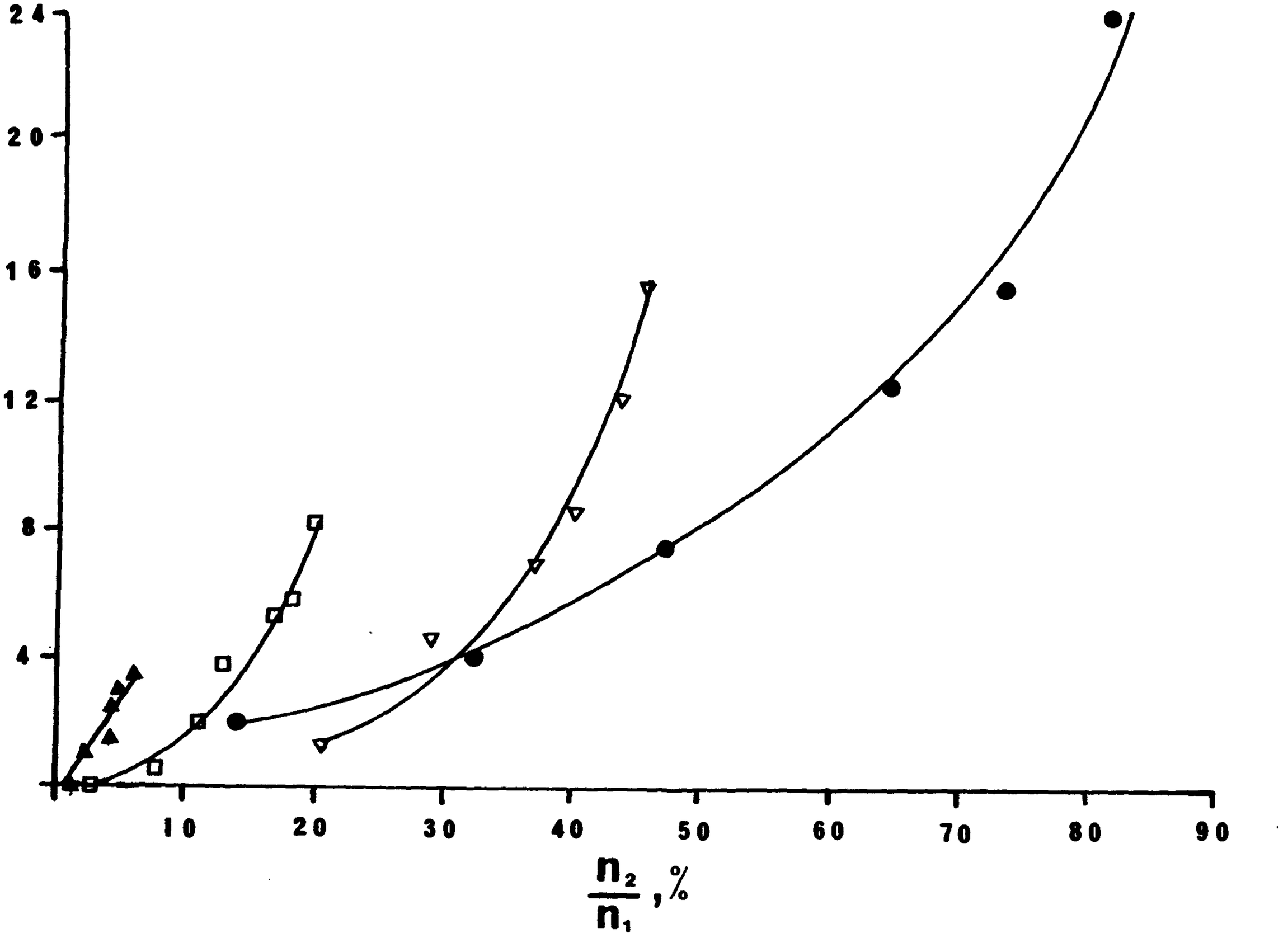

Figure 9.10: Correlation between permanent set and recombination efficiency, $\frac{n_2}{n_1}$, of unfilled conventional (▽), black-filled conventional (●), black-filled soluble EV (□) and black-filled peroxide (▲) NR vulcanizates. See Figure 9.8 for details of formulations.

n_1/N to show a correlation between n_2/n_1 and n_1/N for a particular stress. The results are shown in Figure 9.11. The results show a more-or-less linear relationship between n_2/n_1 and n_1/N for each vulcanizate used in this investigation. The percentage of crosslinks which break increases with increasing stress. The recombination efficiency for the conventional vulcanizates is always higher than that of soluble EV and peroxide vulcanizates. The results are again in accord with those of Brown, Porter and Thomas (39) for the unfilled NR vulcanizates.

9.6 Effects of pre-stressing on ENRs and SBR

The rubbers were all filled with 50 pphr of HAF black and a conventional sulphur vulcanization system was used. They were pre-stressed to 22 MPa for one minute and allowed to relax for 24 hours before swelling in toluene for three days. Then they were deswelled and dried down to constant weight before carrying out the tear test. The results are shown in Table 9.7. It is observed that the permanent set increased and that the tearing energy decreased with increasing degree of strain-crystallizability of the rubber. The results here agree with those obtained from split tear tests, where the stress giving the orientation was maintained during the test. This clearly shows that, whether the stress giving the orientation was maintained during the test or not, the rubber which strain crystallizes the most will give the highest strength anisotropy. However, the anisotropy after pre-stressing is associated with the set, and the question arises how does strain-crystallizability affect tearing?

A suggestion is now put forward in an attempt to explain this. When a strain-crystallizing rubber is highly pre-stressed, the crystals formed may produce stress amplification, thus giving sufficiently high stresses in the amorphous rubber near to them to produce crosslink failure. The higher the degree of crystallinity, the more these crystals form in the bulk of the rubber and the more likely that the crystallinity will increase the number of crosslink failures. However, the set is controlled by the recombination efficiency of the broken crosslinks. It seems likely that the higher the proportion of crosslinks broken, the higher the probability that two active ends will meet and recombine. This

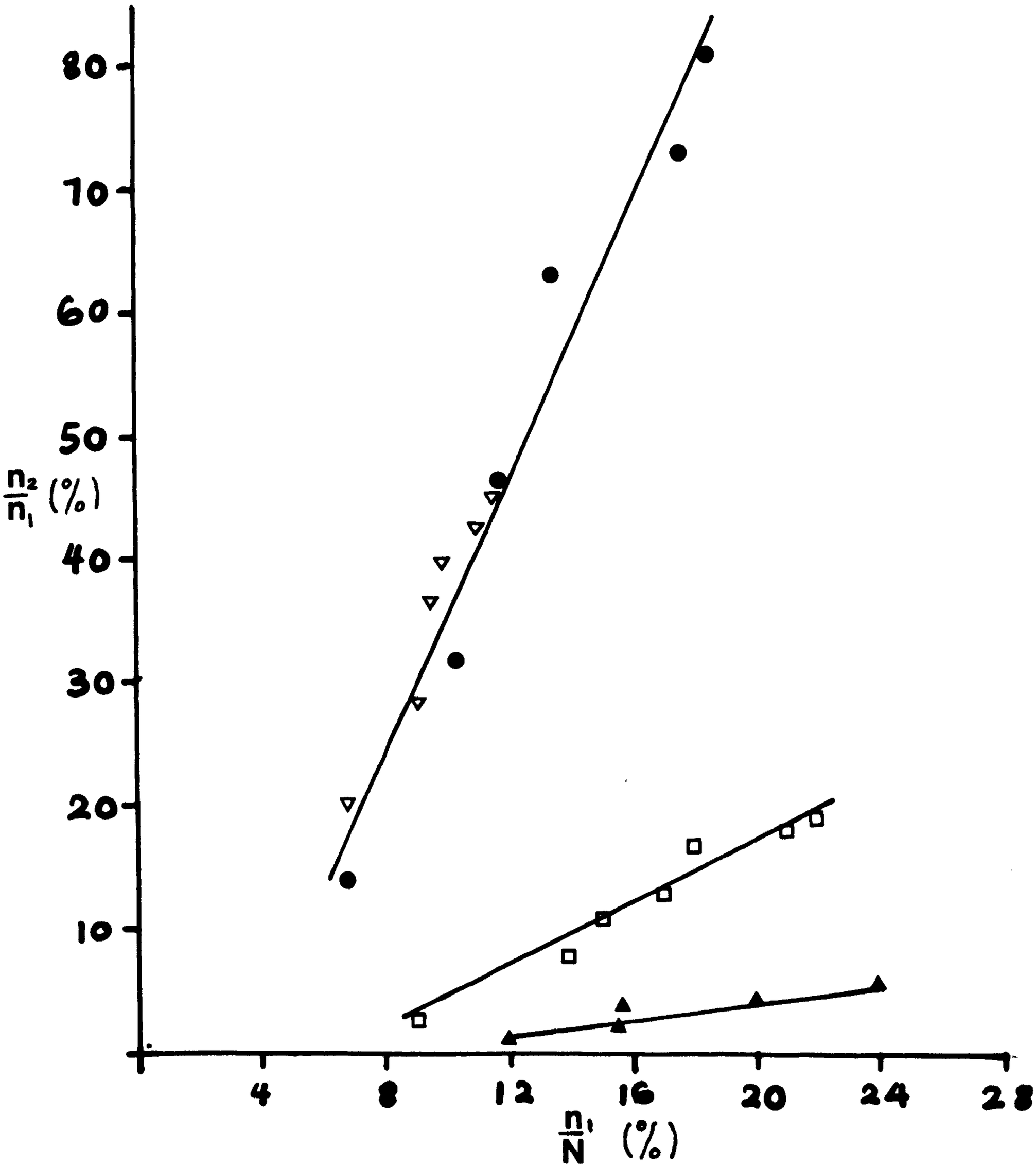

Figure 9.11: Correlation between recombination efficiency, $\frac{n_2}{n_1}$, and percentage of broken crosslink, $\frac{n_1}{N}$, for unfilled conventional (▽) and black-filled (●) NR vulcanizates, black-filled soluble EV (□) and peroxide (▲) NR vulcanizates. All black-filled contain 50 pphr HAF See Figures 9.8a and 9.8b for details of formulation.

Table 9.7: Effect of strain-crystallization on permanent set

Rubber	NR	ENR-25	ENR-50	SBR
Set (%)	24	17	12.4	5.2
T (kJ m^{-2})	2.33	3.25	7.66	12.97
*°crystallization	11	11	10	0
Types of tear	s	s	s.s	s+s.s

* Data obtained from reference number 50

All rubbers contained 50 pphr of HAF black. Conventional cure system (S 2.5 MBS 0.5) was used in each case, using the base mix formulations shown in Table 4.2 in Chapter Four. All the samples were pre-stressed to 22 MPa. Samples were swollen, deswelled and dried to a constant weight. Tearing measurements were carried out at a rate of 830 μm s^{-1} at 23°C in the direction of the extension previously applied.

s - steady tearing

s.s - stick-slip

suggestion is consistent with the experimental observations shown earlier in Figures 9.8 and 9.11, where both the fractions of crosslinks broken (n_1/N) and the recombination efficiency (n_2/n_1) increased with increasing pre-stressing level. Figure 9.12 provides convincing evidence on the effect of strain crystallization on n_1/N and n_2/n_1. Below 12 MPa, the proportions of crosslinks broken did not differ greatly between strain-crystallizing NR vulcanizates and non-strain- crystallizing SBR vulcanizates. Above 12 MPa, where crystallization became pronounced, the NR vulcanizates showed higher proportions crosslink breakage than did the SBR vulcanizates. By raising the pre-stress level from 12 MPa to 22 MPa, the proportion of crosslink breakage increased by 50% in the NR vulcanizates, whereas in the SBR vulcanizates it increased by about 5% only. Infact, the proportion of crosslink breakage in black-filled SBR vulcanizates at a stress level of 22 MPa was similar to that observed in unfilled NR vulcanizates as shown earlier in Figure 9.8b. It appears as if the effect of stress amplification produced by the crystals in unfilled NR was equivalent to the stress amplification produced by 50pphr HAF in SBR vulcanizates. This gives a strong indication that the crystals provide a substantial stress amplication, and also that the crystals themselves act as reinforcing fillers. Figure 9.13 shows an almost linear relation between the proportion of crosslink which break, n_1/N, and the recombination efficiency n_2/n_1 which is consistent with the results shown in Figure 9.11. In summary, it can be said that tearing energy after pre-stressing decreased with increasing order of degree of strain-crystallizability of the rubber. This appears to be attributable to stress amplification produced by the crystals causing substantial proportions of the crosslinks to break. The increased proportion of crosslink breakage increases the recombination efficiency, leading to high permanent set, and hence to anisotropy retained after pre-stressing. The findings from the present investigation are consistent with the observation of Gent and Kim (47) who did not find a significant effect of prestretching in non-strain-crystallizing black-filled SBR

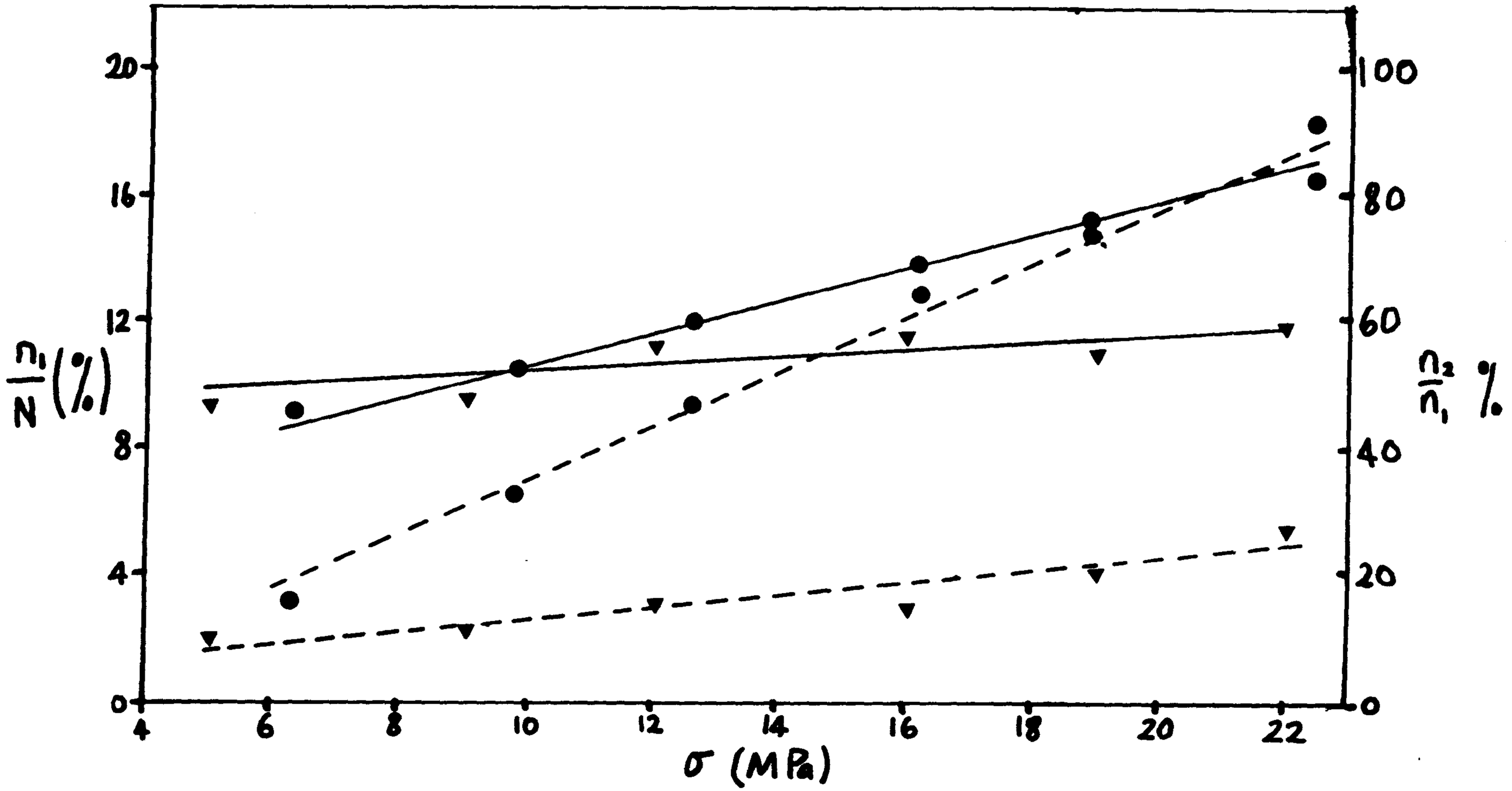

Figure 9.12: Plot of $\frac{n_1}{N}$ and $\frac{n_2}{n_1}$ against tensile stress, σ, of black-filled 50 HAF conventional NR (●) and SBR (▼) vulcanizates. Base mix formulations as shown in Table 4.2, curatives: sulphur 2.5 pphr and MBS 0.5 pphr Full line denotes % of chains broken ($\frac{n_1}{N}$) and broken lines denote recombination efficiency ($\frac{n_2}{n_1}$).

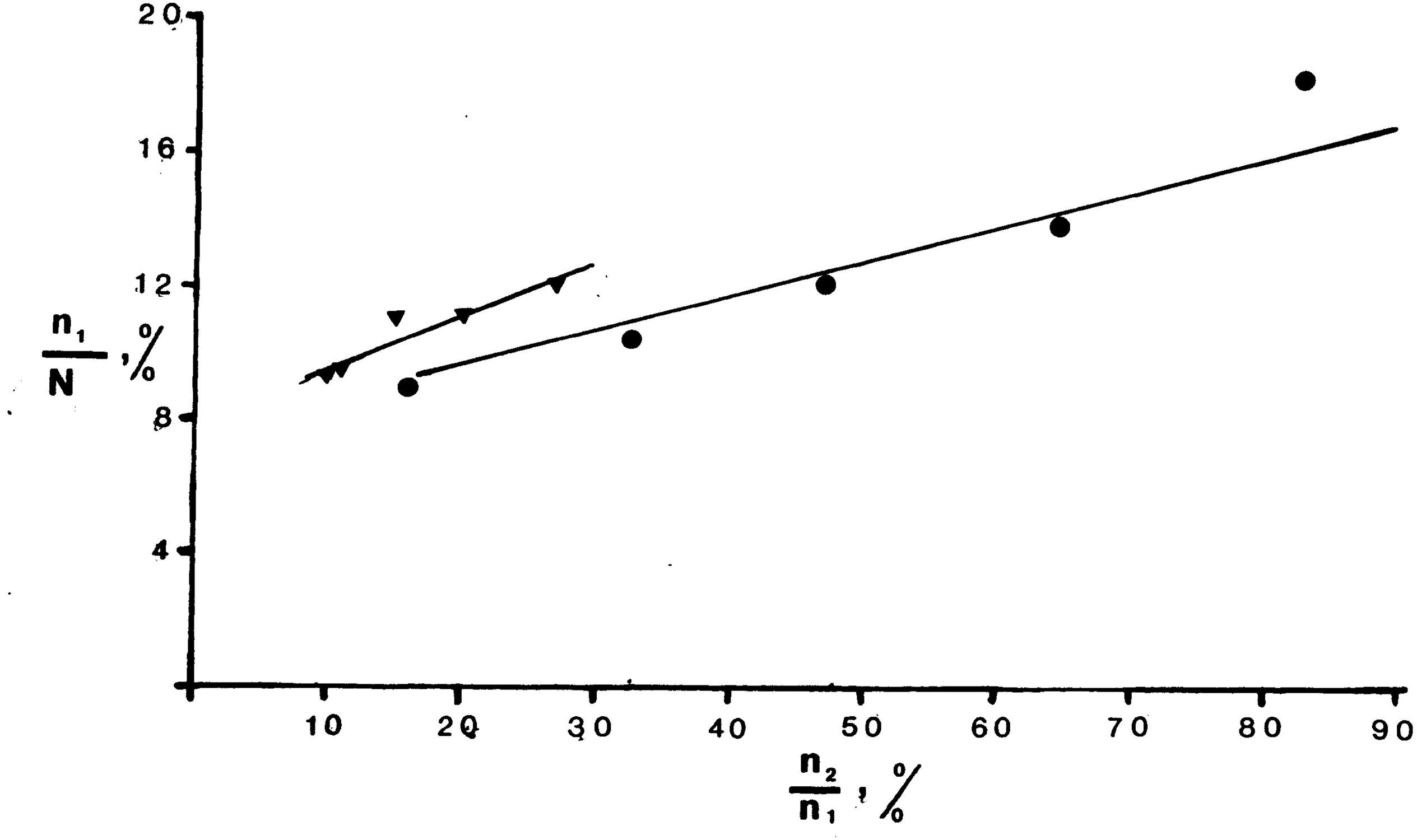

Figure 9.13: Correlation between percentage of crosslinks broken, $\frac{n_1}{N}$, and recombination efficiency, $\frac{n_2}{n_1}$, for black-filled conventional NR (●) and SBR (▼) vulcanizates. See Figure 9.12 for details of of formulations.

vulcanizates, but only in strain-crystallizing black-filled NR vulcanizates.

9.7 Effects of di-n-butyl tetrasulphide (DBTS) on permanent set and tearing energy

When polysulphidic crosslinks are broken, sulphenyl radical groups are likely to be generated at the broken ends (39). These active radicals may recombine to form a second network. The incorporation of di-n-butyl tetrasulphide (DBTS) will interfere with the recombination process, probably by scavenging these radicals and thus terminating their activity. Thomas (38) and more recently Brown, Porter and Thomas (39), have shown that the incorporation of DBTS into the polysulphidic crosslink network reduces both the recombination efficiency and the permanent set. The results so far suggest that the set (strictly speaking the formation of a second network) plays a part in contributing to the strength anisotropy which promotes knotty tearing. DBTS was incorporated into a black-filled polysulphidic crosslinked NR network by the swelling method described in Chapter Eight, to see what effect if any, it has, on the developement of knotty tearing. The results are shown in Table 9.8, where the effect of DBTS at three concentration levels are compared with the control samples and samples containing plasticizer (Dutrex R: a-high-viscosity aromatic oil) at 10 pphr and 15 pphr respectively. The data represent the mean values obtained from three samples in each case. When about 4% by weight of DBTS was incorporated into the vulcanizate, the tearing energy decreased by about 30%, and the permanent set decreased by about 40%. As the amount of DBTS was increased to 12% and 19%, the tearing energy decreased further by about 37% and 55% respectively. Correspondingly, the permanent set also decreased. It is quite unlikely that the decrease in the tearing energy is associated with the plasticizing effect, because samples containing 10 pphr and 15 pphr of commercial plasticizer showed increases in tearing energy of about 35% and 18% respectively. The results here contradict the findings of Brown, Porter and Thomas (39) who found that the decrease in the tearing energy observed in samples containing DBTS was similar to that observed in samples containing paraffin oil diluent. However, it should be noted that their work was based on unfilled NR vulcanizates, where tearing occurred in a stick-slip

Table 9.8: Effect of dibutyl tetrasulphide (DBTS) on tearing energy

DBTS (% by weight)	Control	4	12	19.5	*10phr	15phr
T (kJ m^{-2})	46.2	31.85	29.17	20.96	62.11	54.69
+Set (%)	18.5	11.2	7.2	4.1	-	-

Notes:

* Dutrex R = aromatic oil plasticizer

+ Tension set after pre-stressing to 22 MPa. Set measurement after vulcanizates had been swollen, deswollen and to constant weight. The full formulations are shown in Table 4.4a for mix A6 in Chapter Four.

manner and appears to be affected by the amount of strain crystallization only. However, in knotty tearing the situation is more complex because strength anisotropy is of paramount importance for its occurrence. The strength anisotropy comes not only from the strengthening structures associated with strain-crytallization and carbon black particles, but may also come from the set. Thus it appears that the decrease in the tearing energy of samples containing DBTS may probably be due to a decrease in the contribution to strength anisotropy associated with the set. DBTS had probably reduced the recombination efficiency probably by deactivating the sulphenyl radicals as suggested by Brown, Porter and Thomas (39). The results also show that the plasticizer somewhat increased the tearing energy, probably by allowing rapid development of black structure around the tip, thereby enhancing anisotropy because of the improvement in molecular mobility associated with the increased in free volume due to the plasticizing effect, and also with further improvement in the black dispersion, again associated with the presence of the plasticizer. Thus it appears that polysulphidic crosslinks may play a dual role in promoting strength anisotropy. First, being labile, they can rupture, thereby relieving local stress concentration near the tip, and thus giving a larger region of high stresses where orientation is substantial and can induce strength anisotropy. Secondly, they promote additional anisotropy associated with the formation of a second network whilst in the strained state, as reflected by the strong correlation between tearing energy after pre-stressing and the permanent set shown in Figure 9.2b. These two factors could be responsible for the observation that black-filled conventional NR sulphur vulcanizates produced knotty tearing over a wider range of crosslink concentrations than did the black-filled EV and peroxide NR vulcanizates.

9.8 Tear strength of pre-stressed vulcanizates at different filler loadings

Conventional NR sulphur vulcanizates loaded with different amounts of HAF black were pre-stressed to four different stress levels ranging from 5 MPa to 22 MPa. After one minute pre-stressing, they were relaxed for 24 hours before swelling them in toluene for three days. They were then deswollen and dried down to constant

weight before inserting a cut in a direction parallel to the extension previously applied. Tear test was carried out in an Instron machine by separating the legs of the test-piece at a rate of 100 mm per minute at 23°C. The results are shown in Figure 9.14, where tearing energy is plotted against the pphr of HAF black loading.

There are three interesting observations. The first is that, at each filler loading, the tearing energy after pre-stressing decreased with increasing tensile stress. The difference in the tearing energy between the unstressed control samples and the pre-stressed samples can be very substantial, in particular at filler loadings greater than 25 pphr of HAF black. Secondly, below 25 pphr of HAF loading, the anisotropy retained was not adequate to cause steady tearing in the direction of molecular orientation. As a result, the crack was unstable and propagated in stick-slip manner. This observation accords with observations for split tearing where, below 25 pphr of HAF loading, the crack was also found to be unstable. Thus this suggests, that in order to induce adequate strength anisotropy to promote knotty tearing, the amount of HAF black loading should be greater than 10 pphr. Thirdly, in the regions of steady tearing, the tearing energy increased progressively with increasing filler loading. This again agrees with the results obtained from split tearing tests shown earlier in Chapter Seven. The increase may be attributable to an increased in hysteresis with increasing filler loading (70).

9.9 Effects of tear rates and temperatures on tear strength of pre-stressed vulcanizates

In this investigation, conventional NR sulphur vulcanizates filled with 50 pphr of HAF were pre-stressed to 23 MPa for one minute, after which the loading stress was removed. Then they were swollen and deswollen, and dried down to constant weight as described earlier, before carrying out the tear test. At rates ranging from 4.2 $\mu m\ s^{-1}$ to 8300 $\mu m\ s^{-1}$, tearing was done by means of constant-rate separation method using an Instron machine. Outside this range of rates, tearing was done using the constant-load method. The experimental details are given in Chapter Eight Section 8.2. The results are shown in Figure 9.15, where

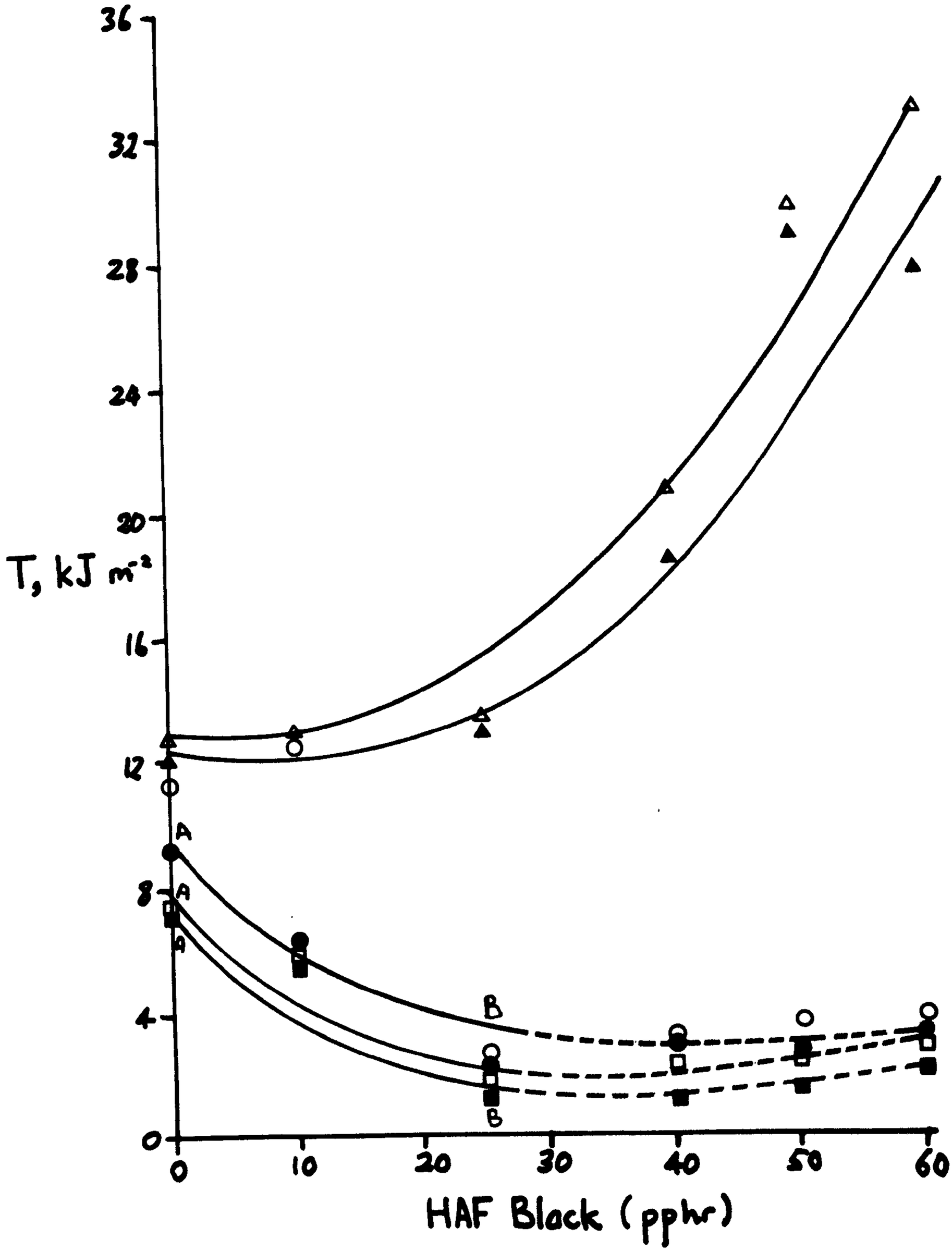

Figure 9.14: Effect of pre-stressing on relationship between tearing energy, and filler loading conventional NR sulphur vulcanizates. The base mix formulations are shown in Table 4.2 in Chapter Four. The curatives: sulphur 2.5, MBS 0.5. Tear rate 830 μm s $^{-1}$. ■ 22 MPa □ 20 MPa ● 18 MPa ○ 15 MPa ▲ 5 MPa △ unstressed control samples. Full line – knotty tearing; Broken lines – steady tearing
A → B – stick-slip tearing

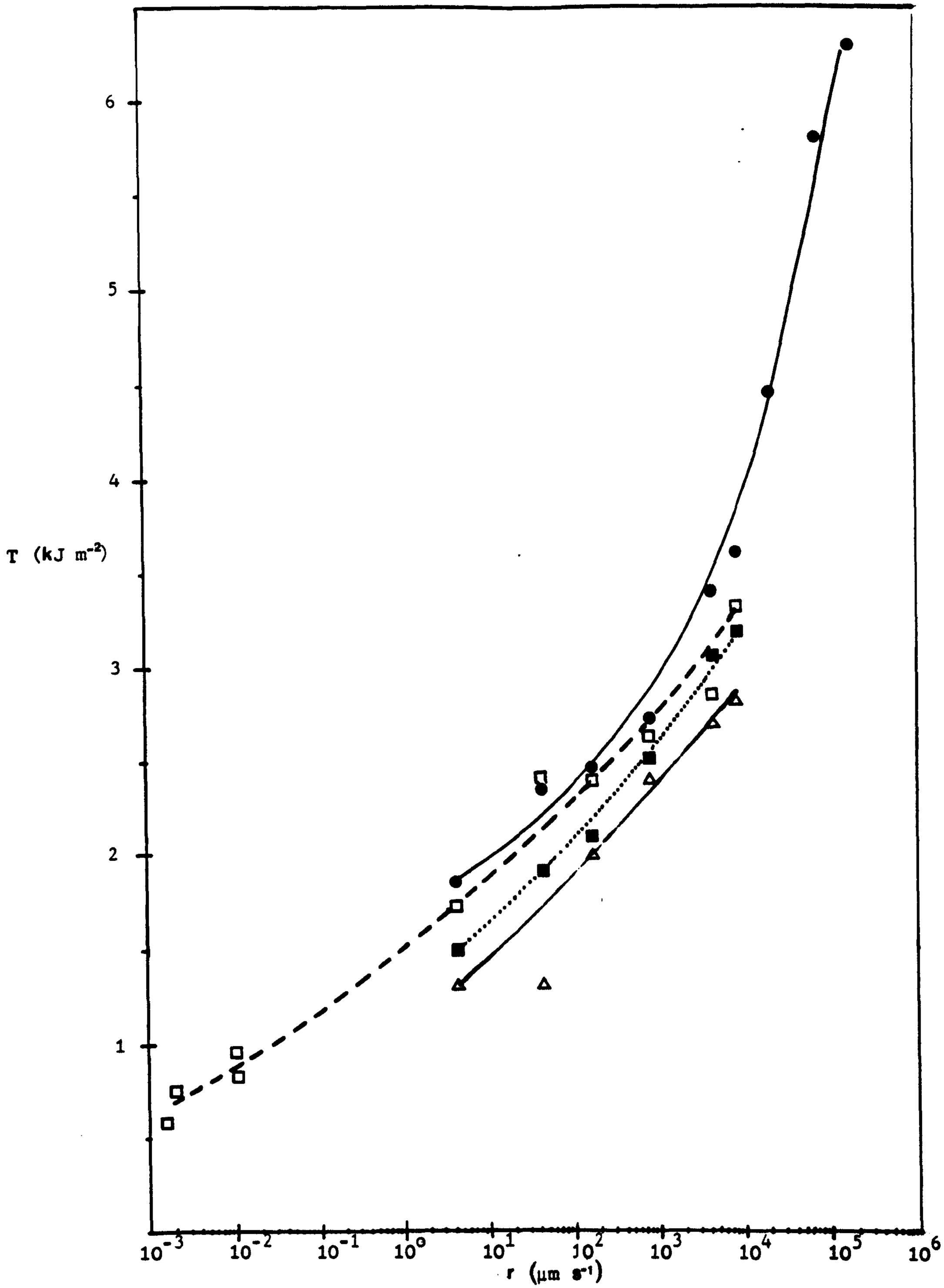

Figure 9.15: Tearing energy, T, vs tear rate, r of black-filled (50 HAF) conventional NR vulcanizate. Samples were pre-stressed to 23 MPa (λ = 5.3) for 1 minute, then swelling, deswelling and drying prior to tearing at (●) 23°C (□) 50°C (■) 70°C (△) 90°C. T - linear scale, r - logarithmic scale. Formulations, mix A6 in Table 4.4a (Chapter Four).

tearing energy, T, at four different temperatures is plotted on a linear scale against crack propagation rate on a logarithmic scale. A linear scale was used for T because the range of tearing energy covered was narrow. A logarithmic scale was necessary for the rate scale because it covered a very wide range. The results in Figure 9.15 show that, at each temperature investigated, the tearing energy increased progresively with rates of tearing. This is attributed to an increase in energy dissipation with rate of tearing (68). However, at 23°C, at tear rates above 8300 μm s^{-1}, there was a sharp increase in the tearing energy, probably because the rubber lost some of its rubbery properties as it approached the glassy behaviour at these high tear rates. In the transition region between the rubbery and glassy states, energy loss is very pronounced since the internal viscosity of the material increases markedly. According to Gent (68), internal energy dissipation determines the tear resistance: the greater the dissipation, the greater the strength. At the highest rates of tear and the lowest temperatures, the tear strength is extremely high, approaching $10^6 J\ m^{-2}$, since the rubbers become first leathery, and eventually glassy (68). In fact Mullins (35) had earlier shown, that there was a strong correlation between tearing energy and the shear loss modulus, G", which gave a measure of energy dissipation.

The dynamic properties of the vulcanizates were independently determined at various temperatures. The results are shown in Figure 9.16, where the loss modulus, E", which gives a quantitative measure of energy dissipation, is plotted against frequency for five different temperatures. The dependence of the loss modulus upon frequency parallels the dependence of tearing energy on tear rate at a particular temperature. The loss modulus increased with increasing frequency at a particular temperature and also with lowering of temperature at a particular frequency. The increase in the loss modulus with frequency is a cosequence of resistance to network deformation increasing with rate of deformation. The tearing energy at a particular rate also decreased as the temperature was raised. This might be attributed to a decrease in energy dissipation since the enhancement of segmental molecular mobility associated with increased thermal motion is expected to reduce the internal viscosity of the material. This observation

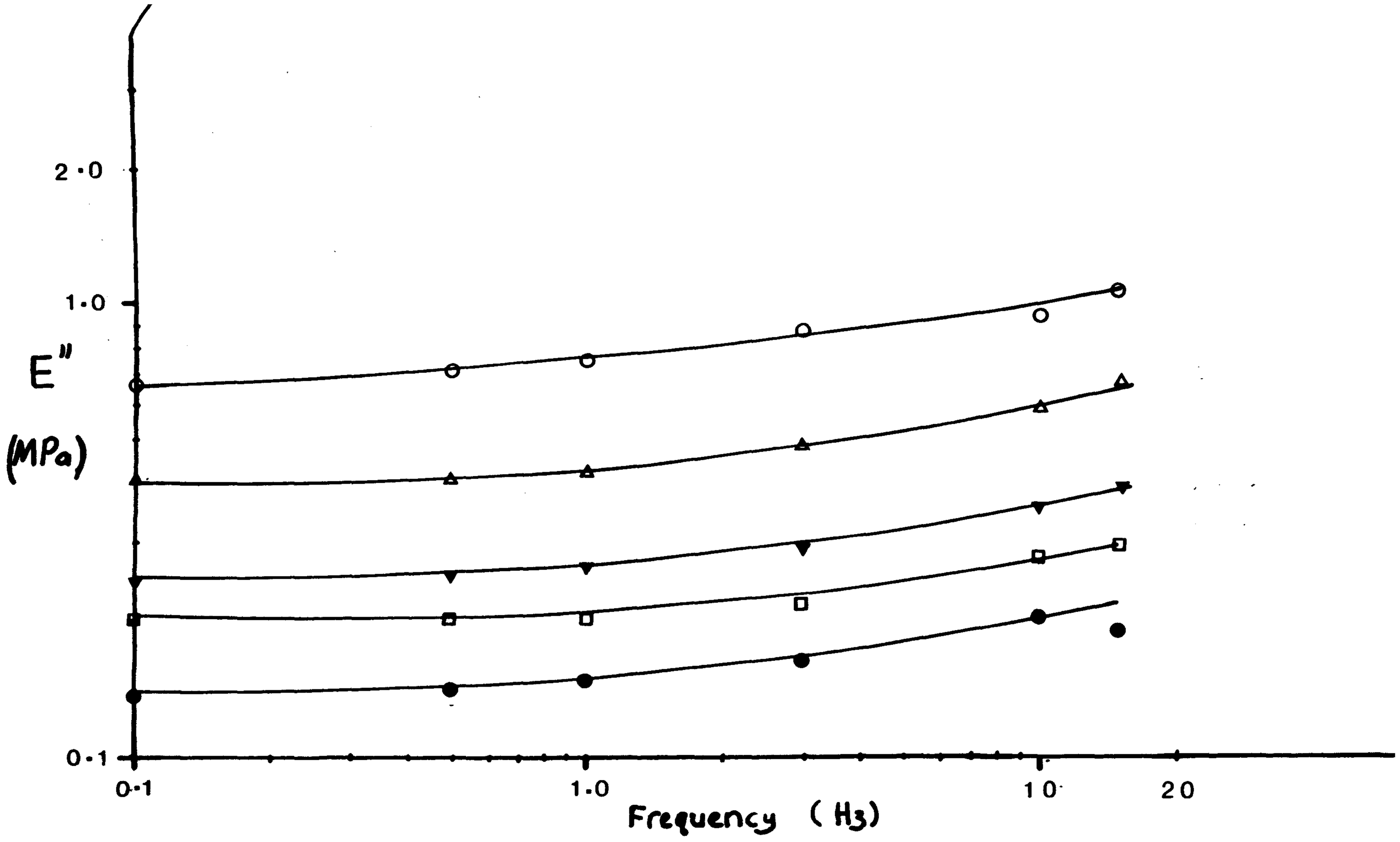

Figure 9.16: Loss modulus, E'', vs frequency at 100% strain amplitude, showing effect of rate of deformation on E'' for black-filled NR vulcanizate (mix H1 shown in Table 4.3b) at temperatures (○) -20°C (△) 0°C (▼) 25°C (□) 50°C (●) 90°C.

again parallels the decrease in the loss modulus as the temperature was raised at a particular frequency.

Mullins (35) had shown that the tearing energy data for unfilled SBR and NBR tearing energy data at different tear rates and temperatures were amenable to time-temperature superposition transformation. By this means, he obtained a single mastercurve covering a wide range of temperatures and tear rates. Mullins (35) observed that the tearing energies of unfilled amorphous SBR and NBR vulcanizates having widely different glass-transition temperatures all fell on a single mastercurve. Tearing energy increased with increasing rate of tearing, as the rate of dissipation of energy by viscous processes increased. Mullins then suggested that the tearing energy is the same for all unfilled amorphous rubbers under conditions of equal segmental mobility, and that the dependence of tearing energy on temperature only indirectly from the effect of temperature upon segmental mobility. The observed interdependence of tearing energy on tearing rate and temperature follows the general pattern expected for a viscoelastic process. It was therefore of interest to see whether the tearing enrgy data shown in Figure 9.15 are amenable to a similar transformation. The method of transformation is described below.

9.10 Tearing energy and loss modulus mastercurves

An attempt was made to construct mastercurves the data shown in Figures 9.15 and 9.16 using the Williams-Landell-Ferry (WLF equation) shown below.

$$\log a_\theta = \frac{-8{\cdot}86(\theta - \theta_s)}{101{\cdot}6 + \theta - \theta_s} \qquad (9.7)$$

where a_θ is the shift factor by which the rate must be multiplied to shift the points to a mastercurve, θ is the temperature of measurement, and θ_s is a reference temperature. The two temperatures were expressed in degrees Kelvin. It was suggested by Williams et al (33) that the reference temperature should be taken as 50°C above the glass transition temperature, θ_g, because of the difficulty of making measurements at temperatures near θ_g. The method was found to work for a wide range of polymers and rate processes. The factors

-8.86 and 101.6 in equation 9.6 are numerical constants. In order to get the mastercurve, first the tearing energy was multiplied by a factor θ_s/θ as a means of making allowance for the change in modulus with temperature (35,87,88,89) since, according to the statistical theory of rubber elasticity, the modulus is proportional to the absolute temperature. Since then, it has become a standard procedure which appears to be a necessary step in obtaining the mastercurve. The same procedure was adopted here, and the temperatures θ and θ_s were expressed in degrees Kelvin. The θ_g of the vulcanizate was determined from DSC measurement and was found to be -68°C. It should also be noted, that the rubber may alter in density with change in temperature. The correction associated with this effect was assumed to be small, and was therefore neglected. The next procedure was to calculate the shift factor, a_θ, at each temperature of test. Each rate of tearing was multiplied with the appropriate value of a_θ to give the abscissae of the points for the mastercurve. Finally, the reduced tearing energy, $T\theta_s/\theta$ was plotted on a linear scale against reduced rate, a_θ(rate) on a logarithmic scale. As shown in Figure 9.17 all the points lay satisfactorily around the mastercurve. The results show that reduced tearing energy increases progressively with reduced rate, implying that energy dissipation is an important factor in affecting the strength. This behaviour is paralleled by the dependence of the loss modulus on frequency, as shown in Figure 9.18. The difference in the shapes between the two mastercurves is a consequence of reduced tearing energy being plotted on a linear scale whereas reduced loss modulus is plotted on a logarithmic scale. Otherwise the shapes are similar. These findings accord with those of Mullins (35).

The WLF transformation is applicable to tearing energy data only when the tearing process is controlled by viscous processes, i.e., by the internal viscosity of the material. Mullins (35) obtained a tearing energy mastercurve for unfilled non-strain crystallizing rubbers so far as they produced steady tearing, but departures occurred when stick-slip tearing prevailed because the tearing process was then affected by structural changes at or near the tips of growing tears. For this reason tearing energy mastercurve cannot be obtained for strain-crystallizing rubbers and black-filled rubbers, unless structural changes at or near the crack

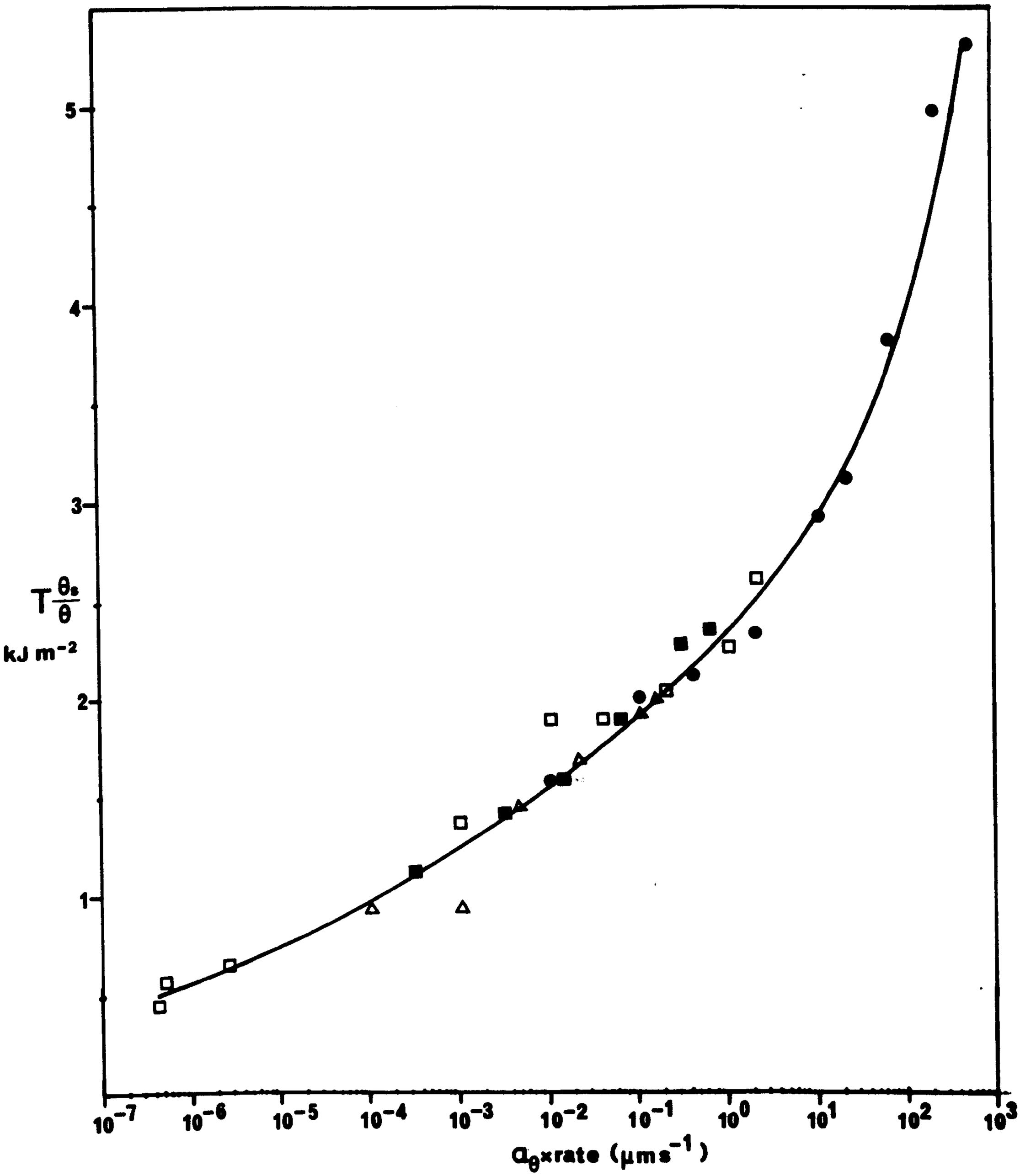

Figure 9.17: Mastercurve for tearing energies covering wide range of tear rates obtained by transforming data shown in Figure 9.1. into a single curve using the WLF transformation.
● 23°C □ 50°C ■ 70°C △ 90°C

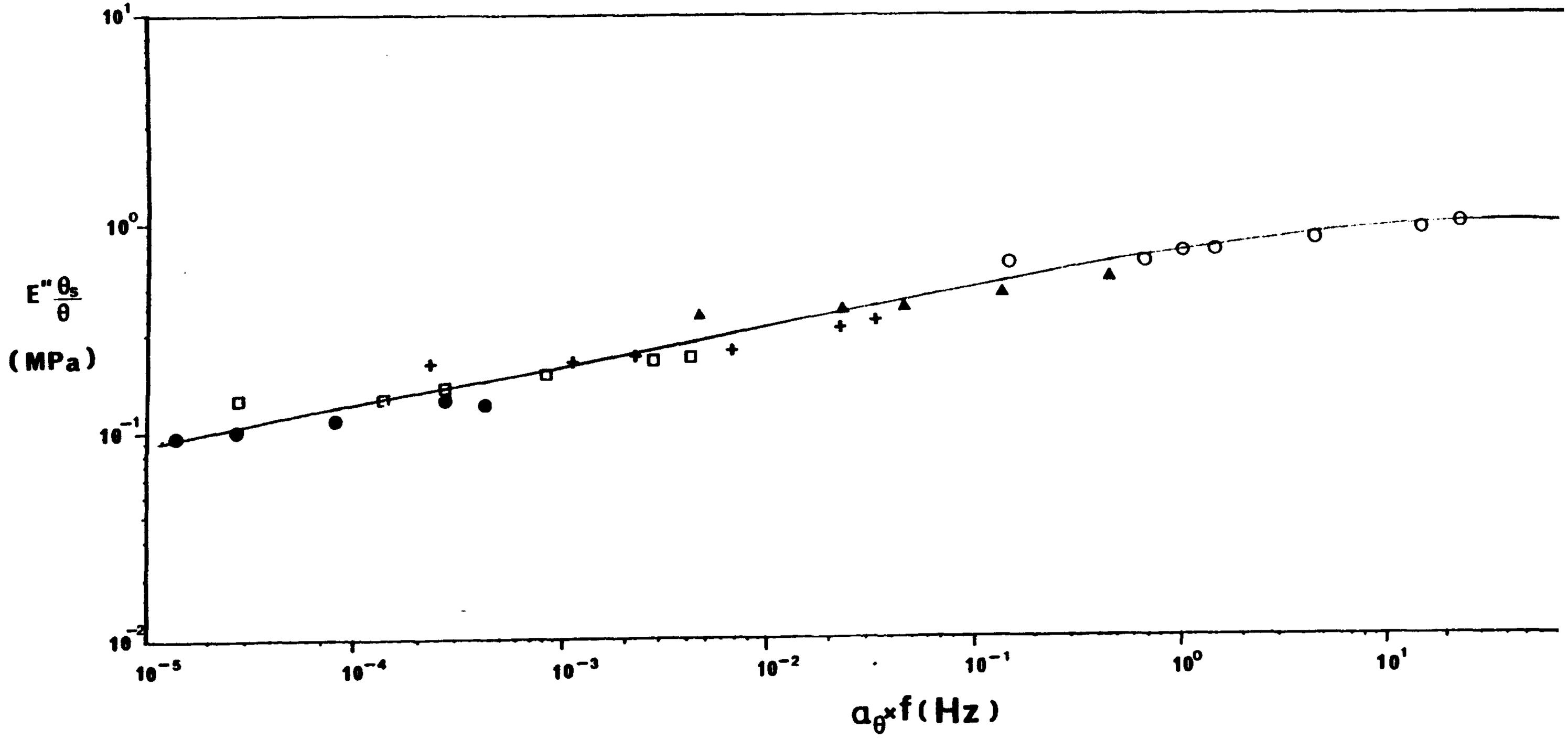

○ −20°C ▲0°C + 25°C □ 50°C ● 90°C

Figure 9.18 : Mastercurve for loss moduli covering wide range of frequencies, f, obtained by transforming data shown in Figure 9.16 into a single mastercurve using the WLF transformation.

tip are prevented. Gent and Henry (42) and later Stacer and co-workers (43,44,45), prevented structural changes at the tear tip by constraining the tip from diverting, as discussed earlier in Chapter Three. They found only by constraining the tip of the tear that they obtained a tearing energy mastercurve for the black-filled vulcanizates.

The success in reducing the tearing energy data in Figure 9.15 to a single mastercurve using the WLF transformation clearly indicates that the tearing process in pre-stressed vulcanizates must be controlled predominantly by the viscoelastic behaviour of the rubber. This is, of course, consistent with the occurrence of steady tearing, and with the fact that the tearing energy increases steadily with tear rate, as shown in Figure 9.17. Besides that, it also suggests that the strengthening structures associated with strain-crystallization and/or black structure at or near the crack tip somehow did not occur, otherwise the mastercurve would not be obtained. It therefore appears as if the set (stricly speaking the second network) formed during pre-stressing inteferes with strain-crystallization at the tip, perhaps by discouraging the chain segments from adopting the regular configuration which are necessary to induce crystallization. This is also consistent with the time-dependent tearing exhibited by the pre-stressed conventional sulphur vulcanizates (black-filled NR) when subjected to constant stress. The time-dependent tearing i.e., the increase in crack length with time under constant stress also indicates that strain-crystallization does not occur at the tip of the tear. Otherwise, time-dependent tearing will not occur. This is another aspect that needs further investigation.

9.11 Influence of cyclic pre-stressing on tear strength and set

It is a well-known fact that, after a strip of vulcanized rubber has first been stretched, the stress required for subsequent deformations is markedly lower. This has been attributed to stress softening (12). This effect is more pronounced in black-filled vulcanizates than in unfilled vulcanizates. It has been suggested that the softening is associated with breakdown or slippage of linkages between filler and rubber, breakdown of filler-filler

aggregates, and breakdown of network chains (12). The main concern here was to study the effects of cyclic pre-stressing on the set and the tearing energy. The test-piece (parallel-sided tensile strip) was subjected to cyclic loadings either at a constant stress or at a constant strain. This was done by pulling the test-piece at a rate of 100 mm per minute to the required stress or extension ratio, and then relaxing it to zero stress before pulling it again to the same stress or extension ratio for the number of cycles required. The set was measured one minute after the completion of all the cycles. A cut was introduced parallel to the direction of extension and tearing was carried out immediately by separating the legs of the test-piece at a rate of 100 mm per minute. The results are shown in Tables 9.9A, B and C.

Table 9.9A shows the effect of cyclic loading (constant stress, 12.4 MPa) on tearing energy. The apparent set was plotted against the number of cycles of pre-stressing. Figure 9.19a (curve a) shows the result. The apparent set after one minute increased progressively with increasing number of cycles. It appears that the set under cyclic loading is more pronounced than under static loading. However, the detailed mechanism is not clear. The effect may perhaps be attributed to the stress-softening mechanisms described above. The tearing energy was also greatly affected by the number of cycles of loading. Although the stress imposed was relatively low, the effect of cyclic pre-stressing was to cause a substantial weakening of the material. For example, by pre-stressing for five times at this particular stress, the decrease in the tearing energy was approximately equivalent to that produced by pre-stressing it once at a large stress of say, 22 MPa. It shows that repeated stressing is more detrimental to tear strength than is static stressing. This, of course, opens a new area for further investigation. The substantial increases in the set which accompany cyclic loading parallel the larger creep observed by Derham and Thomas (90) under tensile loads repeatedly applied than would be expected from observation of the creep under the same load applied continuously. Derham and Thomas suggested that the observed phenomenon was associated with the crystallization of natural rubber under strain. They envisaged that the phenomenon was analogous to the crack-growth behaviour of natural rubber, where repeated stressing produces crack growth, but a static load does

Table 9.9: Effect of pre-stressing under cyclic loading on tearing energy and set (measured after 1 minute of unloading)*

(A) Cyclic loading at a constant stress, σ = 12.4 MPa

No. of cycles	1	2	3	5	7	10
*Set (%)	12	20	27	34	43	55
T (kJ m^{-2})	11.28	5.73	2.7	2.37	1.38	1.24
Type of tear	k	k	s	s	s	s
λ	4.0	4.60	4.9	5.1	5.35	5.9

(B) Cyclic loading at a constant stress, σ = 6.83 MPa

No. of cyclies	1	2	3	5	7	10
*Set (%)	5	7	9.5	10	14	16
T (kJ m^{-2})	17.2	16.02	16.20	15.3	9.12	7.39
Type of tear	k	k	k	k+s	k+s	k+s
λ	3.0	3.2	3.4	3.55	3.7	3.85

(C),Cyclic loading at a constant strain, λ = 4

No. of cycles	1	2	3	5	7	10
*Set (%)	12	17	19	21	23	24
T (kJ m^{-2})	11.28	9.83	9.15	7.08	2.88	2.93
Type of tear	k	k	k	k+s	s	s
σ (MPa)	13.1	8.36	7.33	6.21	5.86	5.6

Notes:

* Set - the set measured 1 minute after the completion of each cycle

k - knotty tearing

s - steady tearing

Tear rate 830 $\mu m\ s^{-1}$ at 23°C

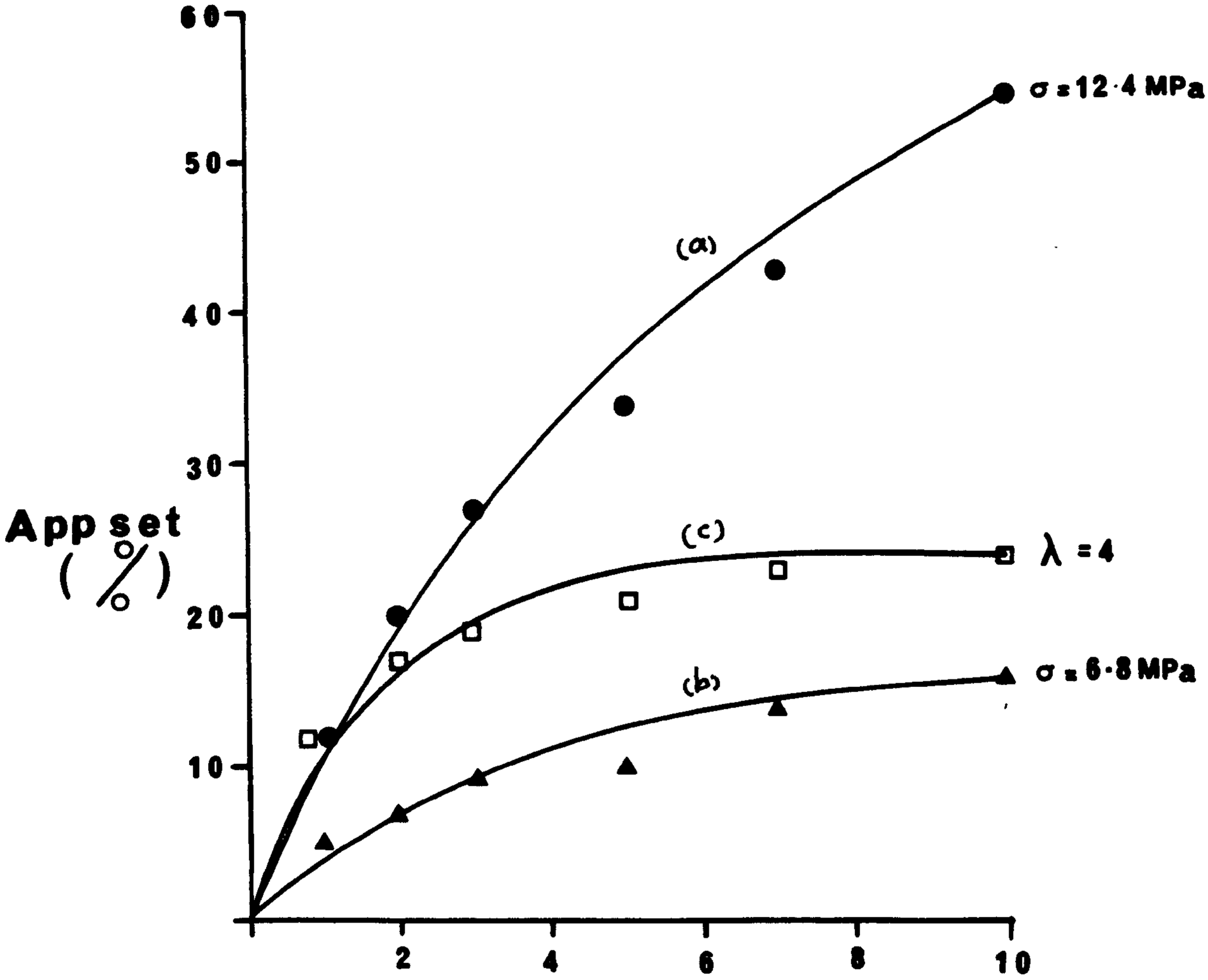

Figure 9.19a: Effect of cyclic pre-stressing on set (mesured 1 minute after the completion of each cycle) for black-filled (50 HAF) conventional NR vulcanizate (mix A6 shown in Table 4.4a).

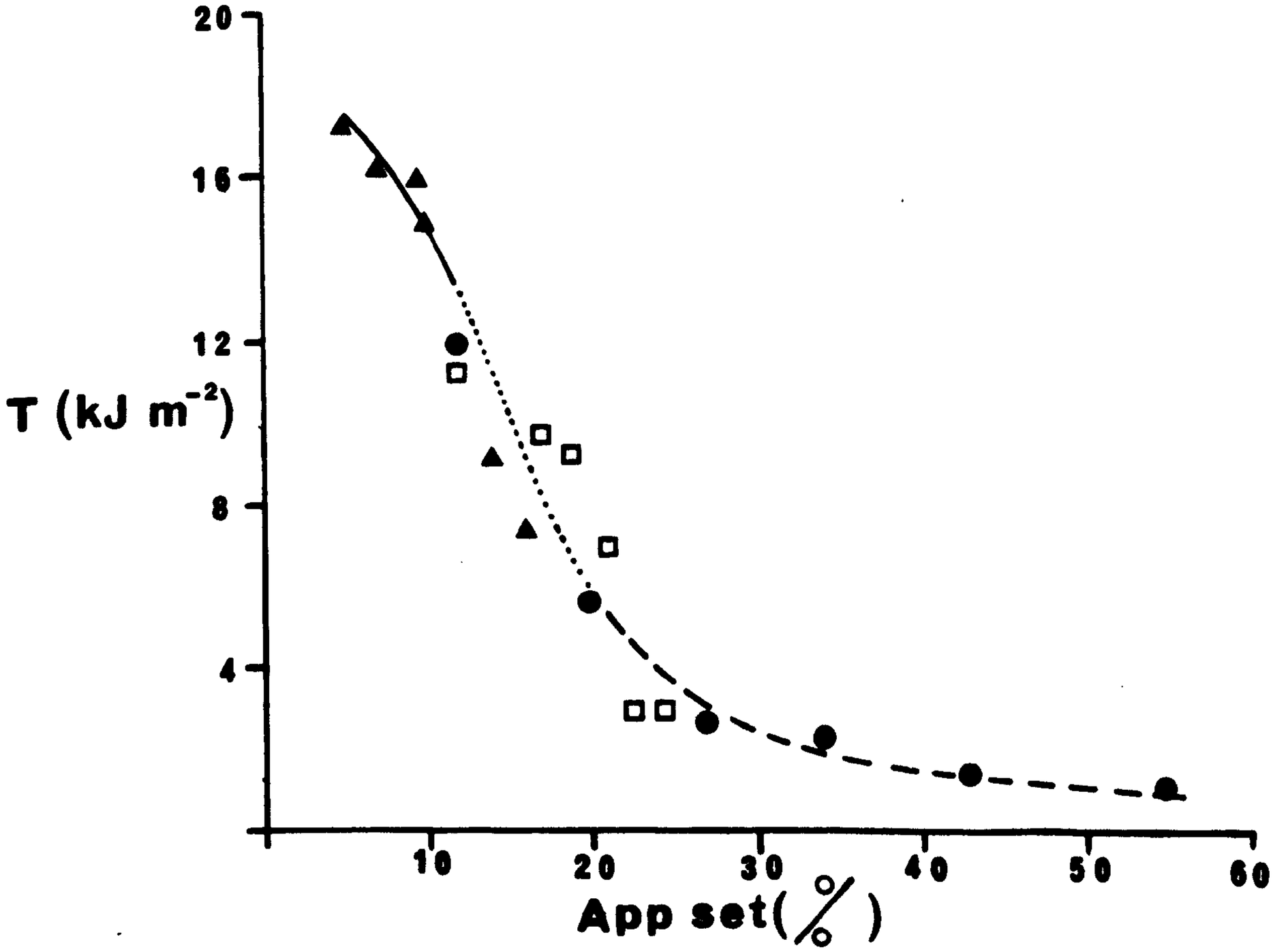

Figure 9.19b: Correlation between tearing energy, T, and set produced by cyclic pre-stressing for the same vulcanizate described in Figure 9.16a. ● 12 MPa, ▲ 6.83 MPa, □ λ 4.

not. Under static loading, strain-crystallization at the tip of the tear prevents bond rupture continuing to its full extent, but after relaxation more bond rupture takes place in a subsequent extension before crystallization again occurs. They also observed that the cyclic creep was much reduced under non-relaxing conditions. This again parallels the non-relaxing cyclic crack growth behaviour of natural rubber.

Table 9.3B shows the effect of cyclic loading, but at a much lower maximum stress, about 6.83 MPa. Similar trends were observed. Figure 9.19 (curve b) shows the correlation between apparent set and the number of cycles of pre-stressing. Again the set and the tearing energy decreased as the number of cycles of loading increased. However, the magnitude of the set was lower, and tearing energies were higher, than those reported in Table 9.9A.

Table 9.3C shows the effect of cyclic pre-stressing at a constant extension ratio (λ=4). Figure 9.19 (curve c) shows the correlation between apparent set and the number of cycles of pre-stressing. Here, the effect was not as severe as in the case of cyclic pre-stressing to constant stress (curve a). This could be attributed to the stress decreasing continuously as the number of loading cycles increased. The observed decrease in stress was attributed to the set introduced after each loading cycle. Nevertheless, the effect of such cyclic pre-stressing on the set and tearing energy was still very pronounced.

In order to see the correlation between tearing energy and the apparent set, the tearing energies given in Tables 9.9A, B and C were plotted against the apparent set. The results are shown in Figure 9.19b. There are three regions of tearing. The full line indicates region of knotty tearing. Knotty tearing occurred if the apparent set was below 12%. This observation is consistent with the the results shown in Figure 9.2b. The dotted lines indicate the transition region between knotty tearing and steady tearing (k + s). In other words the test-piece initially propagated in steady tearing and then reverted to knotty tearing again. The broken lines indicate region of steady tearing. Steady tearing occurred when the apparent set was greater than 20%. It is interesting to see that all the points lie satisfactorily around the tearing energy-apparent set curve, although the test-pieces were cycled to different stresses and strains. Thus the results indicate that, it is the set

which affect the tearing energy and not the method of how the set was obtained.

9.12 Introduction of set at low stresses

The permanent set which is observed after imposing a large stress on a vulcanizate has been attributed to the formation of a second network in the strained state by recombination of the active ends of broken crosslinks. To investigate this aspect further, a rubber mix was initially vulcanized to below its maximum state of cure. This is called first-stage vulcanization. The state of cure was assessed from the Rheometer curve of torque (measured in lbf.in or N.m) versus curing time as shown schematically in Figure 9.20. An oscillating Disk Rheometer is an instrument used to assess the curing characteristics of a rubber mix. The rotor for the Oscillating Disk Rheometer is oscillated through a small degree of arc. The sample of rubber mix is subjected to an oscillary shearing action of constant amplitude. The torque required to oscillate the rotor, which is embedded in the rubber sample confined in a die cavity under pressure and controlled at a desired vulcanization temperature is measured. As vulcanization proceeds, the torque required to shear the rubber increases and a curve of torque versus curing time can be generated. From Figure 9.20, a maximum state of cure is defined as the maximum torque where the curve plateaus. The cure time i.e., the time to vulcanize the rubber to its maximum torque is denoted by t_{100}. The cure time to vulcanize the rubber to 50% of its maximum torque is denoted by t_{50}, and so forth.

24 hours later, a second stage of vulcanization was carried out, the vulcanizate being allowed to attain its maximum state of cure in an autoclave. However, the samples were slightly strained so that the crosslinks introduced during the second stage of vulcanization formed a second network whilst in the strained state, thus simulating the recombination process which is believed to occur in a polysulphidic network and which is believed to give the set. It was interesting to see whether or not set is thereby introduced. Since the rubber was not fully vulcanized, the stress required to extend to 100% extension and below was low, being less than 3 MPa. It is unlikely that such low stresses would rupture the crosslinks.

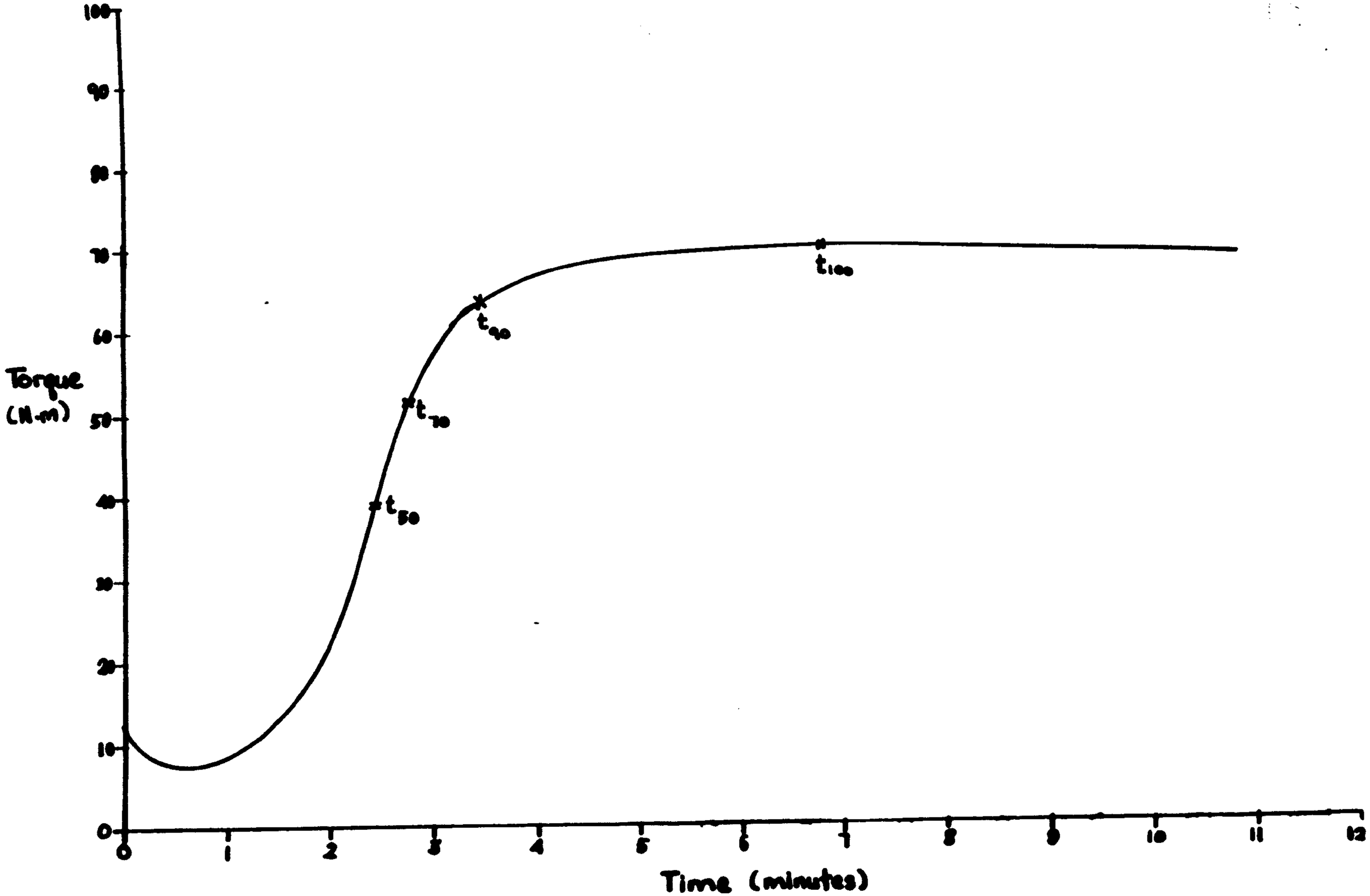

Figure 9.20: Schematic diagram showing a torque-cure time graph obtained from oscillating disc Rheometer.
t_{100} - the time to reach maximum torque, t_{90} - the time to reach 90% of the maximum torque, t_{70} - the time to reach 70% of the maximum torque t_{50} - the time to reach 50% of the maximum torque.

Figures 9.8a and 9.8b indicate that, for appreciable crosslink rupture to occur, the stress imposed should be greater than 4 MPa. Thus it is assumed here that the mechanical stress did not cause crosslink rupture, and thus no recombination of broken crosslinks occurred. The second network introduced in the strained state was therefore attributed solely to the crosslinking which occurred during second-stage vulcanization.

Crosslink concentration after the first-stage and second-stage vulcanizations were determined by equilibrium swelling method described in Section 4.8 in Chapter Four. Suppose that $[X]_1$ is the crosslink concentration introduced in the first-stage vulcanization, and $[X]_2$ is the crosslink concentration at maximum state of cure. The percentage of crosslink concentration introduced in the first-stage vulcanization (q_1) is defined by equation 9.8

$$q_1 = \frac{[X]_1}{[X]_2} \times 100\% \qquad 9.8$$

and the percentage of crosslink concentration introduced in the second-stage vulcanization (q_2) is defined by equation 9.9

$$q_2 = 100\% - q_1 \qquad 9.9$$

Tearing and swelling measurements were also carried out using control samples. Control samples were those which were vulcanized in a compression mould in a steam-heated press to the maximum state of cure (i.e., single-stage vulcanization).

Table 9.10 shows the tensile and swelling properties for vulcanizates having various states of cure. Both the tensile strength and the volume fraction of rubber in the swollen samples were affected by the state of cure. Below 50% maximum state of cure, the crosslink concentration was low. As a result, the tensile strength was low because plastic flow associated with molecular slippage occurred and dissipated the stress before it was sufficiently large to effect reorientation and crystallization. At 70% state of cure and above, the concentration of crosslinks was sufficient to prevent plastic flow, and enabled the network to support high deformations at large stresses. This in turn permitted

Table 9.10: Tensile and swelling properties of black-filled conventional NR sulphur vulcanizates at different states of cure. Full formulations shown in Table 4.4a for mix A6 in Chapter Four.

1st.-stage vuln. Vulcanization time	t_{15}	t_{30}	t_{50}	t_{70}	t_{80}	t_{95}	t_{100}
at 140°C (mins)	11.5	13.5	16	20.5	24.5	35	50
M100 (MPa)	0.62	0.86	1.10	1.69	2.44	2.69	2.70
M200 (MPa)	1.40	2.31	3.07	5.06	7.32	8.07	7.50
M300 (MPa)	3.24	5.14	6.87	9.81	13.5	15.0	13.9
M400 (MPa)	6.01	8.54	12.6	15.5	18.7	22.3	20.8
M500 (MPa)	8.94	12.5	17.3	21.5	22.6	28.7	-
T.S. (MPa)	15.1	18.6	23.6	29.0	29.4	30.0	29.3
E.B. (%)	698	641	608	626	603	518	480
υ_r	0.1515	0.2163	0.2513	0.2879	0.3222	0.3328	0.3407
$[X]_1 x 10^{-2}$ (mole per kg RH)	1.08	2.37	3.34	4.63	6.11	6.64	7.06

t_{15} , t_{30} , t_{50}, t_{70} , t_{80}, t_{95} , denote the time to reach 15%, 30%, 50% 70%, 80% and 95% of the maximum (100%) torque-cure time graph.

appreciable molecular orientation and crystallization to occur thus, giving high tensile strength.

In this investigation, the rubber was initially vulcanized to 80% and 95% state of cure in a compression mould heated in a steam press. The second-stage vulcanization was carried out in an autoclave to the maximum state of cure. The reason for choosing the 80% and 95% states of cure was to avoid prolonged vulcanization in the autoclave. This might have caused degradation due to the presence of oxygen in the air inside the autoclave because the air might not have been completely evacuated before passing in the steam. Furthermore, polysulphidic crosslinks are thermally unstable, and prolonged vulcanization might have caused chemical changes within the first network introduced during the first-stage vulcanization.

Table 9.11 shows the results. One of the interesting observations was the high set introduced at low stresses. For an example, in a 95%-vulcanized sample, the stress to extend to 50% elongation was about 1.2 MPa, and the set introduced was about 25%. The set was associated with the second network introduced during the second- stage vulcanization. The set was measured 7 days after the completion of the second-stage vulcanization after allowing the samples to relax at 23°C, to eliminate any viscoelastic effects. The value remained was unaffected even when swelling and deswelling were carried out after the 7-day period. This confirms that the set measured after 7 days was associated solely with the second network introduced by the crosslinking which occurred during the second-stage vulcanization. The percentage of crosslink concentration in the second network q_2 was about 6%, and this network appears to have produced 25% set. The tearing energy for crack propagating in the direction of molecular orientation was about a factor of 10 lower than that of the control samples. To check further that the vulcanizate consisted of two networks, tear tests were carried out in the transverse direction to the molecular orientation under the same conditions as the previous tests. The average tearing energy in the transverse direction was about 33 kJ m^{-2} (shown by the sign T_h in Table 9.11). This clearly indicates that a two-network vulcanizate indeed produced anisotropy of strength as reflected by the differences in the tearing energies

Table 9.11: Introduction of set at low stress and its effect on tear strength of a black-filled conventional NR sulphur vulcanizate. Full formulations shown in Table 4.4a for mix A6 in Chapter Four.

1st-stage vulcanization Cure time at 140°C	t_{100}	t_{80}	t_{95}	t_{95}	t_{95}	t_{95}
(minutes)	50	24.5	35	35	35	35
$[X]_1 \times 10^{-2}$ (mol per kg RH)	7.06	6.11	6.64	6.64	6.64	6.64
2nd-stage vulcanization in an autoclave at 140°C						
time to reach to t_{100}	-	2.5	15	15	15	15
Strain (%)	-	100	50	75	100	125
Stress (MPa)	-	2.4	1.2	1.7	2.7	3.5
$[X]_2 \times 10^{-2}$ (mol per kg RH)	7.06	7.04	7.05	7.05	7.05	7.05
q_1 (%)	100	87	94	94	94	94
q_2 (%)	-	14	6	6	6	6
Set (%)	-	60	25	40	50	60
T (kJ m^{-2})	35	2.60	3·5	3.2	2.7	2.2
Type of tear	k	s	s	s	s	s
T_b (kJ m^{-2})	-	-	32·8	-	-	-
Type of tear	-	-	k	-	-	-

Footnotes:

$$q_1 = \frac{[X]_1}{[X]_2} \times 100\ \%$$

$q_2 = 100\% - q_1$

t_{100} - the time determined from the torque-cure time curve to reach maximum torque.

t_{95} - the time determined from the torque-cure time curve to reach 95% of maximum torque.

t_{80} - the time determined from the torque-cure time curve to reach 80% of maximum torque.

k - knotty tearing s - steady tearing.

Tear rate 830 μm s^{-1} temperature 23°C.

for crack propagation in the direction parallel and transverse to molecular orientation. This lends support to the hypothesis put forward by Rivlin and Thomas (76) for strength anisotropy introduced by a two-network vulcanizate. Among other observations, the set increased progressively as the amount of pre-stress increased and correspondingly the tearing energy decreased. Also when the proportion of crosslinks in the second network increased, the amount of set also increased.

Finally, these experiments were repeated using a vulcanizate produced by the soluble EV system. The advantage of this vulcanization system over the conventional system is that it produces mainly monosulphidic crosslinks which are more thermally stable than are polysulphidic crosslinks. In this way, it was possible to check whether the crosslinks introduced in the first stage vulcanization of the conventional system were affected by thermal effects or not. The results are shown in Table 9.12. The percentage of crosslink concentration introduced in the first-stage vulcanization, q_1 was about 52%, and the percentage of crosslink concentration introduced in the second network, q_2 during the second-stage vulcanization was about 48%. One of the interesting observations here was the lower permanent set of the soluble EV vulcanizate as compared with that of conventional vulcanizate, although q_2 of the former vulcanizate was approximately 8 times than q_2 of the latter vulcanizate. The higher the crosslink concentration introduced in the second network, the higher would be the expected set, regardless of the type of crosslinks. However, the results here seem to dispute this prediction. The discrepancy could be associated with the thermal instability of the crosslinks produced by the conventional sulphur system. The high set observed in the conventional vulcanizate suggests that more crosslinks were introduced during the second-stage vulcanization than in the first-stage vulcanization. Although the calculated q_2 was about 6%, this might not be the case actually. The calculation was based on the assumption that the crosslinks introduced during the first-stage vulcanization were stable and did not break and reform during the second-stage vulcanization. In the case of conventional vulcanizate, this is not necessarily true, because polysulphidic crosslinks are thermally unstable. It might be that, during the second-stage vulcanization, because of thermal instability some of

Table 9.12: Introduction of set at low stress and its effect on tear strength of a black-filled soluble EV NR sulphur vulcanizate. Full formulations shown in Table 4.4b in Chapter Four.

1st-stage vulcanization	t_{100}	t_{50}	t_{50}	t_{50}	t_{50}
Cure time at 140°C, (mins.)	60	21	21	21	21
$[X]_1 \times 10^{-2}$ (mol per kg RH)	7.07	3.67	3.67	3.67	3.67
2nd-stage vulcanization in an autoclave at 140°C					
Time to reach t_{100} (minutes)	-	39	39	39	39
Strain (%)	0	50	100	150	200
Stress (MPa)	-	1.25	2.68	3.70	3.90
$[X]_2 \times 10^{-2}$ (mol per kg RH)	7.07	7.11	7.11	7.11	7.11
q_1 (%)	100	52	52	52	52
q_2 (%)	-	48	48	48	48
Set (%)	-	17.5	25	37	40
T (kJ m^{-2})	27.24	21.3	3.14	2.36	2.89
Types of tear	k	k	s	s	s

Footnotes;

t_{100} - the time determined from the torque-cure time curve to reach maximum torque.

t_{50} - the time determined from the torque-cure time curve to reach 50% of maximum torque.

$$q_1 = \frac{[X_1]}{[X_2]} \times 100\ \%$$

$q_2 = 100\% - q_1$

k - knotty tearing s - steady tearing

All tear measurements along the molecular orientation ie. parallel to the direction of pre-stressing. Tear rate 830 $\mu m\ s^{-1}$, temp. 23°C.

the crosslinks introduced during the first-stage vulcanization dissociated and reform again during the second-stage vulcanization. As a result, probably more crosslinks were introduced during the second stage vulcanization than appears from the measured crosslink concentrations. Thus the value of q_2 obtained for the soluble EV vulcanizates probably gave a reliable measure of crosslinks introduced in the second network. In contrast, the value q_2 for the conventional vulcanizates may have been somewhat misleading.

A correlation between tearing energy and set was obtained by plotting tearing energies against the set (both apparent and permanent) obtained from various methods of pre-stressing. The results are shown in Figure 9.21. It is interesting to see that all the points lay satisfactorily around the correlation curve regardless of the way the set was obtained. Generally the tearing energy decreases progressively with increasing set regardless of the type of vulcanization system used, the method of pre-stressing (single or multiple) and the manner the second network was introduced (recombination of broken crosslinks or by second-stage vulcanization). Thus the results clearly show that it is the set which affect the tear strength. The higher the set the lower the tearing energy to propagate tearing in the direction of molecular orientation parallel to the direction of pre-stressing. In all cases, when the set was less than 10%, knotty tearing occurred. There is a transition region between the 10% to 20% set. In this transition region, knotty tearing and steady tearing occurred simultaneously, i.e., the tear propagated steadily and then reverted to knotty tearing. However, this behaviour was only observed in cyclic pre-stressing, but not observed if the set was introduced by a single pre-stressing to large extension or by second-stage vulcanization. The scattering of the points in the transition region is attributed to the differences in the mode of tear failure between vulcanizates pre-stressed to large stress and vulcanizates pre-stressed repeatedly either to a constant stress or to a constant extension. When the set was greater than 20% steady tearing occurred regardless of the vulcanization system, the method of pre-stressing and the manner by which the second network was introduced during pre-stressing.

The important feature of these experiments is that they lend

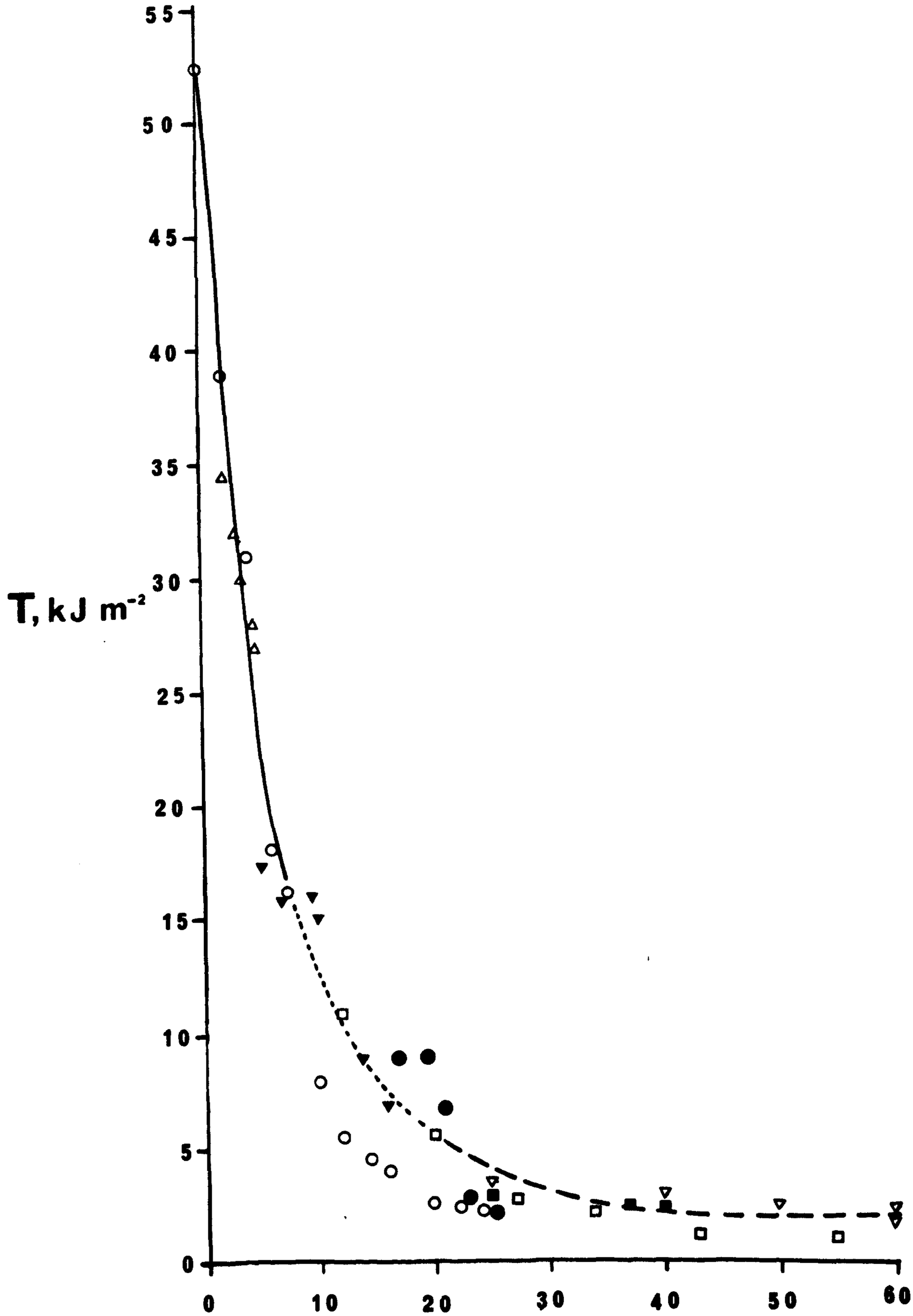

Figure 9.21: Correlation between tearing energy, T, and set obtained by various methods: ○ single pre-stressing, □▼● multiple (cyclic) pre-stressing, ▽ two-stage vulcanization based on black-filled (50 HAF) conventional NR vulcanizate (mix A6 shown in Table 4.4a). △ single pre-stressing, ■ two-stage vulcanization based on black-filled NR soluble EV vulcanizate (shown in Table 4.4b).

support to the hypothesis that the permanent set is a consequence of the presence of two-networks in the final vulcanizate (38,39). The findings discussed in this section indicate that, when a second network is formed in a strained state, a small permanent deformation known as set is established. Besides that, the study here also has some practical applications, for example in continuous vulcanization and in injection moulding. In these cases, vulcanization is carried out at high temperature, say at 190°C and above, using very fast accelerator systems. Because of the short vulcanization time (less than one minute), vulcanization may take place before the rubber has completely filled the mould. The effect is analogous to the formation of two networks in the vulcanizates investigated in this work. It is not surprising that the strength properties, such as the tensile strength and, in particular, the tear strength, of injection-moulded test-pieces show a strong dependence on the direction of orientation (91). The work described in this section provides a good model for interpreting the effect of anisotropy that may be encountered in injection-moulded test-pieces, where the proportion of crosslinks in the first and in the second networks has been varied. The correlation between set and tearing energy would give a quantitative measure of the magnitude and extent of any anisotropy introduced.

9.13 Summary

The work described in this chapter provides good experimental evidence that the anisotropy observed in black-filled NR vulcanizates after pre-stressing is attributable to the presence of two networks in the vulcanizate. This observation is consistent with the hypothesis put forward by Rivlin and Thomas (76). The two networks can be introduced either by imposing large mechanical deformations where crosslinks are broken and recombined during pre-stressing or alternatively by a two-stage vulcanization process. The first mechanism is only possible with vulcanization systems that produce predominantly polysulphidic crosslinks, such as the conventional sulphur/accelerator system. When a large stress is imposed, the polysulphidic crosslinks can break and recombine to form a second network whilst in the strained state, thus giving a permanent set when the loading stress is removed. The tearing energy after pre-stressing is found to correlate strongly with the

set, regardless of the method of pre-stressing, vulcanization system, and the manner in which the second network was introduced in the final vulcanizate. Using the two-network theory suggested by Thomas (38), the fraction of crosslinks broken, and the proportion that recombined, were determined quantitatively. A strong correlation between recombination efficiency and permanent set was also observed. It was also found that pre-stressed vulcanized rubbers showed time-dependent tearing when subjected to constant load. The tearing energy data at different temperatures covering a wide range of rates were transformable into a single mastercurve using the WLF equation, suggesting that the tearing process is controlled by the viscous behaviour of the material. Here, the tear strength is strongly influenced by the energy dissipation.

CHAPTER TEN

TEAR STRENGTH OF CARBON-BLACK-FILLED VULCANIZATES IN STEADY TEARING REGION

One of the interesting observations associated with the tear behaviour of black-filled vulcanizates was the smooth fractured surface produced by steady tearing as shown in Figure 10.1. Clearly its fractured surface is relatively smoother than the fractured surface obtained from a similar unfilled vulcanizate under the same tear-test conditions. Kadir and Thomas (30) suggested that the roughening of the fractured surface observed in unfilled vulcanizates in the rough tearing region is associated with cavitation due to the hydrostatic component of the stress field around the tip of the crack. For unfilled NR vulcanizates, the stress necessary to produce cavitation is about 10^6 N m^{-2} (30). The local tensile stress developed just ahead of the crack tip must be very high in order to break primary chemical bonds, and should be more than adequate to cause such cavitation. In an unfilled vulcanizate, smooth fractured surfaces can be obtained at very high rates of tearing, probably at 10 m s^{-1} and above (30). At such high rates of tearing, the material approaches its glassy state and behaves correspondingly stiffer. Hence the stress necessary to produce cavitation also increases. However, at these high rates of tearing, rupture of the chains occurs before cavitation can take place. In the absence of cavitation, smooth fractured surfaces were obtained (30).

As mentioned above, smooth fractured surfaces can be obtained from black-filled vulcanizates even at tear rates for which rough tearing is observed in the case of the corresponding unfilled vulcanizates. Gent and Lindley (92) observed that cavitation occurred in black-filled vulcanizates less readily than in the corresponding unfilled vulcanizates for reasons which are not entirely clear. They also observed a linear dependence of cracking stress on the Young's modulus, and that, the stiffer the vulcanizate, the higher the cracking stress required to cause cavitation. Their observations agree with the findings of Mullins and Tobin (78), who investigated the volume changes which occur

Figure 10.1: Phtograph showing a fracture surface of HAF-black-filled (50pphr) SBR vulcanizate in steady tearing region.

during strectching of carbon-black loaded NR vulcanizates. Mullins and Tobin found that NR peroxide and sulphur gum vulcanizates increase in volume at low extensions. They attributed this effect to the formation of vacuoles around particles of zinc oxide. With black-filled vulcanizates, no further increases in volume were observed, even though it contained 50 pphr of carbon black. This suggests that there was little or no formation of vacuoles around the carbon black particles. This also implies that cavitation does not appear to occur in black-filled vulcanizates as readily as it does unfilled vulcanizates. When carbon blacks are loaded into rubbers, the stiffness of the rubber increases markedly. The stiffness of the black-filled vulcanizate can be expressed quantitatively in terms of the volume fraction of the filler in the rubber vulcanizate by Guth and Gold (93) equation, i.e.,

$$E = E_o(1 + 2.5\Phi + 14.1\Phi^2) \qquad (10.1)$$

where E is the elastic modulus of the filled rubber, E_o is the the modulus of the rubber without filler and Φ is the volume fraction of the filler i.e., the fraction of the total volume of the vulcanizate which is occupied by the filler. For example with 50 pphr of black loading, $\Phi = 0.2035$, and on substitution into equation 10.1 gives $E = 2.0926E_o$. Thus the stiffness of the black-filled vulcanizate containing 50 pphr of black is twice the stiffness of the gum vulcanizate. According to Mullins (94), the stiffening effect by filler particles is reasonably well understood, at least in qualitative terms. He suggested that the stiffening effect is in part associated with the absence of deformation within the rigid filler particles, and in part with immobilisation of the rubber at the interface between the rubber matrix and the filler particles. Whether or not the increase in the stiffness attributable to these factors is adequate to suppress cavitation is not entirely clear. This is another interesting area which deserves investigation in future work.

Another interesting aspect of the steady tearing of black-filled vulcanizates is the magnitude of their tearing energies. The average tearing energy of SBR filled with 50 pphr of HAF black was about 32 kJ m^{-2} at tear rates ranging from 4.2 μm s^{-1} to 8300 μm s^{-1} at 23°C. This value is 10 or more higher than values

for unfilled vulcanizates at the same tear rate and temperature of test. This suggests that macroscopic lateral tear deviation (knotty tearing) is not the only mechanism by which carbon black enhances the tear strength. This observation contradicts the findings of Gent and Henry (42). They suppressed knotty tearing by preventing lateral tear deviation by close confinement of the crack tip, and found that the tear strength for filled vulcanizates was at the most twice the tear strength for unfilled vulcanizates. They then argued that the instrinsic strength of filled vulcanizate is not greatly improved in the absence of knotty tearing, and suggested that lateral tear deviation is the principal mechanism by which carbon black enhances tear strength. Generally, it is widely accepted that knotty tearing appears to be the main mechanism of tear strength in black-filled vulcanizates. However, by no means it is the sole or the only mechanism by which carbon black can enhance the tear strength. The results presented and discussed in Chapter Five earlier provide some evidence that, in the absence of knotty tearing, the tear strengths of black-filled SBR vulcanizates were at least 10 times higher than those of unfilled vulcanizates. Similar observations were noted by Greensmith (16).

In knotty tearing, the increase in the tearing energy is predominantly due to an increase in the diameter of the tear tip associated with lateral tear deviation. In steady tearing, the effective tip diameter is relatively constant and the strain energy density at break is the dominant factor which influences the tear strength (16). The magnitude of U_b is affected by the tensile strength of the material. The difference between the tensile strengths of unfilled and black-filled SBR vulcanizates is substantial. For example, the black-filled SBR vulcanizates prepared according to the formulations shown in Table 4.3b (H4) in Chapter Four had tensile strengths of about 25 MPa. In comparison, the tensile strength of the unfilled SBR shown in Table 4.4b (G4) was about 2 MPa. Thus the tensile strength of black-filled SBR vulcanizates was a factor of about 12 higher than the tensile strength of unfilled SBR vulcanizates. Based on this ground alone, it would be expected that black-filled SBR vulcanizates would show higher tear strengths than would the corresponding unfilled vulcanizates. This agrees with the findings of Greensmith (23) who observed a close correlation between tensile strength and tear

strength when knotty tearing did not occur. The magnitude of the tip diameter produced by the steady tearing of unfilled vulcanizates in the rough tearing region is about 0.2 mm (16,23). The observed value was in accord with the theoretical value predicted from the relationship $d = TU_b^{-1}$. However, this equation is quantitatively valid when tearing occurs in stick-slip and produces rough fractured surfaces, or in knotty tearing where the tear produces a knot. Steady tearing in the smooth tearing region produces fractured surfaces which are smoother than the fractured surfaces produced by steady tearing in the rough tearing region, and also than the fractured surfaces produced by stick-slip tearing (30).

When the fractured surface is smooth, the relationship $d = TU_b^{-1}$ breaksdown. For example, the tearing energy for the steady tearing of black-filled SBR vulcanizates was about 32 kJ m^{-2}, and the stored energy density at break determined from the area under stress-strain curve at break was about 61 MJ m^{-3}. Substituting these values into $d = TU_b^{-1}$ gives a value for the tip diameter, d, of about 2 mm. Clearly, this value of d is rather high in comparison with the observed roughness of the fractured surface. The calculated value of d overestimates the roughness of the fractured surface by a factor of more than 10, the fractured surface of this type of vulcanizate being smoother (Figure 10.1) than that of the corresponding unfilled vulcanizates. According to Thomas (95), although in the smooth tearing region the tip of tear is very sharp, the radius of the strain distribution at the tip of the tear is larger than the diameter of the tip itself because, in order to break a bond lying across the the fracture plane, it is necessary to take many other bonds in the same chain between crosslinks up to essentially to the breaking point. Every volume element of rubber above and below the fracture plane experiences a strain cycle as the crack approaches and recedes from its vicinity, and therefore energy is dissipated. Greensmith (23) also was aware of this effect when he observed that black-filled SBR vulcanizates could produce high tearing energies in the absence of knotty tearing. He then proposed that mechanical energy losses occur as the material at the neighbourhood of the tip is brought to breaking point or to high extensions close to its breaking point. He further suggested that additional energy losses might also occur in regions adjacent to the tip because, when tearing occurs, each volume

element in the path of the propagating crack is subjected to a strain cycle as the material is subjected to moderate extension and is then relaxed. This additional energy dissipation may well be considerable at high tearing rates where rapid deformation occurs. With black-filled vulcanizates, the effect will be more pronounced and may be encountered even at low rates of tearing. Greensmith (23) then suggested that the effect of hysteresis is analogous to an increase in the effective diameter of the tip of the crack.

It has frequently been proposed in the literature that mechanical hysteresis plays an important role in determining the strength properties of vulcanized rubbers, notably by Mullins (35,79), by Harwood and Payne (56,97), and by Andrews (11,28). There are four main sources of mechanical hysteresis (67,94,96,97) in a rubber vulcanizate, namely:

(i) Hysteresis associated with the breakdown of carbon black aggregates or agglomerates. Hysteresis arising from this this cause is only apparent at low stresses.

(ii) Hysteresis due to stress softening, also known as the Mullins effect. Both unfilled and filled vulcanizates show similar behaviour in this respect.

(iii) Hysteresis at large extensions associated with strain crystallization.

(iv) Hysteresis associated with the viscoelastic behaviour of the rubber, mainly with the internal viscosity of the material.

Generally speaking, black-filled vulcanizates are more hysteresial than are unfilled vulcanizates particularly in the case of non-strain crystallizing rubbers. Carbon black results in an enhancement of the actual strain in the rubber phase, and this leads to an increase in energy losses at a given strain (97). The strong correlation between tearing energy and the loss shear modulus, which gives a quantitative measure of hysteresis as shown by Mullins (35), gives good evidence for the dependence of tear strength on mechanical hysteresis. According to Harwood and Payne (96), the

more energy a rubber can dissipate when stretched, the more applied work it can absorb before breaking. Based on this suggestion, black-filled vulcanizates are expected to have higher tear strengths than the corresponding unfilled vulcanizates, because the former are more hysteresial than the latter. However, the mechanisms by which hysteresis enhances the tear strength are still not entirely clear. Andrews (11,28) suggested that, when a crack propagates in a hysteretic material, the stress concentration at the tip of the tear is substantially less than would be the case if the material were perfectly elastic. The decrease in the stress concentration due to hysteresis is analogous to increasing the effective diameter of the tear tip as suggested by Greensmith (23). It must be reiterated that the detailed mechanisms are still not entirely clear, and thus this area of investigation provides a future challange. The main conclusion reached from this chapter is that, in the absence of knotty tearing, high tear strength can still be obtained. This implies that knotty tearing is not the only mechanism by which carbon blacks enhance the tear strength. In steady tearing, mechanical hysteresis appears to be responsible for the observed increase in the tear strength, although the detailed mechanisms are still obscure. Thus the tear behaviour of black-filled vulcanizates remains complex and not fully understood.

CHAPTER ELEVEN

SUMMARY OF INVESTIGATIONS, CONCLUSIONS AND SUGGESTIONS FOR FURTHER WORKS

There are basically two machanisms by which the tear resistance of rubber vulcanizates can be enhanced. One is by energy dissipation and the other is by blunting of the tip of the tear. In black-filled rubber vulcanizates, blunting of the tear tip appears to be the principal mechanism by which carbon black enhances the tear strength. This is commonly known as knotty tearing. In knotty tearing, the tear deviates almost at right angles from the intended path, and thereby increases the effective tear-tip diameter. As a result, the stress concentration at the tear tip is greatly reduced. Consequently the tear resistance of the vulcanizate is greatly enhanced. The present work has shown that there is a strong correlation between tearing energy and the size of the knot diameter measured in the unstrained state. The tearing energy increases progressively with increasing knot diameter. Over a wide range of tear rates and temperatures, the measured values of knot diameter showed close agreement with the value calculated from the theoretical expression i.e., $T \cong U_b d$.

The magnitude of the knot diameter was found to be affected by temperature and tear rate, suggesting that the development of strengthening structure requires an appreciable time to form. At slow tear rates or at high temperatures where the molecular mobility is enhanced, knotty tearing occurred readily and effectively, as reflected by the increase in the knot diameter. Under these conditions, probably the molecular mobility was sufficiently high such as to permit rapid development of strengthening structures around the tip which give the strength anisotropy necessary for the occurrence of knotty tearing. In contrast, at rapid tear rates, the knot diameter decreases because the strengthening structure has less time to develop. The variations of tearing energy with rate and temperature in the knotty tearing region could well be attributed to variations in the rate of development of the strengthening structures around the tear-tip, which in turn affect the effective size of the tear-tip diameter. This area of work needs further investigation.

In the present investigation, the work done to break per unit volume of rubber, U_b, was determined from standard tensile tests carried out at a rate of 100 mm per minute at 23°C. The value of U_b obtained in this way was used to estimate the size of the knot diameter using the approximate relationship $T \cong U_b d$. It would be more appropriate and proper to determine U_b at the same strain rate and temperature at those at which the tear tests were carried out than to determine U_b at the arbitrary rate and temperature used in the standard tensile test.

Factors which affect the development of knotty tearing were investigated over a wide range of temperatures and tear rates using rubbers which differ widely in their glass-transition temperature and ability to strain-crystallize. In the present work, at least six major factors which affect the development of knotty tearing were identified. These factors were:

(i) the degree of strain-crystallization of the rubber vulcanizate
(ii) the degree of molecular mobility
(iii) the nature of the crosslinks
(iv) the concentration of the crosslink
(v) the concentration and type of carbon black.
(vi) the temperature and rate at which the tear tests were carried out.

It was found that both the degree of crystallinity and the glass-transition temperature, θ_g, of the rubber affect the development of knotty tearing. The range of tear rates and temperatures over which knotty tearing can occur was found to increase with increasing degree of crystallinity of the rubber. Thus a non-strain crystallizing rubber such as SBR showed a limited region of knotty tearing at a particular tear rate and temperature. This seems to suggest that strain-crystallization helps to enhance further the strength anisotropy already induced by the carbon black. The molecular mobility also plays an important role in promoting knotty tearing, in particular in rubbers that have high glass-transition temperatures such as ENR 50. At fast tear rate and low temperatures, the region of knotty tearing was small probably because the molecular mobility of the rubber did not allow rapid

development of 'black structure' around the tip of the crack which would thereby produce the strength anisotropy necessary for the occurrence of knotty tearing. In future work, it would be informative to investigate the development of knotty tearing in vulcanizates based on isomerized NR and ENRs, so that complications arising from strain-cystallization are avoided. Isomerized rubbers are preferred to synthetic non-strain- crystallizing rubbers because although strain-crystallization is suppressed, the chemistry of vulcanization is not greatly affected. This would ensure that any changes in the tear behaviour observed would be attributable only to the absence of strain-crystallization and would not be complicated by any variations in network structure. It would also be interesting to ascertain whether or not if tear tests are carried out at the same segmental molecular mobility, the various vulcanizates show similar regions of knotty tearing.

The test conditions, such as tear rate and temperature, affect the development of knotty tearing by affecting the molecular mobility of the rubber chains as noted above. The next important factor is the vulcanizing system. The present work has shown, that conventional sulphur vulcanizing systems, which produce mainly polysulphidic crosslinks, give vulcanizates having a wider region of knotty tearing than those produced by the efficient vulcanizing (EV) and the peroxide systems, which produce predominantly monosulphidic and carbon-carbon crosslinks respectively. Polysulphidic crosslinks are labile and break easily when highly stressed. When the polysulphidic crosslink yields, it relieves the local stress concentration near the crack tip, thus giving a larger region of high stresses where both orientation and the consequent strength anisotropy are substantial. Besides that, the ability of the broken polysulphidic crosslinks to recombine to form a second network whilst in the strained state has been invoked as an additional source of strength anisotropy which will be discussed again later.

It was observed also that, for a particular vulcanizing system, the development of knotty tearing depended upon the crosslink concentration. At very low crosslink concentrations below 4.0×10^{-2} mol per kg of rubber hydrocarbon, strain-crystallization did not occur because the stress was dissipated by plastic flow before the critical stress required to produce the molecular alignment and

orientation necessary for the occurrence of crystallization was reached. As a consequence of the absence of strain-crystallization and the inability of the crosslinked network to support large stresses, the high strength anisotropy necessary for the occurrence of knotty tearing was not achieved, and hence steady tearing occurred. At crosslink concentration greater than 4.0×10^{-2} mol per kg of rubber hydrocarbon, all the three vulacanizing systems (conventional, EV and peroxide) produced vulcanizates which showed knotty tearing. In the knotty tearing region, the tearing energy decreased with increasing crosslink concentration. A suggestion was put forward that the decrease in the tearing energy was associated with decrease in the extent of strain-crystallization accompanying increasing crosslink concentration. This was attributed to an increasing number of restrictions on molecular segments attempting to orientate and align with neighbouring chain segments. The overall effect is that the degree of orientated crystallization would reduce as also would the strength anisotropy. Corresponding to this, the tearing energy decreased, since tearing became less knotty as reflected by the progressive decrease in the size of the knot diameter observed. At very high crosslink concentrations, say, above 7.0×10^{-2} mole per kg of rubber hydrocarbon, the EV and the peroxide systems produced vulcanizates which showed steady tearing, whereas conventional system produced vulcanizates which showed knotty tearing for the reasons given above. At any particular crosslink concentration, the conventional sulphur vulcanizing system produced vulcanizates having higher tearing energies than did the EV vulcanizing system, and the EV vulcanizing system produced vulcanizates having higher tearing energies than did the peroxide system.

Among the other factors which affect the development of knotty tearing are the carbon black loading and the nature of the carbon black i.e., particle size, structure and surface activity. It was observed that, with fine HAF black, the loading required to produce knotty tearing in strain-crystallizing rubbers was at least 25 parts per hundred of rubber. With large-size MT black particles, only NR would give knotty tearing over a narrow range of tear rates at 23°C, at 50 parts per hundred of rubber. This may be attributed to large-size MT black particles adhered less strongly to the rubber matrix than the fine HAF particles, based on the evidence of the

work of Andrews and Walsh (11). The bond at the interface between the rubber and the MT carbon black breaks down at low stresses before the stress is sufficiently high to produce high strength hysteresis or the strength anisotropy necessary to produce knotty tearing.

It has been suggested by Russe (15) and Greensmith (16), that the occurrence of knotty tearing requires the development of local strength anisotropy around the tip of a tear. The effect of strength anisotropy on the tear strength was investigated in this work by using split-tear test-pieces which were first pre-strained by applying a pre-straining force, F_B. If anisotropy was introduced by F_B, on the application of the tearing force, F_A, the crack propagated in the direction of F_B, and the observed tearing energy would give a quantitative measure of strength anisotropy. The degree of strength anisotropy introduced by pre-straining was found to be affected by the following factors:

(i) the amount of pre-straining applied
(ii) the degree of crystallization of the rubber.

It was found that the tearing energy of pre-strained vulcanizates for a tear propagating in the direction of molecular orientation (i.e., parallel to F_B) was very low, being a factor of about 10 or more lower than the tearing energy obtained from measurements using trouser tear test-pieces. The higher the pre-strain level, the lower was the tearing energy for a tear propagating in the direction of molecular orientation. This throws some light on why strength anisotropy is an essential requirement for the occurrence of knotty tearing. When an advancing tear approaches the highly-oriented regions of local anisotropy around the tip of the tear, the tear splits along the direction of molecular orientation because its tear resistance is very low, as is reflected by low tearing energy for crack propagating in this direction. Thus the splitting of the tear in the direction of molecular orientation, i.e., parallel to the anisotropic zone, appears to be the cause of the tear deviation that lead to knotty tearing.

It was suggested earlier that strain-crystallization in rubbers

promotes knotty tearing, so that knotty tearing occurs more readily and effectively in these vulcanizates than it does in non-strain-crystallizing rubbers. The reason for this is believed to be that crystallization gives a further source of strength anisotropy, perhaps by giving extra molecular orientation and extra reinforcement by the crystals formed. It was found that in pre-strained vulcanizates, the tearing energy of a crack propagating in the direction of molecular orientation decreased with increasing degree of crystallinity of the rubber. Since high strength anisotropy gives a low tearing energy in the direction of molecular orientation, this indicates that the higher the degree of crystallinity, the stronger is the anisotropy. This observation clearly indicates that crystallization provides a source of enhancement of strength anisotropy, and is consistent with the suggestion put forward above. The fact that SBR black-filled vulcanizates did not produce stable crack propagation in the direction of molecular orientation gives further evidence for the importance of strain-crystallization in providing a further source of strength anisotropy. However, this does not mean that strain-crystallization is an essential feature for knotty tearing to occur. If this were the case, then SBR vulcanizates would never produce knotty tearing. The fact that SBR tears in a knotty manner under certain conditions of test suggests that the important factor is the degree of strength anisotropy. One interesting area for future work is to carry out split-tear tests on black-filled SBR vulcanizates at temperatures where knotty tearing occurs, to see if the anisotropy of strength under this condition will produce stable crack propagation in the direction of molecular orientation.

It was also found that, at the same level of molecular orientation, the tearing energy of pre-strained vulcanizates decreased with increasing crosslink concentration. This indicates that, in the absence of knotty tearing, mechanical energy dissipation is the dominant factor in determining strength. Vulcanizates having low crosslink concentrations dissipate more energy than do vulcanizates having high crosslink concentration. It was also observed that, at any particular crosslink concentration, the tearing energy of pre-strained vulcanizates increased in decreasing order of the bond strength of the crosslink, i.e., the tearing energies of the various vulcanizates decreased in the order

conventional > EV > peroxide. This conclusion agrees with the work of Brown, Porter and Thomas (40) on unfilled vulcanizates. In the knotty tearing region, the dependence of the tearing energy on the nature of crosslinks was less marked, probably being outweighed by the effect of tip diameter on tear strength.

Finally, there was also an unexpected finding associated with the tear behaviour of a pre-strained black-filled strain-crystallizing rubber vulcanizate under constant stress. It is well-known that, both unfilled and filled strain-crystallizing elastomers do not show time-dependent crack growth under constant stress, because of the development of crystalline region at the tip of the tear. If such a filled material is pre-strained sufficiently, however, time-dependent crack growth can occur in the direction of pre-straining, i.e., presumably between the crystallites. By contrast, if a carbon-black-filled non-strain crystallizing elastomer is held stretched, time-dependent crack growth in the direction of stretching was not observed and the crack was unstable.

The effect of pre-stressing on tear strength was also investigated. The stress giving the orientation was maintained for one minute, and then the loading stress was removed. Samples after pre-stressing were swollen to eliminate viscoelastic effects, and then deswollen and dried down to constant weight prior to tear testing. The strength anisotropy introduced by pre-stressing was found to be affected by the following factors:

(i) viscoelastic recovery
(ii) the amount of permanent set
(iii) nature of the crosslinks
(iv) the degree of crystallization of the rubber

The tearing energy of pre-stressed vulcanizates was found to be lower before the completion of viscoelastic recovery than after the completion of viscoelastic recovery by swelling and deswelling. The tearing energy of pre-stressed vulcanizates was also found to correlate strongly with the permanent set. A suggestion was put forward that the anisotropy retained after pre-stressing was associated with the set. The higher the set, the higher was the

anisotropy retained and the lower was the tear resistance in the direction of molecular orientation. Thus the set gives a quantitative measure of anisotropy retained after pre-stressing, and the tearing energy in the direction of molecular orientation gives a quantitative measure of strength anisotropy produced by the set. It was found that the effect of pre-stressing was more pronounced in vulcanizates produced by the conventional sulphur system than in vulcanizates produced by the soluble EV system, because the former gave substantially higher set than the latter. In conventional vulcanizates, if the set introduced by pre-stressing was greater than 12% , the tearing mode changed from knotty to steady tearing. The tearing energy of pre-stressed vulcanizates decreased by a factor of about 20 or more compared to the unstressed control vulcanizates.

The set can be introduced into the vulcanizate by a single pre-stressing, multiple pre-stressings and by 2-stages vulcanization method. When the tearing energies of these vulcanizates were plotted against the set, an interesting correlation between tearing energy and set was obtained. All the points lie satisfactorily on a single curve, regardless of the way the set was obtained. Apparently, the tearing energy-set correlation was also independent of the nature of crosslink since the points for different vulcanization systems also lie on the same curve. This observation leads to a conclusion that the anisotropy retained after pre-stressing is associated with the set. When a black-filled vulcanizate is pre-stressed, the carbon black particles are oriented in the direction of extension. If the two-networks form during pre-stressing, on releasing the stress, the carbon black particles are locked in the oriented state because of the presence of the set. Weak paths are left in the rubber as a consequence of anisotropy introduced by the set and thus allowing easy tearing in the direction of pre-stressing. This conclusion has some practical importance. It is clearly evident from the tearing energy-set correlation, that the set is a potential cause of weakening a rubber vulcanizate. It is important that care should be taken as not to introduce set into the vulcanizate prior to its service or for quality control tear tests. Thus when stripping a vulcanized sheet of rubber from the mould, it is important that it should be removed with a minimal stripping force. The use of mould lubricant can ease

stripping of the vulcanized sheet from the mould. In the case of a high temperature vulcanization, it is important that the viscosity of the rubber mix is sufficiently low to allow rapid flowing of the rubber, so as to avoid vulcanization taking place before the rubber completely fills the mould. If vulcanization starts before the rubber fills the mould, the final vulcanizate will contain two networks, viz, one network which forms before the mould is completely filled, and the second network which forms after the mould is completely filled. Such a vulcanized sheet will be somewhat distorted and will never lie flat when it is put on a flat table. Such vulcanizate should never be used.

When the tearing energies of pre-strained vulcanizates were compared with the tearing energies of pre-stressed vulcanizates, two important observations were noted. Firstly, it was found that tearing energies of pre-strained vulcanizates where the stress giving the orientation was maintained constant during the test were about half those of the corresponding pre-stressed vulcanizates. This indicates that the anisotropy introduced by pre-stressing was substantial. It also implies that once the two-networks (set) have occurred, the orientation maintained during pre-straining contributed little strength anisotropy but nevertheless is still significant. Thus this shows that the strength anisotropy comes not only from the strengthening structure associated with strain-crystallization and the carbon black structure, but also from the set. Secondly, the tearing energy of pre-stressed vulcanizates was found to decrease with increasing degree of crystallization of the rubber. This complements the observation that the set increased with increasing degree of crystallization. This observation is also consistent with the results for strength anisotropy introduced by pre-straining, where the tearing energy of pre-strained vulcanizates decreased with increasing degree of crystallization.

Independent measurements of tension set and volume fraction were carried out. Using the two-network theory developed by Thomas (38), the proportions of crosslinks broken, and the subsequent recombination efficiency of the broken crosslinks to form a second network, were determined quantitatively. The high set observed in conventional sulphur vulcanizates was attributed to high recombination efficiency of the broken polysulphidic crosslinks to

form a second network. The low set observed in soluble EV vulcanizates was attributed to low recombination efficiency. The incorporation of di-n-butyl tetrasulphide (DBTS) into a polysulphidic network reduced the amount of set markedly, and the tearing energy decreased significantly since tearing became less knotty. The decrease in the tearing energy was not attribute to the plasticizing effect of the DBTS, because vulcanizates containing aromatic oil plasticizer had significantly improved tear strength compared to vulcanizates containing DBTS and those without plasticizer. This suggests that the decrease was probably because the contribution to anisotropy associated with the set was markedly reduced. Thus the anisotropy associated with the set may play an important role in giving further anisotropy of strength, which is consistent with the observation that conventional sulphur vulcanizates produce knotty tearing more readily than do EV and peroxide vulcanizates over a wide range of crosslink concentration.

The present work lends support to the hypothesis put forward by Rivlin and Thomas (76) that anisotropy of strength could develop in two-network vulcanizates. Two-stage vulcanizations were carried out to provide a means of testing the hypothesis that the permanent set was associated with the formation of a second network whilst in the strained state. After the first-stage vulcanization, the sample containing the first network was pre-strained slightly so that the crosslinks introduced during the second-stage vulcanization produced a second network in a strained state. The observations proved that the set was indeed produced. For future work it would be more appropriate to carry out this work using the peroxide system, in order to avoid the uncertainty associated with the instability of the crosslinks introduced in the first network.

Finally, a further interesting observation concerned the time-dependent crack growth under constant stress displayed by a pre-stressed black-filled conventional sulphur NR vulcanizate which has high set. This suggests that strain-crystallization at the tip of the crack is somewhat suppressed, otherwise time-dependent crack growth would not have occurred. The observation here was consistent with the time-dependent tearing observed in pre-strained vulcanizates where the stress giving the orientation was maintained during the test. Thus it appears that the second network (set)

interferes with the development of strain-crystallization at the tip there. This is consistent with the observation that, a pre-stressed black-filled EV NR vulcanizate which has low set, did not show time-dependent crack growth under constant stress.

The application of WLF transformation to tearing energy data for pre-stressed vulcanizates gave a single mastercurve covering a wide range of tear rates and temperatures. This observation provides further evidence that crack propagation is predominantly controlled by viscous processes. Otherwise WLF transformation would not give a single mastercurve.

For future work, it would be interesting to carry out the following experiments:

(i) X-rays studies on pre-stressed black-filled vulcanizates to see if there is any evidence that the carbon black particles remain locked in an oriented position after pre-stressing.

(ii) Crystallization studies on unfilled NR after pre-stressing. It would be interesting to check if there is any difference in the rate of crystallization across and along the direction of the stress previously applied. This study might provide evidence as to whether the second network interferes with strain-crystallization or not.

(iii) Tear measurement on samples that have been pre-stressed in equibiaxial extension. It would be interesting to ascertain whether the tear behaviour is the same as that obtained by pre-stressing in uniaxial extension.

In the steady tearing regions, the fractured surfaces of black-filled vulcanizates were smoother than those of unfilled vulcanizates under the same conditions of tearing. The tearing energy of black-filled vulcanizates can be very substantial, in particular that of non-strain-crystallizing SBR vulcanizates. This additional strength in the absence of knotty tearing is believed to be associated with the increase in hysteresis provided by the carbon black, although the mechanism is still not entirely clear. This area of work certainly needs attention. In particular, the effect

of cavitation on the fractured surface of black- filled vulcanizate should be investigated. It would be interesting to ascertain whether the smooth fractured surface of black-filled vulcanizates is related to the stiffening effect imposed by the carbon black particles making cavitation less favourable.

The final conclusion that can be drawn from this thesis can be summarised as follows:

(i) Knotty tearing is still the principal mechanism by which carbon black enhances the tear strength of rubber vulcanizates.

(ii) The essential requirement for the occurrence of knotty tearing is the development of local strength anisotropy around the tip of the tear.

(iii) Apart from the carbon black ``structure'' additional anisotropy may come from the contributions associated with strain-crystallization and with set.

(iv) In the absence of knotty tearing, carbon black enhances the tear strength by increasing the mechanical hysteresis.

REFERENCES

1. E.M. Danenberg, Vanderbilt Rubber Handbook, Ed. by Robert O Babbit, Pub., R.T. Vanderbilt Co. Inc., Ch. 7, pg. 408, 1978.
2. E.H. Andrews and A.N. Gent, The Chem. and Phys. of Rubberlike Substance, Ed. by L. Bateman, London: Maclaren and sons Ltd., Ch. 9, 225, 1963.
3. M.J. Gregory and A.S. Tan, Proc. of the Inst. Rub. Conf., Kuala Lumpur, 1975.
4. MRPRA, Tech. Bulletin No.4, 1964 and MRPRA Information sheets no. 67 and no. 76.
5. L.R.G Treloar, Introduction to Polymer Sci., Wykeham Pub. (London) Ltd., London & Winchester, Ch. 6, 81, 1970.
6. Heinze, H.D., Schmieder, K., Schnell, G, and Wolf, K.A, Rub. Chem. Tech., 35, 776, 1962.
7. J.B. Horn, Rub. Tech. and Manufacturer, Ed. by C.M. Blow, Ch. 6, 174, Pub. for IRI by Butterworths, London, 1971.
8. J.J. Brennan, T.E. Jerymyn, and B.B. Boonstra, J. Appl. Polym. Sci., 8, 2687, 1964.
9. Bueche, F., J. Polym. Sci., 33, pg. 259, 1958.
10. Dannenberg, E.M., Trans IRI, 42, T26, 1966.
11. E.H. Andrews and A. Walsh, J. Polym. Sci., 33, 39, 1958.
12. L. Mullins, Elastomers: Criteria for Eng. Design, Ed. by C. Hepburn and R.J.W. Reynolds, Appl. Sci. Pub., Ch. 1, pg 1, 1981.
13. F. Bueche, J. Appl. Polym. Sci., 4, 107, 1960.
14. Harwood, J.A.C, Mullins, L, and Payne A.R., J. Appl. Polym. Sci., 9, 3011, 1965.
15. W.F. Busse, Ind. and Eng. Chem., 26, 1194, 1934.
16. H.W. Greensmith, J. Polym. Sci., 21, 175, 1956.
17. A.A. Griffith, Phil. Trans. Roy. Soc. (London) A221, 163, 1920.
18. E.H. Andrews, Dev. in Polymer Fracture-1, Ed. by E.H. Andrews, Appl. Sci. Pub. Ltd., London, pg. xiii, 1979.
19. R.S. Rivlin and A.G. Thomas, J. Polym. Sci., 10, 291, 1953.
20. A.G. Thomas, J. Appl. Polym. Sci.,3, 8, 168, 1960.
21. G.J. Lake, P.B. Lindley and A.G. Thomas, Pro. 2nd. Int. Conf. of Fracture, Brighton, 13th.-14th. April, 1969.
22. A.G. Thomas, J. Polym. Sci., 18, 177, 1955.
23. H.W. Greensmith, J. Appl. Polym. Sci., 3, 183, 1960.
24. G.J. Lake and A.G. Thomas, Proc. Roy. Soc.A, 300, 108, 1967.

25. G.J. Lake and P.B. Lindley, J. Appl. Polym. Sci., 9, 1233, 1965.
26. L.R.G. Treloar, The Physics of Rubber Elasticity, 3rd. Ed., Clarendon Press, Oxford, 1975.
27. A.K. Bhoumick, A.N. Gent and P. Pulford, Rub. Chem. and Tech., 56, 226, 1982.
28. Andrews E.H., J. Mat. Sci., 9, 887, 1974.
29. H.W. Greensmith and A.G. Thomas, J. Polym. Sci., 18, 189, 1955.
30. A. Kadir and A.G. Thomas, Elastomers: Criteria for Eng. Design Ed. by C. Hepburn and R.J.W. Reynolds, Appl. Sci. Pub., Ch. 5, 67, 1981.
31. G.J. Lake and O.H. Yeoh, J. Polym. Sci., Part B:Polym. Phy. 25, pg. 1157-1190, 1987.
32. H.W. Greensmith, L.Mullins and A.G. Thomas, Trans. Soc. of Rheo.4, 179, 1960.
33. M.L. Williams, R.F. Landel and J.D. Ferry, J. Amec. Chem. Soc., 77, 3701, 1955.
34. F. Bueche, Physical Properties of Polymers, Int. Sci. Pub., John Wiley and Sons, N. York, Ch. 4, 85, 1962.
35. L. Mullins, Trans. Inst. Rub. Ind., 35, 213, 1959.
36. D.J. Elliot, Dev. in Rub. Tech. One, Ed. by A. Whelan and K.S. Lee, Pub. Appl. Sci. London, 1979.
37. Bateman L.,Cunneen J.I. and Moore C.G., The Chem. and Phy. of Rubberlike Substance (Bateman L.,Ed), London:Maclaren and sons Ltd., Ch.19, 1963.
38. A.G. Thomas, J. Polym. Sci., 48, 145, 1974.
39. P. Brown, M. Porter and A.G. Thomas, in press.
40. P.S. Brown, M. Porter and A.G. Thomas, Int. Rub. Conf., Kuala Lumpur, 1985.
41. A.N. Gent, Int. Rub. Conf., Plastics and Rubber Inst. 1987.
42. A.N. Gent, and A.W. Henry, Proc. Inst. Rub. Conf., 193, 1967.
43. R.G. Stacer, E.D. von Meerwall and F.N. Kelly, Rub. Chem. and Tech., 58, 913, 1985.
44. R.G. Stacer, L.C. Yanyo and F.N. Kelly, Rub. Chem. and Tech., 58, 421, 1985.
45. R.G. Stacer and F.N. Kelly, ACS Rub. Div. Mtg., Los Angeles April 23-26, 1985.
46. R. Houwink and H.J.J. Janssen, Rub. Chem. and Tech., 29, 409, 1956.
47. A.N. Gent and H.J. Kim, Rub. Chem. and Tech., 51, 35, 1978.
48. R. Chasset and P. Thirion, Proc. Int. Rub. Conf., Washington DC 349, 1959.

49. A.I. Medalia, Rub. Div. Mtg., ACS, New York, NY,, April 8-11, 1986.
50. C.K.L. Davies, S.V. Wolfe, A.G. Thomas and I.R. Gelling, Polymer, 24, 107, 1983.
51. C.S.L. Baker, I.R. Gelling and Azemi bin Samsuri, J. Nat. Rub. Res., 1(2), 1986.
52. M. Porter, Rub. Chem. Tech., 40 (3), 866, 1967.
53. G.M. Bristow, and M. Porter, J. Appl. Polym. Sci., 11, 2215, 1967.
54. M. Porter, Private communication, 1986.
55. P.J. Flory and J. Rehner, Jr., J. Chem. Phys., 521, 1943.
56. P.J. Flory, J. Chem. Phys., 18, pg. 108, 1950.
57. G.M. Bristow, J. Appl. Polym. Sci., 9, 1571, 1965.
58. J. Glazer and F.H. Cotton, The Appl. Sci. of Rubbers, Ed. by W.J.S. Nauton, Ch.12 (part 1), pg. 922
59. A.G. Thomas, private communication, 1989.
60. NR Formulary and Property Index, MRPRA, 1984. 61.
61. G.J. Van Der Bie, J.M. Rellage, and C. Vervloet, same as ref. 7, Chapter 4, 84.
62. E. Southern, PhD. Thesis, Univ. of London, 1969.
63. A.K. Bhoumick and A.N. Gent, Rub. Chem. Tech., 56, 845, 1984
64. Azemi bin Samsuri, A.G. Thomas, I.R. Gelling and E. Southern Int. Rub. Tech. Conf., Kuala Lumpur, 1985
65. W.S. Penn, Synthetic Rubber Tech., Vol. 1, Ch.3, 16, Pub. Maclaren and Sons, Ltd., London, 1960.
66. Gee, G., J. Polym. Sci., 2, 451, 1947.
67. Harwood J.A.C. and A. Schallamach, J. Appl. Sci., 12, 889, 1968.
68. Gent, A.N., In Sci. and Tech. of Rubber, Ed. by F.R. Eirich, Academic Press, New York, 419, 1978.
69. L. Mullins, Rub. Chem. Tech., 33 (2), 315, 1960.
70. M.J. Gregory, C. Metherell and J.F. Smith, Plastics and Rubber: Materials and Applications, 37, 1978.
71. P. Mason, J. Appl. Polym. Sci., 4 (11), 212, 1960
72. E.M. Dannenberg, Rubber Age, 98(9,10), 82, 1966.
73. G.M. Bristow, Private communication, 1989.
74. B.B. Boonstra, same ref. as no. 7, Ch. 7, pg. 227.
75. Greensmith, H.W., J. Appl. Polym. Sci., 7, 993, 1963
76. R.S. Rivlin and A.G. Thomas, Eng. Fracture Mech., 18, 389, 1983.
77. A.G. Thomas, Deformation and Fracture of High Polymers, Ed. by Henning Kausch, J.A. Hassel and Robert Jaffe, Plenum Press, 1974.
78. L. Mullins and N.R. Tobin, I.R.I. Trans., 33, 1956.

79. L. Mullins and N.R. Tobin, J. Appl. Polym. Sci., 9, 2993, 1965.
80. T.K. Lee and M. Porter, Int. Rub. Conf., Venice, Oct., 1979.
81. M.J. Gregory, Rub. Chem. and Tech., 52, (5), 1979.
82. M. Shepelev and O. Shepelev, Int. Rub. Conf., Venice, Oct., 1979.
83. L. Mullins, Proc. of the 2nd. Rubber Tech. Conf., 179, 1948.
84. M.S. Green and A.V. Tobolsky, J. Chem. Phys., 14, 80, 1946.
85. J.P. Berry, J. Scanlan and W.F. Watson, Trans. Faraday Soc., 52, 2, 1956.
86. Azemi bin Samsuri, unpublished results 1989.
87. J.D. Ferry, Viscoelastic Prop. of Polym., 3rd Ed., Pub. John Wiley and Sons, 1980.
88. A.B. Davey and A.R. Payne, Rubber in Eng. Practice, London Maclaren and Sons Ltd., Ch.2, 24, 1965.
89. T.L. Smith, J. Appl. Phys., 35, 27, 1964.
90. C.J. Derham and A.G. Thomas, Rub. Chem. Tech., 50, 397, 1977.
91. C.M. Metherell, Private communication, 1988.
92. A.N. Gent and P.B. Lindley, Proc. Roy. Soc. A, 249, 195, 1958.
93. E. Guth and R. Simha, Kolloid-Z, 74, 266, 1936.
94. L. Mullins, same reference as no. 30, Ch.1, 1, 1981.
95. A.G. Thomas, private communication, 1989.
96. J.A.C. Harwood and A.R. Payne, J. Appl. Polym. Sci., 9, 2993, 1965.
97. A.R. Payne, J. Appl. Polym. Sci., 57, 368, 1962.

Paper 6. Tear Behaviour of Carbon Black-filled Rubbers

AZEMI BIN HAJI SAMSURI
Rubber Research Institute of Malaysia, Kuala Lumpur, Malaysia

AND

A.G. THOMAS
Consultant, Hertfordshire, United Kingdom

Abstract in English

The enhancement of tear strength by carbon black fillers is thought to be primarily associated with the phenomenon known as knotty tearing when the propagating tear deviates sideways, perhaps at right angles, from the intended tear path. It is suggested that local anisotropy of strength near the tear tip is the cause of this deviation. The effect of this anisotropy has been investigated using the 'split' tear test piece. In this test piece, the crack can be made to propagate in the direction of a previously applied stress, and the results interpreted as the tearing energy for propagation in this direction. Thus, this simulates the development of a 'knot' at the tip in a conventional test piece. As the pre-strain is increased, tearing in this direction becomes progressively easier, the tearing energies decreasing by a factor of ten or more. An approximate calculation suggests that this degree of anisotropy should be quite adequate to produce the observed knotty tearing behaviour.

There is strong evidence that for certain types of vulcanisate, a large stress can produce scission and subsequently some recombination of crosslinks in the deformed state, thus giving some permanent set. The question arises as to whether the anisotropy observed with the 'split' tear test piece, where the stress giving the orientation is maintained during the test, is in fact associated with these molecular changes, so that the strength anisotropy may persist after the stress is removed. Tear measurements on pre-stressed test pieces have been carried out and indicate that indeed most of the anisotropy does remain when the stress is removed, and that moreover, the anisotropy in the carbon black-filled system, correlates strongly with the set. The factors determining the ease with which rubber vulcanisates can be induced to show permanent set after pre-stressing are at least partly understood. The ability to strain-crystallise is very important, as is also the nature of the crosslink. Polysulphidic crosslinks produce the greatest set, followed by monosulphidic and carbon-black crosslinks in decreasing order.

At least some of the substantial differences observed between the tear strengths of carbon black-filled vulcanisates can be understood on this basis, for example the relatively low tear strength of a carbon black-filled peroxide-cured material comparedwith a similar material conventionally cured.